Evolution of the delta family of ionotropic glutamate receptors

Giulio Rosano

Thesis for the degree of Philosophiae Doctor (PhD)
University of Bergen, Norway
2024

UNIVERSITY OF BERGEN

Evolution of the delta family of ionotropic glutamate receptors

Giulio Rosano

Thesis for the degree of Philosophiae Doctor (PhD)
at the University of Bergen

Date of defense: 14.06.2024

Year: 2024

Title: Evolution of the delta family of ionotropic glutamate receptors

Name: Giulio Rosano

Print: Skipnes Kommunikasjon / University of Bergen

Scientific environment

This thesis was conducted in the Lynagh lab at the Michael Sars Centre, partner of the European Molecular Biology Laboratory (EMBL) and part of the University of Bergen's Department of Biological Sciences, under the Faculty of Mathematics and Natural Sciences' PhD program.
The work was funded in part by the Michael Sars Centre (Research Council of Norway project number 234817) and in part by the European Research Council (Horizon 2020 grant agreement 803714).

Acknowledgements

These four years in Bergen wouldn't have been the same without the people who, for better (and for worse), helped me through this journey. Here, I'm obviously going to talk about the former.
I am especially grateful for the guidance provided by Tim Lynagh, my supervisor, from day one. From the very first moment he came to visit me in my quarantine apartment (from afar), I knew I could count not only on his knowledge and dedication to work but, most importantly, on him. I believe we were always honest with each other, and that really made a difference, even during the hardest times of a mentor-student relation. I hope you don't find this "a little out there!".
Thanks to my co-supervisor, Aurélia E. Lewis. It was always very nice to chat and discuss; your presence was always of great comfort.
Thanks to all members of S15, current and past (and future). Everyone was always ready to help and give great feedback, thanks. Everyone at the Michael Sars Center made me feel part of a big family. Thanks to every single one of you.
Among them, Eudald really helped me during the struggles of being a PhD candidate, and his advice on how to handle the ups and downs of PhD life were invaluable. But most importantly, I found a true friend that goes beyond Bergen, Barcelona or Sant Feliu, thank you "funny guy"! Mark, it's hard to express, but for me you never truly left Norway. I am so grateful of having you as a friend that I would need the entire script of *The Room* to express my feelings. Unfortunately this thesis is far from it.
Noah, Vincenzo, thanks for the time spent together, keep fighting!
Toto, Marianna, Francesco and Veronica thanks for being such great company and such good friends. Bergen is only the beginning of our friendship.

The feeling of (hopefully) being a better scientist today than I was four years ago is incomparable to the feeling of being a better tennis player. Espen, Helge, Camilo, thanks for pushing me becoming a better player and being of great mental support inside and outside the court.
Simone, Emanuele, Riccardo, I love you guys. Also, can you believe that from that middle school class from Taviano there's (at least) two PhDs?
Blandine, you were always supportive of my failed projects and proud of my small achievements. In you, I always find the care and love that I hope to somehow give back, even with my limits. Thank you for always being here with me. I love you.
Mamma, papà, Gaia, nonna. Non c'è posto che io non veda senza portarvi con me. Non è facile starvi lontano da così tanto tempo, ma la sola idea di rendervi orgogliosi mi da una felicità difficile da descrivere e la forza di andare sempre avanti. Vi voglio bene.

Author contributions

I, **Giulio Rosano**, wrote this thesis with the help of comments and revisions from my supervisor Timothy Lynagh.

Yuhong Wang performed experiments with *Rat*GluA2, page 48 figure 5.2 C (Chapter 5.1.2).

Allan Barzasi performed experiments with *Sacco*GluD, page 37 figure 4.5 (Chapter 4.2) and *Aca*GluD in page 61 figure 5.10 (Chapter 5.4).

Timothy Lynagh contributed to much of the experimental design and analysis throughout the work, and also helped perform some of the experiments including page 34 figure 4.3 and page 37 figure 4.5 and site-directed mutagenesis (Chapter 3.2).

Contents

Publication emerging from this thesis

Loss of activation by GABA in vertebrate delta ionotropic glutamate receptors

Giulio Rosano, Allan Barzasi, Timothy Lynagh

Proceedings of the National Academy of Sciences of the USA, 121 (6): e2313853121 (2024),

https://www.pnas.org/doi/10.1073/pnas.2313853121

The publication emerging from this thesis is appended at the end of this thesis in Appendix 2

Foreword

This thesis delves into the world of ionotropic glutamate receptors (iGluRs). Particularly, I focus on the delta family of iGluRs, the only family of iGluRs known for their lack of direct activation by ligands, with a spotlight on the evolutionary journey and functional properties of these receptors across various animal species. The introductory chapter one sets the stage by providing an overview of neuronal signaling mechanisms and the critical role that iGluRs play in modulating synaptic activity. I further narrow down the introduction to the distinct features of delta iGluRs, laying the groundwork for my aims in chapter two and subsequent experimental study. My study makes use of molecular phylogenetics, electrophysiology, and mutagenesis techniques to uncover the evolution and functional properties of various delta iGluRs, methods which are described in chapter three. Chapter four stands as the cornerstone of my thesis, unveiling the surprising activation of numerous invertebrate delta iGluRs by GABA, a neurotransmitter traditionally associated with inhibitory effects in the nervous system. In chapter five, I delve into the pharmacological and biophysical properties of the starfish delta receptor *Aca*GluD and its relation to other iGluRs. In chapter six, by comparing active GABA-gated invertebrate delta receptors to inactive vertebrate delta receptors and using mutagenesis I decipher the molecular basis for the loss of GABA-gated currents observed in vertebrate delta iGluRs. Chapter seven assesses the relevance of these findings for related fields, and overall, this thesis presents a comprehensive analysis of delta iGluRs, offering a new perspective on their evolution and functional diversity.

Abstract (in English)

In the mammalian brain, ionotropic glutamate receptors (iGluRs) are critical in mediating excitatory signals between neurons. These receptors are categorized into four distinct families: AMPA, KA, NMDA, and delta. Unlike other iGluR families, delta receptors are not activated by neurotransmitter binding. This thesis presents a comprehensive analysis combining phylogenetics, electrophysiological experiments, and site-directed mutagenesis, to explore the functional diversity of delta receptors from numerous animals and identify the molecular basis for the functional divergence of mammalian delta receptors. My findings reveal that delta iGluRs in various invertebrate species function similarly to the AMPA/KA receptors found in mammals but, uniquely, are activated by γ-aminobutyric acid (GABA), traditionally recognized as an inhibitory neurotransmitter. This discovery points to a potential excitatory role for GABA in invertebrate neural circuits, challenging conventional paradigms of neurotransmission. Moreover, my analysis identifies nine amino acid substitutions that arose in the vertebrate lineage, significantly contributing to the distinctive functional divergence of mammalian delta iGluRs.

Abstract (på norsk)

I pattedyrhjernen er ionotrope glutamatreseptorer (iGluR) avgjørende for å formidle eksitatorisk nevrotransmisjon. Disse reseptorene deles inn i fire forskjellige familier: AMPA, KA, NMDA og delta. I motsetning til de andre iGluR-familiene aktiveres ikke delta-reseptorene ved binding av nevrotransmittere. Denne avhandlingen presenterer en omfattende analyse som kombinerer fylogenetikk, elektrofysiologiske eksperimenter og stedsrettet mutagenese for å utforske det funksjonelle mangfoldet av deltareseptorer fra en rekke dyr og identifisere det molekylære grunnlaget for den funksjonelle divergensen mellom deltareseptorer hos pattedyr. Funnene mine viser at delta iGluR-reseptorer hos ulike arter av virvelløse dyr fungerer på samme måte som AMPA/KA-reseptorene hos pattedyr, men at de aktiveres av γ-aminosmørsyre (GABA), som tradisjonelt er kjent som en hemmende nevrotransmitter. Denne oppdagelsen peker på en potensiell eksitatorisk rolle for GABA i nevrale kretser hos virvelløse dyr, noe som utfordrer konvensjonelle paradigmer for nevrotransmisjon. I tillegg identifiserer analysen min ni aminosyresubstitusjoner som oppsto i virveldyrlinjen, noe som i betydelig grad bidrar til den særegne funksjonelle divergensen mellom delta iGluR-ene hos pattedyr.

Chapter 1

Introduction

1.1 Neurons and Signal Transmission

The central nervous system (CNS), composed of the brain and spinal cord, serves as the principal control hub of the body's activities and functions and it's responsible for orchestrating a wide range of sensory information and motor responses, from regulating vital processes such as breathing to enabling complex behaviors like thinking, learning, and emotions. Structurally and functionally, it consists of an elaborate network of cells called neurons that have the ability of communicating with each other. Most neurons are composed of a cell body from which protrude numerous dendritic branches and a single, elongated axon. Neurons are interconnected by synapses, the functional point of contact of neurons within the network, where communication occurs through the coupling of a presynaptic axon terminal and a postsynaptic dendrite.

The fundamental basis of neural communication lies in the generation and propagation of electrical signals. These electrical signals manifest as transient shifts in the cell's membrane potential, the electrical voltage difference across the neuron's membrane, resulting from the differential concentration of ions—mainly extracellular sodium (Na^+), calcium (Ca^{2+}) and chloride (Cl^-) and intracellular potassium (K^+) and various organic anions—between the inside and outside of the cell. It is generally stabilized, or polarized, at approximately –70 mV at rest, which is maintained by ion pumps and channels in the cell membrane (Pivovarov et al. (2019)). When the

membrane potential of a neuron becomes sufficiently depolarized, reaching a threshold value (between –50 and –55 mV) it leads to the rapid opening of voltage-gated Na^+ channels and a subsequent influx of Na^+, further depolarizing the membrane and elevating the potential to a peak value near +30 mV. The depolarization also inactivates sodium channels and activates slightly slower voltage-gated K^+ channels, allowing potassium ions to exit the neuron and thus repolarizing the membrane towards the resting potential (Hodgkin and Huxley (1939)). Reaching the end of the repolarization phase there's an overshoot to a hyperpolarized state due to the delayed closing of K^+ channels, momentarily making the neuron less excitable (Yoshimura and Jessell (1989)). These events define an action potential, an all-or-nothing event that once initiated it propagates along the neuron's axon without diminishing in strength, thanks to the continuous opening of ion channels along the axon's length, and culminates in the opening of voltage-gated Ca^{2+} channels leading to an influx of Ca^{2+}. Incoming Ca^{2+} act as a secondary messenger and initiate the fusion of neurotransmitters-containing vesicles with the presynaptic membrane. This allows the neurotransmitters to infuse the synaptic gap, a 20 nm space between the presynaptic and the postsynaptic neuron, and specifically bind to neurotransmitter receptors that are localized on the postsynaptic membrane (Teleanu et al. (2022)).

This conversion of electrical signal to chemical one opens the door to a wide array of events. Namely, the type of receptor involved dictates the nature of the response within a neuron. In the case of ionotropic receptors a swift alteration of their structure upon neurotransmitter binding, and consequent pore opening, allows the passage for ions such as Na^+, K^+, or Ca^{2+} within milliseconds, that leads to rapid changes in the neuronal membrane potential and facilitating fast synaptic transmission. Metabotropic receptors, in contrast, initiate a more prolonged response by activating G-proteins, which in turn can trigger various other downstream signaling pathways. Based on the specific neurotransmitter or receptor involved, the postsynaptic neuron may receive a signal that is either excitatory or inhibitory. When ionotropic receptors allow the influx of cations, the neuron's membrane potential becomes more positive, which typically leads to excitatory postsynaptic potentials (EPSP) that triggers voltage-dependent Na^+ channels

and a dendritic action potential that propagates along the dendritic membrane towards the axon. Conversely, when ionotropic receptors selectively allow the influx of Cl^- ions or the efflux of K^+, the neuron's membrane potential becomes more negative, a process known as hyperpolarization, thus diminishing or completely abolishing an EPSP (Takagi (2000)). The accuracy in distinguishing these processes is crucial because it underlines how neural networks manage the balance between excitation and inhibition, a fundamental aspect of their function.

1.2 GABA and $GABA_A$ receptors

Most inhibitory synapses in the brain and spinal cord use either γ-aminobutyric acid (GABA) or glycine as neurotransmitters. GABA, the most prevalent inhibitory neurotransmitter in the CNS, operates primarily through $GABA_A$ receptors, ionotropic receptors from the pentameric ligand-gated ion channel (pLGIC) superfamily. In addition to ionotropic receptors, GABA also acts on metabotropic $GABA_B$ receptors, which are G-protein coupled receptors that modulate neurotransmission over longer periods of time and influence a wide range of intracellular signaling pathways that lead to longer-lasting effects on neuronal excitability. GABAergic signaling is crucial in brain physiology and its dysfunction can lead to pathological conditions such as epilepsy. This typically occurs when the equilibrium between excitation and inhibition within the network is disrupted (Treiman (2001)). $GABA_A$ receptors consist of five symmetric subunits. 19 different $GABA_AR$ subunits have been cloned in the mammalian CNS and this diversity enables significant variability in the composition of $GABA_AR$ (Olsen and Sieghart (2009)). Each subunit is characterized by an extracellular domain (ECD) that includes "half" of the intersubunit binding site for GABA binding, a transmembrane domain made up of four transmembrane helices (TM1-TM4) with the TM2 helix lining the ion channel pore, and a flexible intracellular domain (ICD) (Miller and Aricescu (2014)). The receptor's structure is finely tuned to respond to GABA binding with conformational changes that open the Cl^- channel, a mechanism that is modulated by various pharmacological agents, including benzodiazepines, anaesthetics and neurosteroids (Olsen (2018); Olsen and Sieghart (2009)). These compounds

bind to different sites on the $GABA_A$ receptor complex than GABA, acting as positive allosteric modulators and, consequently potentiating the inhibition of neurons and are used in the treatment of conditions like anxiety, epilepsy, and sleep disorders (Castellano et al. (2021)).
Transitioning from the pharmacological modulation of $GABA_A$ receptors in mature neurons, it is interesting to note the dynamic functionality of these receptors during different life stages in the mammalian brain. During early neural development, the intracellular environment of these neurons is characterized by a higher concentration of Cl^- relative to the extracellular environment and its maintained primarily through the activity of the Cl^- membrane importer protein sodium-potassium-chloride cotransporter 1 NKCC1 (Payne et al. (2003)). Activation of $GABA_A$ receptors under these conditions results in Cl^- ions flowing out of the neuron, leading to membrane depolarization—in stark contrast to the hyperpolarizing, inhibitory effect seen in adult neurons (Ben-Ari and Holmes (2005)). As the brain matures the expression of NKCC1 decreases and an upregulation of potassium-chloride cotransporter 2 (KCC2) take place. KCC2 extrude Cl^- from the inside of the neuron, lowering the intracellular concentration of Cl^- below the equilibrium potential of $GABA_A$ receptor-mediated Cl^- influx (Delpire (2000); Chabwine et al. (2015); Rivera et al. (1999)). Interestingly, the timing of the GABA shift from excitatory to inhibitory function is not uniform across the nervous system but appears strongly dependent on the neuronal type, sex, and species (Peerboom and Wierenga (2021)).

1.3 Glutamate and glutamate receptors

Glutamate is the principal excitatory neurotransmitter in the mammalian CNS and plays a critical role in virtually all aspects of brain function (Johnson and Aprison (1970); Fagg and Foster (1983)) and in turn glutamate receptors play a crucial role in transmitting excitatory signals in neuronal networks. Glutamate receptors are broadly classified into two groups: ionotropic receptors, which are ligand-gated ion channels, and metabotropic receptors, which function through G protein-coupled mechanisms. Ionotropic glutamate receptors (iGluRs) function as cation-selective channels that are directly opened by glutamate, facilitating rapid signal trans-

duction across synapses, while in metabotropic glutamate receptors (mGluRs), glutamate binding alters mGluR interactions with G proteins, leading to relatively slow-acting intracellular signaling cascades (Conn (2003)). Within mammals, the coding of iGluR subunits is accomplished by 18 distinct genes and are categorized into four families based on sequence homology and pharmacological characteristics. Three of these families were named after selective agonists identified during their initial classification: α-**a**mino-3-hydroxy-4-**m**ethylisoxazole-5-**p**ropionic **a**cid (AMPA) receptors, **ka**inate receptors (KA) and **N**-**m**ethyl-**D**-**a**spartate (NMDA) receptors (Hollmann and Heinemann (1994)). Unlike these three, a fourth family, for which no activating agonist has been identified, lead to their classification as 'delta receptors' and their inclusion in the iGluR family was based primarily on sequence similarity (Yamazaki et al. (1992)). A functional iGluR is a tetramer assembled from subunits within the same family, allowing for the formation of either homomers, which consist of identical subunits, or heteromers, composed of different subunits. In mammals, the AMPA receptor family is composed of four subunits (GluA1-A4), KA receptors by five subunits (GluK1-K5), NMDA receptors by seven subunits (GluN1, GluN2A-D, GluN3A-B) and delta receptors by two subunits (GluD1-2) (Wisden and Seeburg (1993)).

1.3.1 Evolution of iGluRs

The evolution iGluRs is believed to be marked by substantial adaptability and diversification of these receptors across different species. There are lineage-specific classes that are not present in vertebrates indicating a complex evolutionary history belied by the well-known AMPA, KA, NMDA and delta receptor groups. Recent studies have proposed a reorganization of iGluRs into groups, some of which were previously unrecognized. This reclassification acknowledges the existence of additional receptor types that have evolved distinct characteristics, potentially leading to novel receptor functions that have yet to be fully understood. Ramos-Vicente and colleagues (Ramos-Vicente et al. (2018)) proposed a new classification for iGluRs that better encapsulates their diversity across different animal lineages. This new classification introduces two

novel families, named Epsilon and Lambda, while retaining the NMDA receptors from the existing categorization and merging AMPA/KA/delta families with a new family termed Phi, into the broader AKDF family (Fig. 1.1). The researchers proposed that the foundational structure for these families (Epsilon, AKDF, Lambda and NMDA) was established in the last common ancestor of all animals, implying that the very first animals already possessed all four subfamilies. They suggest that the Epsilon family is the most ancient, found across most animal groups today, while Lambda is restricted to poriferans. The AKDF family is present in poriferans, placozoans, cnidarians and bilaterians while the most known AMPA, KA, delta are restricted to bilateral. This implies that when bilaterians diverged from other animals, the AKDF gene that they inherited from the last common ancestor of bilaterians and cnidarians went through several rounds of duplication and diverged quite early. Subsequently, when bilaterian animals diverged, most of the newer animal lineages inherited an AMPA receptor gene, a KA receptor gene and a delta receptor gene. NMDA receptors are found in cnidarians and bilaterians. (Ramos-Vicente et al. (2018)). Two possible models emerge based on the work of Ramos-Vicente and colleagues. The first model, the one proposed in the study (Ramos-Vicente et al. (2018)), suggests that the last common ancestor of all animals already possessed the families of ionotropic glutamate receptors—Epsilon, Lambda, AKDF, and NMDA—with some families being lost during evolution along different animals. An alternative model suggests a more incremental evolution of these receptor families. Initially, only a precursor of the Epsilon receptors existed in the last common ancestor of all animals. Subsequent gene duplications led to the emergence of the AKDF family in the ancestor of placozoans, cnidarians, and bilaterians, with the Lambda sub-family appearing exclusively in poriferans. Another gene duplication event is proposed to have given rise to the NMDA receptors in cnidarians and bilaterians (Fig. 1.1).

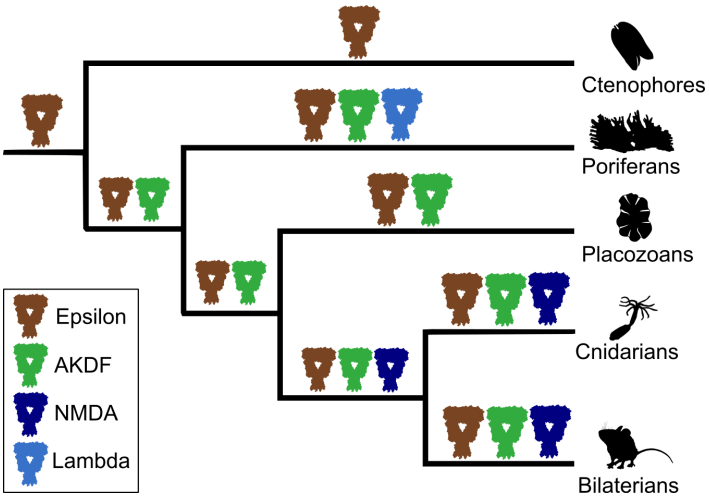

Figure 1.1: **Cartoon tree of model of possible evolution of iGluRs** Cartoon phylogenetic tree illustrating the evolutionary distribution of four iGluR families—Lambda, Epsilon, NMDA, and AKDF—across different animal lineages. Each iGluR family is represented by a distinct color: Epsilon (brown), AKDF (green), NMDA (dark blue) and Lambda (light blue). The model shown in this cartoon tree is the incremental evolution of iGluRs families as opposed to the one reported in Ramos-Vicente et al. (2018).

1.3.2 Topology and structure of iGluRs

The structure of each iGluR subunit consists of four distinct domains: an extracellular amino-terminal domain (NTD) and ligand binding domain (LBD), a trans membrane domain region (TMD) containing three membrane spanning α-helices (M1, M3, M4) and a re-entrant pore loop (M2), and the intracellular C-terminal domain (CTD) (Sobolevsky et al. (2009)). Two subunits first assemble into a dimer, and the receptor complex is the result of a dimer of dimers formation (Rossmann et al. (2011)). In mammalian iGluRs the ATD layer in one dimer is constituted by subunits A and B, while the second dimer is formed by subunits C and D (Fig. 1.2). A structural crossover occurs from the ATD to the LBD where the composition of the dimers shifts so that subunits A and D come together to form one dimer, and subunits B and C form the second dimer in the LBD layer (Fig. 1.2) (Sobolevsky et al. (2009)).

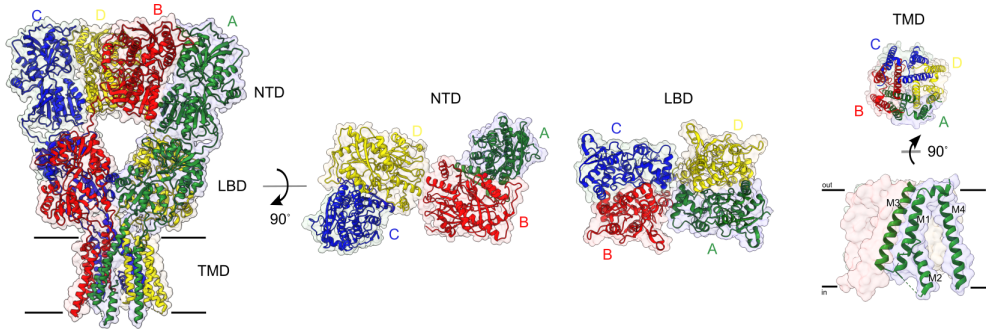

Figure 1.2: **X-ray structure of GluA2 and domain arrangements** Full length X-ray structure of GluA2 with four subunits labelled A-D. Each colour refers to one subunit (PDB:3kg2).

Recent findings shows that homomeric GluD1 receptors do not exhibit this swap of domains between NTD and LBD (Burada et al. (2020a)). Similarly, the low-resolution structure of the extracellular domain of GluD2 appears to maintain a non-domain swapped conformation as well (Burada et al. (2020b)). It seems that among mammalian iGluRs, delta receptors are unique in exhibiting this non-domain swapped architectural feature.

The NTD, including approximately 400-450 amino acids, assumes a semi-independent structural configuration. It has been observed that iGluRs lacking the NTDs can still function as ligand-gated ion channels (Pasternack et al. (2002)), yet the NTD contributes to modulating the kinetics of the ion channel and the formation of the receptor's tetrameric structure (Paoletti et al. (2000)). Moreover the NTD host several N-glycosylation sites that play an important role in modulating the process of receptor desensitization. It has been observed that interactions between these N-glycosylation sites and certain lectins, such as concanavalin A (ConA), can influence this process. Specifically, ConA has been shown to bind to these glycosylated sites (with a preference on KA over AMPA receptors), leading to the potentiation of receptor currents by reducing desensitization of the receptors. (Everts et al. (1997); Thalhammer et al. (2002)). Additionally, NMDA receptors possess a specific site in their NTD for binding zinc (Zn^{2+}) and allosteric modulators (Amico-Ruvio et al. (2011); Perin-Dureau et al. (2002)). The

ATD of GluD2 receptors has been shown to interact with the extracellular cerebellin1 (Cbln1) (Matsuda et al. (2010); Elegheert et al. (2016)), and similar interactions have been identified for GluD1 (Yasumura et al. (2012)).

The LBD is relatively small compared to the NTD (∼250 amino acids) and is structured around two non-continuous extracellular segments: S1 which is between NTD and M1 in primary structure and S2 which is between M3 and M4 (Fig. 1.3 A). These segments are organized into a clamshell-like configuration where the top lobe is called D1 and the lower lobe D2 (Fig. 1.3 B). The binding of an agonist to the space between these two sections leads to the clamshell closing, which in turn by pulling the LBD-TMD linker via structural rearrangements of the transmembrane α-helices initiates the ion channel's opening (Armstrong and Gouaux (2000)). In AMPARs, alternative splicing in the LBD leads to spliced versions of the receptor subunits, which result in different functional properties and are refered as *flip/flop* variants. The *flip* variant tends to show slower desensitization compared to the *flop* variant (Pei et al. (2009)). Glutamate is the endogenous ligand for the majority of subunits, while GluN1, GluN3A-B, and GluD1-2 are known to bind glycine and D-serine (Hansen et al. (2021)).

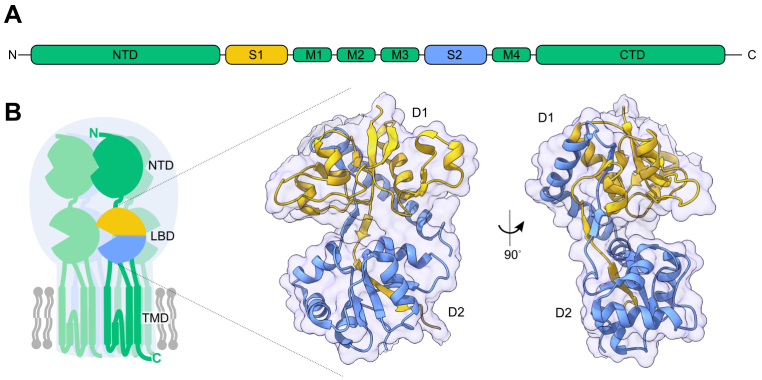

Figure 1.3: **Linear architecture and LBD structure of iGluR** (A) Primary structure of a single subunit of iGluR. (B) Left, cartoon representation of of the iGluR subunit domain arrangement. Right, X-ray structure of the LBD of GluA2 where S1 and S2 domains are colored accordingly to the linear architecture (PDB:3kg2).

The TMD forms the ion channel in iGluRs. The membrane α-helices M1, M3 and M4 span the lipid bilayer of the membrane due to a longer sequence of hydrophobic amino acids while the shorter pore loop M2 is only located in the inner lipid layer (Fig. 1.2). This structure resembles that of a K^+ channel (Kuner et al. (2003);Wood et al. (1995); Wo and Oswald (1995)) with the difference that the pore loop of a K^+ channel goes into the cell membrane from the extracellular side. This lead to the hypothesis that the iGluR channel might originally be an inverted variant of a K^+ channel (Zhorov and Tikhonov (2004)). M1 is located on the periphery of the channel cavity. The short M2 pore loop is where the ”Q/R editing” site is found and plays a crucial role in determining ion permeability. In AMPA/KA receptors mutating a conserved M2 glutamine (Q) to arginine (R) in the laboratory, or as occurs via RNA editing naturally in certain subunits, makes the receptors significantly less permeable to Ca^{2+} (Burnashev et al. (1996)). M3 α-helices are the most inner helices around the upper part of the pore and their movement away from the center allows for ions to flow through the pore in the gating process (Twomey et al. (2017)). This upper M3 segment is also home for the highly conserved SYTANLAAF motif that defines most iGluRs (Hansen et al. (2021)). A naturally occurring point mutation, which replaces the third alanine (A) from the motif to a threonine (T), results in a constitutively open channel in GluD2 receptors, also known as the lurcher mutant (Zuo et al. (1997)). Mutations in this region can also drastically influence the receptor’s desensitization and modify the effectiveness of partial agonists (Schmid et al. (2007); Taverna et al. (2000)). Placed furthest away from the ion cavity, M4 is crucial for the proper tetrameric assembly of subunits and their transport to the plasma membrane (Salussolia et al. (2011)).

The CTD sits entirely in the intracellular side of the cell and possess a intrinsically disordered structure (Choi et al. (2013)). It is integral to the interactions with intracellular proteins that participate in various functions such as second messenger signaling, receptor localization to specific cell regions and receptor stabilization at synapses (Hansen et al. (2021)). Furthermore, The CTD of iGluRs often includes specific sequences that are recognized by PDZ domain-

containing proteins. These PDZ domains, typically located in synaptic proteins, bind to the CTD and are integral to the assembly of signal transduction complexes. This PDZ binding modulates various aspects of iGluR function, including trafficking to the membrane, synaptic localization, and stabilization, as well as the regulation of receptor signaling properties (Tomita et al. (2001)).

1.3.3 Activation and desensitization

Since iGluRs are crucial in the rapid transmission of signals across excitatory synapses, their response time must be inherently fast (Baranovic and Plested (2016)). This necessity for speed is underscored by the dynamics of glutamate release into the synaptic cleft. Upon release from the presynaptic neuron, glutamate concentration swiftly reaches mM concentration for a very brief amount of time (<10 ms), as glutamate transporters promptly clear glutamate from the synapse (Moussawi et al. (2011)). Therefore, the binding of a ligand must be transferred as effectively as possible to the opening of the channel in order to allow fast communication. The initial step in glutamate receptor activation is the binding of glutamate to the LBD, leading to the closure of the binding pocket. Initially, the α-carboxyl group of glutamate interacts with an highly conserved arginine within the D1 domain and the D2 domain is drawn upwards towards the γ-carboxyl group of glutamate. This results in the clam-shell closing and the sealing of the ligand in the ligand binding site. Throughout this process, D1 is stabilized by its interaction with the D1 domain of an adjacent subunit within the dimer. Conversely, as the D2 domain moves up, it draws the connecting TMD linkers towards itself and away from the axis of the pore, transmitting this movement to the transmembrane α-helices leading to the opening of the ion channel pore (Armstrong and Gouaux (2000)). From structural and other biophysical studies of AMPARs, if the ligand remains bound the receptor undergoes a subsequent conformational shift, transitioning into a so-called desensitized state. This change involves the disengagement of D1 domain interactions at the receptor dimer interface, causing these domains to move apart. Consequently, the channel is still closed despite the ligand being still bound (Armstrong et al.

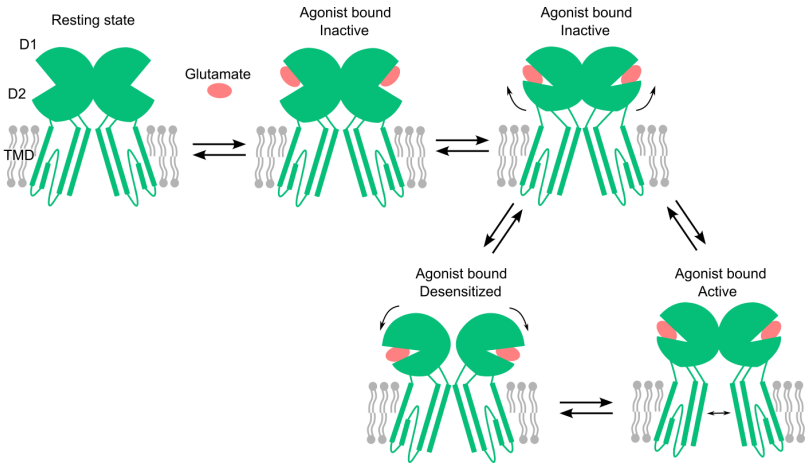

Figure 1.4: **Schematic representation of the conformational changes during activation and desensitization** Cartoon representation of one of the two dimers of the receptor complex. NTDs and CTDs are omitted for clarity. In the resting state the receptor is in a inactive state. The LBD is open, allowing glutamate to interact with the D1 domain, which in turns attracts the D2 domain. The conformational change is transferred via the linkers to the TMD, and the channel is in ac active state. With glutamate still bound, the D1 domains move away from each other, relaxing the linkers and desensitizing the receptor.

(2006)). Upon dissociation of the ligand, the receptor returns to its resting state and can be activated again (Fig. 1.4).

Different compounds or mutations that enhance the interactions between the D1 domains can prevent desensitization. Among these, the lectin Concanavalin A (ConA), which binds to the carbohydrate side chains of the receptors, was found to inhibit the desensitization of KA receptors (Mayer and Vyklicky Jr. (1989)). Specific mutations in the S1 region of AMPA receptors such as L483F have been found to significantly reduce or nearly eliminate desensitization (Stern-Bach et al. (1998)). Interestingly, mutations that affect desensitization are not exclusive to the LBD domain. In fact in homomeric GluA2 receptors, a mutation in the lurcher site (A643V) caused a gain-of-function receptor with substantially diminished desensitization compared to WT (Coombs et al. (2022)). This unreported missense mutation was identified in a patient that suffered from epilepsy seizures, underlining how a finely tuned balance between activation and desensitization states is required in a healty brain.

1.4 Mammalian delta iGluRs

AMPA, KA, and NMDA iGluRs were characterized pharmacologically based on the synthetic agonists they interact with, and biophysically, based on their kinetics and ion conduction (Watkins and Jane (2006)), and when the cDNAs were cloned, heterologously expressed receptors reflected this (Seeburg (1993)). In contrast after delta receptors were cloned and heterologously expressed, they were considered orphan receptors (Hollmann and Heinemann (1994); Zuo et al. (1997)), meaning a likely native agonist was yet to be identified, or their activity was not via typical transmitter ligands. This belief persisted for many years, because of their inability to create functional channels either independently or when combined with other iGluR subunits.

GluD2

The only way to pharmacology characterize delta receptors was via the lurcher mutant, a spontaneous genetic alteration that results in GluD2 ion channels that are constitutive active (Zuo et al. (1997)). This mutation is characterized by a single amino acid mutation in the highly conserved sequence SYTANLAAF motif at the end of M3 in the TMD, where a hydrophobic alanine is replaced by a hydrophilic threonine (A654T). Naur and colleagues showed that D-serine and glycine bind to the LBD of GluD2, leading to a reduction in the spontaneous currents through the GluD2-lurcher channels (Naur et al. (2007)). This indicates that ligand binding prompts a significant structural change that is able to transfer conformational changes to the TMD in order to decrease the constitutive flow of ion across the channel pore. Despite the GluD2-LBD X-ray structure revealing that D-serine induces a closure in the LBD similar to the activation seen in other iGluRs it is not enough to elicit currents at WT GluD2 (Naur et al. (2007)). An interesting aspect of the GluD2-lurcher receptor is the enhancement of constitutive currents in the presence of extracellular Ca^{2+} ions (Wollmuth et al. (2000)). This enhancement is due to two Ca^{2+} ions binding at the LBD dimer interface of GluD2 (Hansen et al. (2009)). Therefore, extracellular Ca^{2+} and D-serine exert opposing effects on the GluD2-lurcher receptors and the presence of Ca^{2+} ions can mitigate the inhibition effect of D-serine of constitutive currents (Hansen et al.

(2009)). It was theorized that D-serine binding at the LBD causes a destabilization of the dimer interface between the D1 domains, leading to a conformational shift akin to desensitization seen in other glutamate receptors. Conversely, Ca^{2+} binding fortifies the dimer interface of the D1 domains within a dimer, thereby maintaining GluD2-lurcher receptor in an open state. Interestingly, breakage of a naturally occurring disulfide bond between C756 and C811 in the D2 domain that has been suggested to limit the conformational changes of GluD2, switched D-serine effect from inhibition to potentiation in GluD2-lurcher. This effect was especially visible when the dimer interface is stabilized by covalent linkage (via P528C + L789C mutations) locking together two adjacent D1 domains. However, the corresponding mutations had no effect on WT GluD2.(Hansen et al. (2009)). By substituting the LBD of GluD2 with that of KA receptor GluK2, functional receptors were created that could respond to different ligands (Schmid et al. (2009)). Conversely, a reverse chimera, consisting of a GluK2 receptor where the LBD has been replaced with that of GluD2, makes receptors that do not respond to D-serine (Schmid et al. (2009)). This finding suggests that the inability of WT GluD2 to elicit ligand-gated currents, even if the ligand is able to bind and conformational changes are observed, is probably due to the characteristics of its LBD. An important step in understanding the gating proprieties of GluD2 came recently. It was known for some time that delta receptors plays a crucial role in the formation and stabilization of synapses (Matsuda et al. (2010); Fossati et al. (2019)). GluD2 receptors, for example, interact with cerebellin-1 (Cbln1), a soluble protein released by granule cells. Cbln1 forms a trimer that can connect via a disulfide bond with another trimer, creating a hexamer structure capable of dimerizing through its cysteine-rich region with the extracellular domain of the presynaptic protein neurexin (Matsuda et al. (2010)). The neurexin-Cbln-1 complex is able to bind the NTD of GluD2 in the postsynaptic membrane thereby creating a stabilizing bridge for the parallel fibers-Purkinje cells (PF-PC) synapses (Elegheert et al. (2016)). This interaction seems to be not purely structural. Glycine and D-serine are capable of activating GluD2 receptors in HEK-293T cell clusters with the neurexin-Cbln-1 complex and in synaptically connected cultured cerebellar neurons (Carrillo et al. (2021)). This activation process

involves a gating mechanism that necessitates the binding of the NTD to presynaptic scaffold proteins, or in the absence of that, through the formation of cysteine cross-links in the NTD, restricting its movement an in turn creating a more compact NTD layer between the two dimers (Carrillo et al. (2021)).

GluD1

Whether the lurcher mutation in GluD1 also leads to the formation of constitutively open channels remained unclear for some time, as it was reported that the same A654T mutation in GluD1 does not produce constitutively open channels (Williams et al. (2003)). Nonetheless, an alanine scanning study of the M3 α-helix demonstrated that GluD1 is in principle capable of forming homomeric receptor complexes. Mutations such as A650C, L652A, A654C, and F655A near the lurcher site led to the formation of constitutively open channels (Yadav et al. (2011)) very much like GluD2-lurcher. Analogous to GluD2-lurcher constitutive currents of GluD1-F655A could be potentiated by extracellular Ca^{2+} ions, suggesting that the same mechanism of dimer stabilization of GluD2 by Ca^{2+} is also at play in GluD1. Only recently, near the end of my PhD studies, it was demonstrated that in human GluD1 receptors, where C645I and A654T mutations were introduced in order to generate consitutive activity, D-serine and the classical inhibitory transmitter GABA enhanced the constitutive currents of the receptor (Piot et al. (2023)). Moreover, structural data of the isolated LBD in complex with GABA/D-serine revealed that the molecular determinant of GABA-binding in GluD1 is E446, located in D1. In the X-ray structure from that study, the carboxylate side chain of E446 interacts with the γ-amino group of GABA. This interaction is absent in the case of D-serine-bound GluD1. In fact, replacing the negatively charged E446, with polar uncharged amino acids serine and glutamine, or the shorter carboxylate amino acid aspartate eliminated the enhancement of constitutive currents by GABA on GluD1-C645I-A654T. The same mutation did not affect D-serine enhancement (Piot et al. (2023)). Interestingly, GluD2-lurcher seemed to be unresponsive to GABA and no modulation was observed even though E446 in conserved in both GluD1 and GluD2 receptors

(Piot et al. (2023)). This implies that additional factors within GluD1 play a role in conferring GABA selectivity among mammalian delta receptors and E446 is not the sole determinant of this sensitivity.

Non-ionotropic functions of delta iGluRs

GluD1 is prominently expressed in the neocortex, hippocampus, striatum, and cerebellum. Its expression is particularly enhanced during synaptogenesis and maintained at high levels during adulthood, indicative of a crucial role in the development and maintenance of synaptic connections (Hepp et al. (2015)). GluD1 was shown to be involved in the formation of excitatory synapses in the cerebellum through its expression at parallel fiber synapses on molecular layer interneurons (Konno et al. (2014)). Recently it was found to be involved in the regulation of inhibitory synapses in cortical pyramidal neurons (Fossati et al. (2019)). Co-expression of GluD1 with metabotropic receptor mGlu1 in HEK cells resulted in a slow depolarizing current mediated by GluD1 that was elicited by 3,5-dihydroxyphenylglycine (DHPG), an agonist for mGlu1 (Benamer et al. (2018)). Similar activity was observed in dopamine neurons where both receptors are expressed. In midbrain slices, the mGlu1 agonist-evoked slow postsynaptic currents were absent in the dead-pore mutant GluD1-V617R, suggesting the participation of native GluD1 channels in these currents. Furthermore, these mGlu1-dependent currents were suppressed in GRID1 knockout mice, which display schizophrenia-relevant endophenotypes (Benamer et al. (2018)). GluD1 receptors were shown to carry a tonic inward current that is critical for setting the baseline excitability of dorsal raphe neurons. This tonic activity is enhanced by the activation of α-1-adrenergic receptors triggered by noradrenaline, which further amplifies the inward current and supports continuous, pacemaker-like firing of these neurons (Gantz et al. (2020)). Interestingly, GluD1 act as a postsynaptic organizer for inhibitory synapses, required for their formation and the regulation of GABAergic synaptic transmission. GluD1 interacts with cerebellin-4, a scaffolding protein secreted by somatostatin-expressing interneurons, which bridges GluD1 with presynaptic neurexins. This interaction enables GluD1 to elicit non-ionotropic postsynap-

tic signaling through the activation of the guanine nucleotide exchange factor ARHGEF12 and the regulatory subunit of protein phosphatase 1 PPP1R12A, but only when GluD1 binds to its agonists glycine or D-serine (Fossati et al. (2019)). These challenge the traditional view of ionotropic glutamate receptors as solely ionotropic receptors and places GluD1 at the center of promoting synaptic organization, both excitatory and inhibitory.

Contrarily to the more widespread expression of GluD1 in the CNS, GluD2 expression is more restricted to Purkinje cells in the cerebellum, specifically limited to PF-PC synapses during development and in its mature state (Zhao et al. (1998); Araki et al. (1993)). It plays a crucial role in modulating long-term depression (LTD) by binding D-serine secreted by Bergmann glia and prompting the internalization of AMPA receptors in the developing brain (Kakegawa et al. (2011)). Absence of the receptor in the synapses and mutations at the D-serine binding site can significantly diminish LTD. This suggests that D-serine may initiate a structural change within the receptor, activating downstream intracellular signaling pathways dependent on the CTD of GluD2 (Kakegawa et al. (2011)). Similarly to GluD1, it has been discovered that GluD2 gating can be activated by mGlu1 receptors (Ady et al. (2014)). In HEK cells this process requires a functional GluD2 ion channel and DHPG-induced mGlu1 stimulation relies on protein canonical signaling pathway, specifically phospholipase C (PLC) and protein kinase C (PKC). These findings were corroborated ex-vivo in experiments at the cerebellar PF-PC synapse (Dadak et al. (2017)).

The biophysical properties and the physiological roles of mammalian delta receptors are therefore clearly multifaceted. Despite the absence of observable ligand-gated activity in isolated WT delta receptors, compelling evidence suggests that these receptors are indeed capable of binding agonists, with subsequent conformational changes induced upon ligand binding. This is exemplified by studies on lurcher mutants and further supported by experiments involving chimeras and targeted mutagenesis, which have collectively hinted at a capability for ligand-gated currents in delta receptors. Furthermore, delta receptors share a common evolutionary

history with other ligand-gated glutamate receptors, such as AMPA and KA receptors. This shared lineage prompts intriguing questions about the molecular changes that led to the loss of typical ligand-gated channel activity that have defined the current receptor function in the nervous system. The central question remains: do delta receptors mediate their physiological effects exclusively through interactions with other proteins, or can they be directly activated by specific agonists? And how did mammalian receptors evolve to lose their ligand-gated activity, transitioning instead to mediate their effects through protein-protein interactions and through intracellular signaling pathways? This thesis aims to delve into the evolution of delta receptors and examine their variations across different animal species. Such an investigation could shed light on their functional diversity and evolutionary significance, potentially unveiling novel aspects of their mechanism of action.

Chapter 2

Aims

Since little is known on (1) the molecular determinants of the divergent function in delta iGluR receptors and (2) if/how they are readily activated by endogenous and pharmacological modulators the aims, of my PhD project are:

1. To establish a clear functional and evolutionary picture of the delta family, using molecular phylogenetics, heterologous expression of diverse delta iGluRs, and electrophysiology.
2. To dissect the amino acid substitutions that gave rise to the unique function of mammalian delta iGluRs with site directed mutagenesis and electrophysiology.

Chapter 3

Methods

3.1 Sequence assembly and phylogenetic analysis

To conduct the phylogenetic analysis and investigate the presence of putative delta iGluR genes throughout the metazoans, iGluR amino acid sequences were sought from four chordates (*Rattus norvegicus*, *Danio rerio*, *Branchiostoma belcheri*, and *Ciona intestinalis*), two hemichordates (*Ptychodera flava* and *Saccoglossus kowalevskii*), two echinoderms (*Acanthaster planci* and *Anneissia japonica*), one ecdysozoan (*Strigamia maritima*), two spiralians (*Crassostrea gigas* and *Schmidtea mediterranea*), two xenoturbellids (*Xenoturbella profunda* and *Xenoturbella bocki*), two acoels (*Diopisthoporus longitubus* and *Hofstenia miamia*), two nemertodermatids (*Meara stichopi* and *Nemertoderma westbladi*), two cnidarians (*Hydra vulgaris* and *Nematostella vectensis*), one placozoan (*Trichoplax sp* H2), one poriferan (*Oscarella carmela*), and two ctenophores (*Euplokamis dunlapae* and *Pleurobrachia bachei*).

Rat sequences were retrieved from UniProt. Other sequences were retrieved via BlastP (Altschul et al. (1997)) search with *Rattus norvegicus* GluD2 (NCBI XP_038964327.1) as query in KEGG Genome Database, https://www.genome.jp/kegg/genome/ (*Nematostella vectensis*); Compagen Japan, http://compagen.unit.oist.jp/ (*Osarella carmela* OCAR_T-CDS_130911 dataset); OIST Marine Genomics Unit, https://marinegenomics. oist.jp/acornworm/viewer/info?project_id=33; a published dataset for xenacoelamorphs (Andrikou et al. (2019)) ; and NCBI (Johnson et al.

(2008)) (all other species). I included an additional two plant sequences from *Arabidopsis thaliana* (NCBI) as an outgroup. The sequences were aligned using MAFFT (Katoh et al. (2002)) v7.450 in Geneious Prime (Geneious) and sequences that were > 95% identical to another or that were excessively long or incomplete were removed. The resulting alignment contained 246 sequences with 4692 amino acids position (including gaps). From this alignment I generated a maximum-likelihood phylogenetic tree with IQ-Tree (Minh et al. (2020)) using the ModelFinder option that automatically determines the best-fit model for the alignment. Q.pfam+G4 substitution model (Minh et al. (2021), El-Gebali et al. (2019)) was found to be the best model that fitted my model (log-likelihood of model – 410679). Branch support was estimated with SH-aLRT method (Guindon et al. (2010)) and ultrafast bootstrap (Hoang et al. (2018)).

3.2 Nucleotide synthesis and mutagenesis kits

Sequences selected for complementary DNA (cDNA) synthesis, cRNA transcription and expression were *Rattus norvegicus* delta 2 NM_024379.2 and delta 1 NM_024378.3, *Danio rerio* AAI62459.1, *Acanthaster planci* XP_022085687.1, *Saccoglossus kowalevskii* XP_002732006.1, *Diopisthoporus longitubus* c29957_g1_i2 and *Meara stichopi* 16765.1 from transcriptome in Andrikou et al. (2019), *Crassostrea gigantea* XP_011428248.2. The sequences were selected based on their position in the putative delta iGluR family and to cover a broad diversity of animal lineages. In an effort to improve their expression *Crassostrea gigantea* XP_011428248.2 and *Danio rerio* AAI62459.1 sequences were codon-optimized for *Xenopus laevis* in iCodon (Diez et al. (2022)) after I learnt of this tool. cDNA for all sequences was commercially synthesized and subcloned (Genscript) between SalI and BamHI sites in a pSP64 (polyA) vector (Promega) preceded by a loosely Kozak consensus sequence, flanked by *Xenopus laevis* β-globin 5' and 3' untranslated and containing a C-terminal cMyc tag (for the exception of *Saccoglossus kowalevskii* XP_002732006.1) (Appendix A). *Rattus norvegicus* GluA2 (flip isoform) in the pRK5 vector was a gift from David MacLean (University of Rochester Medical

Center), and human TARPγ2 (CACNG2) in the pcDNA3.1(+) vector was a gift from Stephan Pless (University of Copenhagen).

Site-directed mutagenesis for single- and double-mutant cDNA was designed with partly overlapping mutant primers (Xia et al. (2015)) that I designed and ordered (Merck). Mutant plasmids were generated with with Phusion Hotstart II High Fidelity polymerase (Fisher Scientific) following supplier's protocol. Chimeras were generated by combining fragments cloned with custom primers using and according to the GenBuilder Cloning Kit (Genscript) (Fig. 3.1). All WT and mutant sequences were confirmed by Sanger sequencing (Genewiz) (Fig. 3.2). Prior to cRNA transcription cDNAs were linearized with EcoRI site just after the poly(A) sequence for constructs in the modified pSP64 vector via HindIII for *Rattus norvegicus* GluA2. cRNA was transcribed with mMESSAGE mMACHINE SP6 Transcription Kit (Thermo Fisher Scientific) utilizing the upstream SP6 site.

Figure 3.1: **Primers design for two chimera constructs** Primer design for (A) *Aca*GluD$^{\text{RatNTD}}$ and (B) *Aca*GluD$^{\text{RatNTDlink}}$ chimera constructs. Annotations in red refers to primer design. Annotations in yellow refers to the linker sequence of *Aca*GluD (A) and *Rat*GluD2 (B). Sequences visualized in in Geneious Prime (Geneious).

Primers name	Sequence	T_m(°C)	PCR protocol
*Aca*GluD_S713A_for	TAACAGC**GC**CCTGCATGACTTCTTC	68.9	98°C - 30 s 98°C - 10 s 69°C - 30 s 25 x 72°C - 3 min 72°C - 10 min
*Aca*GluD_S713A_rev	ATGCAGG**GC**GCTGTTAAGGATGGTG	72	

Sanger sequencing results

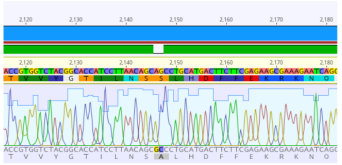

Primers name	Sequence	T_m(°C)	PCR protocol
*Rat*GluD2_A654T_for	CAAATCTTGCC**ACG**TTCCTCACTATCACCC	71.4	98°C - 30 s 98°C - 10 s 70°C - 30 s 30 x 72°C - 45 s 72°C - 5 min
*Rat*GluD2_A654T_rev	GAGGAA**CGT**GGCAAGATTTGCTGTATAAGATG	70	

Sanger sequencing results

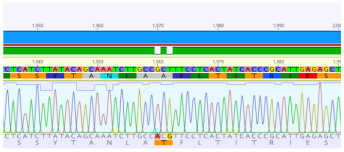

Figure 3.2: **Example of primers design for two mutant constructs** Primer design for mutants *Aca*GluD S713A (top) and *Rat*GluD2 A654T (bottom). From left to right. Names of the designed primers for mutagenesis and related sequence and calculated melting temperature (in bold nucleotides that differs from template sequence). PCR protocol used for generating the according mutant. Sequencing results visualized in in Geneious Prime (Geneious).

3.3 Heterologous expression in *Xenopus laevis* oocytes, electrophysiology and data analysis

Collagenase-treated *Xenopus leavis* stage V/VI oocytes were commercially acquired (EcoCyte Bioscience) kept in 50% (in water) Leibovitz's L-15 medium (Gibco) supplemented with additional 0.25 mg/mL gentamicin, 1 mM L-glutamine, and 15 mM HEPES, pH 7.6 at 18 °C. Occytes were injected (Nanoliter 2010, World Precision Instruments) with 20 ng cRNA (WT, mutants and chimera constructs. For *Rat*GluA2 experiments: 10 ng GluA2 cRNA + 1 ng TARPγ2 cRNA). Two-electrode voltage clamp experiments were performed three to four days after injection, during this time unhealthy oocytes were removed regularly and remaining cells were moved to fresh dishes and new media.

1 M stocks of glycine, GABA, D-serine, monosodium glutamate and 0.1 M stocks of CGP-78608 and 5,7-dichlorokynurenic acid (DCKA) were prepared in Ca_{2+} and $MgCl_2$-free bath solution (see below) and stored at -20. Stocks of 0.1 M pentamidine, 6-cyano-7-nitroquinoxaline-

2,3-dione (CNQX), 6,7-dinitroquinoxaline-2,3-dione (DNQX) and 2,3-dioxo-6-nitro-7-sulfamoyl-benzo[f]quinoxaline (NBQX) were prepared in water.

In experiments, oocytes were continuously perfused with a bath solution containing (in mM) 96 NaCl, 2 KCl, 1.8 $CaCl_2$, 1 $MgCl_2$, and 5 HEPES, pH 7.6 with NaOH based on delta iGluR experiments performed elsewhere (Naur et al. (2007)), in a plastic recording chamber (RC-3Z, Warner Instruments). For zero-Ca^{2+} experiments, $CaCl_2$ and $MgCl_2$ were replaced with 2 mM $BaCl_2$. Oocytes were impaled with Borosilicate micropipettes containing KCl (3 M) and voltage clamped at –80 mV with an OC-725D amplifier (Warner Instruments) controlled via an Axon Digitata interface and pClamp v11 (Molecular Devices). Current was sampled at 1000 Hz and filtered at 200 Hz. Drugs dissolved in bath solution were applied via an eight-channel, gravity-driven perfusion system (VCS-8-pinch, Warner Instruments). In most experiments, ligands were applied for 10 seconds, and oocytes were washed with bath solution for 30 s before another application. In the case of ligand-gated currents, oocytes were washed for 30 s before another ligand application. Horizontal bars above currents in figures indicate application of ligands. Current recordings were additionally filtered (50 Hz, Bessel 8-pole) and measured in Clampfit (Molecular Devices). Data were plotted in Prism v9 (GraphPad). For simple plots, all data points are shown. For concentration–response experiments peak current amplitude was plot against drug concentrations and fitted with the Hill equation. EC_{50} values for each individual oocyte were calculated by variable slope nonlinear regression in Prism v9 and used to calculate the means reported in text. In figures, the mean ± SEM data points are shown, along with a curve fit to these mean data points, for display.

3.4 Immunolabeling of *Xenopus laevis* injected oocytes

To check the expression of *C. gigantea* XP_011428248.2, *A. planci* XP_022085687.1 WT and F640Y, S713A, R721K, P741N, D825P mutants, cRNA-injected oocytes were washed twice with phosphate-buffered saline (PBS) and fixed with 4% paraformaldehyde in PBS overnight at 4 °C. Fixed oocytes were embedded in 3% low-gelling point agarose and sliced with a vibratome

(Leica) in 100-µm sections. Slices were washed with PBS containing 0.2% bovine serum albumin (BSA) and 0.1% Tween 20 for 3 h at room temperature. Slices were then incubated with mouse anti-Myc tag monoclonal IgG1 antibody (Myc.A7, Invitrogen MA121316, Fisher Scientific) 1:500 in blocking buffer (PBS containing 1% BSA and 0.1% Tween-20) overnight at 4 °C. Subsequently they were washed three times with PBS, incubated with goat anti-mouse polyclonal IgG (H+L) Alexa Fluor 568 conjugate (Invitrogen A11004, Thermofisher) 1:1000 in blocking buffer for 1 h at room temperature, and washed three times with PBS. Slices were mounted on a glass slide in 50% glycerol, and raw images were acquired on an Olympus FLUOVIEW FV3000 confocal laser scanning microscope with standard PMT detectors, 20× air and 30× and 40× silicon oil immersion lenses. Raw images were visualized and processed with Fiji software (Schindelin et al. (2012)).

3.5 Structural model of *Aca*GluD ligand binding domain

The structural model for the *Aca*GluD ligand binding domain (LBD) was generated using the AlphaFold2 algorithm through Colab-Fold v2 (Jumper et al. (2021), Mirdita et al. (2022)).

3.6 Homology model of *Aca*GluD

To illustrate the position of the 41 mutations in *Aca*GluD I generated an homology model of the full-length receptor by uploading the sequence to SWISS-MODEL server (Waterhouse et al. (2018)). The template used for building the model was that of GluA2 X-ray structure (PDB: 3KG2). The .pdb file generated is visualized in Fig. 6.5 A using ChimeraX 1.4 software (Meng et al. (2023)).

3.7 Computational Ligand Docking

Dockings were conducted using AutoDock 4.2 (Morris et al. (2009)). The structure file (.pdb) generated by AlphaFold2 was used for the docking experiments of *Aca*GluD, while *Rat*GluD2 was docked using the PDB structure file (PDB: 2V3U) (Naur et al. (2007)) after removing unnecessary molecules such as water and D-serine from the X-ray structure. Both GABA and D-serine molecules used as ligands were retrieved from https://pubchem.ncbi.nlm.nih.gov/ (Compound CID: 119 and 71077 respectively). Employing a blind docking approach, 100 experiments were carried out for each ligand, with a maximum of 25 million energy evaluations per experiment using the Lamarckian genetic algorithm and default parameters from AutoDock4.2. The resulting configurations were clustered into ligand binding modes with <2.0 Å rmsd from each other. Clusters of energetically favorable configurations typically included over 10 similar binding modes. Fig. 5.5 shows the first five most energetically favorable binding poses from the first, most energetically favorable, cluster and images of the ligand-receptor complex were generated using ChimeraX 1.4 (Meng et al. (2023)).

3.8 N-Linked Glycosylation Site Prediction

To identify the number of potential N-linked glycosylation sites in *Aca*GluD, *Rat*GluD2, and *Rat*GluD1 I used the NetNGlyc 1.0 web service tool (Gupta and Brunak (2002)) using the amino acid sequences as input. The parameters used for the NetNGlyc 1.0 analysis were kept at default settings.

Chapter 4

Results I - Exploring the broader delta iGluR family

In exploring the functional diversity within the broader delta iGluR family, especially if and how mammalian receptors differ from those of distantly related species, it was crucial to first establish a clear phylogenetic framework. This framework not only delineates the evolutionary breadth of the family, e.g. which types of animals have delta iGluRs, but it also sets the stage for subsequent functional analyses, e.g. which receptors should be tested to best assess the functional signature of the family.

4.1 Phylogenetic analysis of the glutamate receptor genes

The phylogenetic analysis was designed to cover a broad spectrum of species, thus providing a comprehensive view of the delta iGluR family. To do that, representative species were selected from diverse animal lineages. This selection included species from major bilaterian groups such as deuterostomes, protostomes, and xenacoelomorphs and non-bilaterian groups like cnidarians, placozoans, poriferans and ctenophores (two plant iGluR genes from *Arabidopsis thaliana* were also included and used as an outgroup for the phylogenetic tree).

All iGluR genes were retrieved using the Basic Local Alignment Search Tool (BLAST) (Meth-

ods, page 21) and a total of 246 non-redundant sequences were obtained and utilized to construct a maximum likelihood tree (Fig. 4.1).

Figure 4.1: **Animal iGluR phylogeny** (A) Maximum likelihood phylogeny (IQ-Tree Minh et al. (2020), Q.pfam+G4 calculated substitution model). Branch support values, SH-aLRT and ultrafast bootstrap (/100). Values near tips are omitted for clarity. Colors for selected iGluR families. (B) Animal lineages and species used for iGluR search.

Previously characterized mammalian GluD1 and GluD2 genes are found in a well-supported

branch including genes from numerous other bilaterians, and I delineate this branch as the delta family (dark green in Fig. 4.1). Here, the closest relatives of the delta family are identified as the AMPA and KA family (dark pink and light pink respectively in Fig. 4.1) and these 3 families, together with other uncharacterized paraphyletic relatives genes have been proposed to form the larger AMPA/KA/delta/phi (AKDF) branch (Ramos-Vicente et al. (2018); Stroebel and Paoletti (2021)) that is exclusive to bilaterian animals. In alignment with previous findings (Ramos-Vicente et al. (2018)) my analysis reaffirms that delta iGluR genes are exclusive to bilaterians but their presence seems to be not constant among all bileterian animals. In fact genes belonging to the putative delta family includes sequences from xenacoelomorphs: a group of simple, soft-bodied marine animals that represent a unique and relatively recently recognized phylum (Hejnol and Pang (2016); Cannon et al. (2016) (with sequences from nemertodermatids *Nemertoderma westbladi* and *Meara stichopi*, acoels *Hofstenia miamia* and *Diopisthoporus longitubus*, xenoturbellids *Xenoturbella profunda* and *X. bocki*); deuterostomes such as vertebrate chordates (*Rattus norvegicus* and *Danio rerio*), non-vertebrate chordates (*Ciona intestinalis* and *Branchiostoma belcheri*), hemichordates (acorn worms *Saccoglossus kowalevskii* and *Ptychodera flava*) and echinoderms (e.g. starfish sequences from *Anneissia japonica* and *Acanthaster planci*). In contrast, the delta family seems to be not well represented in protostomes as I was able to find only one sequence from *Crassostrea gigas* that appear as the earliest branching gene within the delta family (Fig.4.1 - 4.2). The findings of my phylogenetic analysis suggest that delta genes emerged when an ancient AKDF gene diversified into ancient delta and AMPA/KA genes probably after cnidarians diverged from bilaterians. This is because I can't identify AMPA/KA or delta genes in cnidarians and I can only find cnidarian sequences in other AKDF branches, along with other bilaterian other AKDF genes. The fact that I could identify delta sequences in xenacoelomorphs, which have been proposed to be the sister group to deutorostomes and protostomes (Cannon et al. (2016)), in various deuterostomes, and in one protostome suggests the fact that the earliest delta gene was probably present when the first bilaterian animal emerged.

4.2 Functional characterization of the delta receptors family

Our current understanding of the delta iGluR family's biophysical function is predominantly based on studies of inactive wildtype (WT) and the constitutively active and D-serine-inhibited 'lurcher'mutant mammalian delta iGluRs (Zuo et al. (1997)). As mammalian channels are a small part of the delta iGluR family (Fig. 4.2), the functional characteristics of the delta family are actually poorly understood. In an effort to fill this gap, I have selected putative delta iGluR genes that (1) came from diverse bilaterian lineages and (2) come from various parts of the delta branch; I then made cRNA, injected it into *Xenopus laevis* oocytes and used two-electrode voltage clamp to test for responses to the application of different neurotransmitters (e.g. glutamate, D-serine, glycine and GABA). The putative GluD genes I chose were two xenacoelomorphs: *Diopisthoporus longitubus* ("*Dio*GluD") and *Meara stichopi* ("*Mea*GluD"), two ambulacrarian deuterostomes *Acanthaster planci* ("*Aca*GluD") and *Saccoglossus kowalevskii* ("*Sac*GluD"), a protostome deuterostome *Crassostrea gigas* ("*Cra*GluD") and vertebrate deuterostomes *Danio rerio* ("*Dan*GluD2A") together with previously characterized genes from *Rattus norvegicus* GluD1 ("*Rat*GluD1") and GluD2 ("*Rat*GluD2") (Fig. 4.2).

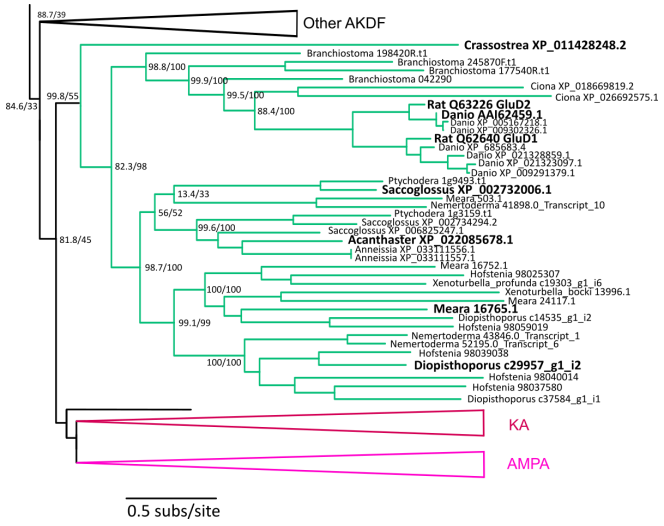

Figure 4.2: **Phylogenetic analysis of the delta iGluR family** Delta iGluR branch from broader iGluR phylogeny. SH-aLRT and ultrafast bootstrap (/100) are shown; Bold, genes tested in this thesis.

Vertebrate deuterostome delta iGluRs

As expected, *Rat*GluD1 and *Rat*GluD2 showed no response to any of the four ligands tested. The same lack of response was observed when I tested the same ligands on a previously uncharacterized vertebrate chordate *Dan*GluD2A (n = 6) (Fig. 4.3 A). All three WT vertebrate delta iGluRs thus showed the same inactivity when tested, and I next determined if lurcher-mutant versions were also similar. I therefore generated A654T *Rat*GluD2 and A654T *Dan*GluD2A (*Rat*GluD2^{Lc} and *Dan*GluD2A^{Lc}), as this *Rat*GluD2 lurcher mutant was previously shown to mediate measurable constitutive current that is inhibited by glycine and D-serine (Naur et al. (2007)). I generated A654C *Rat*GluD1 ("*Rat*GluD1^{AC}") as this mutant showed greater constitutive activity than the A-T mutant (Yadav et al. (2011)). *Rat*GluD2^{Lc} constitutive current was reduced upon application of D-serine (IC_{50} = 2 ± 0.2 mM, n = 4) and glycine (IC_{50} > 3 mM, n = 4), while it was insensitive to glutamate and only 30 mM GABA had relatively small activity (Fig. 4.3 B). In contrast to *Rat*GluD2^{Lc}, other vertebrates receptors *Dan*GluD2A^{Lc} and *Rat*GluD1^{AC} demonstrated additional sensitivity to GABA. Specifically, GABA induced inactivation of 58 ± 8% (n = 4) for *Dan*GluD2A^{Lc} receptors and 86 ± 5% (n = 10) for *Rat*GluD1^{AC}, compared to the inactivation caused by D-serine (Fig. 4.3 C-D). Thus, while WT vertebrate delta iGluRs are inactive, this suggests that some of these receptors have the capability to bind GABA, the classical inhibitory neurotransmitter. This results also support recent discoveries concerning the binding of GABA to vertebrate GluD1 receptors (Piot et al. (2023)). Although Piot and colleagues have used different mutations in GluD1 to observe a potentiation of constitutive current by GABA (they used a double-mutant A654T-C645I whereas I used A654C) our results align nicely with the emerging paradigm where GABA, traditionally recognized for its inhibitory neurotransmitter role, also affects vertebrate delta receptors indicating a potentially broader spectrum of physiological implications than previously understood. Notably, unlike the predominantly inactive WT delta iGluRs found in vertebrate deuterostomes, the WT delta iGluRs in other bilaterians exhibit a distinctly active profile.

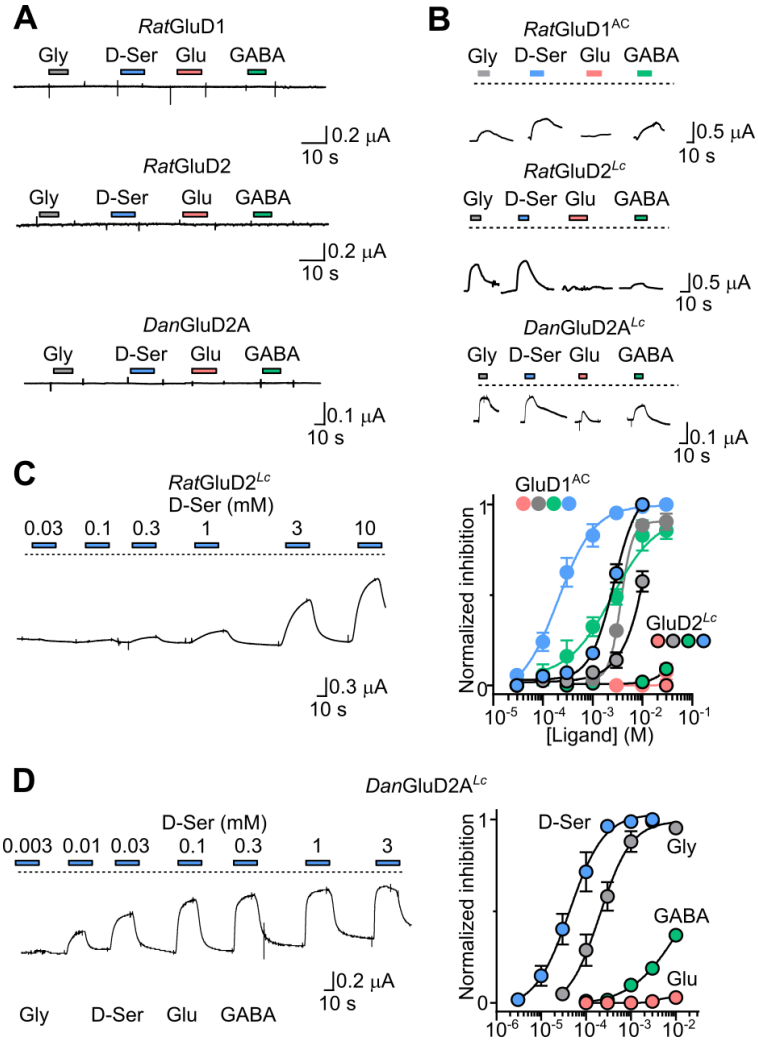

Figure 4.3: **Experimental characterization of vertebrate delta iGluRs** (A) Example recordings at *Xenopus* oocytes expressing indicated WT genes. (B) Example recordings at *Xenopus* oocytes expressing lurcher mutation of indicated genes. The dashed line indicates zero current. (C) Left, Example recordings at *Xenopus* oocytes expressing *Rat*GluD2^{Lc} to increasing concentrations of D-serine. Right, mean normalized (±SEM, n = 4) responses reflect ligand-induced inhibition of constitutive current to maximum inhibition of constitutive current in *Rat*GluD1^{AC} and *Rat*GluD2^{Lc}. (D) Left, Example recordings at *Xenopus* oocytes expressing *Dan*GluD2A^{Lc} to increasing concentrations of D-serine. Right, mean normalized (±SEM, n = 4) responses reflect ligand-induced inhibition of constitutive current to maximum inhibition of constitutive current.

Ambulacrarian deuterostome delta iGluRs

*Aca*GluD, from the crown-of-thorns-starfish *Acanthaster planci* an ambulacrarian deuterostome, showed significant large inward ligand-gated current activity when I tested GABA and glutamate in oocytes expressing *Aca*GluD receptors (I_{max} = 8.2 ± 1.2 µA (n = 4); I_{max} = 1.9 ± 0.4 µA (n = 9) respectively). Glycine and D-serine on the other hand had smaller but detectable currents (I_{max} = 0.19 ± 0.02 µA (n = 9); I_{max} = 0.75 ± 0.10 µA (n = 9) respectively) (Fig. 4.4 A). GABA, in fact was the most potent agonist with EC_{50} = 13 ± 3 µM (n = 5) compared to glutamate EC_{50} = 7.8 ± 0.2 mM (n = 3) and glycine EC_{50} = 2.0 ± 0.1 mM (n = 4) (Fig. 4.4 B).

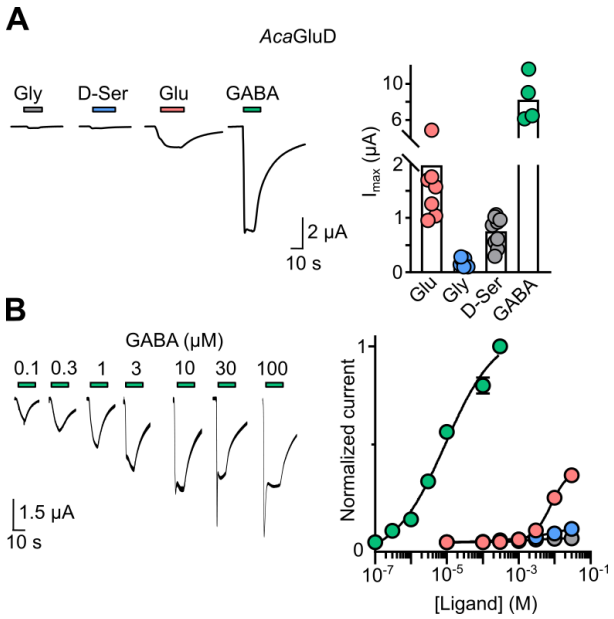

Figure 4.4: **Functional characterization of *Aca*GluD** (A) Left, TEVC recordings of responses to different ligands in oocytes injected with *Aca*GluD. Right, I_{max} at different oocytes (dots) and resulting means (columns). (B) Left, Representative recording to increasing concentrations of GABA in oocytes injected with *Aca*GluD, and (right) mean ± SEM current responses (normalized to GABA-gated current amplitude) to increasing ligand concentrations in oocytes injected with *Aca*GluD.

Another ambulacrarian putative delta iGluR gene that I tested was from acorn worm *Saccoglossus kowalevskii*, *Sac*GluD, but measuring ligand potency proved to be more challenging

compared to *Aca*GluD due to the small currents recorded and expression variability between different batches of oocytes (Fig. 4.5 A). To try and overcome this obstacle I engineered the equivalent of the lurcher mutation in *Sac*GluD, A621T, (*Sac*GluD^{Lc}) hoping that this mutation would reveal the ligand sensitivity somewhat hidden in the WT form. *Sac*GluD^{Lc} exhibit greater constitutive current than WT (279 ± 79 nA, n = 20 and 96 ± 29 nA, n = 20 respectively) (Fig. 4.5 C) but these constitutive currents paled in comparison to ligand-gated currents in the mutant receptor. The most striking difference between WT and lurcher-mutant was the robust inward GABA/glutamate-gated currents observed in the latter, while no currents were recorded when I applied glycine or D-serine (Fig. 4.5 B). As in *Aca*GluD, GABA was the most potent agonist (EC_{50} = 84 ± 14 μM, n = 4) when compared to glutamate (EC_{50} = 0.64 ± 0.16 mM, n = 3). The functional analysis of two ambulacrarian delta iGluRs from distinct species—a starfish (*Aca*GluD) and an acorn worm (*Sac*GluD)—provides compelling evidence of their ligand-gated nature, with a pronounced preference for GABA over glutamate, D-serine and glycine.

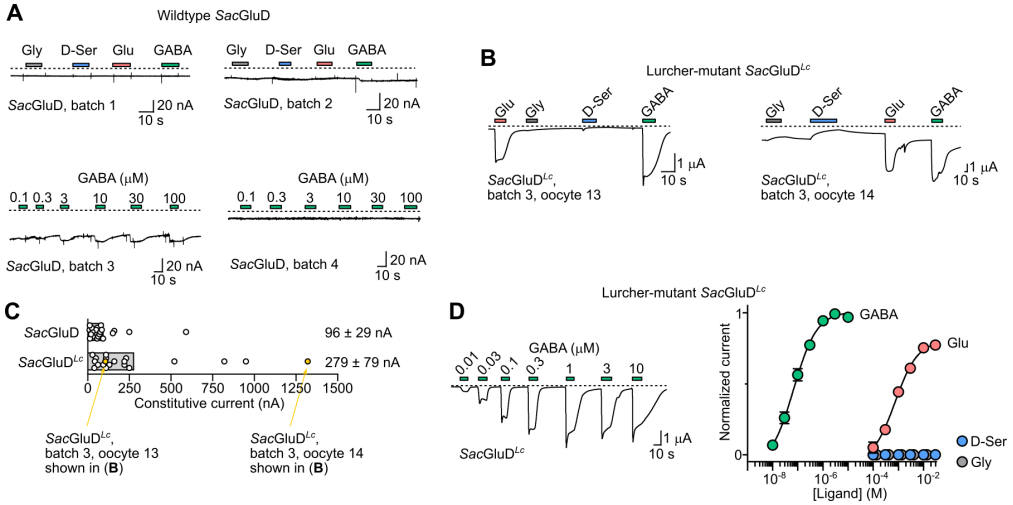

Figure 4.5: **Functional characterization of *Sac*GluD** (A) TEVC recordings in oocytes of four different batches, injected with WT *Saccoglossus kowalevskii* GluD (*Sac*GluD) mRNA, showing current responses to different potential ligands. Dashed lines, zero current. (B) TEVC recordings of responses to different ligands in oocytes injected with lurcher-mutant *Saccoglossus kowalevskii*. Oocyte batch number is separate from that in panel A. (C) Mean (bars) and individual data points (both n = 20 oocytes, over four different batches) of constitutive current in WT *Sac*GluD-expressing and corresponding lurcher-mutant-expressing oocytes. Two data points are highlighted: shown in panel B. (D) Left, Representative recording, and right, mean ± SEM current responses (normalized to GABA-gated current amplitude) to increasing ligand concentrations in oocytes injected with lurcher-mutant *Sac*GluD^{Lc}. n = 4 (GABA), 3 (Glu), or 5 (D-Ser and Gly).

Xenacoelomorph delta iGluRs

In comprehensively exploring the diversity of delta iGluR genes, I next targeted two genes from the other, xenacoelomorph-specific sub-branches, as delineated in the phylogenetic tree (Fig. 4.2). In turn, in my selection of xenacoelomorph genes I tried to represent both sub-branches therein, and thus a gene from the nemertodermatid *Meara stichopi*, *Mea*GluD, and another from the acoel *Diopisthoporus longitubus*, *Dio*GluD. My experimental attempts to detect ligand-gated currents in the WT *Mea*GluD were unsuccessful. Further exploration using a lurcher-like mutant variant, A611T (*Mea*GluD^{Lc}), also did not yield the anticipated results, as there was no discernible constitutive activity observed (Fig. 4.6 A). This leads to the consideration that either the *Mea*GluD gene or its Lc-mutant variant may not express effectively

in *Xenopus* oocytes. Contrasting the results from *Mea*GluD, in oocytes expressing *Dio*GluD, I observed small yet consistent ligand-gated activity (Fig. 4.6 B). Remarkably, GABA was identified as the exclusive agonist capable of inducing currents, with an EC_{50} value of 180 ± 20 µM (n = 6) (Fig. 4.6 C). This finding holds significant implications for our understanding of the evolution of delta iGluRs. The presence of GABA-gated activity in *Dio*GluD, a gene from a non-deuterostome xenacoelomorph, alongside similar findings in deuterostome species, underscores the ancient nature of this functional trait. It suggests that the ability of delta iGluRs to respond to GABA is an ancestral trait that was present in the earliest delta iGluRs, before the evolutionary split between deuterostomes (like starfish and vertebrates) and non-deuterostomes (like the xenacoelomorphs). Subsequently, in early vertebrates, delta iGluR genes underwent significant evolutionary changes, leading to the loss of GABA-gated function.

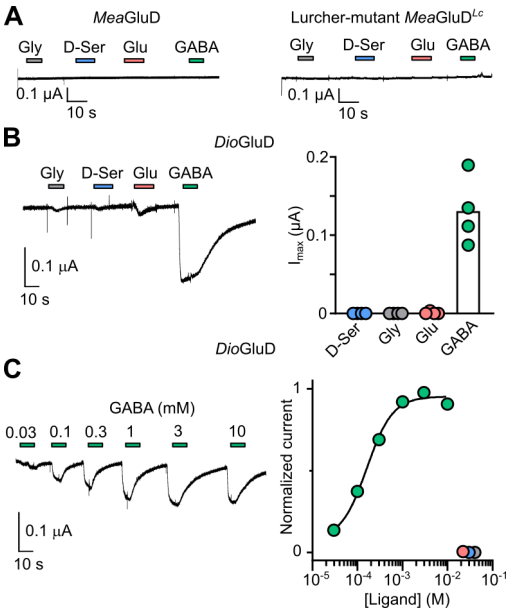

Figure 4.6: **Functional characterization of Xenacoelomorph delta iGluRs** (A) Left, Example recordings at *Xenopus* oocytes expressing WT *Mea*GluD and (right) lurcher-mutant *Mea*GluD^{Lc} (B) Left, TEVC recordings of responses to different ligands in oocytes injected with *Dio*GluD. Right, I_{max} at different oocytes (dots) and resulting means (column). (C) Left, Representative recording to increasing concentrations of GABA in oocytes injected with *Dio*GluD, and (right) mean ± SEM current responses (normalized to GABA-gated current amplitude) to increasing ligand concentrations in oocytes injected with *Dio*GluD.

Protostome delta iGluRs

But to unravel the functional characteristics of the ancestral delta iGluR, I turned to the earliest-branching gene in the delta iGluR branch, that of the mollusc *Crassostrea gigas*, *Cra*GluD. Basal branches represent the earliest points of divergence from the common ancestor within a phylogenetic tree, serving as crucial markers for understanding the evolutionary history and ancestral traits of a group. Therefore, exploring the functionality of *Cra*GluD was not just an effort in characterizing another variant of delta iGluRs, but a critical step towards reconstructing the evolutionary narrative of these receptors. In testing both WT and lurcher mutant (A567T) variants of *Cra*GluD, no ligand-gated currents were detectable in either (Fig 4.7 A). This absence of measurable activity could be attributed to potential limitations in the expression of *Cra*GluD within the oocyte membrane. To test this I checked the expression of *Cra*GluD in the oocyte membrane via immunolabelling. This experiment revealed no difference in fluorescence between oocytes injected with WT *Cra*GluD and those that were uninjected (Fig 4.7 B). This suggests that the lack of functional currents in *Cra*GluD may stem from insufficient receptor expression at the oocyte membrane rather than an inherent lack of receptor functionality. Consequently, due to the absence of detectable currents and the apparent limitations in membrane expression in *Xenopus* laevis oocytes of *Cra*GluD, it becomes challenging to draw conclusions regarding the ancestral properties of delta iGluRs drawn from this particular gene.

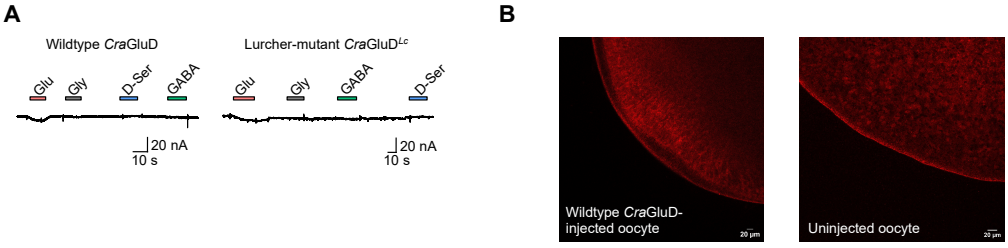

Figure 4.7: **Functional characterization of *Cra*GluD** (A) TEVC recordings in oocytes expressing *Cra*GluD and *Cra*GluD^{Lc} showed no significant ligand-gated current. (B) Anti-myc fluorescent immunolabelling of oocyte injected with -myc mRNA and uninjected oocyte suggests absence of *Cra*GluD surface expression.

4.3 Conclusion

My phylogenetic analysis, aimed at establishing a functional and evolutionary picture of the delta family, spanned a broad array of animal species to ensure a thorough examination of this receptor class. This analysis positions mammalian GluD1 and GluD2 genes within a robustly supported branch that includes a diverse array of bilaterian sequences, defining what I termed the delta family. The delta iGluR family is also closely related to the AMPA and KA receptor families, and contributes to the broader AMPA/KA/delta/phi (AKDF) branch. My findings suggest the delta genes originated from the diversification of an ancestral AKDF gene, likely after the divergence of cnidarians from bilaterians (Fig. 4.8). The identification of delta sequences in xenacoelomorphs—considered a sister group to both deuterostomes and protostomes-supports the notion that the earliest delta gene emerged with the first bilaterian animals. Notably, while delta iGluR genes are exclusive to bilaterians, their distribution is not uniform across all bilaterian animals, as protostomes sequences (I included sequences from *Schmidtea mediterranea*, *Crassostrea gigas* and *Strigamia maritima* in my analysis) are absent from the delta family but for a single sequence from *Crassostrea gigas*. Therefore, upon the divergence of deuterostomes and protostomes, the delta gene may have been lost in several major protostome lineages. Instead, protostomes might have retained this ancestral AKDF/delta gene, but it then diversified rapidly across various protostome species. In such scenarios, certain sequences—like that of *Crassostrea gigas*—could have evolved to resemble delta genes more closely than they do other protostome sequences, but others may have evolved so much that they no longer share enough similarity with delta genes to appear here in the tree.

My attempt in functionally characterizing sequences from the putative delta iGluR family unveiled that a large number of invertebrate delta iGluRs are ligand-gated channels activated by the classical inhibitory transmitter GABA. Given that this functional signature is widespread throughout the delta iGluR branch, it is reasonable to postulate that GABA sensitivity developed relatively early following the emergence of the ancestral delta iGluR gene, although deducing the functional properties of the ancestral delta receptor is challenging, especially with the lack

of functional data from the basal-branching delta iGluR sequence from *Crassostrea gigas*. I propose that delta receptors originated in an early bilaterian organism, possessing the distinctive feature of being GABA-gated. These GABA-gated delta iGluRs have been inherited and retained in various present bilaterian lineages: from xenacoelomorphs to invertebrate deuterostomes like starfish and acorn worms. In lineage to vertebrates, however, delta iGluRs underwent two substantial changes, losing activation by ligand and lost selectivity for GABA. However, the sequence of evolutionary events—whether the loss of ligand-gated currents preceded the alteration in ligand selectivity, or vice versa—remains unclear and underscores the necessity for further comparative studies across a broader range of species within the chordate lineage to delineate the sequence of events that shaped delta receptors function in vertebrates.

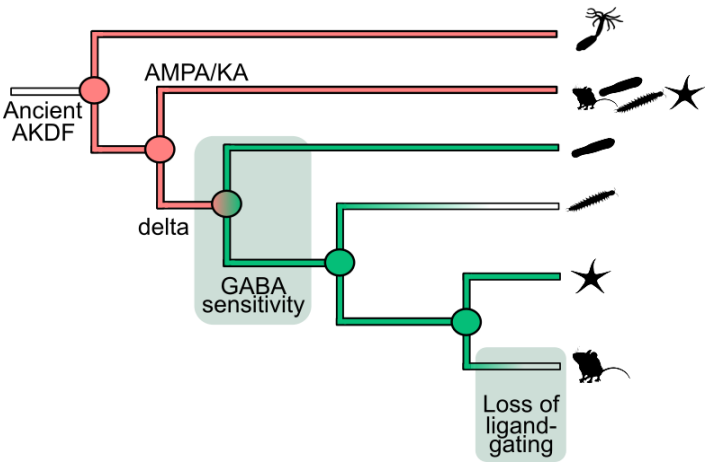

Figure 4.8: **Summary of proposed evolution of the delta receptor gene** Delta iGluRs genes emerged from an ancestral AKDF gene after the separation of cnidarians and bilaterians. Delta iGluR genes are predominantly found in bilaterians (with sparse representation in protostomes) and became sensitive to GABA relatively soon after their emergence. In the lineage leading to vertebrates, delta iGluRs experienced by the loss of activation by ligand binding and a reduction in GABA selectivity.

Chapter 5

Results II - Pharmacological and biophysical properties of *Aca*GluD and relation to other iGluRs

Delta iGluRs are important for structural synaptic integrity in the cerebellum (Kakegawa et al. (2011)) and hippocampus (Dai et al. (2021)). It has been demonstrated that GluD2 gating can be triggered by mGlu1 receptor activation (metabotropic glutamate receptor 1), a process that occurs both in heterologous expression systems and in native neuronal environments such as Purkinje cells where GluD2 is highly expressed (Ady et al. (2014)). Deletions or mutations of delta iGluRs are linked to neurological disorders such as cerebellar ataxia (Coutelier et al. (2015)), schizophrenia and autism (Benamer et al. (2018)). Pharmacological modulators that enhance or inhibit GluD1 and GluD2 iGluR function may therefore help unravel the role of delta iGluRs within neural circuits and perhaps lead to novel therapeutics. However, as mammalian delta iGluRs typically do not show ligand-gated currents in conventional heterologous expression systems (page 34), electrophysiological experiments testing pharmacological modulation of delta iGluR function have not proceeded like they have for other iGluRs (Brogi et al. (2019)). There is evidence suggesting that delta iGluRs share some pharmacological properties with NMDA receptors. Most obviously, GluD1 and GluD2 subunits and NMDA receptor GluN1

subuntis bind glycine and D-serine (Naur et al. (2007); Matsui et al. (1995)). Additionally, the GluN1-specific NDMA receptor competitive antagonist 7-chlorokynurenic acid (7-CKA) was found to inhibit GluD2^{Lc} currents by a homologous site (Kristensen et al. (2016)). Moreover pentamidine, which inhibits NMDA receptors in the low µM range (Reynolds and Aizenman (1992)) showed moderate inhibition of GluD2^{Lc} currents, and had almost no effect on AMPA receptors at concentrations tested (Williams et al. (2003)).

Yet my phylogenetic analysis suggested that delta iGluRs are more closely related to AMPA/KA receptors than to NMDA receptors (page 30), which would perhaps imply a more shared pharmacological profile with AMPARs. As one of the main findings from previous chapter is that certain invertebrate WT delta iGluRs show robust ligand-gated currents in oocytes, I was in a better position to unravel the pharmacological and biophysical properties of the delta iGluR family, which should in future enable pharmacological developments for vertebrate delta iGluRs and also offer insight into relationships among iGluRs families. Therefore in this chapter, I offer the first broad functional characterization of an active WT delta iGluRs. This characterization extends to the analysis of channel pore features, the pharmacology of competitive antagonists, the modulation by extracellular calcium ions (Ca^{2+}) and computational studies focused on ligand binding. I focused on characterizing the crown-of-thorns starfish *Aca*GluD receptor, as it demonstrated better expression levels in *Xenopus laevis* oocytes among the receptors I tested and pharmacological interrogation was now feasible due to its large, robust currents. Consequently, the upcoming sections of my thesis will primarily center around the *Aca*GluD receptor.

5.1 Channel pore properties of *Aca*GluD

5.1.1 Current-voltage relationship of *Aca*GluD

Because the current-voltage (IV) relationship, reflecting relative ion permeability and conductance, in iGluRs determines whether their activation excites or inhibits neurons, it is an important aspect of their biophysical characterization. I therefore recorded GABA-gated currents in

*Aca*GluD-expressing oocytes in increasing holding potentials from –80 to 60 mV both in the presence and in the absence of extracellular calcium (Ca^{2+}) (Fig 5.1). The IV relationship of *Aca*GluD shows a reversal potential of –16 mV and inward rectification with only minimal outward currents observable at voltages exceeding 50 mV, regardless of the presence of divalent cations. This tells us several things about the delta iGluR pore. As the reversal potential is –16 ± 2 mV (n = 4) the channel is not a K^+-selective channel, whose currents would reverse at around –80 mV, is not a Na^+-seclective channel, whose currents would reverse at around +50 mV, and is instead a mixed cation channel, like most animal iGluRs (Chang et al. (1994)). This would make *Aca*GluD an excitatory GABA receptor, which is remarkable given the role of GABA in inhibitory signaling in most animals (Sigel and Steinmann (2012)). The removal of extracellular Ca^{2+} does not affect this reversal potential, suggesting that Ca^{2+} permeates relatively little, however the small currents in the absence of Ca^{2+} and the inward rectification and thus flat IV relationship make it difficult to measure the reversal potential in this condition. The large inward currents in regular extracellular solution indicate the absence of block by extracellular Mg^{2+} ions and thus ions can flow relatively freely across the membrane when this delta iGluR is activated at the typical resting membrane potential of neurons. This too is more similar to AMPA receptors (Schmid et al. (2009)).

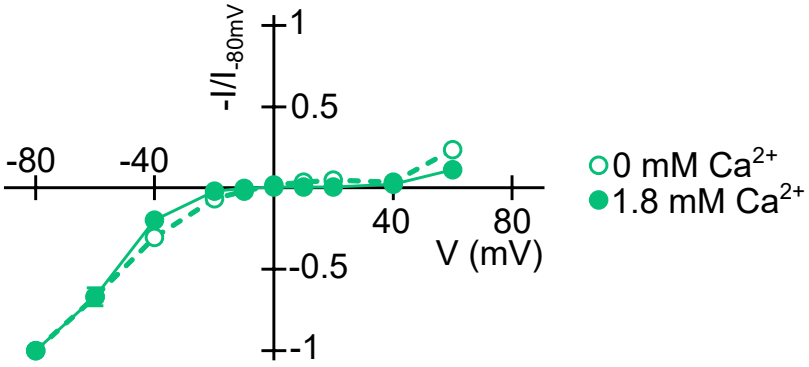

Figure 5.1: **IV curve for *Aca*GluD** Normalized current ($I/I_{-80\,mV}$)-voltage relationship of GABA-gated currents through *Aca*GluD-expressing oocytes in the presence (filled circles) and absence (empty circles) of extracellular calcium. Data points mean ± SEM (n = 4), joined by straight lines.

5.1.2 Pentamidine modulation in *Aca*GluD

Channel blockers inhibit iGluR activity by docking within the channel pore and thus obstructing the flow of ions. They may have various physico-chemical structures, but iGluR channel blockers typically have a cationic moiety (Zhorov and Tikhonov (2004)). Therefore, I decided to test the effect of a known iGluR pore blocker, pentamidine, on different iGluRs. Other studies demonstrated that pentamidine blocks 100% glutamate/glycine-induced current at NMDA receptors with an IC_{50} of 0.5 µM, while it inhibits *Rat*GluD2^{Lc} constitutive current only 74 ± 8 % with an IC_{50} of 6.8 µM (Williams et al. (2003)). My experiments on *Rat*GluD2^{Lc} corroborate this finding where pentamidine at 100 uM is not able to fully block the constitutive current of *Rat*GluD2^{Lc} but reduced it of 68 ± 5 % (n = 4) (Fig. 5.2 A). Similarly, in oocytes expressing *Aca*GluD receptors, when I applied an EC_{100} concentration of GABA and glutamate in the presence of 100 µM pentamidine, currents were substantially smaller than in the presence of EC_{100} GABA or glutamate alone (Fig. 5.2 B). Specifically, 100 µM pentamidine blocked 68 ± 5 % (n = 5) of the GABA-gated current and 78 ± 2 % (n = 7) of the glutamate-gated current (Fig. 5.2 B). This shows that 100 µM pentamidine blocks 100 % of ligand-gated currents at NMDA receptors but a full block with the same concentration of pentamidine is not achieved in GABA/glutamate-gated current at *Aca*GluD or on constitutive currents on *Rat*GluD2^{Lc}. Pentamidine effects at AMPARs have not been studied in detail, so with the help of Yuhong Wang, a PhD candidate in my lab, we tested the effects of 100 µM pentamidine on AMPARs. As AMPARs desensitize quickly, it can be difficult to assay their pharmacology in oocytes. We therefore co-expressed rat GluA2 with human TARPγ2, which leads to bigger and slower-desensitizing currents, allowing us to measure pharmacological modulation (Ishii et al. (2020)). 1 mM glutamate-gated currents at *Rat*GluA2 were reduced by 37 ± 3 % (n = 5) in the presence of 100 µM pentamidine for both transient and sustained current (Fig. 5.2 C). This indicates a pattern of sensitivity among different types of ionotropic glutamate receptors where the pore blocker pentamidine exhibit more potent inhibition at NMDA receptors, and less potent inhibition at delta and AMPA receptors.

Experiments involving an active, ligand-gated delta iGluR have illuminated several key as-

pects of the delta iGluR pore's characteristics. Firstly, this receptor functions as a non-selective cation channel, aligning with the general pore behavior observed across other iGluRs, despite being activated by GABA—a neurotransmitter typically associated with inhibitory actions. Secondly, the channel is subject to blockade by high concentrations of pentamidine (high μM range). This requirement for elevated pentamidine levels to inhibit without achieving a full block of ion flux mirrors the pharmacological profile of AMPA receptors. This behavior differs from that of NMDA receptors, where significantly lower μM concentrations of pentamidine are sufficient to achieve a complete blockade of ligand-induced currents.

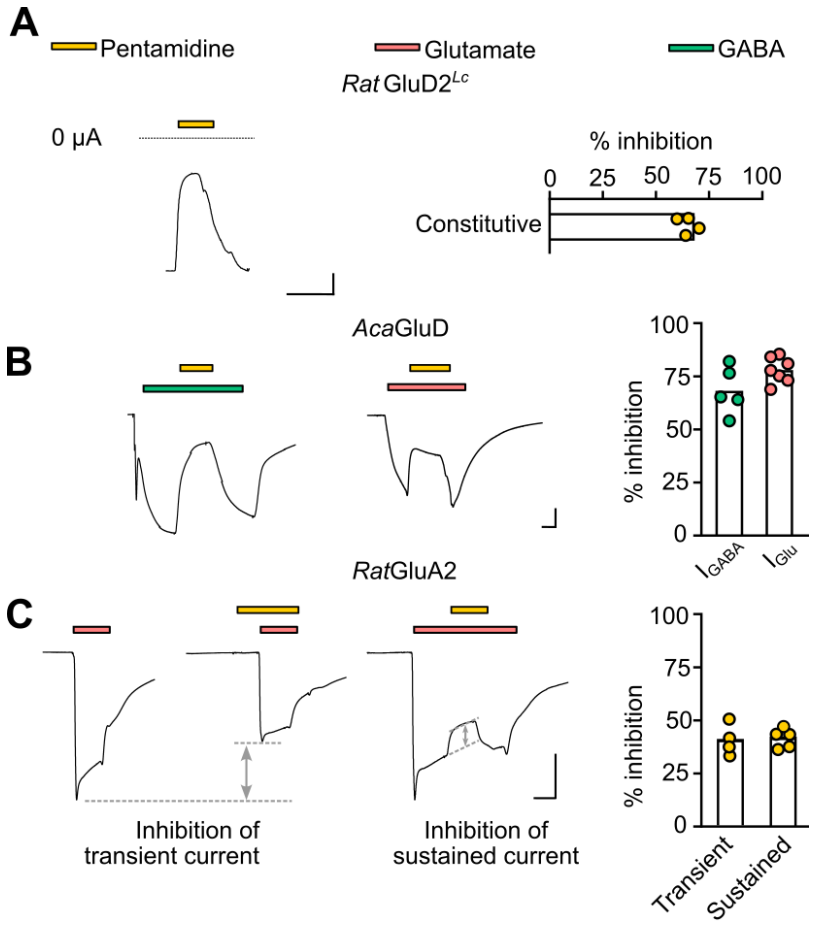

Figure 5.2: **Effect of pentamidine at *Rat*GluD2^{Lc}, *Aca*GluD, *Rat*GluA2** (A) Example recording in oocytes expressing *Rat*GluD2^{Lc} in response 100 µM pentamidine. The dashed line indicates zero current (scale bars x, 15 s; y, 0.2 µA). Right, % inhibition of constitutive current modulated by 100 µM pentamidine. (B-C) Left, example recordings of ligand-gated current modulated by 100 µM pentamidine in oocytes expressing (B) *Aca*GluD (scale bars x, 5 s; y, 1 µA) and (C) *Rat*GluA2 and human TARPγ2 (CACNG2) (scale bars x, 10 s; y, 1 µA). Right, % inhibition of ligand-gated current by pentamidine at different oocytes (dots) and resulting means (columns).

5.2 Ligand binding domain properties of *Aca*GluD

One of the striking properties of *Aca*GluD is the fact that it's more sensitive to GABA than glycine or D-serine. This indicates that the LBD must differ from other delta iGluRs biophys-

ically. To unravel the molecular basis of this distinct ligand preference, I performed a combined computational and functional investigation, comparing the ligand-binding properties of *Aca*GluD with those of the glycine- and D-serine-sensitive *Rat*GluD2.

5.2.1 Computational and functional analysis of ligand binding

Central to this investigation was the application of computational docking techniques to explore the interactions between GABA and D-serine with starfish *Aca*GluD AlphaFold structural model (Jumper et al. (2021)) and *Rat*GluD2 X-ray structure (Naur et al. (2007)). After inputting the amino acid sequence of the receptor's ligand binding domain (LBD) (Fig. 5.3 A–B), AlphaFold provided five models (ranked 1 to 5) of its three-dimensional structure (Mirdita et al. (2022)) (Fig. 5.3 D). The Predicted Local Distance Difference Test (pLDDT) scores are a measure of confidence for the local accuracy of the predicted model on a per-residue basis. Scores close to 100 indicate regions modeled with high confidence, while scores between 70 and 90 indicates that the regions are expected to be modelled with reasonably confidence. Regions with pLDDT below 70 are modelled with low confidence and should be considered with caution. The plot shows that for the entire *Aca*GluD LBD structure, AlphaFold is quite confident in its prediction, as indicated by the scores predominantly above 90 across all five models (Fig. 5.3 C). For the whole subsequent analysis, I used the first ranked model generated from AlphaFold because it had a higher overall pLDDT compared to the other four. Within this model I checked which regions had lower pLDDT score. The first region is in the upper lobe in position 15 to 25 and is a loop formed by two β-strands just before the B helix. This region seems to be quite flexible, pointing away from the rest of the structure and relatively far from the putative ligand binding site. The second region with a lower confidence score is found on the rear side of the lower lobe of the LBD from positions 195 to 200. Like the first region, this is a short loop that connects helix I to the subsequent β-strand and its comparatively low pLDDT shouldn't affect the overall structure and goodness of the model (Fig. 5.3 D). The AlphaFold model of *Aca*GluD LBD is predicted with very high confidence and it stands as a solid base for my subsequent analysis of

its ligand binding proprieties.

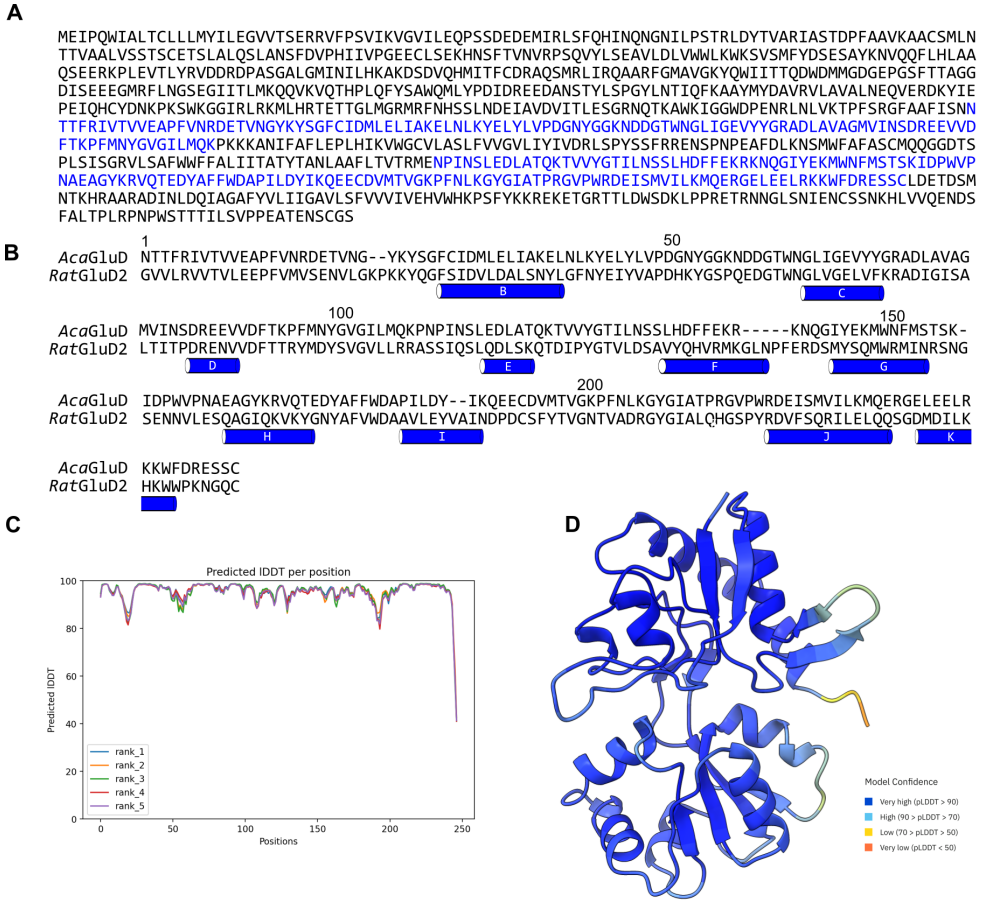

Figure 5.3: **AlphaFold Predictions for *Aca*GluD LBD** (A) Amino acid sequence of *Aca*GluD. Blue, ligand binding domain. (B) Amino acid sequence alignment of *Aca*GluD and *Rat*GluD2 LBDs. Alpha helices from secondary structure are shown below alignment (taken from *Rat*GluD2 Naur et al. (2007)), numbers above alignment refers to positions in *Aca*GluD LBD. (C) Predicted Local Distance Difference Test (pLDDT) score across different model ranks, indicating per-residue confidence. Higher scores represent greater confidence in the predicted structure. Position numbers refers to *Aca*GluD LBD numbering shown in (B). (D) Structures of the first ranked AlphaFold model of *Aca*GluD LBD, colored by rank pLDDT score.

In the absence of molecular dynamics simulations, my assessment of ligand binding affinity would require a closed clamshell LBD, the conformation stabilized by ligand-binding and

which leads to channel opening (Armstrong and Gouaux (2000)). I therefore examined whether the model generated was in a more 'open' or 'closed' conformation. To this end I defined a 2D coordinate (Σ1,Σ2) that expresses the distance between the upper and lower lobes of the LBD (Yu et al. (2015)). Σ1 represents the distance between the center-of-mass of non-hydrogen atoms within residues 547-549 in the upper lobe and the center-of-mass of non-hydrogen atoms within residues 713- 714 in the lower lobe. Σ2 represents the distance between the center-of-mass of non-hydrogen atoms within residues 474-476 in the upper lobe and the center-of-mass of non-hydrogen atoms within residues 746-748 in the lower lobe (Fig. 5.4). The model displayed (Σ1,Σ2) = (10.4, 9.7 Å). For apo *Rat*GluD2 X-ray structure (PDB: 2V3T) (Σ1,Σ2) = (12.7, 10.1 Å) and D-serine bound *Rat*GluD2 (PDB: 2V3U) (Σ1,Σ2) = (9.6, 7.4 Å)) (Chin et al. (2020)). Based on these parameters, it is plausible to deduce that my *Aca*GluD LBD model is not exhibiting a fully closed state, rather it appears to be in a partially closed conformation.

Figure 5.4: **Openness of the LBD *Aca*GluD structural model** Σ1: distance between residues 547-549 and residues 713- 714, Σ2: distance between residues 474-476 and residues 746-748 shown in grey lines.

Following validation of the AlphaFold structural model, I adopted a blind docking approach to investigate the interactions of GABA and D-serine with both the computationally modeled *Aca*GluD receptor and the experimentally resolved GluD2 X-ray structure but with the ligand

removed (PDB: 2V3U). By doing so I did not presuppose a binding site, allowing for an unbiased exploration of potential ligand-binding sites across the entire surface of each receptor. Consistent with canonical ligand-induced activity of *Aca*GluD and with structurally determined binding sites in *Rat*GluD2, both ligands docked to the expected binding site of the receptors (Fig. 5.5 A–B). GABA showed a stronger docking affinity compared to D-serine in *Aca*GluD (Fig. 5.5 A), while the reverse pattern was observed in *Rat*GluD2 (Fig. 5.5 B). This is consistent with my experiments, which showed that GABA not only induced larger currents but also emerged as a more potent agonist than D-serine in *Aca*GluD.

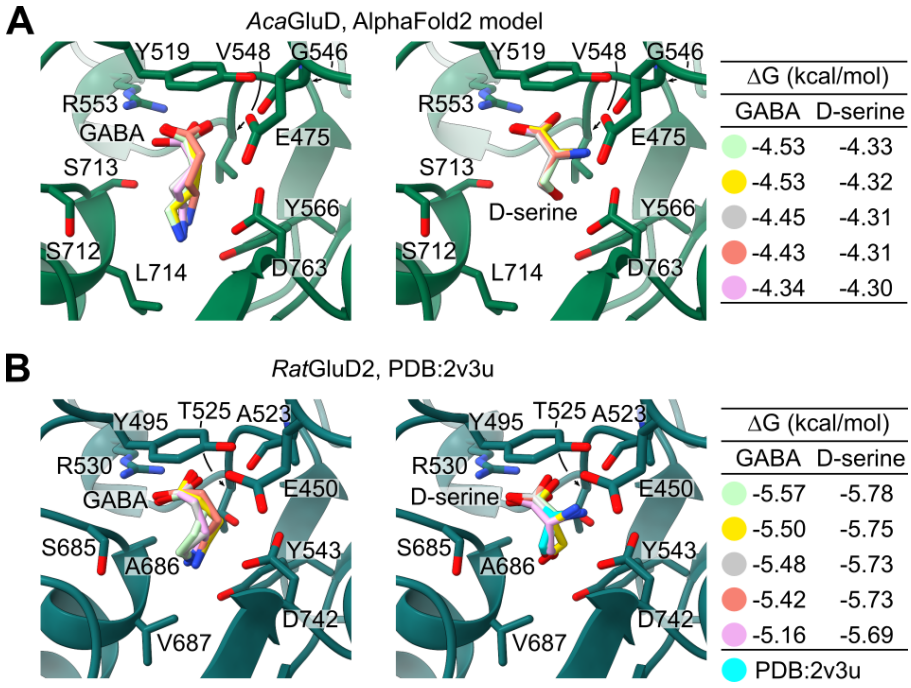

Figure 5.5: **Computational ligand docking to *Aca*GluD and *Rat*GluD2** Five most energetically favorable binding poses for GABA and D-serine at *Aca*GluD model (A) and *Rat*GluD2 X-ray structure (PDB: 2V3U) (B).

In questioning the molecular basis for the preference of different ligands in *Aca*GluD and *Rat*GluD2, I aligned LBD residues. Interestingly, the ligand-binding residues shows only minor differences between GABA-selective and D-serine/glycine-selective receptors (Fig. 5.6 A).

Indeed, in both receptors, the same major interaction between R553/R530 (from the upper lobe) and the GABA and D-serine carboxylate and between conserved D763/D742 (from the lower lobe) and the GABA γ-amine and D-serine α-amine are observed in my dockings.(Fig. 5.5 A-B). Only three differences were found in the vicinity of the ligand in *Aca*GluD and *Rat*GluD2 receptors, which may underpin their divergent ligand specificities. First, at position 546 in the upper lobe of the ligand-binding domain, *Aca*GluD has a glycine residue (G546), while *Rat*GluD2 features an alanine (A523) (Fig. 5.6 A). Second, residue V548 in *Aca*GluD is hydrophobic and, consequently, lacks the capacity for polar interactions with the α-amine of D-serine implied in my dockings (Fig. 5.6 A). The equivalent position in *Rat*GluD2, occupied by a polar threonine (T525) can engage in such an interaction in my dockings and in the published X-ray structure (Naur et al. (2007)). Third, in the lower lobe of the binding site *Aca*GluD possesses a polar serine (S713), where *Rat*GluD2 features a small, nonpolar alanine (A686) at the corresponding position (Fig. 5.6 A). Therefore I decided to mutate the residues at these positions in the *Aca*GluD receptor to mirror the corresponding D-serine-selective-residues in *Rat*GluD2, generating *Aca*GluD mutants G546A, V548T and S713A. I anticipated an increase in the receptor's sensitivity to D-serine or decrease in sensitivity to GABA. Contrary to expectations, the ligand selectivity profile of these *Aca*GluD mutant receptors was similar to that of wildtype and showed no increase in D-serine activity (Fig. 5.6 B–C).

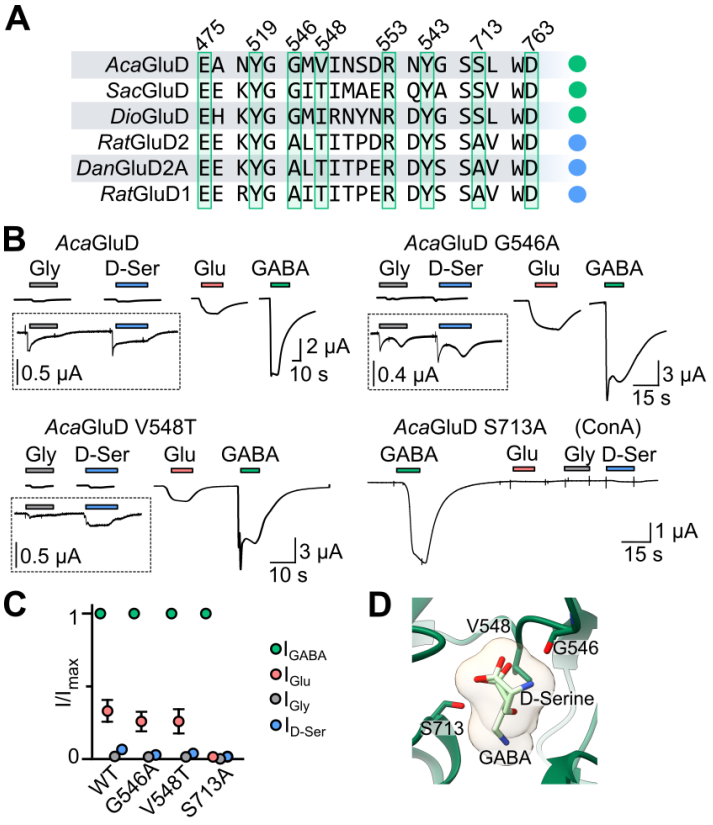

Figure 5.6: **Comparative ligand-selectivity analysis** (A) Amino acid sequence alignment of selected LBD segments (*Aca*GluD numbering. Green circle, GABA-selective receptors. Blue circle, D-serine-selective receptors). (B) Example recording of oocytes expressing the indicated mutant *Aca*GluD receptors to different ligands. (Oocytes expressing S713A receptors only responded after concanavalin A treatment ("ConA", 10 µM). (C) Mean (± SEM, n = 4) and normalized responses for mutants tested in (B). (D) Structural representation of *Aca*GluD highlighting the positions of mutated residues. GABA and D-serine in their most favorable binding poses.

The fact that the G546A mutation had no effect on ligand selectivity confirms that it is the main chain carboxyl group of this residue that is important for ligand binding. Similarly, the side chain of A686 in *Rat*GluD2 is perhaps too far from the ligand to interact directly, suggesting that the S713A mutation might also be expected to contribute little to potency directly. The V548T result was somewhat surprising, as the hydroxyl group of the threonine seems ideally placed to interact specifically with the amino group of D-serine and not with the CH2 groups

of GABA (Fig. 5.6 D). Nonetheless, it is consistent with my observation (page 37) that invertebrate receptor *Sac*GluD has pronounced selectivity for GABA over D-serine (Fig. 4.5) even with the upper lobe threonine residue similar to that of T525 in *Rat*GluD2 (Fig. 5.6 A). The conserved D763/D742 residue seems particularly important, as it binds to the ligand amine whether slightly higher in the site for D-serine or lower in the site for GABA. Together these results might indicate that ligand selectivity is not solely determined by individual amino acid differences within the ligand-interacting residues but perhaps some other aspects contribute significantly to the determination of ligand specificity. In line with this, a recent study has showed that E475/E450 residue contributes to GABA vs D-serine preference in *Rat*GluD1 receptors and NMDA receptor GluN1 subunits (Piot et al. (2023)), yet it is conserved in GABA-selective and D-serine selective GluD receptors (Fig. 5.6 A). This analysis suggests that the underlying reason for this dual sensitivity likely lies in the structural adaptability of the ligand-binding residues, including D742, which demonstrate the necessary flexibility and the carboxylate side chain to accommodate both GABA and D-serine.

5.3 Modulation by competitive antagonists in *Aca*GluD

In exploring the pharmacological profile of *Aca*GluD, I evaluated the effects of potential competitive antagonists on the receptor. Competitive antagonists bind to the binding site of the receptor but without inducing LBD closure and they prevent the agonist from binding and activating. Some competitive antagonists such as quinoxalinediones CNQX, DNQX and NBQX (see Methods, page 24,25) are known to be more selective inhibitors of AMPA/KA receptors compared to NMDA receptors (Sheardown et al. (1991)), while the opposite has been reported for compounds such as DCKA (McNamara et al. (1990)) and CGP-78608 (see Methods, page 24) (Auberson et al. (1999)), which are glycine site (GluN1) antagonists of NMDA receptors. Since *Aca*GluD is able to bind not only GABA but also glutamate (like AMPA/KA receptors) and glycine/D-serine (like NMDA receptors) I wanted to check whether *Aca*GluD is sensitive to AMPA/KAR- or NMDAR-competitive antagonists.

When applied in isolation, classical antagonists of AMPA/KA receptors, CNQX, DNQX, and NBQX at a concentration of 100 μM, failed to elicit any detectable currents through *Aca*GluD (Fig. 5.7 A). However, when these antagonists were co-applied with GABA at an approximate EC_{30} GABA concentration, CNQX, DNQX, and NBQX inhibited the GABA-induced currents by 81 ± 4%, 53 ± 3%, and 61 ± 3% respectively (each n = 5, Fig. 5.7 B). This inhibition of current was comparable to that of the pore blocker pentamidine (Fig. 5.2 B). I also noted that DNQX and NBQX enhanced glutamate-gated currents by 34 ± 3%, while CNQX had no discernible effect (each n = 5, Fig. 5.7 B). Enhancement by such competitive antagonists seems unusual but it's worth noting that both CNQX and DNQX can act as partial agonists at AMPA receptors when co-expressed with TARP-type auxiliary subunits (Menuz et al. (2007)) and that, in the case of Lurcher-mutant GluA1 receptor, CNQX was converted from antagonist to a potent agonist (Taverna et al. (2000)).

This shows us that at both delta and AMPA iGluRs, quinoxalinediones can inhibit or enhance receptor activity depending on context: inhibition or enhancement depends on particular agonist in delta iGluRs; and no activation or activation depends on simple or complex AMPAR oligomerization. This prompted me to test the effects of these compounds on WT *Rat*GluD2 receptors: if we had drugs activating or at least modulating the activity of relatively inactive delta iGluRs, we might be able to better probe their physiological role. I observed that these drugs had no effect on *Xenopus laevis* oocytes expressing WT *Rat*GluD2 (Fig 5.8 A). Subsequent testing on the mutant *Rat*GluD2^{Lc} receptors showed that NBQX, CNQX, and DNQX respectively reduced constitutive currents by 9 ± 0.2%, 10 ± 0.2%, and 11 ± 0.2% (each n = 4, Fig 5.8 B).

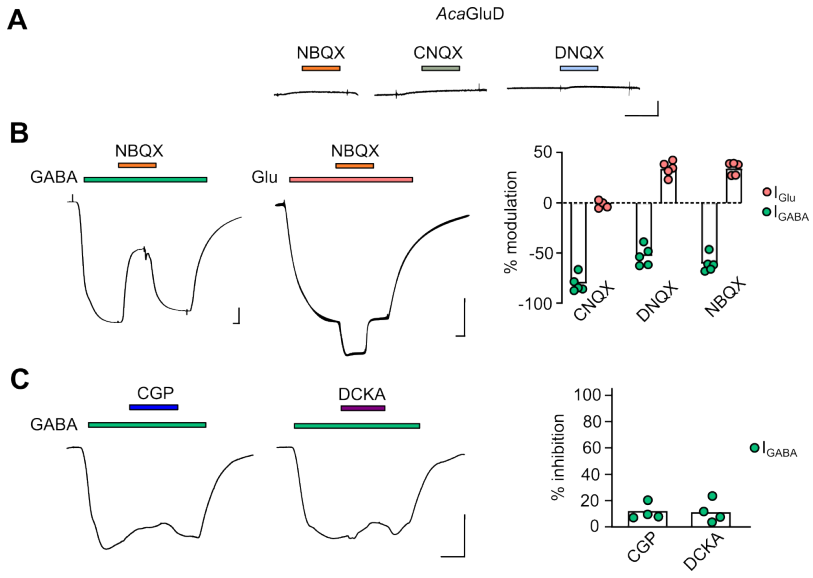

Figure 5.7: **Effects of competitive antagonists in *Aca*GluD** (A) Example recordings of competitive antagonists application NBQX, CNQX, and DNQX (100µM) at *Aca*GluD-expressing oocytes (scale bars x, 10 s; y, 0.2 µA). (B) Left, Representative current traces illustrating the modulatory effects of NBQX on GABA and glutamate induced currents in *Aca*GluD (scale bars x, 5 s; y, 1 µA). Right, Percent modulation of current by CNQX, DNQX, and NBQX for GABA/glutamate-gated currents (columns, mean; circles, individual data points). (C) Left: Representative current traces showing the impact of NMDA receptor glycine site antagonists CGP and DCKA on GABA-induced currents in *Aca*GluD (scale bars x, 10 s; y, 1 µA). Right: Percent inhibition of GABA-gated currents by CGP and DCKA (columns, mean; circles, individual data points).

In contrast to classical AMPAR antagonists, GluN1 competitive antagonists DCKA and CGP-78608 at 100 µM exhibited minimal effect on GABA-gated currents in *Aca*GluD, with only 11 ± 5% and 9 ± 3% inhibition respectively (each n = 4, Fig. 5.7 C) current reduction. Thus, in terms of competitive antagonists, delta receptors appear more closely related to the AMPA/KA receptor subfamily rather than the NMDAR subfamily, reflecting the close phylogenetic relationship of AMPA and delta iGluRs, despite the fact that GluN1 and delta subunits bind glycine and D-serine as agonists.

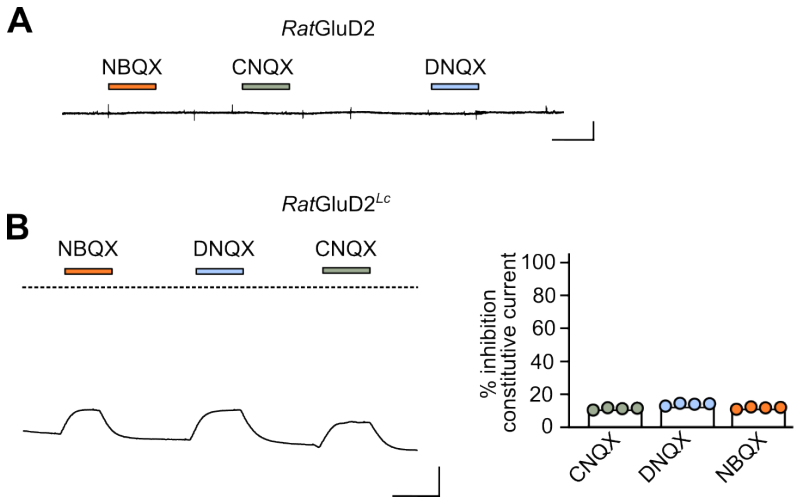

Figure 5.8: **Effects of competitive antagonists in *Rat*GluD2 and mutant *Rat*GluD2^{Lc}** (A) Example recordings of competitive antagonists application NBQX, CNQX, and DNQX (100µM) at *Rat*GluD2-expressing oocytes (scale bars x, 10 s; y, 0.2 µA). (B) Left, Example recordings of competitive antagonists application NBQX, CNQX, and DNQX (100µM) at consitutive active *Rat*GluD2^{Lc}-expressing oocytes (scale bars x, 10 s; y, 1 µA). Right, Percent inhibition of consitutive current by CNQX, DNQX, and NBQX (columns, mean; circles, individual data points).

5.4 Modulation of *Aca*GluD by extracellular calcium

As I continued to characterize the functional profile of *Aca*GluD receptors, my investigation next focused on the potential effects of extracellular calcium ions (Ca^{2+}). This was motivated by prior research that demonstrated the modulation of mutant *Rat*GluD2^{Lc} by extracellular calcium (Hansen et al. (2009)). Specifically, extracellular Ca^{2+} exerts two effects on *Rat*GluD2^{Lc}; enhancement of constitutive activity and reduction of D-serine potency in inhibiting its constitutive current. I tested *Aca*GluD receptors for these effects. In the absence of Ca^{2+}, the maximal current amplitudes induced by GABA, glutamate, and glycine were small while the introduction of 1.8 mM Ca^{2+} to the extracellular solution resulted in a substantial enhancement of these currents. For instance GABA-evoked currents increased from 0.30 ± 0.03 µA (n = 5) to 6 ± 1 µA (n = 5), glutamate-gated currents from 0.42 ± 0.13 µA (n = 4) to 5.8 ± 0.6 µA (n = 3) and glycine-gated currents from 0.062 ± 0.007 µA (n = 4) to 0.32 ± 0.01 µA (n = 4) (Fig. 5.9

A). Interestingly, agonist potency, as measured by EC_{50} values, was not substantially affected by the presence of extracellular calcium. GABA and glycine-EC_{50} values in Ca^{2+}-free solution were 4.8 ± 0.6 µM (n = 5) and 1.6 ± 0.2 mM (n = 5) respectively. The presence of 1.8 mM Ca^{2+} in the extracellular solution increased the GABA EC_{50} threefold to 13 ± 3 µM (n = 5), and glycine EC_{50} was almost unchanged with a value of 2.0 ± 0.1 mM (n = 4) (Fig. 5.9 B). This suggests that the principal effect of Ca^{2+} is to increase agonist efficacy rather than significantly alter agonist affinity. Whether the absence of Ca^{2+} ions leads to decreased single channel conductance, a number of inactive receptors, or an altered gating equilibrium would require further investigation, although by homology with Cl^- and Na^+ modulation of AMPARs and KARs, I think the latter two are more likely (Plested and Mayer (2007)).

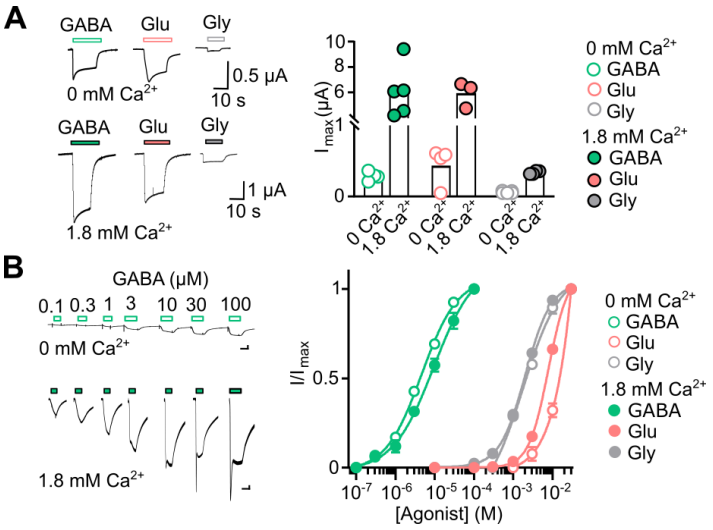

Figure 5.9: **Calcium modulation of *Aca*GluD** (A) Left, electrophysiological traces for *Aca*GluD, showing current responses different ligands in the absence (top) and presence of 1.8 mM Ca^{2+} (bottom). Right, Maximum current amplitudes elicited by GABA, glutamate, and glycine in the absence (0 mM) and presence (1.8 mM) of Ca^{2+} (columns, mean; circles, individual data points). (B) Left, Dose-response curves normalized to maximum current in respective condition, (I/I_{max}) (mean ± SEM, n = 5 to 7) and (Right) example responses to increasing concentrations of GABA in the absence or presence of extracellular Ca^{2+} (scale bars x, 10 s; y, 0.15 µA).

To understand how ligand-gated currents are modulated in *Aca*GluD by extracellular Ca^{2+}, I referred to a previous study which showed that the carboxylate side chains of E531, D535,

and D728, located at the back of the LBD in *Rat*GluD2^{Lc} receptors, play a key role in Ca^{2+} modulation (Hansen et al. (2009)). As these residues were also conserved in *Aca*GluD (Fig. 5.10 A-C) I decided to verify their contribution to the Ca^{2+} enhancement of ligand-gated I observed in *Aca*GluD. With the help of Allan Barzasi, a visiting master's student in our lab, we mutated these carboxylate residues to alanine, which has a small, nonpolar side chain thereby disrupting any putative contribution of that residue to Ca^{2+} enhancement. *Aca*GluD mutants E554A, D558A and D801A showed no enhancement of ligand-gated currents by Ca^{2+} (Fig. 5.10 E). This was the case with both 100 µM and 3 mM GABA (Fig. 5.10 D), confirming that the absence of enhancement was not due to the use of subsaturating GABA concentrations at mutant receptors. The mutations themselves had little effect on GABA potency, with EC_{50} values differing little between WT and mutants (WT = 13 ± 3 µM (n = 5), D558A = 18.3 ± 4.6 µM (n = 3), D801A = 6.1 ± 3.6 µM (n = 4)) although E554A showed threefold increased GABA potency (E554A = 3.0 ± 0.3 µM (n = 4)).

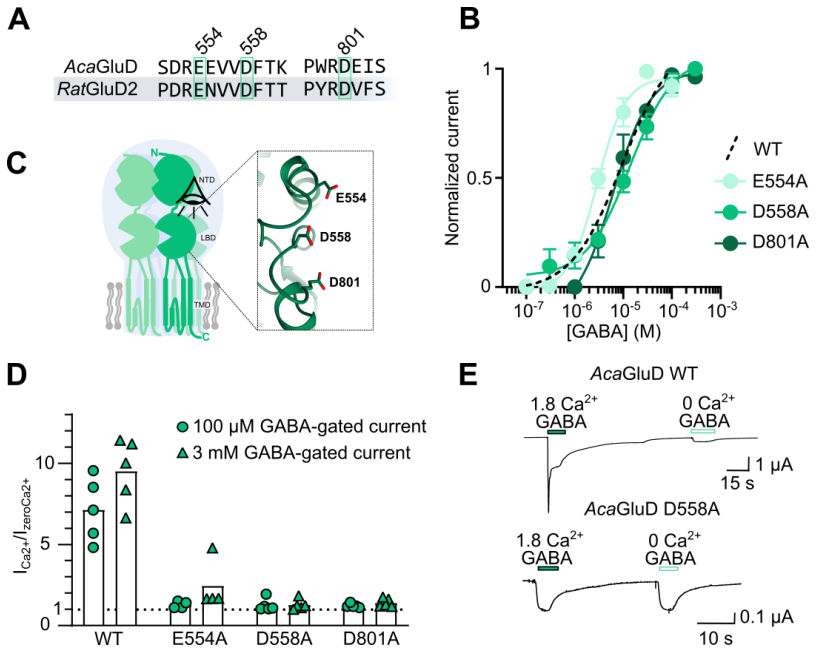

Figure 5.10: **E554, D558 and D801 are responsible for calcium modulation in *Aca*GluD** (A) Sequence alignment of *Aca*GluD with *Rat*GluD2, highlighting conserved residues implicated in calcium binding (*Aca*GluD numbering). (B) *Aca*GluD E554A, D558A and D801A mean ± SEM (n = 3, D801A; n = 4, all others) normalized (to maximum GABA-gated current at each oocyte) current amplitude in response to increasing GABA concentrations. (C) Cartoon illustrating structural domains of typical iGluR tetramer, one subunit highlighted, showing amino-terminal domain (NTD), ligand-binding domain (LBD), and transmembrane channel domain (TMD). Cell membrane in gray. (Inset) Alphafold structural model of *Aca*GluD indicating the positions of residues E554, D558, and D801 (top view). (D) Ca^{2+}-induced enhancement of GABA-gated currents ($I_{Ca2+}/I_{zeroCa2+}$) was similar for 100 µM GABA- and 3 mM GABA-gated currents (columns, mean; circles, individual data points). (E) Electrophysiological traces for *Aca*GluD WT and D558A mutant, showing current responses to 100 µM GABA in the absence and presence of 1.8 mM Ca^{2+}.

5.5 Conclusion

In this section of my thesis, I have sought to elucidate the pharmacological and biophysical properties of delta iGluRs. The study was driven by the discovery that numerous invertebrate wildtype delta iGluRs show ligand-gated currents in *Xenopus laevis* oocytes. Central to this investigation was the crown-of-thorns starfish *Aca*GluD receptor, which was selected for its

robust expression and significant ligand-gated current responses in the oocytes.

My work shows several ways in which the biophysical or pharmacological properties of delta receptors reflect their close evolutionary relationship with AMPA/KA receptors. Active delta iGluRs lack Mg^{2+} block, like AMPA/KA receptors. This means that invertebrate delta iGluRs could depolarize neurons in response to brief pulses of neurotransmitter and thus serve as principal synaptic receptors, as opposed to NMDARs which require prior depolarization by other means to release Mg^{2+} block and conduct. Furthermore, given that these receptors are mixed cation channels gated by GABA, their activation could lead to depolarizing excitatory currents, unlike type-A GABA receptors ($GABA_A$ receptors) that are predominantly chloride channels which exert inhibitory effects upon GABA binding. This implies that in the context of invertebrate delta iGluRs, GABA might play a unique excitatory role, diverging from its classical inhibitory function. However, this hypothesis regarding the putative excitatory role of delta iGluRs upon GABA binding and its functional implications within synaptic networks needs further investigation through in vivo/ex vivo studies.

In addition the pharmacological characterization of an active delta iGluR shows that delta iGluRs are modulated by AMPAR modulators. This suggests that physiological studies using e.g. DNQX to asses AMPAR contributions to circuits could also inadvertently alter delta iGluR function. This could result in misinterpretation of the role and significance of AMPARs in synaptic transmission and plasticity, as the observed effects might be partially attributed to the off-target modulation of delta iGluRs. Results from mutagenesis experiments on *Aca*GluD, combined with the observed effects of extracellular Ca^{2+} on current modulation, draw a parallel with the established mechanisms of calcium modulation in *Rat*GluD2^{Lc}. In *Rat*GluD2^{Lc} the proposed mechanism of potentiation of spontaneously active currents involves the stabilization of the dimer interface which in turn mitigates the structural adjustments responsible for desensitization (Hansen et al. (2009)). Calcium-mediated stabilization of the dimer interface could therefore be a biophysical signature of delta iGluRs, possibly an ancestral one, extending from vertebrate to invertebrate synapses. Given that the putative calcium-binding sites are located between up-

per lobes of adjacent ligand-binding domains, from two adjacent subunits, as in *Rat*GluD2, it's likely that calcium binding reinforces the coupling between these subunits. This strengthened interaction might ensures that upon agonist binding, the lower lobe undergoes more pronounced conformational changes that are then conveyed to the ion channel domain, resulting in robust activation.

When comparing the ligand-interacting amino acid residues between GABA- and D-serine-selective delta iGluRs my results shows that divergent residues close to the ligand do not alone determine ligand potency. In fact, as I was not able to find amino acid substitutions that govern ligand potency among clearly divergent residues, other factors might be responsible for the change in ligand sensitivity between vertebrate and invertebrate delta iGluRs. The notion that residues that do not directly interact with ligands can influence the potency and selectivity of ligand binding in iGluRs is not new. In fact, in GluD2 receptors the hinge region, situated between the two lobes of the ligand-binding domain, was identified as a critical determinant for D-serine affinity. In fact, mutations in the hinge region significantly altered the receptor's ligand-binding characteristics suggesting that the flexibility and conformational dynamics of the hinge region, which does not directly interact with the ligand, are paramount in tuning the receptor's response to the ligand, thereby affecting both potency and selectivity (Tapken et al. (2017)). Similarly, for the AMPA receptor GluA2 subunit, mutating Leu-650 to Thr, a residue outside the immediate ligand-binding site, caused a marked alteration in the receptor's responsiveness to AMPA and KA (Armstrong et al. (2003)). The crystallographic analyses of the mutant L650T receptor bound to different ligands revealed varying degrees of domain closure each associated with different ligand efficacies. I could expect that the same phenomenon might be at play in determining ligand sensitivity in delta receptors. My results suggests that elements beyond the immediate ligand-binding site, such as the overall conformational flexibility of the receptor, the spatial arrangement of amino acid residues, and potential allosteric sites, could be influential. My docking results omitted water molecules, a factor that likely impacts the outcomes, given that ligand binding in iGluRs frequently involves water interactions (Sahai and Biggin (2011)).

While the presence of water is not imperative for predicting the correct binding pose of ligands within these receptors, it does contribute significantly to the favorable interaction energy (Vijayan et al. (2010)). This suggests that, although preliminary docking can provide insights into potential binding configurations, a comprehensive understanding of ligand-receptor interactions within iGluRs would benefit from considering the role of water in mediating these processes. Detailed structural analyses, such as cryo-electron microscopy, can offer high-resolution images of the receptor in various states (e.g., resting, active or desensitized), elucidating the role of distant residues in ligand binding and receptor activation. Furthermore, molecular simulations might offer insights into the conformational changes that accompany ligand binding, providing a deeper understanding of the mechanisms at play and the determinants of GABA– or D-serine–affinity within the delta receptor family.

Chapter 6

Results III - Molecular basis for loss of GABA-gated currents in vertebrate delta iGluRs

The previous chapters of my thesis elucidated the functional characteristics of delta iGluRs, revealing the ability of these receptors to act as ligand-gated channels without the necessity for auxiliary protein, a characteristic that has been retained in delta iGluR of several invertebrate species. This, paired with phylogenetic insights that place delta iGluRs in close relationship with other ligand-gated channels such as AMPA/KA receptors points towards the hypothesis that when ancestral delta iGluRs first diverged from AMPA/KA receptors, they were ligand-gated channels that quickly evolved to be GABA-selective. When the major bilaterian animals diverged from each other, these GABA-gated delta iGluR were inherited by each lineage, but we observe remarkable functional divergence of delta iGluRs of vertebrates: the loss of ligand-gated channel activity and the switch to selective glycine and D-serine binding. Through a combination of comparative analysis, site-directed mutagenesis and functional characterization, this next section will delve into the molecular basis of this functional divergence, again mostly using *Aca*GluD as a template for mutagenesis analysis.

6.1 The N-terminal domain does not determine ligand-gated current in *Aca*GluD

I first focused my attention on the N-terminal domain (NTD) and sought to determine its contribution to the ligand-gated activity of starfish delta iGluR. It is well established that this large clamshell-like domain formed by ~400 amino acids facilitates subunit assembly, can accommodates certain allosteric modulators and can contribute to gating properties in most iGluRs, perhaps especially NMDA receptors (Hansen et al. (2010)). In AMPA receptors deletion of the NTD does not significantly impact functions such as transport to the cell surface, ligand binding properties and agonist-triggered channel activation (Pasternack et al. (2002)). In mammalian GluD2 receptors the NTD serves as platform for binding of extracellular protein cerebellin-1 (Cbln1) that in complex with presynaptic β-neurexin1 (β-NRX1) is important in maintaining synaptic stabilization and promoting synaptogenesis at parallel fibre–Purkinje cell synapses (Elegheert et al. (2016)). Moreover, it was also recently reported that the conformational flexibility of the NTD, with its splayed arrangement in vertebrate delta iGluRs, might be the cause of receptor inactivity, whereas a more compact structural arrangement, possibly facilitated by complexing with β-NRX1-Cbln1, enables agonist-induced current in GluD2 receptors (Carrillo et al. (2021); Elegheert et al. (2016)). Furthermore, comparative sequence analysis between *Aca*GluD and *Rat*GluD2 reveals a notably low sequence identity of 19% in the NTDs, in contrast to the 38% identity observed in both the ligand-binding and transmembrane domains (Fig. 6.1). This significant variability in the NTD suggests it may play a pivotal role in the functional divergence observed in vertebrate delta iGluRs, potentially contributing to their inactivity, for example by altered interactions between adjacent NTDs or NTDs and LBDs. To test if divergent NTDs in vertebrate delta iGluRs are the cause of their inactivity I decided to replace the NTD of *Aca*GluD with the one of *Rat*GluD2 and test whether this change would render the starfish receptor unable to be gated by GABA.

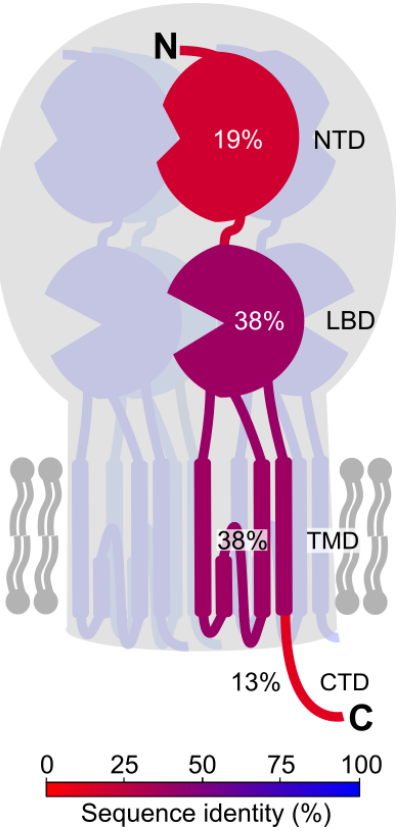

Figure 6.1: **Domain-specific comparative sequence identity between *Aca*GluD and *Rat*GluD2** Cartoon illustrating the percentage of sequence identity across different domains when comparing *Aca*GluD and *Rat*GluD2 iGluR subunits. The N-terminal domain (NTD), ligand-binding domain (LBD), and transmembrane domain (TMD) are shown with corresponding sequence identity percentages.

I created two chimeric *Aca*GluD constructs (see Methods page 23). These constructs were engineered by substituting the NTD of *Aca*GluD with that of *Rat*GluD2, while varying the NTD-LBD linkers between species. The first construct, named *Aca*GluD$^{\text{RatNTD}}$ integrates the *Rat*GluD2 NTD while preserving the original NTD-LBD linker from *Aca*GluD. The second construct, *Aca*GluD$^{\text{RatNTDlink}}$ incorporates both the NTD and its corresponding NTD-LBD linker from *Rat*GluD2. This allowed me to measure ligand-gated currents and assess the functional impact of these domains and their linkers (Fig. 6.2).

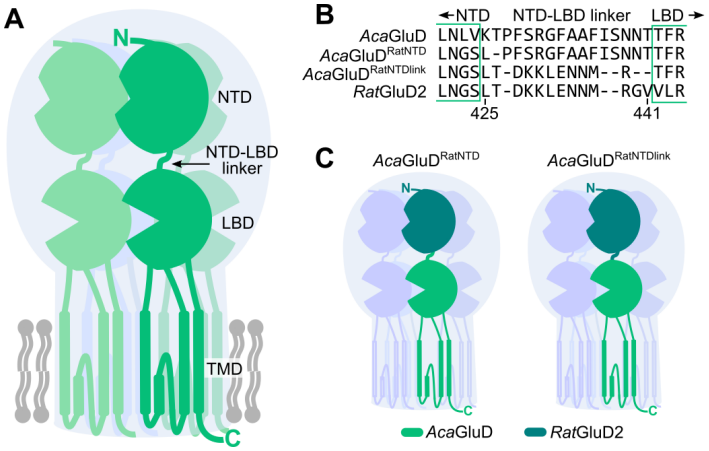

Figure 6.2: ***Aca*GluD$^{\text{RatNTD}}$ and *Aca*GluD$^{\text{RatNTDlink}}$ chimera design** (A) Cartoon illustrating structural domains of typical iGluR tetramer, one subunit highlighted, showing amino-terminal domain (NTD), ligand binding domain (LBD), and transmembrane channel domain (TMD). Cell membrane in gray. (B) Amino acid sequence alignment of linker region and illustrating chimera design. (C) Cartoon illustrating chimeras with color specific domain.

Contrary to expectations based on recent research suggesting that the high flexibility of the NTD in *Rat*GluD2 is the primary determinant of receptor inactivity (Carrillo et al. (2021)), the substitution of *Rat*GluD2 NTD into *Aca*GluD had minor, if any, impact on ligand-gated activity. Both chimeric constructs, *Aca*GluD$^{\text{RatNTD}}$ and *Aca*GluD$^{\text{RatNTDlink}}$ exhibited significant GABA-gated currents, similar to those observed in wildtype *Aca*GluD (Fig. 6.3). The only difference I found when testing the chimeras was small increase in relative D-serine efficacy in *Aca*GluD$^{\text{RatNTDlink}}$ when compared to *Aca*GluD$^{\text{RatNTD}}$ or wildtype *Aca*GluD (Fig. 6.3). The construct retaining both the N-terminal domain and the NTD-LBD linker of *Rat*GluD2 had a relative efficacy of D-serine ligand-gated currents of 20 ± 3 % (n = 3) relative to GABA, while relative efficacy of D-serine at *Aca*GluD$^{\text{RatNTD}}$ and wildtype *Aca*GluD was only 4.5 ± 0.5 % (n = 3) and 12 ± 3 % (n = 7) respectively (Fig. 6.3). This is in line with findings on NMDARs that demonstrates that the region formed by the GluN2 subunit (GluN2A to GluN2D) N-terminal domain and the short linker connecting the NTD to the agonist-binding domain controls the subunit-specific gating proprieties and agonists potency of NMDARs (Gielen et al.

(2009)). Thus, the change in ligand efficacy among the chimeric constructs suggests that the NTD-LBD linker is coupled to the channel gating apparatus, but overall these results show that the substantial differences in the NTDs between *Aca*GluD and *Rat*GluD2 do not play a key role in the loss of function observed in vertebrate delta iGluRs compared to delta iGluRs in other deuterostomes.

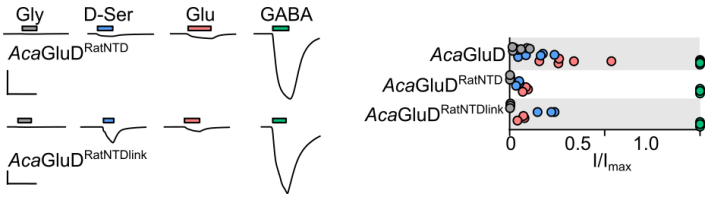

Figure 6.3: **RatGluD2 NTD does not abolish the activity of starfish *Aca*GluD iGluRs** Left, Ligand-gated currents in oocytes expressing mutant *Aca*GluD receptors containing the NTD from at GluD2 (*Aca*GluD^{RatNTD}) or the NTD and NTD-LBD linker from *Rat*GluD2 (*Aca*GluD^{RatNTDlink}). (Scale bars: x, 10 s; y, 2 µA). Right, Summarized data normalized to maximum GABA-gated current at each oocyte from experiments illustrated left.

6.2 *Rat*GluD2-like mutations in the LBD and TMD significantly alter *Aca*GluD activity

Chapter 6.1 results indicate that the molecular determinants of vertebrate delta iGluRs inactivity must be found outside the NTD, namely in the ligand binding domain (LBD), transmembrane domain (TMD) or in the intracellular C-terminal domain (CTD) of the receptor. Presumably, in early vertebrate delta iGluRs, mutations must have occurred at amino acid positions important for ligand-gated channel activity in the LBD, TMD and/or CTD, and at these positions, extant inactive vertebrate delta iGluRs must differ from active invertebrate delta iGluRs. Moreover, the active delta iGluRs probably show conservation of biophysical properties of the amino acids at these positions, whereas the amino acids at these positions might differ among inactive delta iGluRs which have already lost activity. I therefore generated a sequence alignment of active and inactive delta receptors, including those characterized in Chapter 4: *Aca*GluD, *Sac*GluD, *Dio*GluD (active ligand-gated receptors); and *Dan*GluD2A, *Rat*GluD1, and *Rat*GluD2 (rela-

tively inactive receptors). I focused on the LBD and TMD, excluding the long intracellular CTD from this analysis, because in mammalian delta iGluRs the CTD is mostly responsible for receptor trafficking (Tao et al. (2019)), exhibits an intrinsically disordered conformation (Choi et al. (2011)), and its deletion does not render receptors inactive (Maki et al. (2012); Puddifoot et al. (2009); Burada et al. (2020a)). Among roughly 410 positions of the LBD and TMD, I looked for amino acid residues that were (1) conserved or biophysically similar in active delta iGluRs and (2) different from this in inactive delta iGluRs. From this analysis I identified a total of 41 sites (Fig. 6.4).

Continuing with *Aca*GluD as my primary experimental model, I embarked on a comprehensive mutational analysis. Each of the 41 amino acid residues identified in my alignment was substituted with its counterpart from the inactive *Rat*GluD2. For efficiency, in two cases, two residues that were close together were mutated together in single constructs. This led to the creation of 39 mutant *Aca*GluD receptors. Figure 6.5 A shows the 41 positions on an homology model of *Aca*GluD receptor based on the X-ray structure of rat GluA2 receptor (Sobolevsky et al. (2009)) (this is higher resolution than the full-length GluD1 cryoEM structure (Burada et al. (2020a))). In order to assess the functional impact of these substitutions, I tested the responses of these mutants to high concentrations of GABA, glutamate, glycine and D-serine and looked for loss of or significant reduction in ligand-gated currents relative to WT. Out of the 41 amino acid substitutions, thirty-one exhibited minimal impact on the receptor's activity. These mutant receptors continued to demonstrate robust responses to GABA and comparatively smaller currents to glutamate, glycine and D-serine (Fig. 6.5 B–C) indicating that the vertebrate-like mutation at play did not alter the receptor's gating by GABA or other ligands.

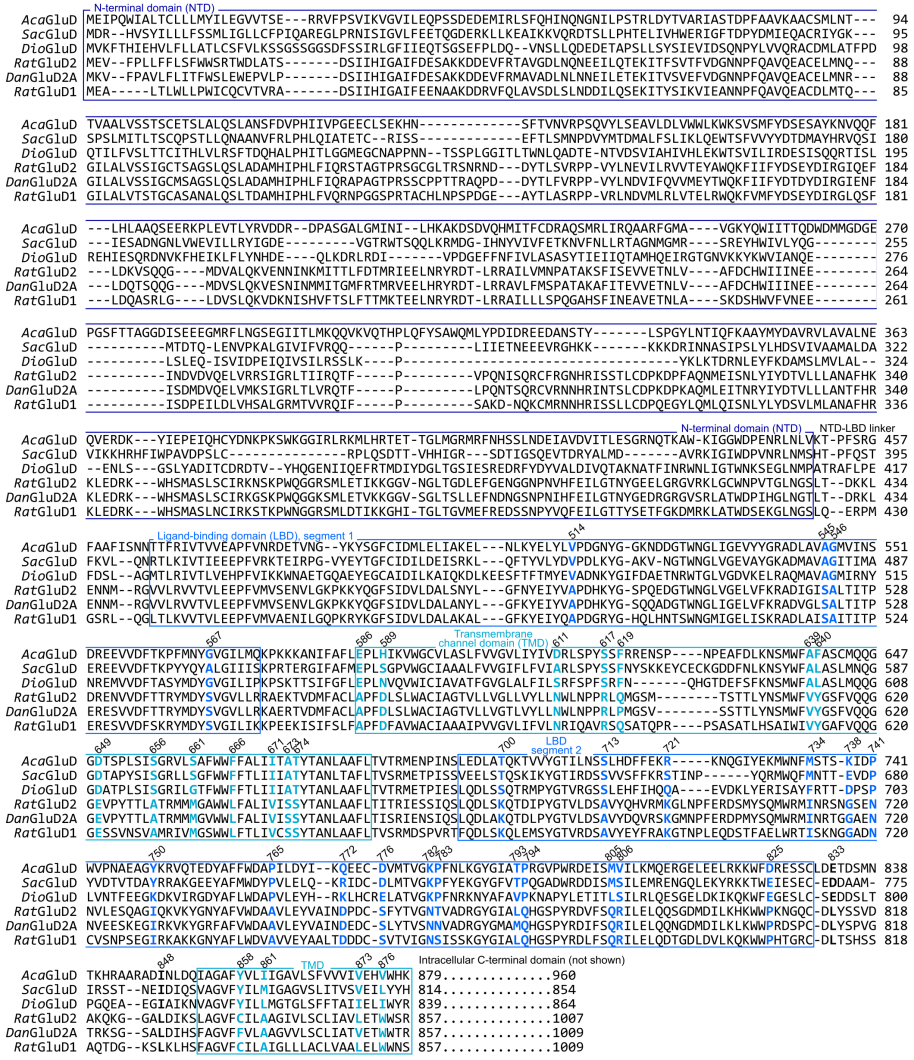

Figure 6.4: **Alignment of active and inactive delta iGluRs** Major tertiary structural elements are indicated as boxes and labeled, as inferred from high-resolution structures of mouse GluD1 N-terminal domain (Elegheert et al. (2016)) and rat GluD2 ligand-binding domain (Naur et al. (2007)) and moderate-resolution structures of human GluD1 and GluD2 full-length receptors (Burada et al. (2020a); Burada et al. (2020b)). Bold cyan and blue, residues that differ between active *Aca*GluD, *Sac*GluD, and *Dio*GluD iGluRs and verified inactive vertebrate delta iGluRs receptors. Numbers refer to *Aca*GluD positions that were mutated.

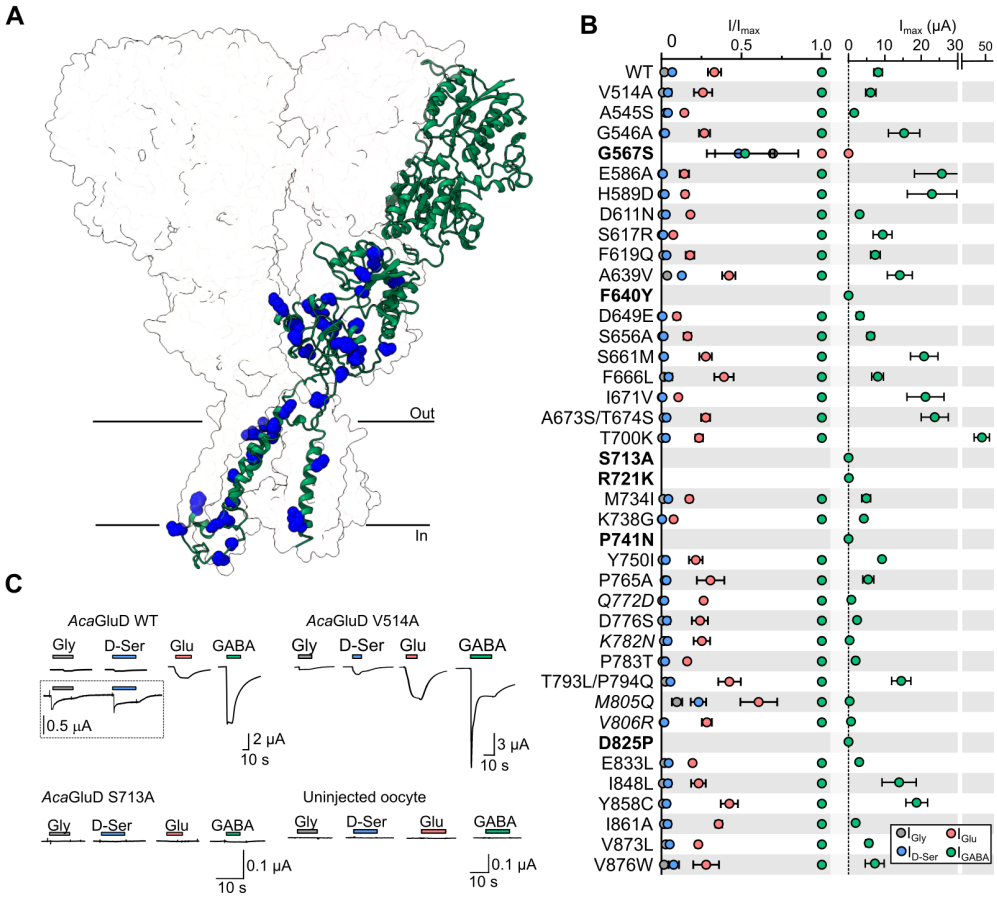

Figure 6.5: **Comparative analysis** (A) 41 amino acid residues (blue spheres) selected for mutagenesis scanning in a single subunit of homology model *Aca*GluD. (B) Relative ligand-gated current amplitude ("I/I_{max}", left) and maximum current amplitude ("I_{max}", right) at wild-type (WT) and mutant *Aca*GluD receptors (mean ± SEM, n = 3 to 5). Bold, mutations that substantially altered receptor function. Italic, mutations that decreased maximum GABA-gated current amplitude to less than 1 μA. (C) Ligand-gated currents in oocytes expressing indicated mutant *Aca*GluD receptors or uninjected oocytes.

Six mutations substantially altered receptor function (bold labels in Fig. 6.5 B). Oocytes injected with *Aca*GluD G567S showed substantial change in relative agonist efficacies and greatly reduced current amplitude of all four agonists tested (Fig. 6.5 B). Oocytes injected with *Aca*GluD mutants F640Y, S713A, R721K, P741N, and D825P displayed no ligand-gated receptor activity, with their responses comparable to those observed in uninjected oocytes (Fig.

6.5 B–C). To determine whether this absence of activity was due to decreased surface expression or other functional changes, I performed immunolabeling assays to detect *Aca*GluD on the cell surface via an engineered c-Myc tag in the *Aca*GluD C-terminal, a mouse anti-cMyc primary antibody, and a goat anti-mouse fluorescent dye conjugate secondary antibody. This showed that F640Y, S713A, and R721K mutants were reasonably well expressed on the oocyte surface, indicating that their loss of activity primarily resulted from alterations in channel function rather than decreased surface expression. However, for the P741N and D825P mutants, while surface expression was detectable under the confocal microscope, it was substantially reduced compared to WT (Fig. 6.6 A–B). This could indicate that the lack of ligand-gated activity in these mutants can be attributed to a combination of altered channel function and, to some extent, diminished receptor presence at the oocyte surface.

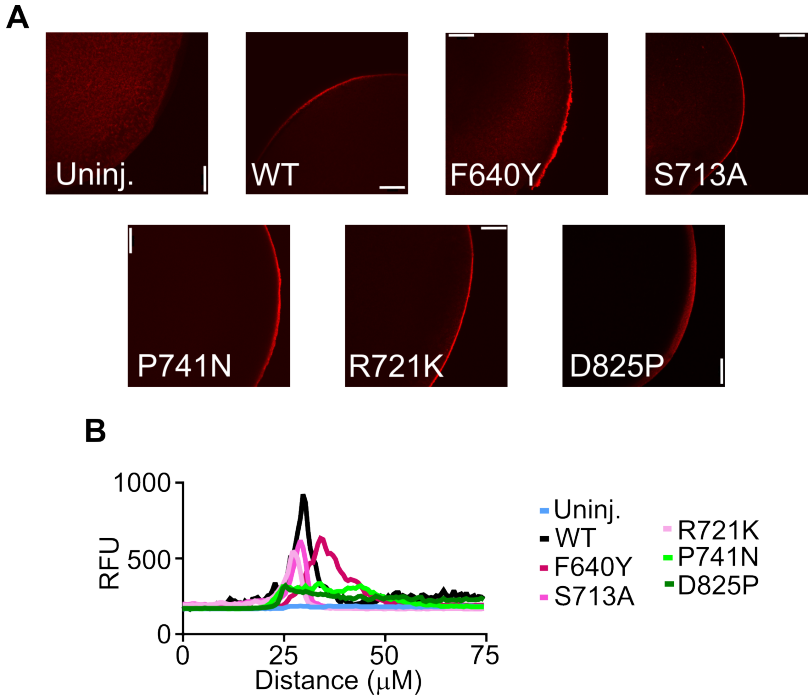

Figure 6.6: **Immunolabeling c-Myc tag in *Aca*GluD C-terminal** (A) Example micropgraphs of uninjected, WT and mutants *Aca*GluD receptors (White scale bars, 100 μm). (B) Random fluorescence units (RFU) plotted against relative radial distance, peaking at the oocyte surface.

In addition, I observed that four other mutants—Q772D, K782N, M805Q, and V806R—exhibited less pronounced, yet still noticeable, changes in receptor function (italic labels in Fig. 6.5 B). These four variants demonstrated a noticeable decrease in their maximum GABA-gated current amplitude, dropping to less than 1 µA (Fig. 6.5 B). This is a substantial reduction compared to the 8.2 ± 1.1 µA observed in WT receptors (n = 4). Despite this decrease in current amplitude, these mutants maintained the typical agonist selectivity profile characteristic of the WT receptors (Fig. 6.5 B). This observation suggests that these particular amino acid positions, while not critically essential for maintaining receptor activity, do play a role in the receptor's response to its agonists, whether by altered agonist potency, gating equilibrium, or surface expression.

In exploring the potential influence of these 10 residues on receptor function, I considered their locations within the receptor's tertiary structure. In doing so, I looked at the homologous residues in the context of published cryo-electron microscopy structure of rat AMPA receptor GluA2 (Twomey et al. (2017)) (Fig. 6.7 B). This indicated that only one of these positions (F640) is found in the TMD of the receptor in the second helix, abutting the channel pore (Fig. 6.7). Its mutation might induce some conformational changes in the pore that could render the channel inactive or might result in an improper folding of the receptor.

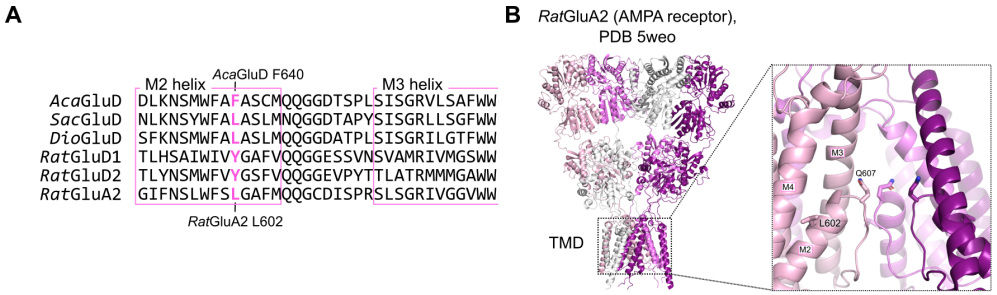

Figure 6.7: **Position of *Aca*GluD F640 in corresponding *Rat*GluA2 structure** (A) Amino acid sequence alignment of membrane-embedded helical segments M2 and M3 from selected delta iGluRs and rat AMPA receptor (*Rat*GluA2). (B) Cryo-electron microscopy structure of RatGluA2 (PDB: 5WEO, Twomey et al. (2017)) and magnified view of the channel pore showing the location of *Rat*GluA2 L602, equivalent to *Aca*GluD F640, in comparison to pore-lining residue RatGluA2 Q607. Helices and selected residues for one subunit are labeled.

The remaining nine residues are all positioned within the ligand binding domain of the receptor and for insight into their position I have utilized the *Aca*GluD AlphaFold structural model introduced in Chapter 5.2.1. Interestingly, seven of these nine amino acid residues (G567, S713, R721, P741, K782, Q772 and D825) are found in the lower lobe of the LBD clamshell (Fig. 6.8). This region is known for its role in the gating process of glutamate receptors: its upwards movement during binding of the neurotransmitter is a crucial conformational change that via the LBD-M3 linker pulls the M3 helix away from the center of the pore allowing the channel to open (Twomey et al. (2017), Chen et al. (2017)). Finally, M805 and V806 are found on the upper lobe of the ligand binding domain. It's important to note that with the exception of S713 all the remaining positions in the ligand binding domain are not in close proximity to the putative bound ligand and in fact G567, R721, D825, and K782, located in the lower lobe, along with M805 and V806 in the upper lobe, are positioned on the back side of the ligand binding domain. It is therefore possible that they interact with the corresponding back of an adjacent ligand binding domain, as LBDs from two subunits form one of the two dimers that form the homotetrameric structure of the receptor. This interface is also of great importance as it was demonstrated that in AMPA receptors, desensitization is achieved via a rearrangement of the dimer interface where there's a significant dissociation of the two adjacent upper lobes and thus the tearing apart this interface causes the receptor to be in a closed but non conductive state (Twomey et al. (2017); Sun et al. (2002); Stern-Bach et al. (1998)). The interface, especially regarding lower lobe residues, is also important for recovery from desensitization in AMPARs and KARs, ensuring that receptors avoid long lived desensitized states (Carbone and Plested (2012)).

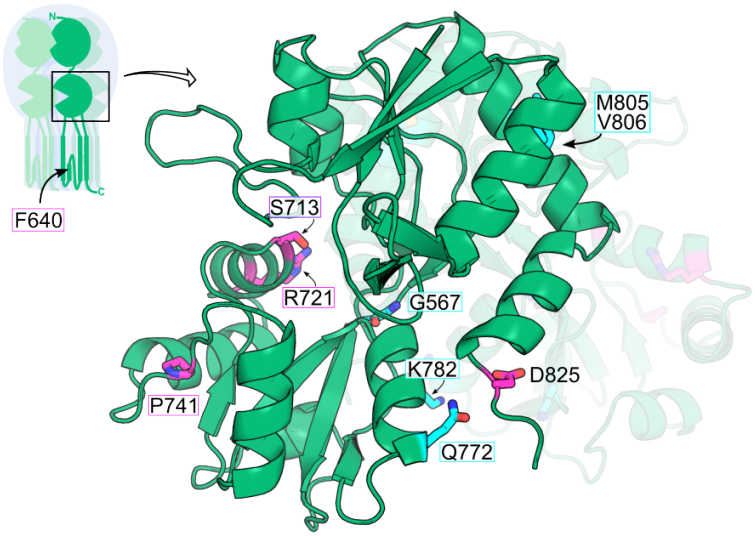

Figure 6.8: **Structural analysis of *Aca*GluD ligand binding domain highlighting key functional residues** AlphaFold model of two adjacent *Aca*GluD LBDs (rear LBD faded). Selected amino acid residues colored and shown as sticks. Magenta, drastic loss of function; cyan, moderate loss of function. Inset cartoon shows LBDs within full-length receptor and approximate position of F640 residue.

Thus, my comparative analysis identifies 10 residues situated in critical regions of the receptor that could determine the inactivity of vertebrate delta iGluRs. In the next section I will focus on the five specific mutations that led to the inactivation of *Aca*GluD, hoping to establish how these residues alter receptor activity.

6.2.1 Vertebrate-like mutations in the lower lobe of the LBD induce an inactive channel state in *Aca*GluD

It is well established that in AMPA/KA iGluRs, the interplay between interfacing LBDs is crucial for modulating the receptor's response to agonists by governing the transitions into and out

of desensitized states (Carbone and Plested (2012)). Given the close evolutionary relationship between delta iGluRs and their AMPA/KA counterparts highlighted in Chapter 4.1, and noting the location of the *Aca*GluD substitutions S713A, R721K, P741N, and D825P at or near the LBD interface, I hypothesized that the inactivity observed in the mutants may be due to perturbed LBD dynamics, potentially leading to heightened desensitization relative to the WT *Aca*GluD. For AMPA/KA receptors, the desensitization process can be modulated by lectins, in particular by plant lectin concanavalin A (ConA), a protein that can bind to specific carbohydrate molecules including glycans that are added to receptor asparagine side chains through the process of N-glycosylation (Kehoe (1978); Mayer and Vyklicky Jr. (1989)). Because ConA, via its desensitization-inhibiting effect, potentiates currents in AMPA receptors and even more so in KA receptors (Everts et al. (1997)) I decided to treat oocytes injected with *Aca*GluD-mutants that had no ligand-gated receptor activity with 10 µM ConA (calculated for the tetrameric ConA) and test for restoration of GABA-gated currents, which might indicate that their inactivity was due to desensitization. Remarkably, the application of ConA to *Aca*GluD mutants F640Y, S713A, and R721K produced an extraordinary enhancement of receptor activity leading to an increase in GABA-gated currents of 533 ± 143 (n = 4), 171 ± 59 (n = 4) and 76 ± 17 (n = 5) fold respectively bringing the responsiveness of these mutants into a range similar to that observed in WT channels (Fig. 6.9). This pronounced recovery of function starkly contrasts with the effects seen in the P741N and D825P mutants. While the latter did exhibit a modest 4 ± 1 (n = 4) fold increase in current amplitude with ConA treatment, bringing it closer to WT levels (6 ± 1, n = 3) the P741N mutant showed no restored function in ConA (Fig. 6.9).

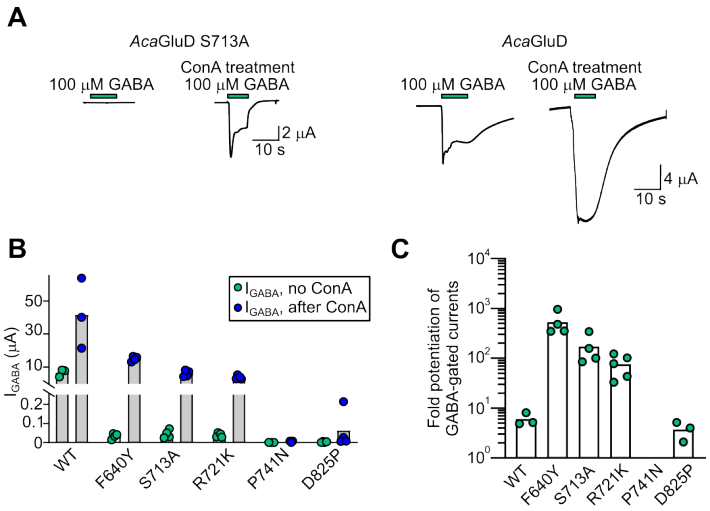

Figure 6.9: **Impact of ConA on loss-of-function-*Aca*GluD mutants** (A) Electrophysiological traces comparing the response of *Aca*GluD S713A mutant and wild-type *Aca*GluD to 100 µM GABA before and after ConA (10 µM) treatment. (B) Summarized current responses to 100 µM GABA ("I_{GABA}") in WT or mutant *Aca*GluD-expressing oocytes before or after treatment with ConA. (C) Fold potentiation of GABA-induced currents by ConA treatment across wild-type and selected *Aca*GluD mutants (logarithmic scale; columns, mean; circles, individual data points).

This result suggests that the mutations which render active delta iGluRs inactive do so by increasing the receptor's preference for a desensitized or another functionally inactive state. Specifically, two substitutions that mimic those found in vertebrate delta iGluRs in the lower lobe of the ligand binding domain (S713A and R721K) appear to lock the receptor in a desensitized state, a condition that can be at least partially reversed by ConA treatment. Similarly, F640Y seemed to induce a desensitized state, but in contrast to the other positions, F640 is in the TMD, in the short M2 α-helix and adjacent to the lower pore. Perhaps the relatively small addition of a hydroxyl moiety to the F640 side chain induces desensitization by pushing on the pore, but it seems curious that ConA would rescue the channel from this mechanism. Instead, it could be that F640Y allosterically alters the activity of the LBD, as has been suggested for e.g. upper-M3 mutations in AMPA receptors, where the mutation A643V in homomeric GluA2 receptors has been showed to cause a gain-of-function phenotype with altered desensitization when compared to WT receptors (Coombs et al. (2022)). Meanwhile, two other substitutions

akin to those in vertebrate delta iGluRs predominantly impede the receptor's surface expression. The fact that desensitization or inactivation could be responsible for the lack of observable currents in *Aca*GluD channels carrying vertebrate delta iGluR-like mutations, led me to consider if WT vertebrate delta iGluRs are inactive due to a similar mechanism. I therefore tested the effects of ConA on WT rat delta receptors. Despite these efforts, the ConA treatment did not elicit any change in activity; GluD1 and GluD2 receptors remained as unresponsive as their untreated counterparts (Fig. 6.10 A). My findings indicate that the persistent inactivity of WT vertebrate delta iGluRs cannot be solely rescued by ConA treatment, suggesting that either (1) the relationship between desensitization and loss of function in *Aca*GluD mutants does not reflect the evolutionary loss of function in vertebrate GluD receptors or (2) vertebrate GluD receptors lack the relevant glycosylation sites that enable it to be probed this way (Fig. 6.10 B,C), and would need other drugs to test this hypothesis.

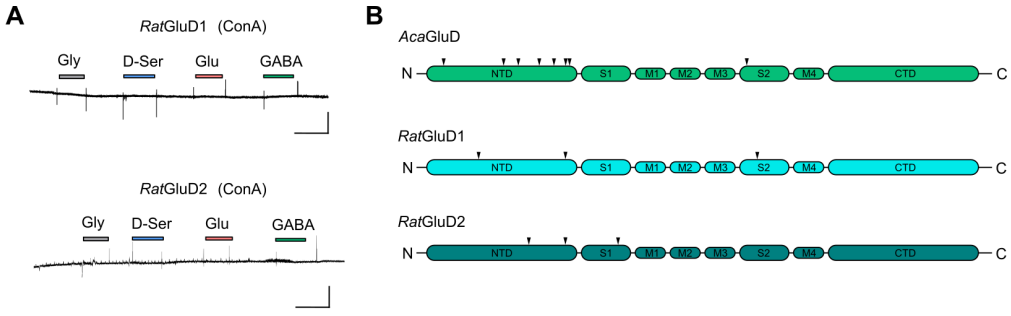

Figure 6.10: **Impact of ConA on *Rat*GluD1 and *Rat*GluD2 and predicted N-glycosylation sites in *Aca*GluD and *Rat*GluD1/2** (A) Example recordings of oocytes expressing wildtype *Rat*GluD1 or *Rat*GluD2 after oocytes were incubated in 10 µM ConA for 5-10 min. (Scale bars: x, 10 s; y, 0.2 µA). (B) Approximate position of NXS/T sites predicted from the web server NetNGlyc in *Aca*GluD and *Rat*GluD1/2 shown as triangles.

6.3 Starfish-like mutations partly reawaken inactive *Rat*GluD2 receptors

If the ten mutations previously discussed were indeed central to the change in function of *Aca*GluD receptors, where 5 mutations abolished ligand-gated currents, 4 mutations greatly reduced it and one additional mutation caused a change in ligand sensitivity, it stands to reason that introducing active starfish-like mutations in the equivalent positions of the dormant vertebrate receptors might restore their activity. Pursuing this line of investigation, I introduced these modifications to *Rat*GluD2, substituting specific residues with their counterparts from the functionally active starfish delta iGluR. The resulting multiple-mutant constructs were *Rat*GluD2^{5x} that carried Y613F, A686S, K694R, N720P, and P806D substitutions, combining the mutations that abolished ligand-gated current in *Aca*GluD receptors (highlighted in pink in Fig. 6.11) and *Rat*GluD2^{9x} that carried the same 5 mutations from *Rat*GluD2^{5x} with the additional N763K, D753Q, Q786M, and R787V mutations that greatly reduced ligand-gated current in *Aca*GluD receptors (highlighted in cyan in Fig. 6.11).

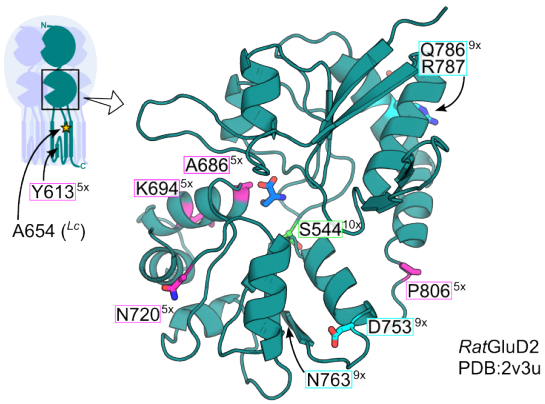

Figure 6.11: **Gain-of-function residues highlighted on X-ray structure of ligand binding domain of *Rat*GluD2** D-serine bound RatGluD2 from X-ray structure (PDB: 2V3U (Naur et al. (2007))). Selected amino acid residues are indicated, colored, shown as sticks, and labeled 5×, 9×, 10× according to the multiple mutants they were incorporated into. 10× mutant included 10×, 9×, and 5× positions. 9× included 9× and 5×. 5× included only 5×. The Inset cartoon shows LBD within full-length receptor and approximate position of Y613 and lurcher mutation.

Furthermore, anticipating the potential persistence of inactivity in these mutants, I created A654T (Lc) mutant versions—*Rat*GluD2$^{Lc\text{-}5x}$ and *Rat*GluD2$^{Lc\text{-}9x}$. The rationale behind this approach was the hypothesis that the constitutively active Lc-variants might reveal subtle nuances of ligand sensitivity and still valuable insight, should the initial mutant constructs fail to exhibit restored function. Electrophysiological experiments revealed that neither mutant-*Rat*GluD2^{5x} and *Rat*GluD2^{9x}-responded to glycine, D-serine, GABA, or glutamate also in oocytes treated with ConA (Fig. 6.12). It could be that among the other 31 substitutions that have accumulated in rat delta iGluRs, there are some that are not enough to render *Aca*GluD inactive on their own in my experiments; but the full activity of delta iGluRs via the crucial 10 residues discussed may be contingent upon the identity of these less "noticeable" 31 amino acid residues. This absence of activity underscores the complexity of receptor function and suggests that these particular mutations do not singularly dictate the ligand-gated activity in vertebrate delta iGluRs.

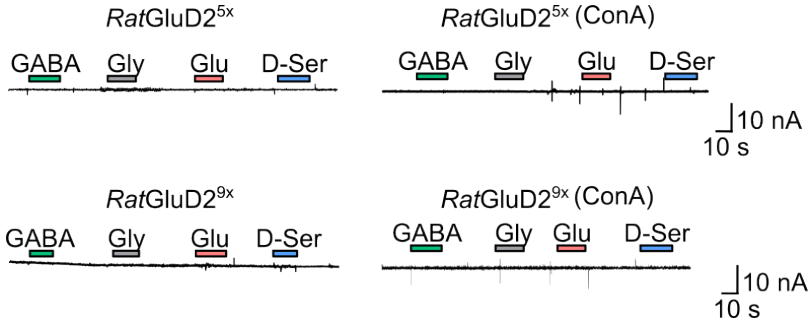

Figure 6.12: ***Rat*GluD2^{5x} and *Rat*GluD2^{9x} are not ligand-gated receptors** Example recordings of oocytes expressing *Rat*GluD2^{5x} and *Rat*GluD2^{9x} to different neurotransmitters ligands (30 mM) without (left) and with (right) 10 µM ConA incubation for 5-10 min.

Examining the Lc-version *Rat*GluD2$^{Lc\text{-}5x}$ and *Rat*GluD2$^{Lc\text{-}9x}$ mutants was illuminating. The *Rat*GluD2$^{Lc\text{-}5x}$ variant displayed characteristics akin to the standard Lc mutant, *Rat*GluD2^{Lc}, maintaining constitutive activity that was inhibited by the application of glycine, D-serine (30 mM each) and by the pore blocker pentamidine (100 µM). When glutamate (L-Glutamic acid monosodium salt monohydrate (MSG), 30 mM) was applied to *Rat*GluD2$^{Lc\text{-}5x}$, a small inward current was detected (Fig. 6.13 A, D). This inward current can be postulated to result from an

increase in the concentration of sodium ions in the extracellular environment from MSG that flow through the channel. However, the *Rat*GluD2$^{Lc\text{-}9x}$ mutant presented a remarkable departure from this behavior; it remained inactive at rest yet exhibited discernible inward currents upon glycine application that were inhibited by pentamidine (Fig. 6.13 B, D). In a continued effort to elucidate the effect of all the 10 mutations that altered the function of *Aca*GluD, my investigation extended to the creation of *Rat*GluD2$^{Lc\text{-}10x}$. This construct included the S544G mutation (highlighted in green in Fig. 6.11), a reverse of the G567S substitution in *Aca*GluD that was previously found to modify ligand selectivity (Fig. 6.5 B on page 72). Notably, this additional mutation did induce a perceptible change; *Rat*GluD2$^{Lc\text{-}10x}$ receptors showed inward currents when exposed to both 30 mM of glycine and D-serine (Fig. 6.13 C), indicating a change in ligand selectivity (Fig. 6.13 D). Therefore, simply incorporating key amino acids from active delta iGluRs into their inactive vertebrate counterparts is not sufficient to restore their activity. However, within the context of an engineered Lc-mutant, this strategy awakens the gating mechanism, resulting in *Rat*GluD2 channels that are at rest and gated by the binding of glycine and D-serine.

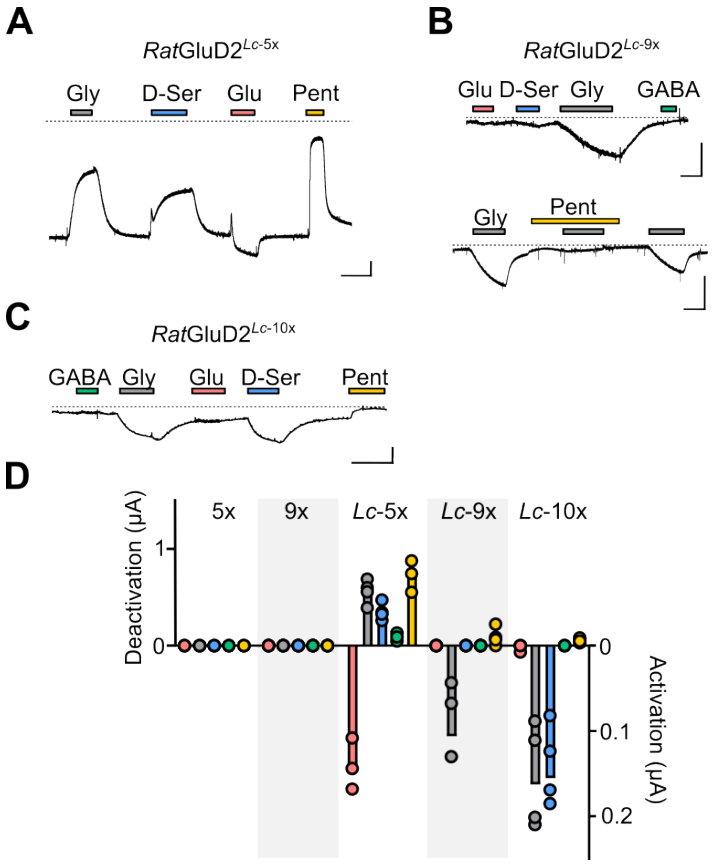

Figure 6.13: ***Rat*GluD2$^{Lc\text{-}5x}$, *Rat*GluD2$^{Lc\text{-}9x}$ and *Rat*GluD2$^{Lc\text{-}10x}$ exhibit different biophysical characteristics** (A)-(C) Example current responses to different neurotransmitter ligands (30 mM) and to pore blocker pentamidine (Pent, 100 µM) in oocytes expressing indicated *Rat*GluD2 mutants. The dashed line indicates zero current baseline. (Scale bars: x, 10 s; y, 0.1 µA). (D) Individual (dots) and mean (columns) responses to ligands in oocytes expressing indicated *Rat*GluD2 mutants (n = 4 to 5).

Upon observing that the S544G mutation induced a shift in ligand sensitivity within the *Rat*GluD2$^{Lc\text{-}10x}$ receptors-as observed with the reverse G567S in *Aca*GluD mutation-I decided to investigate the effect of this mutation when introduced in isolation to the *Rat*GluD2^{Lc} mutant context. The S544G mutation in the *Rat*GluD2^{Lc} context resulted in an enhanced inhibitory response to both glycine and D-serine compared to the lurcher variant and an enhanced sensitivity to glutamate (Fig. 6.14 A,B). Specifically, D-serine exhibited an inhibition of 88 ± 7 % (n =

4), glycine 92 ± 3 % (n = 4), and glutamate 25 ± 2 % (n = 3), in relation to the inhibition by pentamidine. This contrasts with *Rat*GluD2^{Lc} mutant alone, which showed a lower inhibition by D-serine at 69 ± 1 % (n = 5), glycine at 49 ± 1 % (n = 5), and glutamate at 5 ± 1 (n = 5) % relative to that of pentamidine (Fig. 6.14 C).

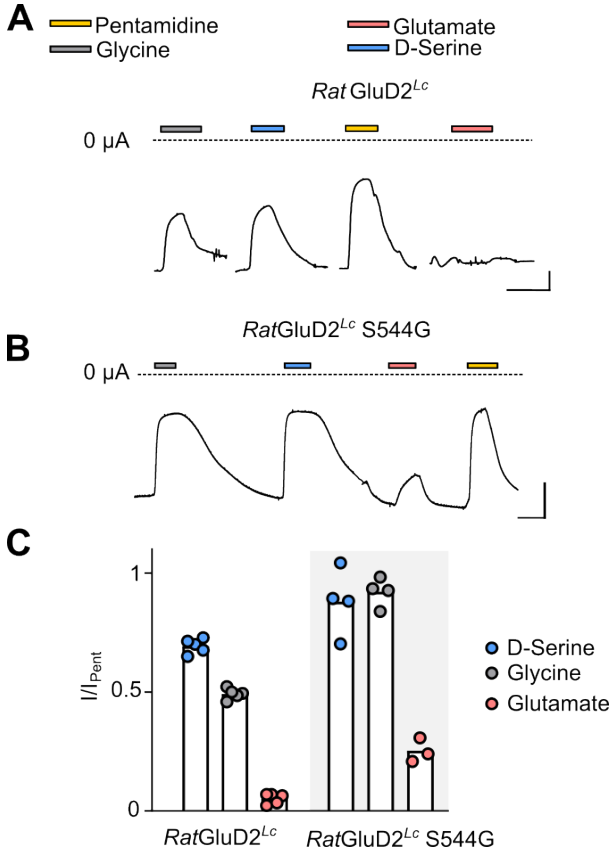

Figure 6.14: **Effect of S544G mutation in *Rat*GluD2^{Lc}** (A) – (B) Example current responses to different neurotransmitter ligands (30 mM) and to pore blocker pentamidine (100 µM) in oocytes expressing (A) *Rat*GluD2^{Lc} and (B) *Rat*GluD2^{Lc} S544G mutant. The dashed line indicates zero current baseline. (Scale bars: x, 10 s; y, 0.5 µA). (C) Fraction of current inhibited by different neurotransmitter ligands relative to 100 µM pentamidine. Individual (dots) and mean (columns) responses to ligands in oocytes expressing *Rat*GluD2^{Lc} and *Rat*GluD2^{Lc} S544G mutant.

In summary, the data reveal the intricate dynamics of receptor functionality and ligand sensitivity, underscored by the pivotal role of the S544G mutation. This residue is situated within

the hinge region of the ligand binding domain, two β-strands that link upper and lower lobes and are seven to nine Å behind the bound ligand. This region, serving as a critical juncture for conformational flexibility, presumably enables the ligand binding domain to undergo the necessary adjustments for receptor activation.

6.4 Conclusion

In this section of my thesis, I aimed to uncover the molecular determinants behind the loss of GABA-gated currents in vertebrate delta iGluRs. This was motivated by my observations suggesting that while the core gating machinery of vertebrate delta iGluRs appears intact (Naur et al. (2007)), key evolutionary changes might underlie their inactivity. My initial investigations centered on the receptor's N-terminal domain. Its splayed conformation was demonstrated to be crucial for the inactivity of rat GluD2 receptors (Carrillo et al. (2021)), yet complete deletion of the domain caused only minor effects on GluD2 (Carrillo et al. (2021)), AMPA (Bedoukian et al. (2006)) and NMDA receptors (Gielen et al. (2009)). Substituting the NTD from inactive vertebrate delta iGluR into the active starfish delta receptor (*Aca*GluD) proved to not compromise the receptor's activity. The change in ligand sensitivity observed in *Aca*GluD receptors incorporating the NTD from *Rat*GluD2 and the short linker bridging the NTD and LBD (Fig. 6.3, page 69) aligns with findings from NMDA receptor (Gielen et al. (2009)). In the cited study, swapping the NTD and the linker region between different GluN2 subunits resulted in changes in the receptor's maximal open probability (P_0) and sensitivity to endogenous inhibitors. With the data presented here I can therefore suggest that the linker region plays a key role in determining also delta receptors pharmacological characteristics, likely by influencing the conformational dynamics between the NTD and LBD but the overall loss of function of vertebrate delta iGluRs is likely not to be a result of mutations occurred in the NTD.

Comparing amino acids sequences between active and inactive delta iGluRs revealed profound insights into the molecular mechanisms that govern receptor activity. In particular, five mutations that occurred in the vertebrate lineage of delta iGluRs caused a striking loss of function

when introduced to the active starfish delta iGluR. Two of these mutations, P741N and D825P, lead to a reduced cell surface expression probably causing an improper folding, assembly, or trafficking of the receptor complex to the membrane of the cell. Three other mutations, two of which are located in the lower lobe of the LBD (S713A and R721K) and one in the TMD (F640Y) rendered the receptor inactive by potentially locking the receptor in a desensitized, or another inactive, state. The phenomenon of receptor desensitization is a critical regulatory mechanism in neurotransmission, allowing for the fine-tuning of synaptic strength and preventing overexcitation that could lead to neurotoxicity (Shaffer et al. (2013); Choi et al. (1988)). Based on the results from introducing vertebrate-like mutations into active delta receptors, it becomes plausible to speculate that the inherent inactivity observed in vertebrate delta iGluRs may come from the receptors being in a more desensitized-like state.

My efforts aimed at reversing loss-of-function mutations within vertebrate delta iGluRs revealed that reverse substitutions alone were insufficient to restore ligand-gated activity. This outcome could suggest that vertebrate delta iGluRs have accrued additional mutations over evolutionary time, complicating the reactivation of these receptors. It could be that a specific set, possibly involving up to 41 potential reverse mutations, could reanimate these receptors, despite single mutations at these positions not significantly impairing function in starfish delta iGluRs. Interestingly, a particular set of reverse mutations introduced into *Rat*GluD2 with the Lc-mutant background successfully resulted in the formation of ligand-gated channels. The interplay between the lurcher mutation and a series of nine invertebrate-like mutations in generating receptors that transition from a state of constitutive activity to being closed at rest and responsive to ligand gating is unclear. This phenomenon, however, was similarly observed with another invertebrate delta iGluR (*Sac*GluD), wherein the lurcher mutation transforms receptors from relatively inactive channels into inactive at rest and robustly activated by GABA (Fig. 4.5, page 37). In AMPA receptors, incorporating the lurcher mutation results in channels exhibiting a small amount of spontaneous activity without the presence of an agonist, but still capable of eliciting inward current responses and at which CNQX was transformed from a competitive an-

tagonist into a potent agonist (Taverna et al. (2000)). It is therefore interesting to observe how a single point mutation in the M3 helix in the TMD can have such diverse effect on different iGluRs and the precise impact of lurcher mutations on the gating mechanisms still requires further investigation.

G567 in *Aca*GluD proved to be a key position in determining ligand selectivity. This mutation strongly decreased macroscopic currents and also reduced GABA selectivity in starfish receptor, and when mutating the same position in *Rat*GluD2^{Lc} I observed an enhancement of inhibitory responses to glycine, D-serine and glutamate. The critical role of the hinge region in modulating the binding affinity and receptor function through conformational flexibility is also supported by previous molecular dynamics simulations findings. In NMDA receptors the variability in the action of partial versus full agonists is reported to be coupled to β-strand conformation in the hinge region (Kaye et al. (2006)). Mutating G567/S544 likely induces a structural variation of the hinge region giving more or less conformational flexibility in response to different ligands and therefore determining their efficacy. Moreover, high flexibility in this region might be needed in order to transmit the conformational changes induced by ligand binding to the gating apparatus (Tapken et al. (2017)).

Chapter 7

Conclusion

The primary goal of my PhD research was to establish a clear functional and evolutionary picture of the delta iGluR family. With an approach that combined molecular phylogenetics, heterologous expression, and electrophysiological experiments, I established a comprehensive functional picture of the delta receptor family. Secondly, by using site-directed mutagenesis and electrophysiological experiments I uncovered the amino acid substitutions that likely set apart mammalian delta iGluRs from active, invertebrate delta receptors.

Divergence of delta receptors and evolvability of ligand sensitivity

My investigation into the evolution and biophysical properties of the delta iGluR family has established three significant advances. (1) Delta iGluRs are exclusive to bilaterians, and they probably emerged from an AKDF duplication in an early bilaterian animal shortly after bilaterian and cnidarian lineages diverged. (2) The emergence of GABA selectivity in delta iGluRs occurred relatively early after the genesis of the ancestral delta gene. This early evolutionary development is supported by the presence of GABA sensitivity in diverse delta iGluRs, including those from early-branching bilaterians xenacoelomorphs, invertebrate deuterostomes, and even retained within certain vertebrate delta iGluRs. (3) In the lineage of chordates, or subsequently within vertebrates, delta iGluRs underwent a significant change, transitioning to a sensitivity for glycine/D-serine and experiencing a loss of their ligand-gated activity. My findings only

define delta receptors from vertebrates as the 'first' inactive delta receptors, but it's possible that the loss of ligand-gated activity happened before the emergence of the first vertebrate animals. For this, we would require electrophysiological characterization of delta receptors from early-branching chordates, e.g., cephalochordates and tunicates. Such research might also indicate whether the observed absence of ligand-gated activity in vertebrate delta iGluRs occurred before or after a shift in ligand selectivity from GABA to glycine/D-serine, also observed in the vertebrate lineage.

Determining ligand specificity for iGluRs solely through sequence similarity poses significant challenges (Alberstein et al. (2015); Li et al. (2016); Ramos-Vicente et al. (2018)), and my work further shows that the ligand-binding residues of GABA-gated channels do not differ obviously from those of glycine and D-serine-gated channels. This observation underscores the ease with which ligand sensitivity can evolve across various ligand-gated ion channel families and animal species, thus highlighting the need for caution when assigning neuronal functions based on the presence of specific ligand-gated ion channel genes due to the rapid evolvability of ligand sensitivity and ion permeability in different receptor families and animal species (Mayer (2021); Dent (2010); Janovjak et al. (2011)). Given that functional predictions based solely on sequences are inherently prone to unanticipated functional shifts, integrating electrophysiological characterization of ligand-gated ion channels, as presented in this thesis, is crucial. Electrophysiological studies, by directly measuring receptor activity and ligand specificity, offer invaluable insights that are fundamental for supplementing the limitations of relying solely on genomic and transcriptomic predictions, thereby offering a more comprehensive framework for the future evaluation of neuronal systems.

An exciting role for GABA

My thesis set out into the heterologous expression and biophysical characterization of various invertebrate delta iGluRs, with a special focus on *Aca*GluD from *Acanthaster planci*. Fortuitously, another laboratory studied the expression pattern of this very receptor (Roberts et al.

(2018)), although they didn't have a picture of its function, and their phylogeny was not extensive enough to classify the receptor's relation to other iGluRs. Significantly, this gene was reported be predominantly expressed in the radial nerve, but also found in the sensory tentacles and tube feet of the starfish ("gKAR2" in Roberts et al. (2018)). Thus it seems that *Aca*GluD, an excitatory GABA receptor, is expressed in specific tissues of *Acanthaster planci* and I considered more of the echinoderm literature to speculate on the physiological functions of the native receptor. Contrasting with its typically inhibitory function in vertebrates, applying GABA to isolated tube feet preparations induces contraction of tube feet in sea urchins (Florey et al. (1975)) and in the starfish *Asterias amurensis* (Protas and Muske (1980)). Unlike the typical hyperpolarizing response mediated by $GABA_A$ receptors in vertebrates, which is associated with an increase in Cl^- conductance, when Na^+ was removed from the extracellular medium, GABA-evoked tube-feet contractions were abolished. Thus, these observations provide compelling evidence for a contrasting effect of GABA in echinoderms relative to vertebrates. However, the precise roles of *Aca*GluD (and delta receptors in general) in Na^+-dependent GABA-evoked contractions in echinoderm tube feet and other potential functions remain to be elucidated. Establishing a direct link between the receptor's function and the physiological response necessitates further investigations on native preparations, employing genetic or pharmacological knockdown of *Aca*GluD. Although this remains speculative until such experiments are performed, the groundwork laid by these findings opens new possibilities in exploring whether delta iGluRs can indeed mediate the excitatory effect of GABA discovered in echinoderms. Beg and Jorgensen showed that in *Caenorhabditis elegans*, a GABA-gated cation channel emerged from the pLGIC superfamily (Beg and Jorgensen (2003)). They showed that GABA mediates enteric muscle contraction in *C. elegans*. Moreover the authors demonstrates that GABA invokes this excitatory response through cation permeability via the postsynaptic EXP-1 receptor, a novel cation-selective, GABA-gated channel of the pentameric ligand-gated ion channel superfamily (also including typical $GABA_A$ receptors). This highlights the diversity and evolutionary adaptability of GABAergic systems, and the notion that GABA can act as an excitatory neuro-

transmitter through various receptor types across different species.

Pharmacological insights

The currents observed by the reawakened, mutant rat delta iGluRs, together with the large GABA-gated currents in several invertebrate delta iGluRs that I uncovered, could establish a practical framework for characterizing potential pharmacological agents on delta iGluRs. Using invertebrate delta iGluRs as a model for drug testing comes with the assumption that their pharmacological characteristics align closely with those of vertebrate GluD1 and GluD2 iGluRs. My findings seem to corroborate this assumption, as both vertebrate and invertebrate delta iGluRs showed similar sensitivity to certain competitive antagonists and a pore-blocker. A potential scenario for the use of such invertebrate ”surrogate” pharmacological templates is de novo mutations in genes encoding delta receptors. Drugs that enhance of inhibit invertebrate delta iGluR function might be useful in upregulating underactive or downregulating overactive mutant receptors in humans. Furthermore, if de novo mutations in human delta iGluRs are identified as linked to specific diseases, we could then harness the active invertebrate delta iGluRs to test the effects of these mutations. This approach would offer a unique opportunity to directly assess how genetic variations influence receptor behavior and pharmacological response, providing critical insights into the disease mechanism at a molecular level. By employing invertebrate models as a proxy, we can rapidly evaluate the therapeutic potential of compounds on mutated receptors, accelerating the path from genetic discovery to targeted drug development. Moreover, my research relates to the analysis of the composition of synaptic iGluRs by using modulators traditionally asso- ciated with AMPA/KA receptors. The discovery that delta iGluRs are also susceptible to mod- ulation by these classical agents highlights a layer of complexity in discerning receptor-specific effects within synaptic environments.

References

V. Ady, J. Perroy, L. Tricoire, C. Piochon, S. Dadak, X. Chen, I. Dusart, L. Fagni, B. Lambolez, and C. Levenes. Type 1 metabotropic glutamate receptors (mGlu1) trigger the gating of GluD2 delta glutamate receptors. *EMBO Rep*, 15(1):103–109, 2014. doi: 10.1002/embr.201337371. 17, 43

R. Alberstein, R. Grey, A. Zimmet, D. K. Simmons, and M. L. Mayer. Glycine activated ion channel subunits encoded by ctenophore glutamate receptor genes. *Proc Natl Acad Sci U S A*, 112(44):6048–57, 2015. doi: 10.1073/pnas.1513771112. 90

S. F. Altschul, T. L. Madden, A. A. Schäffer, J. Zhang, Z. Zhang, W. Miller, and D. J. Lipman. Gapped BLAST and PSI-BLAST: A new generation of protein database search programs, 1997. ISSN 03051048. 21

S. A. Amico-Ruvio, S. E. Murthy, T. P. Smith, and G. K. Popescu. Zinc effects on NMDA receptor gating kinetics. *Biophysical Journal*, 100(8), 2011. ISSN 15420086. doi: 10.1016/j.bpj.2011.02.042. 8

C. Andrikou, D. Thiel, J. A. Ruiz-Santiesteban, and A. Hejnol. Active mode of excretion across digestive tissues predates the origin of excretory organs. *PLoS Biol*, 17(7):e3000408, 2019. doi: 10.1371/journal.pbio.3000408. 21, 22

K. Araki, H. Meguro, E. Kushiya, C. Takayama, Y. Inoue, and M. Mishina. Selective Expression of the Glutamate Receptor Channel δ2 Subunit in Cerebellar Purkinje Cells. *Biochemical and Biophysical Research Communications*, 197(3):1267–1276, 1993. doi: https://doi.org/10.1006/bbrc.1993.2614. 17

N. Armstrong and E. Gouaux. Mechanisms for activation and antagonism of an AMPA-sensitive

glutamate receptor: crystal structures of the GluR2 ligand binding core. *Neuron*, 28(1):165–181, 2000. doi: 10.1016/s0896-6273(00)00094-5. 9, 11, 51

N. Armstrong, M. Mayer, and E. Gouaux. Tuning activation of the AMPA-sensitive GluR2 ion channel by genetic adjustment of agonist-induced conformational changes. *Proc Natl Acad Sci U S A*, 100(10):5736–5741, 2003. doi: 10.1073/pnas.1037393100. 63

N. Armstrong, J. Jasti, M. Beich-Frandsen, and E. Gouaux. Measurement of conformational changes accompanying desensitization in an ionotropic glutamate receptor. *Cell*, 127(1):85–97, 2006. doi: 10.1016/j.cell.2006.08.037. 11

Y. P. Auberson, P. Acklin, S. Bischoff, R. Moretti, S. Ofner, M. Schmutz, and S. J. Veenstra. N-Phosphonoalkyl-5-aminomethylquinoxaline-2,3-diones: In vivo active AMPA and NMDA(glycine) antagonists. *Bioorganic & Medicinal Chemistry Letters*, 9(2):249–254, 1999. doi: https://doi.org/10.1016/S0960-894X(98)00720-3. 55

J. Baranovic and A. J. Plested. How to build the fastest receptor on earth, 2016. ISSN 14374315. 11

M. A. Bedoukian, A. M. Weeks, and K. M. Partin. Different domains of the AMPA receptor direct stargazin-mediated trafficking and stargazin-mediated modulation of kinetics. *Journal of Biological Chemistry*, 281(33), 2006. ISSN 00219258. doi: 10.1074/jbc.M600679200. 85

A. A. Beg and E. M. Jorgensen. EXP-1 is an excitatory GABA-gated cation channel. *Nature Neuroscience*, 6(11):1145–1152, 2003. doi: 10.1038/nn1136. 91

Y. Ben-Ari and G. L. Holmes. The multiple facets of γ-aminobutyric acid dysfunction in epilepsy, 2005. ISSN 13507540. 4

N. Benamer, F. Marti, R. Lujan, R. Hepp, T. G. Aubier, A. A. M. Dupin, G. Frebourg, S. Pons, U. Maskos, P. Faure, Y. A. Hay, B. Lambolez, and L. Tricoire. GluD1, linked to schizophrenia, controls the burst firing of dopamine neurons. *Mol Psychiatry*, 23(3):691–700, 2018. doi: 10.1038/mp.2017.137. 16, 43

S. Brogi, G. Campiani, M. Brindisi, and S. Butini. Allosteric Modulation of Ionotropic Glutamate Receptors: An Outlook on New Therapeutic Approaches to Treat Central Nervous

System Disorders. *ACS Medicinal Chemistry Letters*, 10(3), 2019. ISSN 19485875. doi: 10.1021/acsmedchemlett.8b00450. 43

A. P. Burada, R. Vinnakota, and J. Kumar. Cryo-EM structures of the ionotropic glutamate receptor GluD1 reveal a non-swapped architecture. *Nat Struct Mol Biol*, 27(1):84–91, 2020a. doi: 10.1038/s41594-019-0359-y. 8, 70, 71

A. P. Burada, R. Vinnakota, and J. Kumar. The architecture of GluD2 ionotropic delta glutamate receptor elucidated by cryo-EM. *Journal of Structural Biology*, 2020b. ISSN 10478477. doi: 10.1016/j.jsb.2020.107546. 8, 71

N. Burnashev, A. Villarroel, and B. Sakmann. Dimensions and ion selectivity of recombinant AMPA and kainate receptor channels and their dependence on Q/R site residues. *J Physiol*, 496 (Pt 1(Pt 1):165–173, 1996. doi: 10.1113/jphysiol.1996.sp021674. 10

J. T. Cannon, B. C. Vellutini, J. Smith 3rd, F. Ronquist, U. Jondelius, and A. Hejnol. Xenacoelomorpha is the sister group to Nephrozoa. *Nature*, 530(7588):89–93, 2016. doi: 10.1038/nature16520. 31

A. L. Carbone and A. J. Plested. Coupled control of desensitization and gating by the ligand binding domain of glutamate receptors. *Neuron*, 74(5):845–857, 2012. doi: 10.1016/j.neuron.2012.04.020. 75, 77

E. Carrillo, C. U. Gonzalez, V. Berka, and V. Jayaraman. Delta glutamate receptors are functional glycine- and D-serine-gated cation channels in situ. *Sci Adv*, 7(52):eabk2200, 2021. doi: 10.1126/sciadv.abk2200. 14, 15, 66, 68, 85

D. Castellano, R. D. Shepard, and W. Lu. Looking for Novelty in an "Old" Receptor: Recent Advances Toward Our Understanding of GABAARs and Their Implications in Receptor Pharmacology, 2021. ISSN 1662453X. 4

J. N. Chabwine, K. Talavera, L. Van Den Bosch, and G. Callewaert. NKCC1 downregulation induces hyperpolarizing shift of GABA responsiveness at near term fetal stages in rat cultured dorsal root ganglion neurons. *BMC Neuroscience*, 16(1), 2015. ISSN 14712202. doi: 10.1186/s12868-015-0180-4. 4

H. Chang, S. Ciani, and Y. Kidokoro. Ion permeation properties of the glutamate receptor channel in cultured embryonic Drosophila myotubes. *The Journal of Physiology*, 476(1), 1994. ISSN 14697793. doi: 10.1113/jphysiol.1994.sp020107. 45

S. Chen, Y. Zhao, Y. Wang, M. Shekhar, E. Tajkhorshid, and E. Gouaux. Activation and Desensitization Mechanism of AMPA Receptor-TARP Complex by Cryo-EM. *Cell*, 170(6): 1234–1246, 2017. doi: 10.1016/j.cell.2017.07.045. 75

A. C. Chin, R. A. Yovanno, T. J. Wied, A. Gershman, and A. Y. Lau. D-Serine Potently Drives Ligand-Binding Domain Closure in the Ionotropic Glutamate Receptor GluD2. *Structure*, 28 (10):1168–1178, 2020. doi: 10.1016/j.str.2020.07.005. 51

D. W. Choi, J. Koh y., and S. Peters. Pharmacology of glutamate neurotoxicity in cortical cell culture: Attenuation by NMDA antagonists. *Journal of Neuroscience*, 8(1), 1988. ISSN 02706474. doi: 10.1523/jneurosci.08-01-00185.1988. 86

U. B. Choi, S. Xiao, L. P. Wollmuth, and M. E. Bowen. Effect of Src kinase phosphorylation on disordered C-terminal domain of N-methyl-D-aspartic acid (NMDA) receptor subunit GluN2B protein. *Journal of Biological Chemistry*, 286(34), 2011. ISSN 00219258. doi: 10.1074/jbc.M111.258897. 70

U. B. Choi, R. Kazi, N. Stenzoski, L. P. Wollmuth, V. N. Uversky, and M. E. Bowen. Modulating the intrinsic disorder in the cytoplasmic domain alters the biological activity of the N-methyl-D-aspartatesensitive glutamate receptor. *Journal of Biological Chemistry*, 288(31), 2013. ISSN 00219258. doi: 10.1074/jbc.M113.477810. 10

P. J. Conn. Physiological Roles and Therapeutic Potential of Metabotropic Glutamate Receptors. In *Annals of the New York Academy of Sciences*, volume 1003, 2003. doi: 10.1196/annals.1300.002. 5

I. D. Coombs, J. Ziobro, V. Krotov, T. L. Surtees, S. G. Cull-Candy, and M. Farrant. A gain-of-function GRIA2 variant associated with neurodevelopmental delay and seizures: Functional characterization and targeted treatment. *Epilepsia*, 63(12), 2022. ISSN 15281167. doi: 10.1111/epi.17419. 12, 78

M. Coutelier, L. Burglen, E. Mundwiller, M. Abada-Bendib, D. Rodriguez, S. Chantot-Bastaraud, C. Rougeot, M.-A. Cournelle, M. Milh, A. Toutain, D. Bacq, V. Meyer, A. Afenjar, J.-F. Deleuze, A. Brice, D. Héron, G. Stevanin, and A. Durr. GRID2 mutations span from congenital to mild adult-onset cerebellar ataxia. *Neurology*, 84(17):1751–1759, 2015. doi: 10.1212/wnl.0000000000001524. 43

S. Dadak, N. Bouquier, E. Goyet, L. Fagni, C. Levenes, and J. Perroy. mGlu1 receptor canonical signaling pathway contributes to the opening of the orphan GluD2 receptor. *Neuropharmacology*, 115, 2017. ISSN 18737064. doi: 10.1016/j.neuropharm.2016.06.001. 17

J. Dai, C. Patzke, K. Liakath-Ali, E. Seigneur, and T. C. Südhof. GluD1 is a signal transduction device disguised as an ionotropic receptor. *Nature*, 595(7866):261–265, 2021. doi: 10.1038/s41586-021-03661-6. 43

E. Delpire. Cation-chloride cotransporters in neuronal communication. *News in Physiological Sciences*, 15(6), 2000. ISSN 08861714. doi: 10.1152/physiologyonline.2000.15.6.309. 4

J. A. Dent. The evolution of pentameric ligand-gated ion channels. *Advances in Experimental Medicine and Biology*, 683, 2010. ISSN 00652598. doi: 10.1007/978-1-4419-6445-8{_}2. 90

M. Diez, S. G. Medina-Muñoz, L. A. Castellano, G. da Silva Pescador, Q. Wu, and A. A. Bazzini. iCodon customizes gene expression based on the codon composition. *Scientific Reports*, 12 (1):12126, 2022. doi: 10.1038/s41598-022-15526-7. 22

S. El-Gebali, J. Mistry, A. Bateman, S. R. Eddy, A. Luciani, S. C. Potter, M. Qureshi, L. J. Richardson, G. A. Salazar, A. Smart, E. L. Sonnhammer, L. Hirsh, L. Paladin, D. Piovesan, S. C. Tosatto, and R. D. Finn. The Pfam protein families database in 2019. *Nucleic Acids Research*, 47(D1), 2019. ISSN 13624962. doi: 10.1093/nar/gky995. 22

J. Elegheert, W. Kakegawa, J. E. Clay, N. F. Shanks, E. Behiels, K. Matsuda, K. Kohda, E. Miura, M. Rossmann, N. Mitakidis, J. Motohashi, V. T. Chang, C. Siebold, I. H. Greger, T. Nakagawa, M. Yuzaki, and A. R. Aricescu. Structural basis for integration of GluD receptors within synaptic organizer complexes. *Science*, 353(6296):295–299, 2016. doi: 10.1126/science.

aae0104. 9, 14, 66, 71

I. Everts, C. Villmann, and M. Hollmann. N-glycosylation is not a prerequisite for glutamate receptor function but is essential for lectin modulation. *Molecular Pharmacology*, 52(5), 1997. ISSN 0026895X. doi: 10.1124/mol.52.5.861. 8, 77

G. E. Fagg and A. C. Foster. Amino acid neurotransmitters and their pathways in the mammalian central nervous system. *Neuroscience*, 9(4), 1983. ISSN 03064522. doi: 10.1016/0306-4522(83)90263-4. 4

E. Florey, M. A. Cahill, and M. Rathmayer. Excitatory actions of GABA and of acetylcholine in sea urchin tube feet. *Comparative Biochemistry and Physiology. Part C, Comparative*, 51 (1), 1975. ISSN 03064492. doi: 10.1016/0306-4492(75)90031-3. 91

M. Fossati, N. Assendorp, O. Gemin, S. Colasse, F. Dingli, G. Arras, D. Loew, and C. Charrier. Trans-Synaptic Signaling through the Glutamate Receptor Delta-1 Mediates Inhibitory Synapse Formation in Cortical Pyramidal Neurons. *Neuron*, 104(6), 2019. ISSN 10974199. doi: 10.1016/j.neuron.2019.09.027. 14, 16, 17

S. C. Gantz, K. Moussawi, and H. S. Hake. Delta glutamate receptor conductance drives excitation of mouse dorsal raphe neurons. *Elife*, 9, 2020. doi: 10.7554/eLife.56054. 16

M. Gielen, B. S. Retchless, L. Mony, J. W. Johnson, and P. Paoletti. Mechanism of differential control of NMDA receptor activity by NR2 subunits. *Nature*, 459(7247), 2009. ISSN 00280836. doi: 10.1038/nature07993. 68, 85

S. Guindon, J.-F. Dufayard, V. Lefort, M. Anisimova, W. Hordijk, and O. Gascuel. New Algorithms and Methods to Estimate Maximum-Likelihood Phylogenies: Assessing the Performance of PhyML 3.0. *Systematic Biology*, 59(3):307–321, 2010. doi: 10.1093/sysbio/syq010. 22

R. Gupta and S. Brunak. Prediction of glycosylation across the human proteome and the correlation to protein function. *Pac Symp Biocomput*, pages 310–322, 2002. 27

K. B. Hansen, P. Naur, N. L. Kurtkaya, A. S. Kristensen, M. Gajhede, J. S. Kastrup, and S. F. Traynelis. Modulation of the dimer interface at ionotropic glutamate-like receptor delta2

by D-serine and extracellular calcium. *J Neurosci*, 29(4):907–917, 2009. doi: 10.1523/JNEUROSCI.4081-08.2009. 13, 14, 58, 60, 62

K. B. Hansen, H. Furukawa, and S. F. Traynelis. Control of assembly and function of glutamate receptors by the amino-terminal domain, 2010. ISSN 15210111. 66

K. B. Hansen, L. P. Wollmuth, D. Bowie, H. Furukawa, F. S. Menniti, A. I. Sobolevsky, G. T. Swanson, S. A. Swanger, I. H. Greger, T. Nakagawa, C. J. McBain, V. Jayaraman, C. M. Low, M. L. Dell'Acqua, J. S. Diamond, C. R. Camp, R. E. Perszyk, H. Yuan, and S. F. Traynelis. Structure, Function, and Pharmacology of Glutamate Receptor Ion Channels. *Pharmacol Rev*, 73(4):298–487, 2021. doi: 10.1124/pharmrev.120.000131. 9, 10

A. Hejnol and K. Pang. Xenacoelomorpha's significance for understanding bilaterian evolution. *Curr Opin Genet Dev*, 39:48–54, 2016. doi: 10.1016/j.gde.2016.05.019. 31

R. Hepp, Y. A. Hay, C. Aguado, R. Lujan, L. Dauphinot, M. C. Potier, S. Nomura, O. Poirel, S. El Mestikawy, B. Lambolez, and L. Tricoire. Glutamate receptors of the delta family are widely expressed in the adult brain. *Brain Structure and Function*, 220(5), 2015. ISSN 18632661. doi: 10.1007/s00429-014-0827-4. 16

D. T. Hoang, O. Chernomor, A. von Haeseler, B. Q. Minh, and L. S. Vinh. UFBoot2: Improving the Ultrafast Bootstrap Approximation. *Molecular Biology and Evolution*, 35(2):518–522, 2018. doi: 10.1093/molbev/msx281. 22

A. L. Hodgkin and A. F. Huxley. Action potentials recorded from inside a nerve fibre [8], 1939. ISSN 00280836. 2

M. Hollmann and S. Heinemann. Cloned glutamate receptors, 1994. ISSN 0147006X. 5, 13

T. Ishii, J. R. Stolz, and G. T. Swanson. Auxiliary proteins are the predominant determinants of differential efficacy of clinical candidates acting as AMPA receptor positive allosteric modulators. *Molecular Pharmacology*, 97(5), 2020. ISSN 15210111. doi: 10.1124/MOL.119.118554. 46

H. Janovjak, G. Sandoz, and E. Y. Isacoff. A modern ionotropic glutamate receptor with a K(+) selectivity signature sequence. *Nat Commun*, 2:232, 2011. doi: 10.1038/ncomms1231. 90

J. L. Johnson and M. H. Aprison. The distribution of glutamic acid, a transmitter candidate, and other amino acids in the dorsal sensory neuron of the cat. *Brain Research*, 24(2), 1970. ISSN 00068993. doi: 10.1016/0006-8993(70)90107-1. 4

M. Johnson, I. Zaretskaya, Y. Raytselis, Y. Merezhuk, S. McGinnis, and T. L. Madden. NCBI BLAST: a better web interface. *Nucleic acids research*, 36(Web Server issue), 2008. ISSN 13624962. doi: 10.1093/nar/gkn201. 21

J. Jumper, R. Evans, A. Pritzel, T. Green, M. Figurnov, O. Ronneberger, K. Tunyasuvunakool, R. Bates, A. Zidek, A. Potapenko, A. Bridgland, C. Meyer, S. A. A. Kohl, A. J. Ballard, A. Cowie, B. Romera-Paredes, S. Nikolov, R. Jain, J. Adler, T. Back, S. Petersen, D. Reiman, E. Clancy, M. Zielinski, M. Steinegger, M. Pacholska, T. Berghammer, S. Bodenstein, D. Silver, O. Vinyals, A. W. Senior, K. Kavukcuoglu, P. Kohli, and D. Hassabis. Highly accurate protein structure prediction with AlphaFold. *Nature*, 596(7873):583–589, 2021. doi: 10.1038/s41586-021-03819-2. 26, 49

W. Kakegawa, Y. Miyoshi, K. Hamase, S. Matsuda, K. Matsuda, K. Kohda, K. Emi, J. Motohashi, R. Konno, K. Zaitsu, and M. Yuzaki. D-serine regulates cerebellar LTD and motor coordination through the delta2 glutamate receptor. *Nat Neurosci*, 14(5):603–611, 2011. doi: 10.1038/nn.2791. 17, 43

K. Katoh, K. Misawa, K. Kuma, and T. Miyata. MAFFT: a novel method for rapid multiple sequence alignment based on fast Fourier transform. *Nucleic Acids Res*, 30(14):3059–3066, 2002. doi: 10.1093/nar/gkf436. 22

S. L. Kaye, M. S. Sansom, and P. C. Biggin. Molecular dynamics simulations of the ligand-binding domain of an N-methyl-D-aspartate receptor. *J Biol Chem*, 281(18):12736–12742, 2006. doi: 10.1074/jbc.M512728200. 87

J. Kehoe. Transformation by concanavalin A of the response of molluscan neurones to L-glutamate. *Nature*, 274(5674):866–869, 1978. doi: 10.1038/274866a0. 77

K. Konno, K. Matsuda, C. Nakamoto, M. Uchigashima, T. Miyazaki, M. Yamasaki, K. Sakimura, M. Yuzaki, and M. Watanabe. Enriched expression of GluD1 in higher brain

regions and its involvement in parallel fiber-interneuron synapse formation in the cerebellum. *Journal of Neuroscience*, 34(22), 2014. ISSN 15292401. doi: 10.1523/JNEUROSCI.0628-14.2014. 16

A. S. Kristensen, K. B. Hansen, P. Naur, L. Olsen, N. L. Kurtkaya, S. M. Dravid, T. Kvist, F. Yi, J. Pøhlsgaard, R. P. Clausen, M. Gajhede, J. S. Kastrup, and S. F. Traynelis. Pharmacology and structural analysis of ligand binding to the orthosteric site of glutamate-like GluD2 receptors. *Molecular Pharmacology*, 2016. ISSN 15210111. doi: 10.1124/mol.115.100909. 44

T. Kuner, P. H. Seeburg, and H. R. Guy. A common architecture for K+ channels and ionotropic glutamate receptors? *Trends in Neurosciences*, 26(1), 2003. ISSN 01662236. doi: 10.1016/S0166-2236(02)00010-3. 10

Y. Li, P. Dharkar, T. H. Han, M. Serpe, C. H. Lee, and M. L. Mayer. Novel Functional Properties of Drosophila CNS Glutamate Receptors. *Neuron*, 92(5), 2016. ISSN 10974199. doi: 10.1016/j.neuron.2016.10.058. 90

B. A. Maki, T. K. Aman, S. A. Amico-Ruvio, C. L. Kussius, and G. K. Popescu. C-terminal domains of N-methyl-D-aspartic acid receptor modulate unitary channel conductance and gating. *Journal of Biological Chemistry*, 287(43), 2012. ISSN 00219258. doi: 10.1074/jbc.M112.390013. 70

K. Matsuda, E. Miura, T. Miyazaki, W. Kakegawa, K. Emi, S. Narumi, Y. Fukazawa, A. Ito-Ishida, T. Kondo, R. Shigemoto, M. Watanabe, and M. Yuzaki. Cbln1 is a ligand for an orphan glutamate receptor delta2, a bidirectional synapse organizer. *Science*, 328(5976):363–368, 2010. doi: 10.1126/science.1185152. 9, 14

T. Matsui, M. Sekiguchi, A. Hashimoto, U. Tomita, T. Nishikawa, and K. Wada. Functional Comparison of d-Serine and Glycine in Rodents: The Effect on Cloned NMDA Receptors and the Extracellular Concentration. *Journal of Neurochemistry*, 65(1), 1995. ISSN 0022-3042. doi: 10.1046/j.1471-4159.1995.65010454.x. 44

M. L. Mayer. Glutamate receptors from diverse animal species exhibit unexpected structural and functional diversity. *Journal of Physiology*, 599(10), 2021. ISSN 14697793. doi: 10.

1113/JP279026. 90

M. L. Mayer and L. Vyklicky Jr. Concanavalin A selectively reduces desensitization of mammalian neuronal quisqualate receptors. *Proc Natl Acad Sci U S A*, 86(4):1411–1415, 1989. doi: 10.1073/pnas.86.4.1411. 12, 77

D. McNamara, E. C. R. Smith, D. O. Calligaro, P. J. O'Malley, L. A. McQuaid, and R. Dingledine. 5,7-Dichlorokynurenic acid, a potent and selective competitive antagonist of the glycine site on NMDA receptors. *Neuroscience Letters*, 120(1):17–20, 1990. doi: https://doi.org/10.1016/0304-3940(90)90157-5. 55

E. C. Meng, T. D. Goddard, E. F. Pettersen, G. S. Couch, Z. J. Pearson, J. H. Morris, and T. E. Ferrin. UCSF ChimeraX: Tools for structure building and analysis. *Protein Sci*, 32(11):e4792, 2023. doi: 10.1002/pro.4792. 26, 27

K. Menuz, R. M. Stroud, R. A. Nicoll, and F. A. Hays. TARP auxiliary subunits switch AMPA receptor antagonists into partial agonists. *Science*, 318(5851):815–817, 2007. doi: 10.1126/science.1146317. 56

P. S. Miller and A. R. Aricescu. Crystal structure of a human GABAA receptor. *Nature*, 512 (7514), 2014. ISSN 14764687. doi: 10.1038/nature13293. 3

B. Q. Minh, H. A. Schmidt, O. Chernomor, D. Schrempf, M. D. Woodhams, A. von Haeseler, and R. Lanfear. IQ-TREE 2: New Models and Efficient Methods for Phylogenetic Inference in the Genomic Era. *Mol Biol Evol*, 37(5):1530–1534, 2020. doi: 10.1093/molbev/msaa015. 22, 30

B. Q. Minh, C. C. Dang, L. S. Vinh, and R. Lanfear. QMaker: Fast and Accurate Method to Estimate Empirical Models of Protein Evolution. *Syst Biol*, 70(5):1046–1060, 2021. doi: 10.1093/sysbio/syab010. 22

M. Mirdita, K. Schutze, Y. Moriwaki, L. Heo, S. Ovchinnikov, and M. Steinegger. ColabFold: making protein folding accessible to all. *Nat Methods*, 19(6):679–682, 2022. doi: 10.1038/s41592-022-01488-1. 26, 49

G. M. Morris, R. Huey, W. Lindstrom, M. F. Sanner, R. K. Belew, D. S. Goodsell, and A. J.

Olson. AutoDock4 and AutoDockTools4: Automated docking with selective receptor flexibility. *J Comput Chem*, 30(16):2785–2791, 2009. doi: 10.1002/jcc.21256. 27

K. Moussawi, A. Riegel, S. Nair, and P. W. Kalivas. Extracellular glutamate: Functional compartments operate in different concentration ranges. *Frontiers in Systems Neuroscience*, (NOVEMBER 2011), 2011. ISSN 16625137. doi: 10.3389/fnsys.2011.00094. 11

P. Naur, K. B. Hansen, A. S. Kristensen, S. M. Dravid, D. S. Pickering, L. Olsen, B. Vestergaard, J. Egebjerg, M. Gajhede, S. F. Traynelis, and J. S. Kastrup. Ionotropic glutamate-like receptor delta2 binds D-serine and glycine. *Proc Natl Acad Sci U S A*, 104(35):14116–14121, 2007. doi: 10.1073/pnas.0703718104. 13, 25, 27, 33, 44, 49, 50, 53, 71, 80, 85

R. W. Olsen. GABAA receptor: Positive and negative allosteric modulators, 2018. ISSN 18737064. 3

R. W. Olsen and W. Sieghart. GABAA receptors: Subtypes provide diversity of function and pharmacology, 2009. ISSN 00283908. 3

P. Paoletti, F. Perin-Dureau, A. Fayyazuddin, A. Le Goff, I. Callebaut, and J. Neyton. Molecular organization of a zinc binding N-terminal modulatory domain in a NMDA receptor subunit. *Neuron*, 28(3), 2000. ISSN 08966273. doi: 10.1016/S0896-6273(00)00163-X. 8

A. Pasternack, S. K. Coleman, A. Jouppila, D. G. Mottershead, M. Lindfors, M. Pasternack, and K. Keinänen. α-amino-3-hydroxy-5-methyl-4-isoxazolepropionic acid (AMPA) receptor channels lacking the N-terminal domain. *Journal of Biological Chemistry*, 277(51), 2002. ISSN 00219258. doi: 10.1074/jbc.M208349200. 8, 66

J. A. Payne, C. Rivera, J. Voipio, and K. Kaila. Cation-chloride co-transporters in neuronal communication, development and trauma, 2003. ISSN 01662236. 4

C. Peerboom and C. J. Wierenga. The postnatal GABA shift: A developmental perspective, 2021. ISSN 18737528. 4

W. Pei, Z. Huang, C. Wang, Y. Han, S. P. Jae, and L. Niu. Flip and flop: A molecular determinant for AMPA receptor channel opening. *Biochemistry*, 48(17), 2009. ISSN 00062960. doi: 10.1021/bi8015907. 9

F. Perin-Dureau, J. Rachline, J. Neyton, and P. Paoletti. Mapping the binding site of the neuroprotectant ifenprodil on NMDA receptors. *Journal of Neuroscience*, 22(14), 2002. ISSN 02706474. doi: 10.1523/jneurosci.22-14-05955.2002. 8

L. Piot, C. Heroven, S. Bossi, J. Zamith, T. Malinauskas, C. Johnson, D. Wennagel, D. Stroebel, C. Charrier, A. R. Aricescu, L. Mony, and P. Paoletti. GluD1 binds GABA and controls inhibitory plasticity. *Science*, page eadf3406, 2023. doi: 10.1126/science.adf3406. 15, 16, 33, 55

A. S. Pivovarov, F. Calahorro, and R. J. Walker. Na+/K+-pump and neurotransmitter membrane receptors, 2019. ISSN 13542516. 1

A. J. Plested and M. L. Mayer. Structure and Mechanism of Kainate Receptor Modulation by Anions. *Neuron*, 53(6), 2007. ISSN 08966273. doi: 10.1016/j.neuron.2007.02.025. 59

L. L. Protas and G. A. Muske. The effects of some transmitter substances on the tube foot muscles of the starfish, Asterias amurensis (Lütken). *General Pharmacology*, 11(1), 1980. ISSN 03063623. doi: 10.1016/0306-3623(80)90019-1. 91

C. A. Puddifoot, P. E. Chen, R. Schoepfer, and D. J. Wyllie. Pharmacological characterization of recombinant NR1/NR2A NMDA receptors with truncated and deleted carboxy termini expressed in Xenopus laevis oocytes. *British Journal of Pharmacology*, 156(3), 2009. ISSN 00071188. doi: 10.1111/j.1476-5381.2008.00040.x. 70

D. Ramos-Vicente, J. Ji, E. Gratacos-Batlle, G. Gou, R. Reig-Viader, J. Luis, D. Burguera, E. Navas-Perez, J. Garcia-Fernandez, P. Fuentes-Prior, H. Escriva, N. Roher, D. Soto, and A. Bayes. Metazoan evolution of glutamate receptors reveals unreported phylogenetic groups and divergent lineage-specific events. *Elife*, 7, 2018. doi: 10.7554/eLife.35774. 5, 6, 7, 31, 90

I. J. Reynolds and E. Aizenman. Pentamidine is an N-methyl-D-aspartate receptor antagonist and is neuroprotective in vitro. *J Neurosci*, 12(3):970–975, 1992. doi: 10.1523/JNEUROSCI.12-03-00970.1992. 44

C. Rivera, J. Voipio, J. A. Payne, E. Ruusuvuori, H. Lahtinen, K. Lamsa, U. Pirvola, M. Saarma,

and K. Kaila. The K+/Cl- co-transporter KCC2 renders GABA hyperpolarizing during neuronal maturation. *Nature*, 397(6716), 1999. ISSN 00280836. doi: 10.1038/16697. 4

R. E. Roberts, D. Powell, T. Wang, M. H. Hall, C. A. Motti, and S. F. Cummins. Putative chemosensory receptors are differentially expressed in the sensory organs of male and female crown-of-thorns starfish, Acanthaster planci. *BMC Genomics*, 19(1), 2018. ISSN 14712164. doi: 10.1186/s12864-018-5246-0. 90, 91

M. Rossmann, M. Sukumaran, A. C. Penn, D. B. Veprintsev, M. M. Babu, and I. H. Greger. Subunit-selective N-terminal domain associations organize the formation of AMPA receptor heteromers. *EMBO Journal*, 30(5), 2011. ISSN 02614189. doi: 10.1038/emboj.2011.16. 7

M. A. Sahai and P. C. Biggin. Quantifying water-mediated protein-ligand interactions in a glutamate receptor: A DFT study. *Journal of Physical Chemistry B*, 115(21), 2011. ISSN 15205207. doi: 10.1021/jp200776t. 63

C. L. Salussolia, A. Corrales, I. Talukder, R. Kazi, G. Akgul, M. Bowen, and L. P. Wollmuth. Interaction of the M4 segment with other transmembrane segments is required for surface expression of mammalian α-amino-3-hydroxy-5-methyl-4- isoxazolepropionic acid (AMPA) receptors. *Journal of Biological Chemistry*, 286(46), 2011. ISSN 00219258. doi: 10.1074/jbc.M111.268839. 10

J. Schindelin, I. Arganda-Carreras, E. Frise, V. Kaynig, M. Longair, T. Pietzsch, S. Preibisch, C. Rueden, S. Saalfeld, B. Schmid, J.-Y. Tinevez, D. J. White, V. Hartenstein, K. Eliceiri, P. Tomancak, and A. Cardona. Fiji: an open-source platform for biological-image analysis. *Nature Methods*, 9(7):676–682, 2012. doi: 10.1038/nmeth.2019. 26

S. M. Schmid, C. Körber, S. Herrmann, M. Werner, and M. Hollmann. A domain linking the AMPA receptor agonist binding site to the ion pore controls gating and causes lurcher properties when mutated. *Journal of Neuroscience*, 27(45), 2007. ISSN 02706474. doi: 10.1523/JNEUROSCI.3175-07.2007. 10

S. M. Schmid, S. Kott, C. Sager, T. Huelsken, and M. Hollmann. The glutamate receptor subunit delta2 is capable of gating its intrinsic ion channel as revealed by ligand binding domain

transplantation. *Proceedings of the National Academy of Sciences of the United States of America*, 2009. ISSN 00278424. doi: 10.1073/pnas.0900329106. 14, 45

P. H. Seeburg. The TIPS/TINS Lecture: The molecular biology of mammalian glutamate receptor channels, 1993. ISSN 01656147. 13

C. L. Shaffer, R. S. Hurst, R. J. Scialis, S. M. Osgood, D. K. Bryce, W. E. Hoffmann, J. T. Lazzaro, A. N. Hanks, S. Lotarski, M. L. Weber, J. H. Liu, F. S. Menniti, C. J. Schmidt, and M. Hajós. Positive allosteric modulation of AMPA receptors from efficacy to toxicity: The interspecies exposure-response continuum of the novel potentiator PF-4778574. *Journal of Pharmacology and Experimental Therapeutics*, 347(1), 2013. ISSN 00223565. doi: 10.1124/jpet.113.204735. 86

M. Sheardown, E. Nielsen, A. Hansen, P. Jacobsen, and T. Honore. 2 , 3-Dihydroxy-6-nitro-7-sulfamoyl-benzo (F) quinoxaline : A Neuroprotectant for Cerebral Ischemia Author (s): Malcolm J . Sheardown , Elsebet Ø . Nielsen , Anker J . Hansen , Poul Jacobsen and Tage Honoré Published by : American Association for the. *American Association for the Advancement of Science*, 247(4942):571–574, 1991. 55

E. Sigel and M. E. Steinmann. Structure, function, and modulation of GABAA receptors, 2012. ISSN 00219258. 45

A. I. Sobolevsky, M. P. Rosconi, and E. Gouaux. X-ray structure, symmetry and mechanism of an AMPA-subtype glutamate receptor. *Nature*, 462(7274):745–756, 2009. doi: 10.1038/nature08624. 7, 70

Y. Stern-Bach, S. Russo, M. Neuman, and C. Rosenmund. A point mutation in the glutamate binding site blocks desensitization of AMPA receptors. *Neuron*, 21(4):907–918, 1998. doi: 10.1016/s0896-6273(00)80605-4. 12, 75

D. Stroebel and P. Paoletti. Architecture and function of NMDA receptors: an evolutionary perspective. *J Physiol*, 599(10):2615–2638, 2021. doi: 10.1113/JP279028. 31

Y. Sun, R. Olson, M. Horning, N. Armstrong, M. Mayer, and E. Gouaux. Mechanism of glutamate receptor desensitization. *Nature*, 417(6886):245–253, 2002. doi: 10.1038/417245a.

75

H. Takagi. Roles of ion channels in EPSP integration at neuronal dendrites. *Neuroscience Research*, 37(3), 2000. ISSN 01680102. doi: 10.1016/S0168-0102(00)00120-6. 3

W. Tao, C. Ma, M. A. Bemben, K. H. Li, A. L. Burlingame, M. Zhang, and R. A. Nicoll. Mechanisms underlying the synaptic trafficking of the glutamate delta receptor GluD1. *Molecular Psychiatry*, 24(10), 2019. ISSN 14765578. doi: 10.1038/s41380-019-0378-4. 70

D. Tapken, T. B. Steffensen, R. Leth, L. B. Kristensen, A. Gerbola, M. Gajhede, F. S. Jorgensen, L. Olsen, and J. S. Kastrup. The low binding affinity of D-serine at the ionotropic glutamate receptor GluD2 can be attributed to the hinge region. *Sci Rep*, 7:46145, 2017. doi: 10.1038/srep46145. 63, 87

F. Taverna, Z. G. Xiong, L. Brandes, J. C. Roder, M. W. Salter, and J. F. MacDonald. The Lurcher mutation of an α-amino-3-hydroxy-5-methyl-4- isoxazolepropionic acid receptor subunit enhances potency of glutamate and converts an antagonist to an agonist. *Journal of Biological Chemistry*, 275(12), 2000. ISSN 00219258. doi: 10.1074/jbc.275.12.8475. 10, 56, 87

R. I. Teleanu, A. G. Niculescu, E. Roza, O. Vladâcenco, A. M. Grumezescu, and D. M. Teleanu. Neurotransmitters—Key Factors in Neurological and Neurodegenerative Disorders of the Central Nervous System, 2022. ISSN 14220067. 2

A. Thalhammer, I. Everts, and M. Hollmann. Inhibition by lectins of glutamate receptor desensitization is determined by the lectin's sugar specificity at kainate but not AMPA receptors. *Molecular and Cellular Neuroscience*, 21(4), 2002. ISSN 10447431. doi: 10.1006/mcne.2002.1137. 8

S. Tomita, R. A. Nicoll, and D. S. Bredt. PDZ protein interactions regulating glutamate receptor function and plasticity, 2001. ISSN 00219525. 11

D. M. Treiman. GABAergic mechanisms in epilepsy. In *Epilepsia*, volume 42, pages 8–12. Blackwell Science, Inc., epilepsia edition, 2001. doi: 10.1046/j.1528-1157.2001.042Suppl.3008.x. 3

E. C. Twomey, M. V. Yelshanskaya, R. A. Grassucci, J. Frank, and A. I. Sobolevsky. Channel opening and gating mechanism in AMPA-subtype glutamate receptors. *Nature*, 549(7670): 60–65, 2017. doi: 10.1038/nature23479. 10, 74, 75

R. Vijayan, M. A. Sahai, T. Czajkowski, and P. C. Biggin. A comparative analysis of the role of water in the binding pockets of ionotropic glutamate receptors. *Physical Chemistry Chemical Physics*, 12(42), 2010. ISSN 14639076. doi: 10.1039/c004336b. 64

A. Waterhouse, M. Bertoni, S. Bienert, G. Studer, G. Tauriello, R. Gumienny, F. T. Heer, T. A. De Beer, C. Rempfer, L. Bordoli, R. Lepore, and T. Schwede. SWISS-MODEL: Homology modelling of protein structures and complexes. *Nucleic Acids Research*, 46(W1), 2018. ISSN 13624962. doi: 10.1093/nar/gky427. 26

J. C. Watkins and D. E. Jane. The glutamate story, 2006. ISSN 00071188. 13

K. Williams, M. Dattilo, T. N. Sabado, K. Kashiwagi, and K. Igarashi. Pharmacology of delta2 glutamate receptors: effects of pentamidine and protons. *J Pharmacol Exp Ther*, 305(2): 740–748, 2003. doi: 10.1124/jpet.102.045799. 15, 44, 46

W. Wisden and P. H. Seeburg. Mammalian ionotropic glutamate receptors. *Current Opinion in Neurobiology*, 3(3), 1993. ISSN 09594388. doi: 10.1016/0959-4388(93)90120-N. 5

Z. G. Wo and R. E. Oswald. Unraveling the modular design of glutamate-gated ion channels. *Trends Neurosci*, 18(4):161–168, 1995. doi: 10.1016/0166-2236(95)93895-5. 10

L. P. Wollmuth, T. Kuner, C. Jatzke, P. H. Seeburg, N. Heintz, and J. Zuo. The Lurcher mutation identifies δ2 as an AMPA/kainate receptor-like channel that is potentiated by Ca2+. *Journal of Neuroscience*, 20(16), 2000. ISSN 02706474. doi: 10.1523/jneurosci.20-16-05973.2000. 13

M. W. Wood, H. M. VanDongen, and A. M. VanDongen. Structural conservation of ion conduction pathways in K channels and glutamate receptors. *Proc Natl Acad Sci U S A*, 92(11): 4882–4886, 1995. doi: 10.1073/pnas.92.11.4882. 10

Y. Xia, W. Chu, Q. Qi, and L. Xun. New insights into the QuikChange process guide the use of Phusion DNA polymerase for site-directed mutagenesis. *Nucleic Acids Res*, 43(2):e12, 2015.

doi: 10.1093/nar/gku1189. 23

R. Yadav, R. Rimerman, M. A. Scofield, and S. M. Dravid. Mutations in the transmembrane domain M3 generate spontaneously open orphan glutamate delta1 receptor. *Brain Res*, 1382: 1–8, 2011. doi: 10.1016/j.brainres.2010.12.086. 15, 33

M. Yamazaki, K. Araki, A. Shibata, and M. Mishina. Molecular cloning of a cDNA encoding a novel member of the mouse glutamate receptor channel family. *Biochemical and Biophysical Research Communications*, 183(2):886–892, 1992. doi: https://doi.org/10.1016/0006-291X(92)90566-4. 5

M. Yasumura, T. Yoshida, S. J. Lee, T. Uemura, J. Y. Joo, and M. Mishina. Glutamate receptor δ1 induces preferentially inhibitory presynaptic differentiation of cortical neurons by interacting with neurexins through cerebellin precursor protein subtypes. *Journal of Neurochemistry*, 121(5), 2012. ISSN 00223042. doi: 10.1111/j.1471-4159.2011.07631.x. 9

M. Yoshimura and T. M. Jessell. Membrane properties of rat substantia gelatinosa neurons in vitro. *Journal of Neurophysiology*, 62(1), 1989. ISSN 00223077. doi: 10.1152/jn.1989.62.1.109. 2

A. Yu, T. Wied, J. Belcher, and A. Y. Lau. Computing conformational free energies of iGluR ligand-binding domains. In *Ionotropic Glutamate Receptor Technologies*, pages 119–132. Springer New York, 2015. ISBN 9781493928125. doi: 10.1007/978-1-4939-2812-5{_}9. 51

H. M. Zhao, R. J. Wenthold, and R. S. Petralia. Glutamate receptor targeting to synaptic populations on Purkinje cells is developmentally regulated. *Journal of Neuroscience*, 18(14), 1998. ISSN 02706474. doi: 10.1523/jneurosci.18-14-05517.1998. 17

B. S. Zhorov and D. B. Tikhonov. Potassium, sodium, calcium and glutamate-gated channels: Pore architecture and ligand action, 2004. ISSN 00223042. 10, 46

J. Zuo, P. L. De Jager, K. A. Takahashi, W. Jiang, D. J. Linden, and N. Heintz. Neurodegeneration in Lurcher mice caused by mutation in delta2 glutamate receptor gene. *Nature*, 388(6644): 769–773, 1997. doi: 10.1038/42009. 10, 13, 32

Appendix 1 - DNA constructs for expression in *Xenopus laevis* oocytes

DNA constructs for expression in *Xenopus laevis* oocytes

All DNA constructs were based on a pSP64 vector (ProMega) modified for expression in *Xenopus* oocytes into which the following delta iGluR inserts were sub-cloned.

ATTTAGGTGACACTATAG, SP6 transcription promoter
AAGCTT, HindIII restriction site
GCTTG etc, beta globin 5’ UTR
GTCGACTCTAGAGGATCC, SalI, XbaI, BamHI, restriction sites
ACC, loose Kozak consensus sequence
cMyc + TAA stop codon,
GGTTA etc, beta globin 3’ UTR
AAAAA etc, poly(A) sequence
GAATTC, restriction site

Modified pSP64 vector

ATTTAGGTGACACTATAGAATACAAGCTTGCTTGTTCTTTTTGCAGAAGCTCAGAATAAACGCTCAACTTTGGCGTCGACTCTAGAGGATCCGAGCAGAAGCTCATCAGTGAGGAAGATCTCTAA
GGTTACCACTAAACCAGCCTCAAGAACACCCGAATGGAGTCTCTAAGCTACATAATACCAACTTACACTTTACAAAATGTTGTCCCCCAAAATGTAGCCATTCGTATCTGCTCCTAATAAAAAGA
AAGTTTCTTCACATTCTAAAAAAAAAAAAAAAAAAAAAAAAAAAAAAAAAAAAAAAAAGAATTCGTAATCATGTCATAGCTGTTTCCTGTGTGAAATTGTTATCCGCTCACAATTCCACACAACATACGAGCCGG
AAGCATAAAGTGTAAAGCCTGGGGTGCCTAATGAGTGAGCTAACTCACATTAATTGCGTTGCGCTCACTGCCCGCTTTCCAGTCGGGAAACCTGTCGTGCCAGCTGCATTAATGAATCGGCCAAC
GCGCGGGGAGAGGCGGTTTGCGTATTGGGCGCTCTTCCGCTTCCTCGCTCACTGACTCGCTGCGCTCGGTCGTTCGGCTGCGGCGAGCGGTATCAGCTCACTCAAAGGCGGTAATACGGTTATCC
ACAGAATCAGGGGATAACGCAGGAAAGAACATGTGAGCAAAAGGCCAGCAAAAGGCCAGGAACCGTAAAAAGGCCGCGTTGCTGGCGTTTTTCCATAGGCTCCGCCCCCCTGACGAGCATCACAA
AAATCGACGCTCAAGTCAGAGGTGGCGAAACCCGACAGGACTATAAAGATACCAGGCGTTTCCCCCTGGAAGCTCCCTCGTGCGCTCTCCTGTTCCGACCCTGCCGCTTACCGGATACCTGTCCG
CCTTTCTCCCTTCGGGAAGCGTGGCGCTTTCTCATAGCTCACGCTGTAGGTATCTCAGTTCGGTGTAGGTCGTTCGCTCCAAGCTGGGCTGTGTGCACGAACCCCCCGTTCAGCCCGACCGCTGC
GCCTTATCCGGTAACTATCGTCTTGAGTCCAACCCGGTAAGACACGACTTATCGCCACTGGCAGCAGCCACTGGTAACAGGATTAGCAGAGCGAGGTATGTAGGCGGTGCTACAGAGTTCTTGAA
GTGGTGGCCTAACTACGGCTACACTAGAAGAACAGTATTTGGTATCTGCGCTCTGCTGAAGCCAGTTACCTTCGGAAAAAGAGTTGGTAGCTCTTGATCCGGCAAACAAACCACCGCTGGTAGCG
GTGGTTTTTTTGTTTGCAAGCAGCAGATTACGCGCAGAAAAAAAGGATCTCAAGAAGATCCTTTGATCTTTTCTACGGGGTCTGACGCTCAGTGGAACGAAAACTCACGTTAAGGGATTTTGGTC
ATGAGATTATCAAAAAGGATCTTCACCTAGATCCTTTTAAATTAAAAATGAAGTTTTAAATCAATCTAAAGTATATATGAGTAAACTTGGTCTGACAGTTACCAATGCTTAATCAGTGAGGCACC
TATCTCAGCGATCTGTCTATTTCGTTCATCCATAGTTGCCTGACTCCCCGTCGTGTAGATAACTACGATACGGGAGGGCTTACCATCTGGCCCCAGTGCTGCAATGATACCGCGAGACCCACGCT
CACCGGCTCCAGATTTATCAGCAATAAACCAGCCAGCCGGAAGGGCCGAGCGCAGAAGTGGTCCTGCAACTTTATCCGCCTCCATCCAGTCTATTAATTGTTGCCGGGAAGCTAGAGTAAGTAGT
TCGCCAGTTAATAGTTTGCGCAACGTTGTTGCCATTGCTACAGGCATCGTGGTGTCACGCTCGTCGTTTGGTATGGCTTCATTCAGCTCCGGTTCCCAACGATCAAGGCGAGTTACATGATCCCC
CATGTTGTGCAAAAAAGCGGTTAGCTCCTTCGGTCCTCCGATCGTTGTCAGAAGTAAGTTGGCCGCAGTGTTATCACTCATGGTTATGGCAGCACTGCATAATTCTCTTACTGTCATGCCATCCG
TAAGATGCTTTTCTGTGACTGGTGAGTACTCAACCAAGTCATTCTGAGAATAGTGTATGCGGCGACCGAGTTGCTCTTGCCCGGCGTCAATACGGGATAATACCGCGCCACATAGCAGAACTTTA
AAAGTGCTCATCATTGGAAAACGTTCTTCGGGGCGAAAACTCTCAAGGATCTTACCGCTGTTGAGATCCAGTTCGATGTAACCCACTCGTGCACCCAACTGATCTTCAGCATCTTTTACTTTCAC
CAGCGTTTCTGGGTGAGCAAAAACAGGAAGGCAAAATGCCGCAAAAAAGGGAATAAGGGCGACACGGAAATGTTGAATACTCATACTCTTCCTTTTTCAATATTATTGAAGCATTTATCAGGGTT
ATTGTCTCATGAGCGGATACATATTTGAATGTATTTAGAAAAATAAACAAATAGGGGTTCCGCGCACATTTCCCCGAAAAGTGCCACCTGACGTCTAAGAAACCATTATTATCATGACATTAACC
TATAAAAATAGGCGTATCACGAGGCCCTTTCGTCTCGCGCGTTTCGGTGATGACGGTGAAAACCTCTGACACATGCAGCTCCCGGAGACGGTCACAGCTTGTCTGTAAGCGGATGCCGGGAGCAG
ACAAGCCCGTCAGGGCGCGTCAGCGGGTGTTGGCGGGTGTCGGGGCTGGCTTAACTATGCGGCATCAGAGCAGATTGTACTGAGAGTGCACCATTCGACGCTCTCCCTTATGCGACTCCTGCATT
AGGAAGCAGCCCAGTAGTAGGTTGAGGCCGTTGAGCACCGCCGCCGCAAGGAATGGTGCATGCAAGGAGATGGCGCCCAACAGTCCCCCGGCCACGGGGCCTGCCACCATACCCACGCCGAAACA
AGCGCTCATGAGCCCGAAGTGGCGAGCCCGATCTTCCCCATCGGTGATGTCGGCGATATAGGCGCCAGCAACCGCACCTGTGGCGCCGGTGATGCCGGCCACGATGCGTCCGGCGTAGAGGATCT
GGCTAGCGATGACCCTGCTGATTGGTTCGCTGACCATTTCCGGGTGCGGGACGGCGTTACCAGAAACTCAGAAGGTTCGTCCAACCAAACCGACTCTGACGGCAGTTTACGAGAGAGATGATAGG
GTCTGCTTCAGTAAGCCAGATGCTACACAATTAGGCTTGTACATATTGTCGTTAGAACGCGGCTACAATTAATACATAACCTTATGTATCATACACATACG

*Aca*GluD (*Acanthaster planci* delta iGluR, after XM_022229986.1 from Genbank)

GTCGACACCATGGAAATACCACAGTGGATAGCTTTAACCTGTCTCCTCCTCATGTATATTCTGGAAGGCGTTGTCACATCTGAGAGGCGTGTTTTCCCGTCAGTCATAAAAGTTGGTGTAATATT
AGAACAGCCGTCGTCAGATGAGGACGAGATGATTCGACTCTCATTCCAACATATAAACCAAAACGGGAACATCTTACCGTCAACCCGATTGGATTATACCGTGGCAAGGATAGCCTCCACAGATC
CCTTTGCAGCCGTTAAAGCAGCATGCTCAATGTTAAATACAACTGTCGCTGCACTTGTGTCTTCTACAAGCTGCGAGACGAGCCTAGCTCTCCAGTCGCTGGCGAACTCTTTCGATGTGCCCCAC
ATTATTGTGCCGGCGAGGAATGCCTCTCGGAAAAGCATAACAGTTTACGGTTAACGTCGCGACCAAGTCAAGTCTACCTGACGGAGCGTCTCGACTTGGTATGGTGCGTGAAATCGAAGAG
TGTCTCTATTGTTCTACGATTCAGAGAGCCCCTATAAGAACGTGCAGCAGTTCCTGCATCTGGCGGCGCAATCGGAGGAGCGCAAGCCGCTGGAGGTGACGCTGTACCGGGTGGACGATAGGGACC
CGGCCAGCGGCGCGCTTGGGATGATTAACATCTTGCACAAAGCTAAGGATTCGGACGTCCAACACATGATCACCTTCTGCGACAGAGCCCAGAGCATGAGGCTGATTAGACAGGCTGCACGTTTT
GGGATGGCCGTGGGGAAATACCAATGGATTATTACAACACAGGACTGGGACATGATGGGAGATGGCGAGCCGGGGAGCTTCACGACGGCTGGCGGGGACATCTCTGAGGAAGAGGGCATGAGATT
CCTCAATGGCTCCGAGGGCATCATCACCTTGATGAAGCAACAGGTCAAAGTTCAGACCCACCCTCTGCAGTTCTACAGCGCCTGGCAGATGCTCTACCCGGACATCGACAGGGAAGAGGACGCTA
ACTCCACTTACTTGTCGCCGGGGTATCTCAACACGATCCAGTTCAAAGCAGCCTATATGTACGACGCCGTACGAGTATTGGCAGTTGCCTTGAACGAACAGGTTGAGCGAGACAAGTACATTGAA
CCCGAGATACAGCATTGCTATGACAACAAACCCAAATCATGGAAAGGGGGCATTCGCCTCCGGAAGATGCTGCACAGGACGGAAACAACTGGGCTGATGGGACGGATGCGGTTTAATCACAGTAG
TCTGAATGATGAGATAGCGGTGGATGTCATTACCTTAGAAAGTGGCCGTAACCAGACCAAGGCATGGAAGATTGGCGGCTGGGACCCGGAAAATCGTCTAAATTTGGTCAAAACACCCTTTTCAA
GAGGTTTTGCTGCTTTTATCAGTAACAACACCACATTTCGCATTGTAACCGTTGTGGAGGGCGCCGTTCGTTAATCGGGACGAGACAGTGAATGGGTACAAGTACTCGGGGTTTGTCATCGACATG
TTAGAACTAATCGCCAAGGAGTTGAACCTGAAGTATGAGTTGTACCTTGTACCAGATGGAAACTACGGAGGAAAGAACGACGACGGGACGTGGAATGGCCTGATTGGGGAAGTTTATTATGGTAG
GGCGGACCTAGCGGTGGCCGGCATGGTCATCAACTCCGCACCGCGAGGAAGTGGTGGACTTCACCAAGCCCTTCATGAACTACGGCGTTGGGATTCCTATGCAAAAGCCCAAGAAGAAGGCCAACA
TCTTCGCCTTCCTGGAGCCGCTCCACATCAAGGTCTGGGGCTGCGTGCTGGCCTCCCTCTTCGTGGTCGGGGTGCTGATCTACATCGTGGACCGGCTCAGCCCTTACAGCAGTTTCCGGCGGGAG
AACAGTCCCAACCCGGAAGCCTTCGACTTGAAGAACAGCATGTGGTTTGCCTTCGCTTCCTGCATGCAACAGGGCGGCGACACCCTCCCGCTGTCCATTTCTGGTCGTGTCCTGAGCGCGTTCTG
GTGGTTCTTCGCCCTCATCATCACCGCTACGTACACCGCCAACCTGGCCGCCTTCCTGACCGTCACCCGCATGGAGAACCCCATCAACTCTCTACAGAGATTTGGCCACGCAGAAAACCGTGGTCT
ACGGCACCATCCTTAACAGCAGCCTGCATGACTTCTTCGAGAAGCGAAAGAATCAGGGTATCTACGAAAAGATGTGGAACTTCATGTCCACCTCCAAGATCGACCCCTGGGTGCCCAACGCCGAG
GCGGGGTACAAGCGCGTCCAGACAGAGGACTACGCCTTCTTTTGGGACGCGCCGATCCTAGACTACATCAAGCAGGAGGAGTGTGACGTCATGACTGTGGGCAAGCCCTTCAACCTGAAGGGATA
CGGCATTGCTACGCCGCGGGGGGTTCCATGGAGAGACGAGATATCAATGGTAATCTTAAAAATGCAAGAGAGGGGCGAACTAGAAGAACTCCGTAAGAAGTGGTTCGACCGGGAATCCAGCTGCC
TGGATGAGACGGACAGCATGAATACGAAACATCGCGCCGCCCGGGCCGACATCAACCTGGACCAGATTGCCGGCGCCTTCTACGTCCTGATCATTGGGGCCGTGTTGTCCTTTGTGGTGGTCATT
GTGGAGCACGTTTGGCACAAGCCGTCCTTCTACAAGAAGCGGGAAAAGGAGACGGGAAGGACCACATTGGACTGGTCAGACAAACTCCCTCCACGGGAAACGAGAAACAATGGTCTTTCTAACAT
TGAAAATTGTTCTTCCAATAAGCATTTAGTTGTTCAAGAGAATGACTCTTTTGCGTTAACACCTTTGAGACCAAACCCATGGAGCACAACGACAATTCTTTCTGTCCCCCCTGAAGCGACAGAAA
ACTCTTGCGGATCC

*Cra*GluD (*Crassostrea gigantea* delta iGluR, after XM_011429946.3 from Genbank)

GTCGACACCATGATACAGTCTACTGGATTTATACTGTTTGTCCTAGCTATTCGATCTTCTGCTAACTGGACAGTGGGAGTCATCTACCAGAGTGACAAGTGGACTGATTTGGGTAAACCACTAAA
TAATGGAAAGGTCACTGCCGTTCAGGAATACCTGTTGCATCAAGTCGATAATTCGGACGCTTTTTCAATGTATCAGAAAGTTTCCAACTTTTCCGAGAGTGGTGTGATTGGAATCGTCGCTTTCA
CATCTTGCCCTACTGCTGCAGTTCTTCAGGAGCAGATCGCTTCTACGAACCTTCCACTGATCACCATAGATAATGAAGTCTGTCCACAAACCTATGACGGCCATCATCATCTGTCCGTGCTTCCA
AACTGCCATAGTCAAAATACACAGTTCATCGATATAGTGCTTCACATGAAGTGGGAACATGTCAACGTCATTTACGATTCAACATCTTCTTACTGCCGTCAGGAACTCATCGTGTTACTGACCAA
AAAGAATGTCTCCAGTAATGCCATATTTCTCCATGAAGGACAACATCTGACGCTGGAAATCTTCCCAGAACTATACTTGGAAGAAGTTATCTACGTGGCTACAGATAAGGAACGGACGCTGGGCA
TTGTCTCCGAGGCTATGACACTGGACATGTTCAACCGTTCCTTCTTCTGGGTTCTGAATTTAGACCCATAGCGTCTGTGGAATAGCTCCTTGTATAAGCCTGTCCATGAAGGATGTGTTCTTCTG
ATATCCTCTGGACTTCAACAGAACGAAACCACGGCAGCTGATTTGCTTTCGGAAGCCCTATCAATATTCCAGCGTGGATTAGATTCTATCGGAGATGGACGAAATATCACAGACTTAACATTTCT
TCGCTTTAACCTCAAGCAATACATGATGGGATCTTCCGACGAAACCGGATTAATAGGAAAGGAATCGCAGATCCGGGTTTCAGTTCTACCAAAGATTACGAAACTCCGTTTGAAGAAGTTGCAG
GTTACTCACAGGATACTCGTAATTTTAATGTAGCTGACGATCGACTTTACAAGTGCATTTTCAAAGACTTTGGCAATAAGACGCTGAAGGTCGTTTCCGTCGAGGGAAAACCTTTCCAAATGCGA
GTGGATAAAGGCAATGGGTCCTTCTACTATTACGGATTTACATACGACCTGCTGAATGAGTTCGCCAAGCAGTTTAACTTCAGATACGAGTTCCTAGATTCAGTAGATGGCCTCTATGGAATAAC
TACAGATGATACCGAAAGTGCTTCAGGGATGATCGGAATGATCATGAGAGGGGAGGCTGATATTGCTGTCGGTGGATTTACAATAACAGCAGACAGAAGAAAAGTTGTAGACTTTCTCTATCCCT
TCCAAGAAGACGGTATCGGAATTATCATGCGAAAGGTTGATAACGAGGCTAACAAGATGTTTCGGGTCTTCAGTTCGCTGGGAACCGACTCTTGGCTTGCTACCGGCGCAGCTGCTTTTGTTGCT
GCCATAGTGTTGTCAATTATCGTCAAGCTGAGTCCGTTTAGTAAGGGACTTCACAACAAGGTATCTGCTAGCTTTTGGTTGGTTTTCTCCGCTTTTCTCCAACAGGGTGAAGAAAAATCCTCCAA
GTCTGCCCCTGCTCGTCTGGATAGGATTCTGGTGGATCTTCACAATTATCGTCATGTCCCTGTATACGGCTAACCTTGCTGCCTTTCTGACAGTATCCCTGGCAAAGGCACCAATAAAAAACT
TGGAGGAACTTGCAGCTCAGTCCGTTTACAAGCCATTAATTAAGAATGGTTCCAATCTTCACACCCTATTCGAGAAAGCTGAAGGAGGTATCTATAAGAAGATTTGGGATATGATGAGAGATGTC
CCTAAAATCATCTCTCCCGATGAAGGATATGAGGATTGATCGTCAAAGGAAATTATGCTTACATGACTGATGAATCGGAAGCCCGTTTCAAAGCTATGAAAGACTGCAAGAATCTAGAAATGGCGGA
TGAAACCTTCCATAAAGCAGAGCTCTCTTTCGTTATACGTAAGAACGCAGAGTTTAAAGAGGCTTTCAATAAACACATGCTGAAAATGGTGCAAAATGGCATCGTGGATAAGTACAAGAAGATAT
GGTGGGATAAGCATTCTTGTCATTCGGCTAATACTGCTACTCGAATTTAAAAGTACAAGTGGAATATTCATTGTCTATTCCGGATTCATTATTTATTTCGGTCATCTGCTGTCTTGTAGAG
CTGTACCTTCGAGGTCGTAAATACCCAAAGAACCGTGTCTCATCCAGTAAACAGAGTCTCGAAGATATTTCTGTCATCATGGTTGATTATGGATCC

*Dan*GluD2A (*Danio rerio* delta iGluR, after AAI62459.1from Genbank)

```
GTCGACACCATGAAAGTTTTTCCGGCAGTACTGTTTCTGATCACATTTTGGTCCCTGGAATGGGAACCTGTTCTTCCCGATTCAATCATTCACATCGGCGCCATTTTTGATGAGTCTGCCAAAAA
GGACGATGAGGTGTTCCGTATGGCAGTCGCGGATCTCAATCTCAACAATGAAATCCTGGAGACAGAGAAGATAACAGTGTCCGTGGAGTTTGTTGATGGAAACAACCCTTTCCAGGCTGTGCAGG
AAGCATGCGAGCTTATGAACAGAGGAATCCTCGCTCTGGTCAGTTCTATCGGCTGCATGTCCGCAGGCTCGCTGCAGTCTTTAGCTGATGCCATGCACATCCCTCACCTGTTCATCCAGAGGGCA
CCCGCGGGCACCCCTCGCTCCAGCTGCCCACCAACAACTCGTGCACAACCCGATGACTACACCCTGTTCGTCCGGCCTCCTGTCTATCTAAATGACGTCATCTTCCAAGTTGTGATGGAGTACAC
TTGGCAGAAGTTCATTATCTTCTACGATACAGACTATGATATCCGTGGAATAGAAAACTTCCTGGACCAGACGTCTCAGCAGGGGATGGATGTGTCTCTGCAGAAGGTTGAATCTAATATTAACA
TGATGATCACTGGAATGTTCCGCACCATGCGAGTGGAAGAACTGCATCGCTACCGAGACACACTGAGACGTGCTGTCCTGTTCATGTCACCCGCCACTGCCAAGGCCTTCATCACCGAAGTGGTG
GAGACCAACCTTGTGGCTTTCGACTGTCACTGGATCATCATAAATGAGGAGATTTCAGATATGGATGTGCAAGAACTGGTCATGAAGTCCATCGGTCGCTTGACCCTGGTGAGACAGACATTCCC
TTTGCCTCAAAACACGAGCCAGCGTTGCGTCCGTAACAATCACCGCATCAACACTTCTCTCTGCGATCCCAAAGACCCTAAGGCACAGATGCTGGAGATTACCAACCGCTACATCTACGACACAG
TACTGTTGCTGGCTAACACATTTCACCGTAAGCTGGAGGATCGTAAGTGGCATTCCATGGCGAGTCTTTCCTGCATCCGTAAGGGCTCCAAACCTTGGCAAGGAGGAAAGTCCATGCTGGAAACT
GTGAAAAAGGGAGGAGTATCTGGTCTGACCTCCCTGCTGGAGTTTAATGATAATGGGTCCAATCCCAACATCCATTTTGAAATCCTGGGTACCAACTACGGTGAGGATCGTGGTCGTGGAGTCTC
CCGTCTGGCTACCTGGGACCCAATCCACGGACTGAATGGAACACTGACCGATAGAAAGCTGGAAAATAACATGCGTGGTGTCGTCCTTCGTGTTGTCACTGTCCTGGAAGAACCGTTTGTTATGG
TGTCTGAAAATGTGCTGGGAAAACCTAAGAAGTACCAGGGATTCTCCATCGATGTGCTGGATGCTCTGGCCAACTATCTCGGATTCAAATATGAGATCTACGTGGCTCCTGATCACAAGTATGGC
AGCCAGCAGGCTGATGGAACGTGGAATGGTCTTATCGGAGAGCTGGTTTTCAAGAGAGCAGACGTAGGACTTTCCGCCCTGACCATCACCCCTGAACGGGAAAGCGTGGTCGATTTCACCACCCG
CTACATGGATTACTCTGTTGGAGTGCTGCTGAGGAAGGCGGAGAGGACCGTCGATATGTTTGCTTGCCTCGCGCCCTTCGACCTGTCCCTGTGGGCTTGTATAGCGGGTACCGTCCTGCTTGTGG
GAACTCTTGTCTATCTGCTCAACTGGCTTAATCCTCCTCGTCTTCCGATGGGCTCTGTCTCCTCAACCACACTCTACAACTCCATGTGGTTTGTCTACGGCTCTTTTGTCCAGCAGGGAGGCGAA
GTGCCCTACACAACTCTGGCTACCCGTATGATGATGGGTGTTTGGTGGCTGTTTGCTCTAATAGTCATCTCCTCCTACACGGCTAATCTGGCTGCTTTTCTTACCATCTCCCGCATTGAGAACTC
CATTCAATCACTGCAGGATTTGGCTAAGCAGACAGATCTCCCTTATGGCACGGTTCTGGACTCCGCCGTCTACGATCAGGTCCGTTCCAAAGGAATGAACCCTTTCGAACGAGACCCTATGTATT
CGCAGATGTGGCGTATGATCAACCGTACAGGAGGAGCCGAAAACAATGTGGAAGAATCAAAAGAAGGAATCCGGAAGGTGAAGTACGGACGTTTTGCATTCGTGTGGGATGCAGCTGTGCTGGAA
TATGTCGCCATTAATGACGAGGACTGTTCGCTGTACACCGTCTCTAACAATGTTGCTGATAGAGGATACGGCATGGCTATGCAGCATGGCAGTCCTTACAGAGACATTTTCTCTCAGCGTATCCT
GGAGCTTCAGCAGAATGGAGATATGGACATCCTGAAGCTTAAGTGGTGGCCAAGGGACAGTCCGTGCGACCTGTACTCTCCAGTCGGAACCCGTAAGAGTGGCAGCGCCCTGGACATCCACAGTT
TTGCTGGAGTCTTCTTTGTTCTAGCGGCAGGTGTGGTCCTGTCCTGTCTGATTGCCACCGTGGAAACGTGGTGGACACGACGTAAGGGCTCCCGTGTCCCATCGAAGGAAGACGATAAAGAAATC
GACCTGGAACACCTGCACCATCGTGTTAACAGCCTGTGCACTGAAGACGAGAGCCCCCACAAACAGTTCTCCACCTCCTCCATCGACCTGACGCCCCTTGATATGGATTCCCTCCCTGCTGCCCG
TCAGGCTCTCGAGCAGATAAGCGACTTCCGTAACACACACATCACCACCACCACCTTTATACCCGAGCAGATTCAGACTCTCTCACGTTCCCTGTCCGCCAAAGCCGCAGCTGGCTTCGCTTTCG
GGGCTGTACAGGATCACCGGACTGGGCGTCCCTTTCGTCAGCGTGCCCCTAATGGCGGCTTCTTTCGCAGCCCTGTCAAAACAATGTCTTCAATCCCTTATCAGCCCACCCCTGCTCCCAACTTT
AGCTATGGAAACGACCCGGATCGAGGAACTTCCATTGGATCC
```

*Dio*GluD (*Diopisthoporus longitubus* delta iGluR, after c29957 from transcriptome in Andrikou 2019)

```
GTCGACACCATGGTCAAGTTTACGCACATCGAACACGTGCTTTTCCTTCTGGCGACGTTATGCTCGTTTGTGCTGAAATCATCGGGTAGCAGTGGTGGAAGTGACTTCAGCTCGATACGGCTCGG
ATTCATCATAGAGCAGACGAGTGGAAGTGAGTTTCCACTTGATCAAGTCAATTCCCTGCTTCAGGATGAGGACGAGACAGCTCCTTCGCTCCTTAGCTATAGCATCGAAGTGATCGACTCTCAGA
ACCCGTACCTAGTAGTGCAGCGTGCGTGCGACATGCTAGCGACGTTCCCCGACCAGACGATCCTATTTGTCAGTCTGACAACGTGCATAACTCACCTGGTGCTACGATCGTTCACTGATCAGCAC
GCGCTGCCACACATTACGCTAGGTGGCATGGAAGGGTGTAATGCGCCGCCCAATAACACGTCCTCTCCATTAGGGGGCATCACGCTTACTTGGAATCTACAGGCCGACACAGAGAATACGGTGGA
TTCAGTGATTGCACACATTGTACACTTGGAAAAATGGACGAGTGTAATATTAATACGAGATGAAAGCATCAGCCAACAGCGGACGATCTCGCTACGGGAGCACATTGAAAGTCAGCGGGATAACG
TCAAATTCCATGAGATCAAACTCTTTCTTTACAATCACGATGAGCAGTTGAAGGACCGACTGCGTGACATCGTACCAGATGGAGAGTTTTTCAACTTCATCGTTCTAGCATCTGCTAGCTACACG
ATTGAAATTATACAGACGGCGATGCATCAAGAAATTAGAGGGACTGGAAACGTCAAGAAGTACAAATGGGTGATAGCTAATCAGGAGTTGAGTCTGGAGCAGATTTCGGTGATCGACCCCGAGAT
TCAGATAGTGTCGATTCTGCGATCATCACTCAAACCGTACAAGCTGAAGACAGACCGAAACTTGGAATACTTCAAGGATGCGATGAGTCTGATGGTTCTTGCACTGGAGAACCTTTCGGGAAGTC
TTTATGCTGATATTACTTGCGACAGAGATACAGTCTATCACCAAGGTGAGAACATCATCCAGGAGTTTAGGACTATGGATATCTACGATGGCCTTACTGGTTCGATCGAATCTCGCGAAGACAGA
TTTTACGACTACGTGGCATTGGACATTGTGCAAACAGCCAAGAATGCGACGTTTATCAATCGCTGGAACCTCATCGGTACGTGGAACAAGAGCGAAGGCCTAAACATGCCCGCGACGCGTGCGTT
TCTTCCCGAGTTCGATTCATTGGCGGGCATGACGCTACGAATTGTCACGCTAGTCGAACATCCATTCGTAATCAAAAAGTGGAATGCCGAAACGGGCCAAGCGGAGTACGAAGGCTGCGCTATCG
ACATTCTGAAGGCCATCCAGAAGGATTTGAAGGAAGAGAGTTTCACCTTCACAATGTACGAGGTGGCAGACAACAAATATGGAATTTTCGACGCTGAAACCAATCGCTGGACAGGCCTCGTCGGG
GATGTGAAAGAGCTGAGAGCGCAGATGGCGGTGGCGGGAATGATACGAAACTACAATCGAGAGATGGTAGTGGACTTCACCGCCTCTTACATGGACTACGGAGTGGGTATTCTCATCCCCAAACC
GTCCAAGACGACGAGCATCTTTGGATTTCTGGAGCCACTCAACGTGCAGGTCTGGATCTGTATCGCCGTGGCAACCTTCGGCGTTGGACTCGCGCTCTTCATCCTCTCCCGGTTCTCGCCCTTCA
GTCGGTTCAATCAACACGGAACCGACGAGTTCAGCTTCAAAAACTCAATGTGGTTTGCGCTCGCTAGCCTCATGCAGCAGGGAGGGGATGCGACGCCGCTCTCAATCTCGGGCAGAATCCTCGGC
ACCTTCTGGTGGTTCTTTACTCTTATTATCATAGCGACGTACACGGCGAATTTGGCGGCTTTCCTGACGGTGACGCGTATGGAGACGCCGATCGAGTCCCTTCAAGACCTGAGTAGCCAGACTCG
GATGCCGTATGGGACGGTGCGCGGCAGTTCGCTCGAACATTTCATACACCAGCAGGCGGAGGTAGACAAACTCTACGAGCGCATCTCAGCCTACTTCAGGACAACCGACCCTTCCCCGCTCGTAA
ACACATTCGAAGAAGGCAAAGATAAAGTCATCAGGGGCGATTACGCATTCCTGTGGGACGCTCCCGTGTTGGAGTACCACCGCAAATTACATTGCAGAGAGCTGGCGACGGTGGGAAAGCCATTT
AACCGCAAAAACTATGCCTTCGCCGTGCCAAAAAATGCGCCGTACCTCGAGACGATCACACTGAGCATCCTCCGTCTACAGGAGTCGGGCGAGCTCGACAAAATCAAGCAGAAGTGGTTCGAGGG
TGAGTCCCTGTGTTCGGAGGACGATTCGCTGACACCCGGTCAGGAGGCTGAGGGAATTGCCATCAAGAACGTCGCCGGTGTCTTTTACATACTGCTGATGGGCACCGGACTATCTTTCTTTACGG
CGATCATCGAGTTGATCTGGTATCGCTATTTCAGAGCGATGGAGGACCTGCGTCCTCCTCTACCCCAAAACAGACAGCGGGCCGAATTGTTGGCTCCTACGGGATCC
```

*Mea*GluD (*Meara stichopi* delta iGluR, after 16765.1 from transcriptome in Andrikou 2019)

```
GTCGACACCATGATTCCACCAAGCTGGCAACATGTATTGGTATTTCTTGTATGGCTATTCCACGTTGCTACCATGCAGCTAAACAAGCTTAAAATCGGGGTCATCATTGAAAATGTACCGATAGA
GGAAGACATTGTTGAAGAAGCAGTGGACATGATAAACAGTGATGATCGATTCAATGGTGTCTTAGAACCGTTGGTGGCGAGTATTGACGGTATAAATCCTGTAACAGTGATCAAGAAAGCCTGTG
ATATGCTTAACAACGATATAAGGTTGATAATAGCAACAACATCATGCGAATCGTTCCCTGGATTGATGGCGTTAGCTACCTCAATACACATGCCACTCATTAACGTCCCGTCCAAGTATTGCAAA
CCCGTTGAGCAAGGCAACGACTTCATACTTGACATAAAGCCCTCGATGAATAACTTACAAGAAGCTGTTCGGGATATAATTAATATCCAAAAATGGAAAAATGTGGTCATATTCTATGACAGTAA
TTTTGGCTGTGAACGACAACAGTCATTGGTGGAGACGTTCGCCAATAACAATGTGTTCTTGTTTAAGACGAACAAAGAGCTCTTGGAAACAGACGGCAACAATGGAATCGTTGAGTTCTTCCAGT
TTATTAAATCCAACGGAACGAACTATAAGTTTGTTGTTATGACTGGAGAAAGAAACAGTATATACCTCATTAATAAAGCTTTGAATATGGGAATGTTCAAATCAACTTACTTATGGCTTCTGGCC
AGCCCGGAGACAAACACGAATTTAATCTCAATGGATAAGATAGCTGCTGGTCAGCTGGTCAGATTGAGGTATAGCATATCAACATGGGGTAAGAGGGAGGAAGCTGAGCTGATTAAGACTCAGAT
CTACAAGGCCATTCTGCGAGCCGCGCTCACAGCTCACAGCATCAAGAGGAGCTTCTGGTCTCCGCCTCGGGGGCTGACCTGCAGACTCGACGGCAACTACACTAATACTCAATGGTTATCAGGAA
GGATGTTTGCCAATAAACTCCGGGCGTTTGAGAACCCTATGGCCGGGGACATGTACTTTGATGACGACAACAAATACTTAAAACAATGGATGATCATAATTGAGATAATAATGGATATAGATGAG
TGGAAACAGGTGGGATCGTGGATGCCAAATTCCAGACTAAATCTCTCTACTACTGCATTCAGTCCTTTCGCCAGTTTGAAATATTTGCATTTAAAAGTAGCCACAGTTGAAGAAGAGCCCTTTGT
GTACAGAACAAAGGAAGGGGTCGTCGAAGGATTTTGTATAGACCTTCTGAACTCTCTACAGAGTGAACTCAACTTCACTTACACTCTCGTCATCAAAGACACCTACGGGACGATGGACCAAGAGA
CCAAGGAATGGAATGGCGGCATCAGAGCTCTCATTGACAAGGAATGCAACATCATGGTAAGCGGAATGACGATCATTGAGTCCAGAGAAACAGTTGTTGATTTTACAGTCCGGTATATGGACTAC
GGTGTAGGCATATTACTCAAAAAACCAATTCCGACAAATGACGTTCTTGGCTTTATCAGACCTCTGGACCTGCAGGTGTGGGGGTGTATCGTGGCCGCCGTCCTGATCGTCGGAGTGATGACGTA
CTTCGTCGTCAAGTTGAGCCCTTATTCAAAGATGGAAGATGGGTCGAACGAGTTCCGATACTTCACATTCGCAAATTCGGTGTGGTTTAGCGTGACCTCGATCTTGCAACAAGGTCCAGAAATGG
TTCCGCAGCCACTTTCTGGCCGGTTGGTGACAGGATTCTGGTGGTTCTTCACTCTCATCATGATCGCCACTTACACTGCCAACCTGGCTGCATTCCTGACTGTAACACGAATGATCACTCCAATA
GAAAGCATTGAGGATTTGGCTCAGCAATCAGACATAAAATACGGCACTCTGCGAGGCTCATCTGTGCAGCAAGCATTCAGCGAGCAGAAGGGCGGTAACTACGTCTTCGAAACCATCAGCCAGTA
TTTCAAGGAAAATCCAGACGTCTTGGTAGATGGAAATATCGAAGGTTTCGAAAGAGTGAAATCTGAGAATTACGCCTTCCTATGGGACTATCCTGTCGTTAAATGGAAGTCTAGTAAAGAATGTG
CTGACTATATTATCGTTGGGAAGCCTTTCTTGCTCAAAGGTTACGGGATAGCTTTGCAGCGAGGCTTCCCTTACCGAGACGACTTCAACTCAGCGATACTGAAGTTTCAAGAGAGCGGGAAGCTC
GCCAAGATGCAGAAGAGTTGGTTCGAGCCTGCCACTACAGTCTGTAAAGAGTCTTCCACCAAGTTCGGCAGCGGGATTGAACTGAAAGATGTAGCCGGTGTCTTTTACGTTCTAATCGTGGGTAA
CGTCCTGGCCTTCATGGCTGCCATTGCTGAGGCTTGCTGGTTCAGGAGAAAAAACCTACAAACCGATCACACAACGTTGATGTCTGAAATAAATTCAGTTGCTGACACGAGAAACGATAGCAAAG
TGCTAATTTCAGTAGATTCTAGAAAATCATTATTTGAATCTCAAGGCCAAGTGAATAGTTATCCAATACAGCATGCGACGAACGACTACCCACCGCCAGCCAATAACTATCCTCAAAGACAGCCG
CCATTGCTGTACACCTCCAGCAGAGAAACAGTGAACACGTATTCTGCATCCGCTATGCATCCCCGCCAATTCTACAATATGGATCAACTACATCCTCTTGAAAAGGAAGCTACCGTTGGATCC
```

*Rat*GluD2 (*Rattus norvegicus* delta 2 iGluR, after NM_024379.2 from Genbank)

```
GTCGACACCATGGAAGTTTTCCCCTTGCTCTTCTTTCTATCCTTCTGGTGGTCTCGAACCTGGGACCTGGCGACCTCCGATTCCATCATCCACATCGGAGCAATTTTTGATGAATCTGCTAAAAA
AGATGATGAAGTATTCCGCACAGCAGTTGGTGACCTCAACCAGAATGAGGAAATCTTACAGACTGAGAAAATCACATTTTCAGTGACATTTGTGGATGGCAACAACCCTTTTCAAGCTGTTCAAG
AAGCATGTGAACTTATGAACCAGGGCATCTTGGCCTTGGTCAGCTCCATTGGTTGCACATCTGCTGGGTCCCTCCAGTCTTTGGCAGACGCCATGCATATCCCTCACCTCTTCATTCAGCGTTCA
ACAGCTGGGACCCCAAGAAGTGGCTGCGGCCTCACCAGGAGCAACAGAAACGATGACTATACCCTTTCAGTTCGTCCACCTGTCTACTTGAATGAAGTCATCCTAAGAGTAGTCACAGAGTATGC
ATGGCAGAAATTTATTATCTTCTATGATAGTGAATATGATATCCGTGGCATACAGGAATTTTTGGACAAAGTTTCCCAGCAGGGAATGGATGTTGCCCTTCAAAAGGTGGAAAACAACATCAATA
AAATGATCACCACGCTCTTTGACACCATGAGGATAGAGGAGTTGAATCGCTATCGAGACACTCTCAGAAGAGCCATCCTTGTTATGAACCCCGCCACAGCCAAATCCTTCATAAGTGAGGTGGTG
GAGACTAATCTGGTTGCTTTTGACTGTCACTGGATCATCATCAATGAGGAAATAAATGATGTGGATGTTCAGGAACTTGTCAGAAGGTCCATTGGAAGGTTAACAATTATTCGGCAGACATTTCC
AGTCCCCCAGAATATAAGTCAGCGCTGTTTCCGTGGCAACCATCGAATTTCTTCAACACTGTGTGATCCCAAGGACCCCTTCGCACAGAATATGGAGATTTCTAACCTTTACATCTATGACACGG
TGCTTCTGCTTGCAAACGCCTTTCATAAGAAGCTGCAGGACCGGAAGTGGCACAGCATGGCGAGCTTGTCCTGTATCAGGAAAAACTCCAAGCCCTGGCAGGGAGGGCGGTCCATGCTGGAGACC
ATCAAGAAGGGTGGAGTTAATGGATTGACTGGAGATCTAGAATTTGGAGAAAATGGAGGTAACCCCAATGTCCACTTCGAAATCCTTGGAACCAACTATGGAGAAGAACTTGGCAGGGGTGTCCG
TAAACTTGGGTGCTGGAATCCTGTCACAGGTCTGAATGGATCACTGACAGACAAGAAACTGGAGAATAACATGCGAGGTGTGGTTCTACGCGTGGTGACTGTATTGGAGGAGCCTTTTGTAATGG
TCTCTGAAAATGTCTTGGGAAAACCGAAGAAATACCAGGGCTTCTCCATTGATGTTTTAGATGCCCTATCTAACTATCTGGGTTTTAACTATGAAATTTATGTTGCACCGGACCACAAATATGGA
AGCCCACAAGAAGATGGGACATGGAATGGACTAGTAGGAGAACTTGTTTTTAAGAGAGCTGACATCGGGATTTCAGCTTTAACCATCACTCCAGACCGGGAGAATGTTGTGGATTTTACAACACG
```

CTACATGGACTACTCAGTAGGGGTCCTACTGCGAAGGGCAGAAAAAACAGTGGATATGTTTGCCTGCCTTGCACCATTTGATCTATCTCTGTGGGCCTGCATTGCCGGCACAGTCCTTCTTGTGG
GACTCCTGGTCTACCTTCTTGAACTCGCTTAATCCCCCACGGTTGCAAATGGGATCAATGACATCTACTACACTCTATAACTCCATGTGTTTGTGTACGGGTCCTTTGTACAGCAAGGTGGGGAA
CTACCATACACACTTTGGCAACCCGAATGATGTGGGGCTTGGTGGTTATTTGCTCTGATTGTCATCTCATCTTATACAGCAAATCTTGCCGCTTTCCTCACTATCACCCGCATTGCAGACGCTC
CATCCAGTCTCTTCAGGATCTGTCCAAGCAAACGGATATCCCTTATGGCACAGTCTTGGATTCCGCAGTATATCAGCATGTTCGCATGAAGGGGCTGAATCCTTTGAGAGGGACAGCATGTATT
CCCAGATGTGGAGGATGATCAACCGAAGCAATGGCTCAGAGAACAATGTTCTGGAGTCCCAAGCAGGCATTCAAAAGGTAAAATATGGAAACTATGCTTTTGTATGGGATGCAGCTGTGTTGAA
TATGTGGCCATCAATGACCCCGACTGTTCCTTCTACACTGTTGGAAATACTGTTGCTGACGGGGGGTATGGCATCGCACTGCAGCATGGCAGTCCCTACCGTGATGTCTTTTCACAAAGGATTCT
GGAGCTGCAGCAGAGTGGCGACATGGACATCCTCAAGCACAAATGGTGGCCTAAGAATGGCCAGTGTGACCTGTACTCCTCAGTAGATGCAAAGCAGAAGGGAGGAGCCCTGGACATCAAGAGTC
TGGCAGGCGTGTTCTGCATCCTGGCCGCGGGGATTGTACTCTCCTGCCTCATAGCCGTCCTCGAGACATGGTGGAGTCGGCGGAAGGGCTCCGAGTCCCATCGAAAGAGGATGACAAGGAAATT
GACCTGGAGCACCTCCATAGACGTGTAAATAGCTTGTGCACAGATGACGACAGCCCCCATAAACAGTTTTCCACCTCGTCAATTGACTTGACCCCTCTGGACATTGACACTTTGCCAACACGACA
AGCCCTGGAGCAGATCAGTGATTTCAGAAACACTCACATCACCACCACCACCTCATCCCAGAGCAGATCCAGACTCTTAGCCGCACAACTCTCAGCAAAAGCTGCCTTTGCCTTCACTTTCGGCA
GTGTGCCCGAGCACCGAACTGGCCCTTTTAGGCACAGGGCCCCTAATGGGGGCTTTTTCAGGAGTCCTATCAAAACAATGTCATCTATTCCTTATCAGCCTACTCCCACTCTGGGGCTCAATCTG
GGCAATGACCCCGACCGAGGCACGTCCATAGGATCC

*Rat*GluD1 (*Rattus norvegicus* delta 1 iGluR, after NM_024378.3 from Genbank)

GTCGACACCATGGAAGCGCTGACGCTGTGGCTTCTTCCCTGGATATGCCAGTGCGTTACGGTGCGGGCCGACTCCATCATCCACATCGGTGCCATCTTCGAGGAGAACGCAGCCAAGGACGACAG
AGTGTTCCAGTTGGCTGTATCAGACTTGAGCCTCAATGATGACATCCTGCAGAGTGAGAAGATCACCTACTCCATCAAGGTCATCGAGGCCAATAATCCGTTCCAGGCGGTGCAGGAAGCCTGTG
ACCTCATGACCCAGGGGATTTTGGCCTTGGTCACGTCCACGGGCTGTGCATCTGCCAACGCCCTGCAGTCCCTCACAGACGCCATGACACATCCCACACCTCTTTGTCCAGCGCAACCCCGGGGGT
TCACCACGTACTGCCTGCCACCTGAACCCTAGCCCCGACGGCGAGGCCTACACACTGGCTTCGAGACCGCCCGTCCGTCTCAATGATGTCATGCTCAGGCTGGTGACAGAACTGCGCTGGCAGAA
GTTCGTCATGTTCTATGACAGCGAGTATGATATCCGTGGGCTCCAAAGCTTTCTGGATCAGGCCTCACGGCTGGGTCTTGACGTCTCTTTACAAAAGGTGGACAAGAACATCAGTCACGTGTTCA
CCAGCCTCTTCACCACCATGAAGACGGAGGAGCTGAATCGCTACCGGGACACACTGCGCCGGGCCATCCTCCTGCTTAGCCCACAGGGGGCGCACTCGTTCATCAACGAGCTGTGGAGACCAAC
TTGGCTTCCAAGGACAGCCACTGGGTCTTCGTGAATGAGGAAATCAGTGACCCCGAGATCCTGGATCTGGTCCACAGTGCCCTTGGCAGGATGACCGTGGTCCGGCAAATCTTCCCATCTGCAAA
GGACAACCAGAAATGCATGAGGAATAACCACCGCATCTCTCCCTGCTCTGTGATCCACAGGAAGGCTACCTCCAAATGCTGCAGATCTCCAATCTCTATCTGTACAGACAGTGTTCTGATGCTGG
CCAACGCCTTCCACAGGAAGCTGGAAGACCGGAAGTGGCATAGTATGGCAAGCCTTAACTGCATACGGAAATCTACCAAGCCATGAAATGCAGGAGGAGATCCATGCTAGACACCATTAAAAGGGA
CACATCACCGGCCTCACAGGAGTTATGGAGTTTCGGGAAGACAGCTCAAATCCCTATGTCCAGTTGAAATCCTTGGCACAACCTATAGTGAGACTTTTGGCAAAGACATGCGCAAGCTGGCGAC
CTGGGACTCAGAGAAGGGCCTGAATGGCAGTCTGCAGGAGAGACCCATGGGCAGCCGCCTCCAAGGACTGACTCTCAAAGTGGTGACTGTCTTGGAAGAGCCTTTTGTGATGGTAGCTGAGAATA
TCCTTGGACAGCCCAAGCGTTACAAAGGGTTCTCCATAGATGTGCTGGATGCATTGGCTAAAGCTCTCGGATTCAAATACGAGATATACCAGGCCCCTGATGGCAGGTATGGCCACCAACTCCAT
AACACTTCCTGGAACGGGATGATCGGGGAGCTCATTAGCAAGAGAGCAGACTTGGCCATCTCTGCTATTACCATCACCCCGGAGAGAGAGAGCGTTGTGGACTTCAGCAAGCGATACATGGACTA
CTCAGTGGGGATTCTCATCAAGAAGCCGGAGGAGAAAATCAGCATCTTCTCCCTTTTCGCCCCCTTGACTTTGCGGTGTGGGCCTGCATTGCTGCAGCCATTCCCGTGGTGGGTGTGCTCATAT
TCGTGTTGAATCGGATACAGGCTGTAAGGTCTCAGAGTGCCACCCAGCCTCGGCCCTCAGCTTCTGCGACTTTGCACAGTGCCATCTGGATCGTCTATGGAGCCTTTGTCCAGCAAGGTGGTGAG
TCTTCGGTGAACTCTGTGGCCATGCGCATCGTGATGGGCAGCTGGTGGCTCTTCACGCTCATTGTATGTTCCTCCTACACAGCCAACCTTGCTGCTTTCCTCCACAGTGCCAGGATGGACAGCCC
CGTAAGAACATTTCAGGACCTGTCCAAGCAACTGGAGATGTCTTATGGCACTGTCCGGGACTCTGCTGTCTATGAGTACTTCAGAGCCAAGGGGACCAATCCCCTGGAGCAGGATAGCACTTTG
CTGAGCTCTGGCGGACCATAAGCAAGAATGGAGGGGCTGACAACTGTGTCCAATCCTTCAGAAGGTATCAGGAAGGCAAAGAAGGGGAACTACGCCTTTCTGTGGGATGTGGCCGTGGTTGAG
TATGCAGCCCTGACAGATGACGACTGCTCAGTGACTGTCATCGGCAACAGCATCAGCAGCAAGGGCTATGGGATTGCCCTGCAACATGGCAGCCCCTACAGGGACCTCTTCTCCCAGAGGATTCT
GGAGCTCGAAGACACAGGGGACCTGGATGTGCTCAAGCAGAAGTGGTGGCCACACACAGGCCGCTGCGACCTCACCAGCCATTCAGTGCACAGACTGATGGTAAATCCCTTAAGCTGCACAGCT
TCGCTGGGGTCTTCTGCATTTTGGCCATTGGCCTCCTTCTCGCCTGCCTCGTGGCTGCTCTAGAGTTATGGTGGAACAGCAACCGGTGCCACCAGGAGACCCCAAAGAGGACAAAGAAGTGAAT
CTGGAACAGGTGCACCGGCGCATCAACAGCCTCATGGATGAAGACATTTCCTCACAAGCAAATTTCCCCAGCATCCATTGAGCTTTCTGCCCTGGAGATGGGGGCCTGGCTCCAAGCCAAGCTTT
GGAGCCCACGAGGGAGTACCAGAACACCCAGCTCTCAGTCAGCACCTTTCTGCCTGAGCAGAGCAGCCATGGCACCAGCCGGACACTGTCGTCAGGGCCCAGCAGCAACCTGCCACTGCCGCTGA
GCAGCTCAGCCACCATGCCCTCAATTCAGTGCAAACACAGGTCGCCCAATGGGGGACTGTTTCGACAGAGTCCGGTGAAGACCCCCATCCCTATGTCTTTCCAGCCCGTGCCTGGAGGCGTCCTT
CCAGAGGCCCTGGACACCTCTCATGGCACCTCCATCGGATCC

*Sac*GluD (*Saccoglossus kowalevskii* delta iGluR, after XM_002731960.1 from Genbank)

GTCGACACCATGGATCGACACGTGTCGTATATTCTGTTGTTGTTTTCGAGTATGTTGATAGGCTTGTTGTTTTCCGATTCAAGCAAGAGAAGGACTACCTCGCAACATCAGCATAGGTGTGTT
ATTCGAAGAAACTCAAGGAGATGAGAGAAAACTTTTAAAAGAAGCAATCAAAAAAGTTCAAAGGGATACTTCATTATTACCTCACACAGAATTAATTGTTCACTGGGAAAGGATTGGATTCACAG
ATCCGTACGACATGATTGAACAAGCATCGCAGAATATATGGGAAGTCGCCTTCATTAATGATAAACATTGACGTCCTGCCAGCCATCTACCTTACTGCAAAATGCTGCTAACGTGTTCAGGTTACCA
CATTTACAGATTGCTACGGAGACCTGCAGGATTAGTTCAGAATTTACGCTAAGTATGAATCCCGATGTCTATATGACTGACATGGCGCTGTTTTCGCTGATCAAGTTACAGGAATGGACTTCATT
TGTTGTTTACTATGACACCGATATGGCATACCACCGAGTGCAGAGCATTATTGAATCGGCCGATAATGGTAATCTAGTTTGGGAAGTCATTTTACTACGCTACATTGGCGATGAAGTGGGTACAC
GCTGGACATCACAACAACTCAAAAGAATGGACGGAATACATAATTATGTGATTGTATTTGAAACCAAAAATGTATTTAATCTTTTACGTACGGCAGGTAACATGGGTATGCGGTCACGTGAATAT
CACTGGATCGTTCTTTATCAGGGAATGACAGACACCCAGCTGGAAAATGTGCCTAAGGCATTGGGTATTGTCATATTTGTCAGACAACAACCTCTCATCATAGAAACGAACGAAGAGGAGGTGAG
AGGTCACAAAAAGAAGAAGAAAGATAGAATAAATAATGCAAGTATACCGTCCCTCTATCTCCATGATAGCGTCATTGTTGCTGCCATGGCACTAGATGCAGTTATCAAGAAACACAGGCATTTTA
TTTGGCCCGCAGTAGACCCGTCGTTGTGTAGACCATTACAGTCTGATACTACTGTACATCATATCGGCAGGTCTGATACTATAGGGTCTCAGGAGGTAACGGATAGATATGCGCTAATGGATGCT
GTGCGAAAGATTGGCATATGGGACCCGGTCAACAGGCTGAACATGTCACACACCCCATTTCAGTCCACTTTTAAAGTTCTACAGAACAGGACTTTGAAGATTGTTACTATAGAGGAAGAGCCTTT
TGTTAGAAAAACCGAGATCCGCCCAGGAGTGTATGAATACACAGGTTTCTGCATAGACATATTAGACGAGATTTCACAAAGTTACAATTCACGTATGTGCTATATGATGTTCCTGATCTGAAAT
ACGGAGCTAAAGTGAATGGTACATGGAATGGGTTAGTCGGAGAAGTGGCATATGGGAAAGCAGACATGGCAGTAGCTGGAATAACAATAATGGCTGAGCGAGAAGAAGTTGTTGATTTCACTAAA
CCGTATTATCAGTATGCCCTGGGAATTATTATCAGTAAGCCCGGACCGAGCGAGGCATCTCGCCTTTATGGAACCATTAAGCGGTCCGGTGTGGGGATGTATAGCAGCAGCCTGTTTGTAGT
GGGAATATTCCTGTTCGTCATAGCCAGGCTTAGTCCATATAGCTCGTTCAATTACTCTAAAAAAGAATATTGTGAATGTAAAGGCGATGACTTTAACTTGAAGAACAGCTACTGGTTTGCATTGG
CATCCCTTATGAACCAAGGTGGTGATACTGCTCCCTACTCCATCTCCGGGAGATTACTGAGCGGTTTCTGGTGGTTTTTCACTTTAATAATCATAGCTACGTACACACAGCTAATTTGACAGCATTT
CTGACAGTGAGCAGGATGGAAACGCCTATATCGTCTGTGGAGGAATTATCAACGCAATCTAAAATCAAATACGGTACAATCCGAGACAGTAGTGTAGTCTCATTTTTTAAAAGATCCACAATAAA
TCCTTATCAGCGAATGTGGCAGTTCATGAATACGACAGAGGTTGATCCATACGTAGACACTGTCACGGACGCATATCGTAGAGCGAAAGGGGAGGAGTAGTGCCTTCATGTGGGATTATCCCGTGT
TGGAGTTACAAAAAAGAATCGATTGCGATCTTATGACTGTGGGAAAGCCTTTCTATGAAAAGGGATACGGTTTTGTAACTCCACAAGGAGCGGATTGGAGAGATGATATATCCATGAGTATTCTG
GAGATGAGGGAGAATGGTCAACTAGAAAAATATCGCAAGAAGACCTGGAAATCGAAAGCGAGTGTGAGGACGATGCGGCTATGATAAGAAGTTCCACAAATGAGATAGATATTCAAAGTGTTGC
TGGTGTGTTCTATATACTTATGATCGGTGCAGGTGTCTCCTGATAACTGTCTCAGTAGAGATATTGTATTATCATTTTTGAGGAAGTGTTGCCGACCAACTATAACAGTCCATCCCAACGTGG
ATGGTAAGGCTATTGAGGTCAGAGAAGAAAAATGCTATAGAAGATGGTAAATCCTTGTCTAATTCCAGAGTTTGAGGATCC

Chimera *Aca*GluD^{RatNTD} (*Acanthaster planci* delta iGluR with NTD replaced with *Rat*GluD2 NTD (purple). *Aca*GluD NTD-LBD linker underlined.)

GTCGACACCATGGAAATACCACAGTGGATAGCTTTAACCTGTCTCCTCCTCATGTATATTCTGGAAGGCGTTGTCACATCTGAGAGGCGTGTTTTCCCGTCCATCATCCACATCGGAGCAATTTT
TGATGAATCTGCTAAAAAAGATGATGAAGTATTCCGCACAGCAGTTGGTGACCTCAACCAGAATGAGGAAATCTTACAGACTGAGAAAATCACATTTTCAGTGACATTTGTGGATGGCAACAACC
CTTTTCAAGCTGTTCAAGAAGCATGTGAACTTATGAACCAGGGCATCTTGGCCTTGGTCAGCTCCATTGGTTGCACATCTGCTGGGTCCCTCCAGTCTTTGGCAGACGCCATGCATATCCCTCAC
CTCTTCATTCAGCGTTCAACAGCTGGGACCCCAAGAAGTGGCTGCGGCCTCACCAGGAGCAACAGAAACGATGACTATACCCTTTCAGTTCGTCCACCTGTCTACTTGAATGAAGTCATCCTAAG
AGTAGTCACAGAGTATGCATGGCAGAAATTTATATCTTCTATGATAGTGAATATGATATCCGTGGCATACAGGAATTTTTGGACAAAGTTTCCCAGCAGGGAATGGATGTTGCCCTTCAAAAGG
TGGAAAACAACATCAATAAAATGATCACCACGCTCTTGAACACCATGAGGATAGAGGAGTTGAATCGCTATCGAGACACTCTCAGAAGAGCCATCCTTGTATGAACCCCGCCACAGCCAAATCC
TTCATAAGTGAGGTGGTGGAGACTAATCTGGTTGCTTTTGACTGTCACTGGATCATCATCAATGAGGAAATAAATGATGTGGATGTTCAGGAACTTGTCAGAAGGTCCATTGGAAGGTTAACAAT
TATTCGGCAGACATTTCCAGTCCCCCAGAATATAAGTCAGCGCTGTTTCCGTGGCAACCATCGAATTTCTTCAACACTGTGTGATCCCAAGGACCCCTTCGCACAGAATATGGAGATTTCTAACC
TTTACATCTATGACACGGTGCTTCTGCTTGCAAACGCCTTTCATAAGAAGCTGCAGGACCGGAAGTGGCACAGCATGGCGAGCTTGTCCTGTATCAGGAAAAACTCCAAGCCCTGGCAGGGAGGG
CGGTCCATGCTGGAGACCATCAAGAAGGGTGGAGTTAATGGATTGACTGGAGATCTAGAATTTGGAGAAAATGGAGGTAACCCCAATGTCCACTTCGAAACCAACTATGGAGAAGA
ACTTGGCAGGGGTGTCCGTAAACTTGGGTGCTGGAATCCTGTCACAGGTCTGAATGGATCACTGCCCTTTTCAAGAGGTTTTGCTGCTTTTATCAGTAACAACACCACATTTCGCATTGTAACCG
TTGTGGAGGGCGCCGTTCGTTAATCGGGACGAGACAGTGAATGGGTACAAGTACTCGGGGTTTTGCATCGACATGTTAGAACTAATCGCCAAGAGTTGAACTTGAAGTATGAGTTGTACCTTGTA
CCAGATGGAAACTACGGAGGAAAGAACGACGACGGGACGTGGAATGGCCTGATTGGGGAAGTTTATTATGGTAGGGCGGACCTAGCGGTGGCCGGCATGGTCATCAACTCCGACCGCGAGGAAGT
GGTGGACTTCACCAAGCCCTTCATGAACTACGGCGTTGGGATCTCATGCAAAAGCCCAAGAAGAAGGCCAACATCTTCGCCTTCCTGCGAGCCGCTCCACATCAAGGTCTGGGGCTGCGTGCTGG
CCCTCCTCTTCGTGGTCGGGGTGCTGATCTACATCGTGACCGGCTCAGCCCTTACAGCAGTTTCCGGCGGAGAACAGTCCCACCCGGAGCCTTCGACTTGAAGAACAGCATGTGGTTTGCC
TTCGCTTCCTGCATGCAACAGGGCGGCGACACCCTCCCGCTGTCCATTTCTGGTCGTGTCCTGAGCGCGTTCTGGTGGTTCTTCGCCCTCATCATCACCGCTACGTACACCCGCCAACCTGGCCGC
CTTCCTGACCGTCACCCGCATGGAGAACCCCATCAACTCTCTAGAGGATTTGGCCACGCAGAAAACCGTGGTCTACGGCACCATCCTTAACAGCAGCCTGCATGACTTCTTCTGAAAGCGAAAGA
ATCAGGGTATCTACGAAAAGATGTGGAACTTCATGTCCACCTCCAAGATCGACCCCTGGGTGCCCAACGCCGAGGCGGGGTACAAGCGCGTCCAGACAGAGGACTACGCCTTCTTTTGGGACGGG
CCGATCCTAGACTACATCAAGCAGGAGGAGTGTGACGTCATGACTGTGGGCAAGCCCTTCAACCTGAAGGATACGGCATTGCTACGCCGCGGGGGGTTCCATGGAGAGACGAGATATCAATGGT
AATCTTAAAAATGCAAGAGAGGGGCGAACTAGAAGAACTCCGTAAGAAGTGGTTCGACCGGGAATCCAGCTGCCTGGATGAGACGGACAGCATGAATACGAAACATCGCGCCGCCCGGGCCGACA
sTCAACCTGGACCAGATTGCCGGCGCCTTCTACGTCCTGATCATTGGGCCGTGTTGTCCTTTGTGGTGGTCATTGTGGAGCACGTTTGGCACAAGCCGTCCTTCTACAAGAAGCGGGAAAAGGA
GACGGGAAGGACCACATTGGACTGGTCAGACAAACTCCCTCCACGGGAAACGAGAAACAATGGTCTTTCTAACATTGAAAATTGTTCTTCCAATAAGCATTTAGTTGTTCAAGAGAATGACTCTT
TTGCGTTAACACCTTTGAGACCAAACCCATGGAGCACAACGACAATTCTTTCTGTCCCCCCTGAAGCGACAGAAAACTCTTGCGGATCC

Chimera *Aca*GluD^{RatNTDlink} (*Acanthaster planci* delta iGluR with NTD and NTD-LBD linker replaced with *Rat*GluD2 NTD and NTD-LBD linker (purple). *Rat*GluD2 NTD-LBD linker underlined.)

GTCGACACCATGGAAATACCACAGTGGATAGCTTTAACCTGTCTCCTCCTCATGTATATTCTGGAAGGCGTTGTCACATCTGAGAGGCGTGTTTTCCCGTCCATCATCCACATCGGAGCAATTTT
TGATGAATCTGCTAAAAAAGATGATGAAGTATTCCGCACAGCAGTTGGTGACCTCAACCAGAATGAGGAAATCTTACAGACTGAGAAAATCACATTTTCAGTGACATTTGTGGATGGCAACAACC
CTTTTCAAGCTGTTCAAGAAGCATGTGAACTTATGAACCAGGGCATCTTGGCCTTGGTCAGCTCCATTGGTTGCACATCTGCTGGGTCCCTCCAGTCTTTGGCAGACGCCATGCATATCCCTCAC
CTCTTCATTCAGCGTTCAACAGCTGGGACCCCAAGAAGTGGCTGCGGCCTCACCAGGAGCAACAGAAACGATGACTATACCCTTTCAGTTCGTCCACCTGTCTACTTGAATGAAGTCATCCTAAG
AGTAGTCACAGAGTATGCATGGCAGAAATTTATTATCTTCTATGATAGTGAATATGATATCCGTGGCATACAGGAATTTTTGGACAAAGTTTCCCAGCAGGGAATGGATGTTGCCCTTCAAAAGG
TGGAAAACAACATCAATAAAATGATCACCACGCTCTTTGACACCATGAGGATAGAGGAGTTGAATCGCTATCGAGACACTCTCAGAAGAGCCATCCTTGTTATGAACCCCGCCACAGCCAAATCC
TTCATAAGTGAGGTGGTGGAGACTAATCTGGTTGCTTTTGACTGTCACTGGATCATCATCAATGAGGAAATAAATGATGTGGATGTTCAGGAACTTGTCAGAAGGTCCATTGGAAGGTTAACAAT
TATTCGGCAGACATTTCCAGTCCCCCAGAATATAAGTCAGCGCTGTTTCCGTGGCAACCATCGAATTTCTTCAACACTGTGTGATCCCAAGGACCCCTTCGCACAGAATATGGAGATTTCTAACC
TTTACATCTATGACACGGTGCTTCTGCTTGCAAACGCCTTTCATAAGAAGCTGCAGGACCGGAAGTGGCACAGCATGGCGAGCTTGTCCTGTATCAGGAAAAACTCCAAGCCCTGGCAGGGAGGG
CGGTCCATGCTGGAGACCATCAAGAAGGGTGGAGTTAATGGATTGACTGGAGATCTAGAATTTGGAGAAAATGGAGGTAACCCCAATGTCCACTTCGAAATCCTTGGAACCAACTATGGAGAAGA
ACTTGGCAGGGGTGTCCGTAAACTTGGGTGCTGGAATCCTGTCACAGGTCTGAATGGATCACTGACAGACAAGAAACTGGAGAATAACATGCGAACATTTCGCATTGTAACCGTTGTGGAGGCGC
CGTTCGTTAATCGGGACGAGACAGTGAATGGGTACAAGTACTCGGGGTTTTGCATCGACATGTTAGAACTAATCGCCAAGGAGTTGAACCTGAAGTATGAGTTGTACCTTGTACCAGATGGAAAC
TACGGAGGAAAGAACGACGACGGGACGTGGAATGGCCTGATTGGGGAAGTTTATTATGGTAGGGCGGACCTAGCGGTGGCCGGCATGGTCATCAACTCCGACCGCGAGGAAGTGGTGGACTTCAC
CAAGCCCTTCATGAACTACGGCGTTGGGATTCTCATGCAAAAGCCCAAGAAGAAGGCCAACATCTTCGCCTTCCTGGAGCCGCTCCACATCAAGGTCTGGGGCTGCGTGCTGGCCTCCCTCTTCG
TGGTCGGGGTGCTGATCTACATCGTGGACCGGCTCAGCCCTTACAGCAGTTTCCGGCGGGAGAACAGTCCCAACCCGGAAGCCTTCGACTTGAAGAACAGCATGTGGTTTGCCTTCGCTTCCTGC
ATGCAACAGGGCGGCGACACCTCCCCGCTGTCCATTTCTGGTCGTGTCCTGAGCGCGTTCTGGTGGTTCTTCGCCCTCATCATCACCGCTACGTACACCGCCAACCTGGCCGCCTTCCTGACCGT
CACCCGCATGGAGAACCCCATCAACTCTCTAGAGGATTTGGCCACGCAGAAACCGTGGTCTACGGCACCATCCTTAACAGCAGCCTGCATGACTTCTTCGAGAAGCGAAGAATCAGGGTATCT
ACGAAAAGATGTGGAACTTCATGTCCACCTCCAAGATCGACCCCTGGGTGCCCAACGCCGAGGCGGGGTACAAGCCGCTCCAGACAGAGGACTACGCCTTCTTTTGGGACGCGCCGATCCTAGAC
TACATCAAGCAGGAGGAGTGTGACGTCATGACTGTGGGCAAGCCCTTCAACCTGAAGGATACGGCATTGCTACGCCGCGGGGGGTTCCATGGAGAGACGAGATATCAATGGTAATCTTAAAAAT
GCAAGAGAGGGGCGAACTAGAAGAACTCCGTAAGAAGTGGTTCGACCGGGAATCCAGCTGCCTGGATGAGACGGACAGCATGAATACGAAACATCGCGCCGCCCGGGCCGACATCAACCTGGACC
AGATTGCCGGCGCCTTCTACGTCCTGATCATTGGGGCCGTGTTGTCCTTTGTGGTGGTCATTGTGGAGCACGTTTGGCACAAGCCGTCCTTCTACAAGAAGCGGGAAAAGGAGACGGGAAGGACC
ACATTGGACTGGTCAGACAAACTCCCTCCACGGGAAACGAGAAACAATGGTCTTTCTAACATTGAAAATTGTTCTTCCAATAAGCATTTAGTTGTTCAAGAGAATGACTCTTTTGCGTTAACACC
TTTGAGACCAAACCCATGGAGCACAACGACAATTCTTTCTGTCCCCCCTGAAGCGACAGAAAACTCTTGCGGATCC

Appendix 2 - Publication emerging from this thesis

PNAS RESEARCH ARTICLE | NEUROSCIENCE OPEN ACCESS

Loss of activation by GABA in vertebrate delta ionotropic glutamate receptors

Giulio Rosano[a], Allan Barzasi[a], and Timothy Lynagh[a,1]

Edited by Mark Nelson, University of Vermont, Burlington, Vermont; received August 23, 2023; accepted December 27, 2023

Ionotropic glutamate receptors (iGluRs) mediate excitatory signals between cells by binding neurotransmitters and conducting cations across the cell membrane. In the mammalian brain, most of these signals are mediated by two types of iGluRs: AMPA and NMDA (i.e. iGluRs sensitive to 2-amino-3-(5-methyl-3-oxo-1,2-oxazol-4-yl)propanoic acid and N-methyl-D-aspartic acid, respectively). Delta-type iGluRs of mammals also form neurotransmitter-binding channels in the cell membrane, but in contrast, their channel is not activated by neurotransmitter binding, raising biophysical questions about iGluR activation and biological questions about the role of delta iGluRs. We therefore investigated the divergence of delta iGluRs from their iGluR cousins using molecular phylogenetics, electrophysiology, and site-directed mutagenesis. We find that delta iGluRs are found in numerous bilaterian animals (e.g., worms, starfish, and vertebrates) and are closely related to AMPA receptors, both genetically and functionally. Surprisingly, we observe that many iGluRs of the delta family are activated by the classical inhibitory neurotransmitter, γ-aminobutyric acid (GABA). Finally, we identify nine amino acid substitutions that likely gave rise to the inactivity of today's mammalian delta iGluRs, and these mutations abolish activity when engineered into active invertebrate delta iGluRs, partly by inducing receptor desensitization. These results offer biophysical insight into iGluR activity and point to a role for GABA in excitatory signaling in invertebrates.

iGluR | neurotransmitter | ion channels | excitatory | GABA

Significance

The neurotransmitters glutamate and GABA activate excitatory sodium ion influx and inhibitory chloride flux across neuronal membranes by binding and activating ionotropic glutamate receptors (iGluRs) and $GABA_A$ receptors, respectively, two superfamilies of ligand-gated ion channels. Curiously, mammalian receptors of the delta iGluR family mediate no sodium influx in response to neurotransmitter binding in most experimental settings, so we investigated delta iGluRs from numerous animal lineages, bioinformatically and experimentally, and found that numerous delta iGluRs are indeed ligand-gated channels. Surprisingly, most are activated by GABA, the classically inhibitory neurotransmitter. Our results identify several amino acid substitutions that occurred during evolution to make mammalian delta iGluRs inactive and reveal a potential excitatory signaling role for GABA in numerous invertebrates.

Rapid signals are conveyed between neurons of the central nervous system via chemical synapses, specialized directional interfaces between adjacent neurons (1). Most synapses in the mammalian brain are glutamatergic and excitatory, where glutamate released by the presynaptic cell binds to ionotropic glutamate receptors (iGluRs) on the postsynaptic cell (2, 3). iGluRs are tetramers assembled by four homologous subunits, each of which has an extracellular N-terminal domain (NTD), extracellular ligand-binding domain (LBD), membrane domain, and intracellular C-terminal domain (CTD). The four membrane domains together form a membrane-spanning, nonselective cation channel (3). The iGluR superfamily is broad, but two main families predominate in mammals and classical model organisms: AMPA receptors, along with close cousins kainate (KA) receptors, are rapidly activated by glutamate and depolarize cells quickly (4); NMDA receptors are slower acting, more calcium-permeable, and require the binding of glutamate and an ambient coagonist, D-Serine or glycine (5).

Additionally, there is a relatively mysterious "delta" family of iGluRs encoded by two genes, GluD1 and GluD2 in rodents and human (6–8). Like most iGluRs, delta iGluRs are expressed in excitatory synapses, their up- or downregulation leads to developmental disorders or neural malfunction, and when expressed heterologously in mammalian cells or frog oocytes, GluD1 and GluD2 subunits form homotetrameric channels (9). In stark contrast to other iGluRs, however, under numerous native and heterologous experimental conditions, no current through GluD1 or GluD2 iGluRs is activated by neurotransmitter binding (7, 10–12). This is despite two major lines of evidence that the ligands D-serine and glycine bind to the canonical iGluR LBD of GluD2 and induce local conformational change. X-ray structures of the excised GluD2 LBD show D-serine binding and LBD closure around the ligand (13), reflecting the first step of channel activation in most iGluRs (3). Second, mutant GluD2 channels carrying the "lurcher" (*Lc*) A654T substitution in the channel pore conduct current constitutively, and the binding of D-serine or glycine inactivates this current, indicative of ligand-induced conformational change in both the LBD and in the channel pore (12, 13).

The absence of typical ligand-gated currents in heterologously expressed delta iGluRs is reflected in relatively unique biological function. Intracellular signaling pathways are suggested to activate delta iGluRs based on mouse cerebellum and midbrain recordings (10, 14, 15), and a principally structural and developmental role is served by delta iGluRs in the hippocampus and cerebellum, where they interact with pre- and intrasynaptic

Author affiliations: [a]Michael Sars Centre, University of Bergen, Bergen 5008, Norway

Author contributions: G.R. and T.L. designed research; G.R. and A.B. performed research; G.R., A.B., and T.L. analyzed data; and G.R. and T.L. wrote the paper.

The authors declare no competing interest.

This article is a PNAS Direct Submission.

[1]To whom correspondence may be addressed. Email: tim.lynagh@uib.no.

This article contains supporting information online at https://www.pnas.org/lookup/suppl/doi:10.1073/pnas.2313853121/-/DCSupplemental.

Published January 29, 2024.

proteins via their large extracellular NTD (16–18). NTD dynamics may in turn relate to the absence of ligand-induced gating in heterologously expressed receptors. The compaction of GluD2 extracellular domains via coexpression with synaptic proteins in densely cultured mammalian cells or via introduced cysteine-linked NTDs leads to small ligand-gated currents in heterologously expressed GluD2 iGluRs (19). Furthermore, delta iGluRs differ from AMPA and NMDA iGluRs in that cryoelectron microscopy structures of full-length GluD1 and GluD2 iGluRs show a "nonswapped" architecture, where the back-to-back NTD dimers of two adjacent subunits sit atop back-to-back LBD dimers of the same two subunits (20, 21), contrasting the "domain-swapped" architecture of other iGluRs (3). Whether nonswapped NTD structure underlies delta iGluR inactivity is doubtful, however, as plant iGluRs are nonswapped yet capable of ligand-gated currents (22).

Delta iGluR function is thus relatively mysterious. This impairs our understanding of the biophysical underpinnings of excitatory signaling, precludes the study of potential delta iGluR pharmacology, and makes biological inferences about the presence of delta iGluR genes in different animals difficult. We therefore sought to establish a molecular and functional signature of the delta iGluR family by investigating beyond the mammalian orthologues, using phylogenetics, electrophysiology, and mutagenesis. This uncovered surprisingly active ligand-gated delta iGluRs in numerous invertebrates, uncovered pharmacological similarities between delta iGluRs and their AMPA receptor cousins, and traced the inactivity of vertebrate delta iGluRs to a distinct part of the iGluR gating machinery.

Results

GABA-gated Channels throughout the Delta iGluR Family. In questioning the divergence of relatively inactive mammalian delta iGluRs from their active, ligand-gated iGluR cousins, we sought a more definitive view of the delta iGluR family and its phylogenetic and functional relation to other iGluRs. We first generated a maximum likelihood phylogeny of iGluR genes from a broad selection of diverse animals (Fig. 1*A* and *SI Appendix*, Fig. S1). Mammalian GluD1 and GluD2 genes are found in a branch we will refer to as the delta family (green in Fig. 1*A*), whose closest relatives in terms of other previously characterized genes are AMPA/KA receptors (dark pink in Fig. 1*A*). Delta and AMPA/KA iGluRs are thus closely related, and together with several uncharacterized paraphyletic relatives make up the AMPA/KA/delta/phi (AKDF) branch that was proposed by others (23, 24). The delta iGluR family comprises genes only from animals of the bilaterian lineage, i.e., xenacoelomorphs, a distinct group of simple marine worms lacking a circulatory system (25); protostomes such as molluscs; and deuterostomes such as vertebrates, hemichordates (e.g., acorn worms), and echinoderms (e.g., starfish, *SI Appendix*, Fig. S1). According to our maximum likelihood phylogeny,

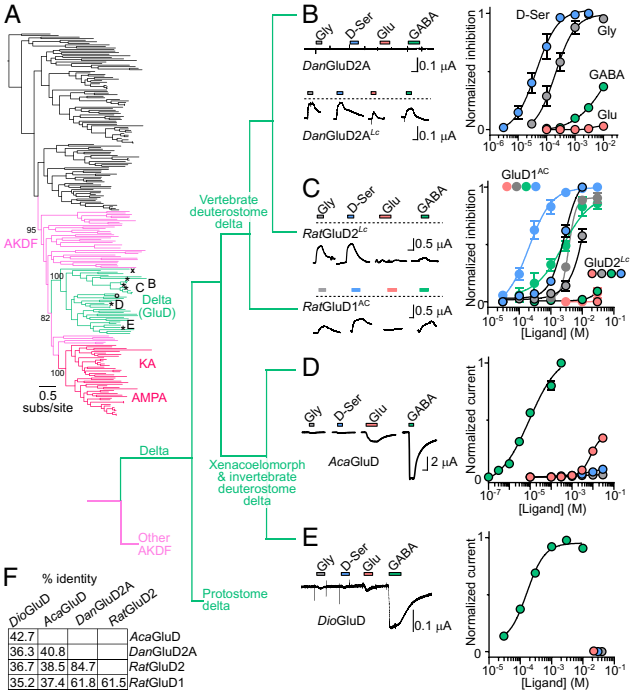

Fig. 1. GABA-gated channels in the delta iGluR family. (*A*) Maximum likelihood phylogeny of animal iGluR genes. Selected iGluR branches are colored and labeled. *, genes characterized in panels *B*–*E*. [X, O], *Crassostrea gigas* GluD and *Saccoglossus kowalevskii* GluD, see *SI Appendix*, Fig. S2. SH-aLRT support for selected branches indicated. Detailed branch support and all gene names in expanded phylogeny, *SI Appendix*, Fig. S1. (*B*–*E*) Example two-electrode voltage clamp recordings of oocytes expressing indicated delta iGluR genes in response to different ligands (*Left*) and mean ± SEM (n = 4 to 6) normalized concentration-dependent responses (*Right*). Scale bars: x, 10 s; y, as indicated. (*B* and *C*) Wild-type channels were inactive; lurcher-mutant (^{Lc}) *Dan*GluD2A and *Rat*GluD2 and A654C-mutant (^{AC}) *Rat*GluD1 channels were constitutively active. The dashed line indicates zero current; mean responses reflect ligand-induced inhibition of constitutive current normalized to maximum inhibition of constitutive current. (*D* and *E*) Wild-type channels were active; mean responses reflect ligand-induced current amplitude normalized to maximum ligand-induced current amplitude. *Dan*, *Danio rerio*. *Rat*, *Rattus norvegicus*. *Aca*, *Acanthaster planci*. *Dio*, *Diopisthoporus longitibus*. (*F*) % amino acid sequence identity of selected delta iGluRs.

protostome delta iGluRs are the earliest branching within the delta family (^{X} in Fig. 1*A*), consistent with a previously published Bayesian phylogeny (23).

Apart from inactive wild-type (WT) and constitutively active, D-serine-inhibited, mutant mammalian delta iGluRs, the functional signature of the delta iGluR family is unknown. We therefore expressed putative delta iGluRs from diverse bilaterian animals in frog oocytes and characterized their function with two-electrode voltage clamp. Genes included "*Dio*GluD" from the acoel *Diopisthoporus longitubus*, (a xenacoelomorph); "*Cra*GluD" from the oyster *Crassostrea gigas* (a protostome); "*Aca*GluD" from the crown-of-thorns-starfish *Acanthaster planci* (an echinoderm) and "*Sac*GluD" from the acorn worm *Saccoglossus kowalevskii* (a hemichordate; both invertebrate deuterostomes); and "*Dan*GluD2A" from the zebrafish *Danio rerio* (a vertebrate deuterostome). Similar to *Rat*GluD1 and *Rat*GluD2, WT *Dan*GluD2A receptors showed no response to the four ligands tested, but lurcher-mutant (*Lc*) *Dan*GluD2A^{Lc} receptors showed constitutive currents that were inactivated by D-serine and glycine (Fig. 1*B*). However, in contrast to *Rat*GluD2^{Lc}, which were only sensitive to glycine and D-serine, *Dan*GluD2A^{Lc} receptors and *Rat*GluD1^{AC} [the *Lc*-like A654C mutation (26)] were also sensitive to GABA, which caused 58 ± 8% (n = 4) or 86 ± 5% (n = 10) inactivation relative to D-serine at these two receptors (Fig. 1 *B* and *C*). This shows that numerous vertebrate delta iGluRs are inactive, but suggests that some of them bind the classical inhibitory neurotransmitter GABA, as indicated by a recent study of *Rat*GluD1 (27).

In stark contrast to WT delta iGluRs of vertebrate deuterostomes, WT delta iGluRs of other bilaterians showed robust ligand-gated currents, and remarkably the most effective agonist was GABA (Fig. 1 *D* and *E*). At invertebrate deuterostome (starfish) *Aca*GluD, the GABA EC_{50} of 13 ± 3 μM (n = 5) was much lower than that of glutamate (7.8 ± 3 mM, n = 3). Fellow invertebrate deuterostome (acorn worm) *Sac*GluD showed smaller currents, making potency difficult to measure, although GABA was more potent than other potential ligands (*SI Appendix*, Fig. S2*A*). This was more evident in lurcher-mutant *Sac*GluD^{Lc}, which showed relatively small constitutive current and inward GABA-gated currents of very high potency (EC_{50} = 84 ± 14 nM, n = 4, *SI Appendix*, Fig. S2 *B*–*D*). At xenacoelmorph (acoel) *Dio*GluD iGluRs, GABA was in fact the only ligand that elicited currents, with an EC_{50} of 180 ± 20 μM (Fig. 1*E*). Finally, we tried measuring the activity of the earliest branching delta iGluR in our tree, protostome (oyster) *Cra*GluD (^{X} in Fig. 1*A*). Unfortunately, we could not establish the function of this receptor, as we detected no ligand-gated currents in oocytes injected with WT or *Lc* mutant *Cra*GluD mRNA, probably due to low surface expression, as assayed by oocyte immunolabeling (*SI Appendix*, Fig. S2 *E* and *F*).

Inferring the putative functional properties of the ancestral receptor at the base of the delta branch is difficult without functional data on early-branching protostome delta iGluRs. However, considering the presence of a) GABA sensitivity in both xenacoelomorph, deuterostome invertebrate, and certain deuterostome vertebrate delta iGluRs, b) the absence of ligand-gated currents in WT vertebrate delta iGluRs, and c) the fact that AMPA/KA iGluR cousins are glutamate-gated channels, we suggest the following. When the first delta iGluR diverged from its AKDF ancestor, it was an active ligand-gated channel that quickly evolved selectivity for the neurotransmitter GABA. After chordates diverged from other invertebrate deuterostomes, ligand-induced channel gating was lost in delta iGluRs of the chordate or subsequent vertebrate lineage. And based on the presence of both GABA and glycine/D-serine sensitivity in vertebrate GluD1 and GluD2 receptors, we tentatively conclude that ligand selectivity changed from GABA to glycine and D-serine in early vertebrates or other chordates.

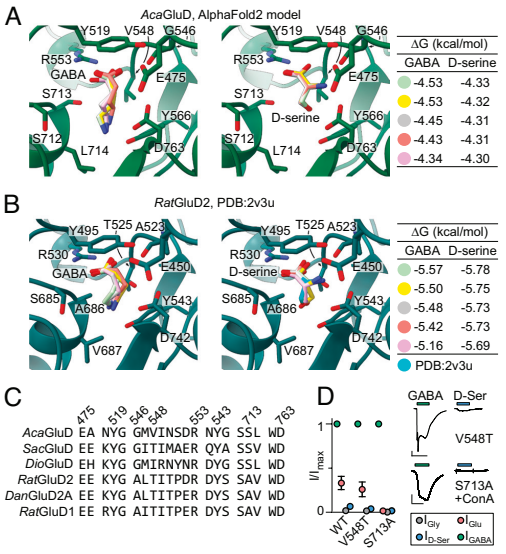

Fig. 2. Computational ligand docking. (*A* and *B*) Five most energetically favorable binding poses for GABA and D-serine at *Aca*GluD model (*A*) and *Rat*GluD2 X-ray structure [PDB:2v3u (13)] (*B*). (*C*) Amino acid sequence alignment of selected LBD segments (*Aca*GluD numbering). (*D*) Example recording and mean (± SEM, n = 4) normalized responses of indicated mutant *Aca*GluD receptors to different ligands. Oocytes expressing S713A receptors only responded after concanavalin A treatment ("ConA", 10 μM).

Computational Analysis of Ligand Binding. One potential explanation for the evolutionary scenario described above would involve substitutions in the ligand-binding residues of the vertebrate delta iGluR LBD, enabling selectivity for α-amino acid D-serine (and glycine) instead of γ-amino acid GABA. We investigated this by computationally docking GABA and D-serine to a starfish *Aca*GluD AlphaFold structural model and the *Rat*GluD2 X-ray structure (13). With an upper lobe–lower lobe separation similar to that of D-serine-bound *Rat*GluD2 (ref. 13 and *SI Appendix*, Fig. S3 *A* and *D*), our model likely represents an active ligand-bound conformation. As expected, based on experimental evidence for *some* sensitivity to GABA and D-serine (Fig. 1 *C* and *D*), both ligands docked to both receptors in the canonical binding site, but with more favorable energies for GABA than D-serine at *Aca*GluD and the converse at *Rat*GluD2 (Fig. 2 *A* and *B* and *SI Appendix*, Fig. S3).

Aligning the ligand-binding residues shows only minor differences between GABA-selective *Aca*GluD and D-serine- (and glycine-) selective *Rat*GluD2 (Fig. 2*C*). Indeed, the major bonding partner of the GABA γ-amine and D-serine α-amine in both receptors is the carboxylate side chain of the conserved lower lobe D763/D742 residue (Fig. 2 *A*–*C*). Similarly, although the upper lobe E475/E450 carboxylate residue was recently shown to contribute to GABA potency in *Rat*GluD1 (27), it is conserved among GABA-selective invertebrate and D-serine-selective vertebrate delta iGluRs (Fig. 2 *A*–*C*), and thus does not determine ligand selectivity.

We did notice two differences between the receptors, however. In the upper lobe, hydrophobic V548 of *Aca*GluD cannot form a polar interaction with the α-amine of D-serine that is formed

by the equivalent but polar T525 of *Rat*GluD2 (Fig. 2 *A*–*C*). And in the lower lobe, invertebrate receptors have a polar S713 side chain where vertebrate receptors have a small, nonpolar A686 side chain (Fig. 2 *A*–*C*). However, when we tested the ligand selectivity profile of mutant V548T and S713A *Aca*GluD receptors, we saw no increase in D-serine activity relative to GABA (Fig. 2*D*), suggesting that these differences do not determine ligand selectivity. This is reflected in the fact that invertebrate *Sac*GluD, which has the upper lobe threonine residue like *Rat*GluD2, shows high GABA selectivity (Fig. 2*C* and *SI Appendix*, Fig. S2*D*). Taken together, these computational and functional data show that most extant delta iGluRs either show GABA selectivity or retain some GABA sensitivity and that ligand-binding residues alone do not determine ligand selectivity in delta iGluRs.

Pharmacological and Biophysical Properties of Delta iGluRs Reflect their Close Relationship to AMPA/KA Receptors. Although phylogenetic relationships suggest that delta iGluRs are closely related to AMPA/KA receptors, previous pharmacological studies have emphasized similarities between delta iGluRs and NDMA receptors, such as glycine and D-serine binding, and channel block by pentamidine (19, 28). We therefore sought a more extensive view of delta iGluR function, incorporating channel pore properties, competitive antagonist pharmacology, and modulation by extracellular calcium ions (Ca^{2+}), utilizing the crown-of-thorns starfish *Aca*GluD receptor because of its large, tractable ligand-gated currents in oocytes.

To establish the channel pore properties of *Aca*GluD receptors we measured current-voltage (IV) relationships and channel block by pentamidine. The IV relationship at *Aca*GluD iGluRs is inwardly rectifying, with small outward currents only appearing at potentials more positive than 50 mV, both in the absence and presence of divalent cations (Fig. 3*A*). This suggests that *Aca*GluD receptors are blocked by intracellular polyamines and not by extracellular Mg^{2+} ions, which is qualitatively similar to AMPA receptors (29) and chimeric receptors carrying KA receptor LBDs and *Rat*GluD2 channel domains (30). Running voltage ramps from −80 to 60 mV during GABA-gated currents in regular extracellular solution yielded a reversal potential of −16 ± 2 mV (n = 4), as expected for a nonselective cation-permeable channel in these conditions (31). This indicates that *Aca*GluD is a mixed cation channel like most iGluRs (3) and thus an excitatory GABA receptor.

Pentamidine is a diarylamidine compound previously shown to block NMDA receptors in the low micromolar range and constitutively active mutant *Rat*GluD2^{Lc} channels in the high micromolar range (28, 32). We observed that pentamidine (100 μM) blocked 68 ± 5% (n = 5) of the GABA-gated current and 78 ± 2% (n = 7) of the glutamate-gated current through *Aca*GluD iGluRs (Fig. 3*B*). As the pentamidine sensitivity of AMPA receptors has been explored relatively little, we tested this ourselves and observed that pentamidine (100 μM) elicited 37 ± 3% (n = 5) inhibition of glutamate-gated current through *Rat*GluA2 AMPA receptors (*SI Appendix*, Fig. S4*A*). Combined with earlier studies, our results show that AMPA receptors and delta iGluRs share moderate pentamidine sensitivity, in contrast to NMDA receptors, which have higher pentamidine sensitivity.

Applied alone, the classical AMPA/KA receptor competitive antagonists CNQX, DNQX, and NBQX (100 μM) elicited no currents at *Aca*GluD iGluRs, but when coapplied with GABA (~EC_{30} GABA concentration) inhibited 81 ± 4%, 53 ± 3%, and 61 ± 3% of the GABA-gated current, respectively (Fig. 3*C*, each n = 5). In contrast, the NMDA receptor glycine site antagonists 5,7-dichlorokynurenic acid (33) and CGP-78608 (34) (both 100 μM) inhibited only 11 ± 5% and 9 ± 3% of the GABA-gated currents, respectively (*SI Appendix*, Fig. S4*B*). Curiously, glutamate-gated currents were *enhanced* 34 ± 3% by DNQX and NBQX, whereas CNQX had no effect (Fig. 3*C*, each n = 5). These quinoxalinedione compounds typically inhibit heterologously expressed AMPA/KA receptors, although CNQX and DNQX act as partial agonists at AMPA receptors coexpressed with TARP-type auxiliary subunits (35). Thus, at both delta and AMPA/KA receptors, certain quinoxalinediones exert complex effects, depending on the specific agonist or oligomeric complex. We observed no effect of CNQX, DNQX, or NBQX on ooyctes expressing WT *Rat*GluD2 (n = 4), but constitutive currents through *Rat*GluD2^{Lc} were inhibited 10 ± 0.2%, 11 ± 0.2%, and 9 ± 0.2% by CNQX, DNQX, and NBQX, respectively (each n = 4, *SI Appendix*, Fig. S4*C*), consistent with the moderate inhibition of *Rat*GluD2^{Lc} currents previously reported for CNQX and another, different quinoxalinedione (36).

Further assessing the functional signature of delta iGluRs, we tested *Aca*GluD for sensitivity to extracellular Ca^{2+}, which was previously shown to enhance the constitutive activity of mutant *Rat*GluD2^{Lc} channels and decrease the potency with which D-serine inhibits constitutive activity (37). We observed that extracellular Ca^{2+} enhanced *Aca*GluD substantially. In nominally Ca^{2+}-free solutions, maximum GABA-, glutamate-, and glycine-gated current amplitudes were 0.42 ± 0.13 μA (n = 4), 0.28 ± 0.02 μA (n = 5), and 0.08 ± 0.01 μA (n = 10), and these were increased to 6.0 ± 1.0 μA (n = 5), 5.8 ± 0.6 μA (n = 4), and 0.33 ± 0.01 μA (n = 4) in the presence of 1.8 mM Ca^{2+} (Fig. 3 *D* and *E*). Enhancement affected maximum current amplitude more than agonist potency, with no more than threefold altered agonist

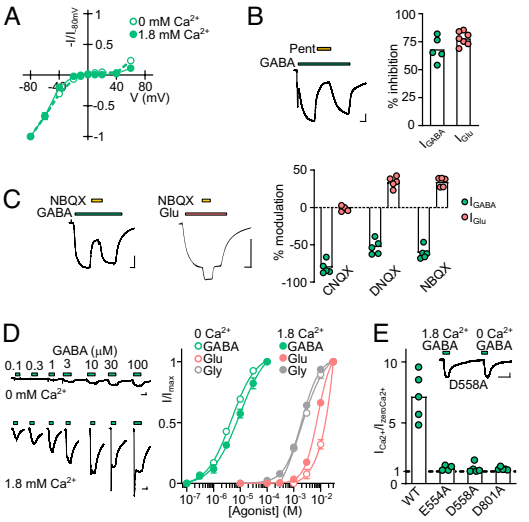

Fig. 3. Pore properties and pharmacology of *Aca*GluD receptors. (*A*) Normalized current ($I/I_{-80\ mV}$) -voltage relationship of GABA-gated currents through *Aca*GluD-expressing oocytes. Data points mean ± SEM (n = 4), joined by straight lines. (*B* and *C*) Example recordings (scale bars x, 5 s; y, 1 μA) and summary data (columns, mean; circles, individual data points) of modulation of GABA- and glutamate-gated current by indicated drugs at *Aca*GluD-expressing oocytes. (*D*) Example responses to increasing concentrations of GABA in the absence or presence of extracellular Ca^{2+} (*Left*) and normalized (to maximum current in respective condition, "I/I_{max}") responses to different agonists (*Right*, mean ± SEM, n = 5 to 7). (*E*) Fold enhancement ("$I_{Ca2+}/I_{zeroCa2+}$") of GABA-gated current by 1.8 mM Ca^{2+} at oocytes expressing WT or indicated mutant *Aca*GluD. *Inset*: example recording from oocyte expressing D558A mutant *Aca*GluD, scale bars in *D* and *E*: x, 10 s; y, 0.15 μA.

EC_{50} values in 1.8 mM Ca^{2+} (Fig. 3*D*; GABA EC_{50} 5 ± 0.6 μM in 0 Ca^{2+} and 13 ± 3 μM in 1.8 mM Ca^{2+}, n = 5; glycine EC_{50} 2 ± 0.1 mM and 2 ± 0.1 mM, n = 4; glutamate EC_{50} ~30 mM and ~10 mM, n = 4). We tested whether *Aca*GluD enhancement by Ca^{2+} is determined by carboxylate side chains on the rear of the LBD as was shown for *Rat*GluD^{Lc} receptors (37). E554A, D558A, and D801A mutant *Aca*GluD iGluRs each showed no enhancement by Ca^{2+} (Fig. 3*E* and *SI Appendix*, Fig. S4*D*), indicating that equivalent, conserved positions determine Ca^{2+} sensitivity in starfish and rat delta iGluRs (*SI Appendix*, Fig. S5). Thus, enhancement by extracellular Ca^{2+} is conserved in diverse delta iGluRs, and mixed cation permeability, inward rectification, quinoxolinedione sensitivity, and sensitivity to high micromolar pentamidine are all conserved in delta iGluRs and their AMPA receptor cousins.

The NTD Does not Determine the Ligand-gated Activity of Starfish Delta iGluRs. Our data suggest that after diverging from other AKDF iGluRs, early delta iGluRs were active, homotetrameric ligand-gated channels, even in the absence of accessory synaptic proteins. And while this ligand-gated activity is conserved in several extant delta iGluRs, delta iGluRs in the lineage to vertebrates lost ligand-gated channel activity. We questioned the molecular basis for this loss, hoping to establish a molecular blueprint for the mysterious function of mammalian delta iGluRs.

In most animal iGluR subunits, the large clamshell-shaped NTD contributes greatly to tetramer assembly but relatively moderately to ligand-gated channel activity (3). However, NTDs are indirectly implicated in the ligand-gated (in)activity of mouse/human delta iGluRs, as the experimental separation of NTDs from each other, or from the LBDs below, impairs channel function (17, 19). We therefore questioned whether substantial divergence in the NTDs—19% amino acid sequence identity between *Aca*GluD and *Rat*GluD2 NTDs *cf* 38% identity between *Aca*GluD and *Rat*GluD2 LBD and channel domains—determines the absence of ligand-gated currents in vertebrate delta iGluRs. To answer this, we measured ligand-gated currents in two chimeric *Aca*GluD constructs in which the NTD was replaced with that of *Rat*GluD2: one retaining the NTD-LBD linker of *Aca*GluD, "*Aca*GluD$^{Rat\text{NTD}}$"; and the other with the NTD-LBD linker of *Rat*GluD2, "*Aca*GluD$^{Rat\text{NTDlink}}$" (Fig. 4 *A* and *B* and *SI Appendix*, Supporting text). Neither chimeric receptor showed drastic differences from WT *Aca*GluD, with each showing large GABA-gated currents (Fig. 4 *C* and *D*). However, we did notice a small increase in the relative efficacy of D-serine at *Aca*GluD$^{Rat\text{NTDlink}}$ (20 ± 3%, n = 3) compared to WT and *Aca*GluD$^{Rat\text{NTD}}$ (12 ± 3%, n = 7, and 5 ± 1%, n = 3, respectively). While confirming that the NTDs and their link to the LBD make some sort of contribution to delta iGluR function (17), these results show that great divergence in the NTDs is unlikely to have determined the stark loss of function in vertebrate delta iGluRs relative to other deuterostome delta iGluRs.

Vertebrate-like Mutations in the Lower Lobe of the LBD Abolish the Activity of Starfish Delta iGluRs. These results suggest that the relative inactivity of vertebrate delta iGluRs such as *Rat*GluD2 derives from amino acid sequence divergence in the remainder of the receptor, i.e., the LBD, transmembrane channel domain (TMD), and the intracellular CTD. We therefore aligned amino acid sequences of delta iGluR subunits, and from ~410 positions comprising the LBD and TMD, we identified 41 at which the amino acid residue shares biophysical properties in *Aca*GluD, *Sac*GluD, and *Dio*GluD and differs in inactive *Dan*GluD2A,

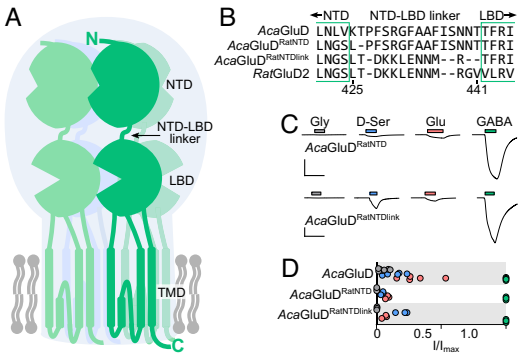

Fig. 4. *Rat*GluD2 NTD does not abolish the activity of starfish *Aca*GluD iGluRs. (*A*) Cartoon illustrating structural domains of typical iGluR tetramer, one subunit highlighted, showing amino-terminal domain (NTD), ligand-binding domain (LBD), and transmembrane channel domain (TMD). Cell membrane in gray. (*B*) Amino acid sequence alignment of linker region, illustrating chimera design. *Numbering*, *Rat*GluD2. (*C*) Ligand-gated currents in oocytes expressing mutant *Aca*GluD receptors containing the NTD from *Rat*GluD2 (*Aca*GluD$^{Rat\text{NTD}}$) or the NTD and NTD-LBD linker from *Rat*GluD2 (*Aca*GluD$^{Rat\text{NTDlink}}$). Scale bars: x, 10 s; y, 2 μA. (*D*) Summarized data from experiments in *C*.

*Rat*GluD1, and *Rat*GluD2 (*SI Appendix*, Fig. S5). As the long CTD is implicated little in channel gating and more in expression and trafficking of iGluRs (3), we excluded it from this analysis. Taking *Aca*GluD again as our active experimental model, we substituted each of these 41 amino acid residues with the equivalent amino acid from inactive *Rat*GluD2, generating 39 mutant *Aca*GluD receptors, which we tested for responses to GABA, glutamate, glycine, and D-serine. (Two of the mutants incorporated substitutions of two adjacent residues for efficiency.)

Thirty-five of the 41 substitutions had little or no effect on *Aca*GluD activity, with the respective mutants showing large responses to GABA and smaller responses to the other agonists (Fig. 5 *A* and *B*). In contrast, six substitutions substantially altered function, with the respective mutants showing either no currents greater than uninjected oocytes (F640Y, S713A, R721K, P741N, and D825P) or a substantial change in relative agonist efficacies combined with decreased current amplitude (G567S; Fig. 5 *A* and *B*). The loss of currents via F640Y, S713A, and R721K substitutions derives primarily from altered channel function and not decreased oocyte surface expression, as the latter was similar to WT, whereas for P741N and D825P, surface expression was evident but greatly reduced compared to WT (Fig. 5*C*). An additional four mutants, Q772D, K782N, M805Q, and V806R, showed milder but noticeable effects, decreasing maximum GABA-gated current amplitude to less than 1 μA (cf. 8.2 ± 1.1 μA at WT, n = 4) and retaining the typical agonist selectivity profile (Fig. 5*B*).

Questioning how these 10 residues contribute to receptor function, we considered their putative location in the receptor tertiary structure. For the LBD, we used the AlphaFold structural model, and for the TMD, we examined the position of homologous residues in published rat delta and AMPA receptor structures (13, 20, 21, 38). From the 10 crucial *Aca*GluD delta iGluR residues, F640 is in the second helix of the TMD, abutting the channel pore (*SI Appendix*, Fig. S6*A*), whereas the other nine residues are all in the LBD, remarkably with seven specifically in the lower lobe of the LBD clamshell (Fig. 5*D*). Ligand-induced activation of iGluRs involves the upward/outward movement of the lower lobe toward the upper lobe, closing the clamshell around the

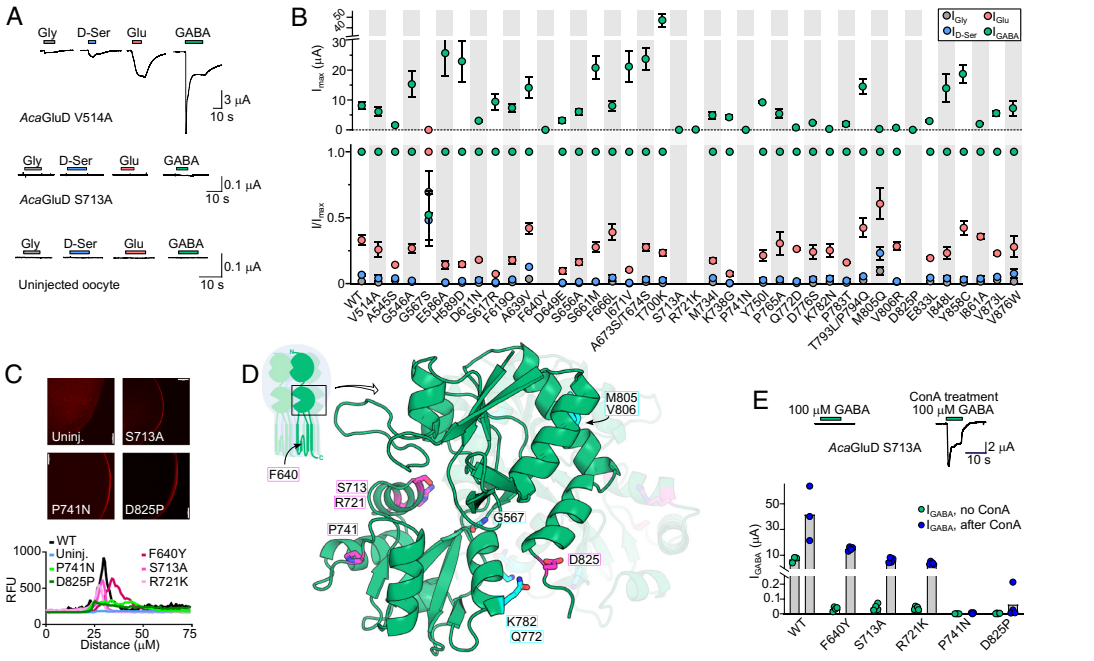

Fig. 5. *Rat*GluD2-like substitutions impair the ligand-gated activity of *Aca*GluD receptors. (*A*) Ligand-gated currents in oocytes expressing indicated mutant *Aca*GluD receptors or uninjected oocytes. (*B*) Maximum current amplitude ("I_{max}", *Upper*) and relative ligand-gated current amplitude ("I/I_{max}", *Lower*) and at wild-type (WT) and mutant *Aca*GluD receptors (mean ± SEM, n = 3 to 5). (*C*) Immunolabeling c-Myc tag in *Aca*GluD C-terminal. *Upper*, example micrographs. *Lower*, Random fluorescence units (RFU) plotted against relative radial distance, peaking at the oocyte surface. White scale bars, 100 μm. (*D*) AlphaFold model of two adjacent *Aca*GluD LBDs (rear LBD faded). Selected amino acid residues colored and shown as sticks. *Magenta*, drastic loss of function; *cyan*, moderate loss of function. Inset cartoon shows LBDs within full-length receptor and approximate position of F640 residue (*SI Appendix*, Fig. S6*A*). (*E*) *Upper*, example, and *Lower*, summarized current responses to 30 mM GABA ("I_{GABA}") in WT or mutant *Aca*GluD-expressing oocytes before or after treatment with concanavalin A ("ConA", 10 μM).

ligand and pulling the pore-lining third TMD helix outward to open the channel (38, 39). Eight of the nine residues are thus in a crucial part of the receptor, close to the putative ligand binding site in the cleft of the LBD clamshell but probably located and/or oriented away from the putative ligand (Fig. 5*D* and *SI Appendix*, Fig. S6*B*). Indeed, G567, R721, D825, and K782 of the lower lobe and M805 and V806 of the upper lobe are all on the "rear" of the LBD, interfacing with the rear of an adjacent LBD within one of two LBD dimers in the homotetramer (Fig. 5*D*). P741 is in the outer lip of the lower lobe, and S713 is more central (Fig. 5*D*), although its hydroxyl moiety is unlikely to interact directly with GABA or other ligands (Fig. 2).

Vertebrate-like Mutations in the Lower Lobe of the LBD Induce an Inactive Channel State. In AMPA/KA iGluRs, interactions between interfacing LBDs control entry into or recovery from agonist-induced desensitization (40–43). Given the relation of delta and AMPA/KA iGluRs, and the position of loss-of-function *Aca*GluD substitutions S713A, R721K, P741N, and D825P in or near the interface of LBDs, we hypothesized that the loss-of-function may derive from altered LBD dynamics and increased desensitization compared to WT *Aca*GluD. We therefore tested responses of mutant *Aca*GluD iGluRs after treatment with concanavalin A, a plant lectin that prevents desensitization and thus uncovers otherwise small responses in some iGluRs (44, 45). Concanavalin A treatment caused a remarkable (>>100-fold) increase in F640Y, S713A, and R721K *Aca*GluD iGluR activity, with GABA-gated currents now resembling those through WT channels (Fig. 5*E*). The same restoration of function was not observed with P741N and D825P mutants, although a relatively small fourfold increase in current amplitude was observed in D825P channels, similar to WT channels (Fig. 5*E*). Thus, active delta iGluRs are rendered inactive by three vertebrate delta iGluR-like mutations that bias the receptor toward desensitization or another inactive state, and two additional vertebrate delta iGluR-like mutations primarily reduce surface expression of active delta iGluRs.

Considering that such desensitization or inactivation may underlie the absence of currents in WT vertebrate delta iGluRs, we tested the effects of D-serine and glycine on *Rat*GluD1 and *Rat*GluD2 after concanavalin A treatment, but we observed no difference to inactive, untreated receptors (*SI Appendix*, Fig. S4*E*). As *Rat*GluD1 and *Rat*GluD2 contain only three predicted N-linked glycosylation sites per subunit compared to eight in *Aca*GluD (seven in the S713A mutant), however, it could be that concanavalin A is incapable of modulating the vertebrate receptors to rescue them from such a state, precluding conclusions along these lines.

Starfish-like Mutations Partly Reawaken Inactive Rat Delta iGluRs. If the 10 mutations discussed above drove the loss of function in vertebrate delta iGluRs, one might expect that the latter could be "reawakened" via active invertebrate delta iGluR-like mutations here. We therefore engineered mutant *Rat*GluD2 iGluRs to contain at these positions the equivalent residues from starfish delta iGluRs. These mutants were *Rat*GluD2^{5x}, containing Y613F, A686S, K694R, N720P, and P806D substitutions (pink

in Fig. 6*A*), and *Rat*GluD2^{9x}, additionally containing N763K, D753Q, Q786M, and R787V (cyan in Fig. 6*A*). We also generated A654T *Lc*-mutant versions, *Rat*GluD2$^{Lc\text{-}5x}$ and *Rat*GluD2$^{Lc\text{-}9x}$, hypothesizing that constitutively active *Lc*-versions could offer tangible insight on ligand sensitivity in case the former mutants remained inactive.

*Rat*GluD2^{5x} and *Rat*GluD2^{9x} mutants showed no responses to glycine, D-serine, GABA, or glutamate (Fig. 6*B*), indicating that these nine mutations alone are not capable of reawakening ligand-gated currents in vertebrate delta iGluRs. On the artificial *Lc*-mutant background, however, tangible effects of the starfish GluD-like mutations were observed. Whereas *Rat*GluD2$^{Lc\text{-}5x}$ behaved much like the typical *Lc*-mutant *Rat*GluD2^{Lc}, *Rat*GluD2$^{Lc\text{-}9x}$ receptors were inactive at rest and conducted inward currents in response to glycine binding (Fig. 6 *C* and *D*). These glycine-gated currents were inhibited by the pore blocker pentamidine (Fig. 6*D*). Finally, we generated *Rat*GluD2$^{Lc\text{-}10x}$, additionally containing S544G (light green in Fig. 6*A*), the converse of the G567S substitution that altered ligand selectivity in starfish *Aca*GluD. Ligand selectivity was slightly altered by the addition of the S544G mutation, as *Rat*GluD2^{10x} receptors showed inward currents in response to both glycine and D-serine (Fig. 6 *E* and *F*). Thus, the reintroduction of key residues from active delta iGluRs into inactive vertebrate delta iGluRs is not enough to reawaken the latter, but on an artificial *Lc*-mutant background, it awakens the gating machinery, leading to *Rat*GluD2 channels that are inactive at rest and activated by glycine and D-serine binding.

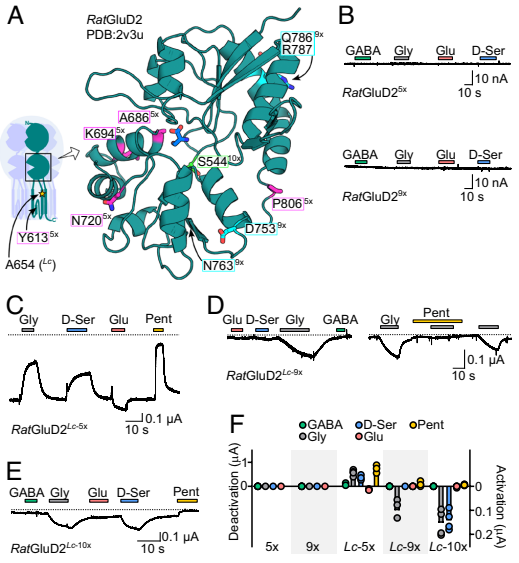

Fig. 6. *Aca*GluD-like mutations alter *Rat*GluD2 receptor function. (*A*) D-serine bound *Rat*GluD2 from X-ray structure PDB:2v3u (13). Selected amino acid residues are indicated, colored, shown as sticks, and labeled 5×, 9×, 10×, and/or *Lc* according to the multiple mutants they were incorporated into. 10× mutant included 10×, 9×, and 5× positions. 9× included 9× and 5×. 5× included only 5×. The *Inset* cartoon shows LBD within full-length receptor and approximate position of two other residues. (*B*–*E*) Example current responses to different neurotransmitter ligands (30 mM) and to pore blocker pentamidine (Pent, 100 μM) in oocytes expressing indicated *Rat*GluD2 mutants. The dashed line indicates zero current baseline. (*F*) Individual (dots) and mean (columns) responses to ligands in oocytes expressing indicated *Rat*GluD2 mutants (n = 4 to 5).

Discussion

The relative inactivity of mammalian delta iGluRs compared to other iGluRs has intrigued biophysicists, impaired pharmacological developments, and confounded our inferences from genome sequencing data. We therefore investigated the evolution and biophysical properties of the delta iGluR family, uncovering GABA-gated delta iGluRs in numerous invertebrates, dissecting their relationships with other iGluRs, and identifying a putative molecular basis for the loss of activity in vertebrate delta iGluRs.

Divergence of Delta Receptors from Other iGluRs. Our phylogenetic analysis finds delta iGluR genes only in bilaterians, consistent with a previous, detailed phylogenetic study (23). But as our study also included xenacoelomorphs, a group of bilaterians that likely branched before the divergence of various nephrozoans (i.e., protostomes and deuterostomes) (46), we now suggest that delta iGluRs emerged from the duplication of an AKDF gene in early bilaterian animals, shortly after they split from cnidarians (e.g., sea anemones and jellyfish).

Delta iGluRs form a family within the AKDF branch of the iGluR superfamily, a branch that includes the AMPA/KA family of fast-activating and deactivating glutamate-gated channels and numerous other uncharacterized genes. We cannot infer the functional nature of the very first delta iGluR, because we were unable to measure the activity of early branching delta iGluRs found in protostomes. Nor do we know the functional nature of the gene from which the first delta iGluR emerged, as much of the sister group to delta iGluRs, the combined [(AMPA/KA)+(Phi)+(uncharacterized AKDF)] branch, is uncharacterized, and branch support toward the base of the AKDF branch is relatively weak (*SI Appendix*, Fig. S1 and ref. 23). However, the presence of GABA sensitivity in xenacoelomorph, invertebrate deuterostome, and even certain vertebrate delta iGluRs, suggests that early delta iGluRs were GABA-sensitive. And the ligand-gated channel activity of numerous delta iGluRs, together with that of AMPA/KA receptors, suggests that mutations in delta iGluR genes of either chordates or vertebrates led to the inactivity of extant vertebrate delta iGluRs.

Biophysical Mechanisms. We identified several mutations that occurred in delta iGluRs of the vertebrate lineage that cause reduced cell surface expression and/or induce inactive, potentially desensitized states. Notably, several of these residues are in the mid-to-rear of the LBD (Fig. 5*D*), a part of the receptor implicated in AMPA/KA iGluR desensitization (40–43), the phenomenon of upper-channel collapse when ligand-bound LBDs separate from each other, loosening the tension between LBDs and channel-forming helices (3). Another vertebrate delta iGluR mutation we identified, G567S in the "hinge" between upper and lower lobes at the rear of the LBD, reduced the GABA selectivity of the invertebrate delta iGluR. How this mutation alters ligand selectivity is not addressed by our experiments, and our dockings to static LBDs do not address, e.g., flexibility of the LBD as determined by residues like G567 in the hinge region. However, previous experimental and computational work on *Rat*GluD2 suggests that D-serine affinity is substantially altered by mutations in the hinge that alter its flexibility (47). That ligand-selectivity may be allosterically controlled is also reflected in the altered glycine/D-serine preference shown by a chimera with an NTD-LBD linker substitution.

Attempting to "reverse" the loss-of-function mutations in vertebrate delta iGluRs and "reawaken" *Rat*GluD2 iGluRs, we found that even when combined, nine reverse substitutions did not reawaken ligand-gated activity. This suggests that additional mutations have accumulated in vertebrate delta iGluRs, and receptor

reawakening is now contingent upon these additional residues. Foreseeably, some combination of up to 41 of the potential reverse mutations would achieve this, despite the fact that many of these forward mutations were not noticeably detrimental to starfish delta iGluR function. Reverse mutations in *Rat*GluD2 iGluRs on the *Lc*-mutant background, however, indeed led to ligand-gated channels, either glycine-gated or glycine- and D-serine-gated, depending on the combination of mutations. This confirms previous work showing that delta iGluR LBDs are capable of substantial ligand-induced conformational change (13, 48) and delta iGluR channels are capable of gating (12, 30), but moreover, it shows that only a few amino acid residues prevent the coupling of these two processes in vertebrate delta iGluRs.

Our results also highlight the fact that the effects of upper-M3 mutations are difficult to predict, as they vary depending on amino acids in the LBD. Four of the above reverse mutations in the LBD caused *Rat*GluD2 *Lc*-mutant channels to be closed at rest. This identifies candidate LBD determinants of the differing effects of M3 mutations in different iGluR families (11, 26, 49, 50). Indeed, despite high conservation of upper-M3 amino acid sequence in various delta iGluRs (*SI Appendix*, Fig. S5), we show that the *Lc*-mutation has very different effects in *Rat*GluD2 and *Sac*GluD, as it converts the latter from a generally inactive channel to one that is largely inactive at rest and potently and efficaciously activated by GABA.

Our experiments suggest that mutations in the NTD played relatively little role in the loss of ligand-gated currents in vertebrate delta iGluRs. However, changes in both the NTDs and LBDs may affect delta iGluR activity via a remarkably similar mechanism. Borrowing from broadly accepted mechanisms of AMPA receptor activation and desensitization (4), delta iGluR activity may depend on tight interfaces at the rear of adjacent LBDs so that clamshell closure at the front of the LBD pulls the lower lobe upward, pulling the channel open via the LBD-channel domain linker. Thus, the inter-LBD interface can be stabilized and channel activity enhanced by either introduced disulfides linking NTDs *or* LBDs (19, 37); pre- and intersynaptic proteins that lock delta iGluR NTDs together to keep the receptor taut (17, 19); or amino acid identity in and around the rear of the LBD (present study).

Pharmacological Avenues. No selective pharmacological modulators of delta iGluRs are known. Whether such modulators would be directly relevant to pharmacotherapy is unclear, as the links between low GluD1 expression and schizophrenia and GluD2 overactivity and cerebellar ataxia may pertain to early development (51–53) and thus be inaccessible to pharmacotherapy. But delta iGluR modulators would drastically improve physiological experiments aiming to dissect the function of delta iGluRs in neural circuitry in vivo/ex vivo.

Small currents through reawakened vertebrate delta iGluRs and certainly large currents through active invertebrate delta iGluRs offer a tangible experimental system for testing the effects of potential drug molecules on delta iGluR function. Such use of invertebrate receptors would rely on their pharmacological profile matching that of vertebrate GluD1 and GluD2 iGluRs, but our study shows that sensitivity to certain competitive antagonists and pore blockers seems similar in vertebrate and invertebrate delta iGluRs. Our study also suggests that care must be taken when dissecting synaptic iGluR composition with classical AMPA/KA receptor modulators, as some of these also affect delta iGluRs.

Excitatory GABA Receptors. The most surprising finding in our study was that many delta iGluRs are activated by the transmitter GABA. GABA mediates most of the rapid *inhibitory* signals in mammalian central synapses via its activation of type-A GABA receptors ($GABA_A$ receptors) of the pentameric (or "Cys-loop") ligand-gated ion channel superfamily (54). The presence of GABA-gated receptors throughout the delta iGluR branch suggests that delta iGluRs became GABA-sensitive early after their emergence, resulting in excitatory GABA receptors that have been inherited by numerous bilaterian animals, including acoels and other xenacoelmorphs, and invertebrate deuterostomes such as starfish and acorn worms. Future studies are needed to determine whether GABAergic neurons synapse onto GABA-gated delta receptors and whether such excitatory GABA receptors also occur in protostomes and early-branching chordates.

There are now numerous examples of ligand-gated ion channels that overturn the conventional view of glutamate as excitatory and GABA and glycine as inhibitory transmitters. Within the iGluR superfamily, there are excitatory glycine-gated NMDA receptors in mammals (55) and numerous glycine-gated and presumably excitatory iGluRs of the "epsilon" family in invertebrates (23, 56). And in the pentameric ligand-gated ion channel superfamily, there are excitatory GABA receptors and inhibitory glutamate receptors (57, 58). The fact that ligand sensitivity and ion permeability are so readily evolvable in different ligand-gated ion channel superfamilies and in different animals means that burgeoning transcriptomic studies must be cautious in assigning neuronal identity to different cells based on the presence of, e.g., iGluR genes. While the prediction of function from sequence will always be susceptible to unidentified switches in function, we foresee that systematic studies of the evolution of receptor families, such as ours, will improve future assessments of neuronal function based on the presence of different ligand-gated ion channel genes.

Methods

Phylogenetics. iGluR amino acid sequences were sought from four chordates (*Rattus norvegicus, Danio rerio, Branchiostoma belcheri,* and *Ciona intestinalis*), two hemichordates *(Ptychodera flava* and *Saccoglossus kowalevskii*), two echinoderms (*Acanthaster planci* and *Anneissia japonica*), one ecdysozoan *(Strigamia maritima*), two spiralians (*Crassostrea gigas* and *Schmidtea mediterranea*), two xenoturbellids (*Xenoturbella profunda* and *Xenoturbella bocki*), two acoels (*Diopisthoporus longitubus* and *Hofstenia miamia*), two nemertodermatids (*Meara stichopi* and *Nemertoderma westbladi*), two cnidarians (*Hydra vulgaris* and *Nematostella vectensis*), one placozoan (*Trichoplax* sp H2), one poriferan (*Oscarella carmela*), and two ctenophores (*Euplokamis dunlapae* and *Pleurobrachia bachei*). Rat sequences were retrieved from UniProt. Other sequences were retrieved via BlastP search with *Rattus norvegicus* GluD2 (NCBI XP_038964327.1) as query in KEGG Genome Database, https://www.genome.jp/kegg/genome/ (*Nematostella vectensis*); Compagen Japan, http://compagen.unit.oist.jp/ (*Osarella carmela* OCAR_T-CDS_130911 dataset); OIST Marine Genomics Unit, https://marinegenomics.oist.jp/acornworm/viewer/info?project_id=33; a published dataset for xenacoelamorphs (59); and NCBI (all other species). We included an additional two plant sequences from *Arabidopsis thaliana* (NCBI) as an outgroup.

Sequences were aligned with MAFFT v7.450 (60) in Geneious Prime (Dotmatics). Sequences that were >95% identical to another and sequences that were excessively long or short were removed. The final alignment contained 246 sequences with 4692 columns (including gaps). From this alignment, we generated a maximum-likelihood phylogenetic tree using IQ-Tree (61) with a Q.pfam+G4 substitution model (62) (log-likelihood of model -410679) and both SH-aLRT (63) and ultrafast bootstrap (64) branch support.

Molecular Biology and Heterologous Expression. Delta iGluR sequences were commercially synthesized and subcloned (Genscript Biotech Netherlands) into a custom vector so that finally each coding sequence had silent mutations to remove internal restriction sites, a C-terminal glycine-serine linker and cMyc tag (except for *Saccoglossus kowalevskii* GluD) and was preceded by a loosely Kozak consensus sequence, flanked by *Xenopus laevis* β-globin 5′ and 3′ untranslated sequences, and followed by a poly(A) tail. *Dan*GluD2 and *Cra*GluD sequences were codon-optimized for *Xenopus leavis* in iCodon as we learnt of this software

(65). Full delta iGluR sequences in *SI Appendix, Supporting Text*. *Rattus norvegicus* GluA2 (flip isoform) in the pRK5 vector was a gift from David MacLean (University of Rochester Medical Center), and human TARPγ2 (CACNG2) in the pcDNA3.1(+) vector was a gift from Stephan Pless (University of Copenhagen). Single- and double-mutant cDNAs were generated by PCR with partly overlapping mutant primers (66) and Phusion Hotstart II High Fidelity polymerase (Fisher Scientific). Chimeras were generated by combining fragments cloned with custom primers using and according to the GenBuilder Cloning Kit (Genscript). Coding sequences of all plasmids were confirmed by Sanger sequencing (Genewiz). Capped mRNA was transcribed from EcoRI (all delta iGluRs), SalI (*Rat*GluA2), or XbaI (TARPγ2) -digested DNAs with the SP6 (delta iGluRs) or T7 (*Rat*GluA2 and *Hom*TARPγ2) Mmessage Mmachine kits (Fisher Scientific) and then purified (RNA Clean & Concentrator kit, Zymo Research). 4 ng (*Aca*GluD), 40 ng (all other delta iGluRs) or 10 ng (*Rat*GluA2 9 ng + *Hom*TARP γ2 1 ng) RNA in 40 nL was injected (Nanoliter 2010, World Pricision Instruments) into collagenase-treated *Xenopus leavis* stage V/VI oocytes (EcoCyte Bioscience) and oocytes were kept in 50% (in water) Leibovitz's L-15 medium (Gibco) supplemented with additional 0.25 mg/mL gentamicin, 1 mM L-glutamine, and 15 mM HEPES, pH 7.6 at 18 °C for two (*Rat*GluA2) or three to four (delta iGluRs) days before experiments.

Electrophysiology. Oocytes were continuously perfused with a bath solution containing (in mM) 96 NaCl, 2 KCl, 1.8 $CaCl_2$, 1 $MgCl_2$, and 5 HEPES, pH 7.6 with NaOH, in a plastic recording chamber (RC-3Z, Warner Instruments). For zero-Ca^{2+} experiments, $CaCl_2$ and $MgCl_2$ were replaced with 2 mM $BaCl_2$. Oocytes were impaled with Borosilicate micropipettes containing KCl (3 M) and voltage clamped with an OC-725D amplifier (Warner Instruments) controlled via an Axon Digitata interface and pClamp v11 (Molecular Devices). Current was sampled at 1,000 Hz and filtered at 200 Hz. Drugs dissolved in bath solution were applied via an eight-channel, gravity-driven perfusion system (VCS-8-pinch, Warner Instruments). For concanavalin A treatment, oocytes were incubated in dishes of concanavalin A-containing (10 μM) bath solution on ice for 5 to 10 min immediately before recording.

Immunolabeling. Oocytes were washed twice with phosphate-buffered saline (PBS) and fixed with 4% paraformaldehyde in PBS overnight at 4 °C. Fixed oocytes were embedded in 3% low-gelling point agarose and sliced with a vibratome in 100-μm sections. Slices were washed with PBS containing 0.2% bovine serum albumin (BSA) and 0.1% Tween 20 for 3 h at room temperature. Slices were incubated with mouse anti-Myc tag monoclonal IgG1 antibody (Myc.A7, Invitrogen MA121316, Fisher Scientific) 1:500 in blocking buffer (PBS containing 1% BSA and 0.1% Tween-20) overnight at 4 °C, washed three times with PBS, incubated with goat anti-mouse polyclonal IgG (H+L) Alexa Fluor 568 conjugate (Invitrogen A11004, Thermofisher) 1:1,000 in blocking buffer for 1 h at room temperature, and washed three times with PBS. Slices were mounted on a glass slide in 50% glycerol, and images were acquired on an Olympus FLUOVIEW FV3000 confocal laser scanning microscope with standard PMT detectors, 20× air and 30× and 40× silicon oil immersion lenses. Images were processed with Fiji software (67).

Data Analysis. Currents were additionally filtered (50 Hz, Bessel 8-pole) and measured in Clampfit (Molecular Devices). Data were plotted in Prism v9 (GraphPad). For simple plots, we have shown all data points, but for concentration–response and IV plots, we have shown only mean ± SEM for clarity. EC_{50} values for each individual oocyte were calculated by variable slope nonlinear regression in Prism v9 and used to calculate the means reported in text. Summary concentration–response curves are fit to mean data points in figures.

Structural Model. An AlphaFold2 structural model of the *Aca*GluD LBD was created using ColabFold v2 without template information (68, 69). For most figures, this was visualized with PyMol v4.6 (Schrödinger).

Computational Ligand Docking. Dockings were conducted using AutoDock 4.2 (70). The structure file generated by AlphaFold2 was used for the docking experiments of *Aca*GluD, while *Rat*GluD2 was docked using the PDB structure file (PDB ID 2v3u) (13) after removing unnecessary molecules such as water and D-serine from the X-ray structure. Both GABA and D-serine molecules used as ligands were retrieved from https://pubchem.ncbi.nlm.nih.gov/ (Compound CID: 119 and 71077 respectively). Employing a blind docking approach, 100 experiments were carried out for each ligand, with a maximum of 25 million energy evaluations per experiment using the Lamarckian genetic algorithm and default parameters from AutoDock4.2. The resulting configurations were clustered ligand binding modes with <2.0 Å rmsd from each other. Clusters of energetically favorable configurations typically included over 10 similar binding modes: Fig. 2 shows the five most energetically favorable; *SI Appendix*, Fig. S3 shows the overall clustering. Images of the ligand–receptor complex were generated using ChimeraX 1.4 (71).

N-Linked Glycosylation Site Prediction. The identification of potential N-linked glycosylation sites in *Aca*GluD, *Rat*GluD2, and *Rat*GluD1 was performed using the NetNGlyc 1.0 tool (72) using amino acid sequences as input. The parameters used for the NetNGlyc 1.0 analysis were kept at default settings, and predicted sites were annotated on amino acid sequence (*SI Appendix*, Fig. S5).

Data, Materials, and Software Availability. All study data are included in the article and/or *SI Appendix*.

ACKNOWLEDGMENTS. This project has received funding from the European Research Council (ERC) under the European Union's Horizon 2020 research and innovation programme (grant agreement no. 803714) and from The Research Council of Norway (project no. 234817). We are grateful to Yuhong Wang (Michael Sars Centre) for help with electrophysiological experiments, Eudald Pascual-Carreras and Sara Brites (Michael Sars Centre) for guidance with immunolabeling, and David MacLean (University of Rochester Medical Center) and Stephan Pless (University of Copenhagen) for plasmids.

1. S. L. Palay, Synapses in the central nervous system. *J. Biophys. Biochem. Cytol.* **2**, 193–202 (1956).
2. J. DeFelipe, L. Alonso-Nanclares, J. I. Arellano, Microstructure of the neocortex: Comparative aspects. *J. Neurocytol.* **31**, 299–316 (2002).
3. K. B. Hansen *et al.*, Structure, function, and pharmacology of glutamate receptor ion channels. *Pharmacol. Rev.* **73**, 298–487 (2021).
4. I. H. Greger, J. F. Watson, S. G. Cull-Candy, Structural and functional architecture of AMPA-type glutamate receptors and their auxiliary proteins. *Neuron* **94**, 713–730 (2017).
5. K. B. Hansen *et al.*, Structure, function, and allosteric modulation of NMDA receptors. *J. Gen. Physiol.* **150**, 1081–1105 (2018).
6. K. Araki *et al.*, Selective expression of the glutamate receptor channel δ2 subunit in cerebellar purkinje cells. *Biochem. Biophys. Res. Comm.* **197**, 1267–1276 (1993).
7. H. Lomeli *et al.*, The rat delta-1 and delta-2 subunits extend the excitatory amino acid receptor family. *FEBS Lett.* **315**, 318–322 (1993).
8. M. Yamazaki, K. Araki, A. Shibata, M. Mishina, Molecular cloning of a cDNA encoding a novel member of the mouse glutamate receptor channel family. *Biochem. Biophys. Res. Comm.* **183**, 886–892 (1992).
9. A. P. Burada *et al.*, Emerging insights into the structure and function of ionotropic glutamate delta receptors. *Br. J. Pharmacol.* **179**, 3612–3627 (2022).
10. V. Ady *et al.*, Type 1 metabotropic glutamate receptors (mGlu1) trigger the gating of GluD2 delta glutamate receptors. *EMBO Rep.* **15**, 103–109 (2014).
11. M. Masternak *et al.*, Differences between the GluD1 and GluD2 receptors revealed by GluD1 X-ray crystallography, binding studies and molecular dynamics. *FEBS J.* **290**, 3781–3801 (2023).
12. J. Zuo *et al.*, Neurodegeneration in Lurcher mice caused by mutation in delta2 glutamate receptor gene. *Nature* **388**, 769–773 (1997).
13. P. Naur *et al.*, Ionotropic glutamate-like receptor delta2 binds D-serine and glycine. *Proc. Natl. Acad. Sci. U.S.A.* **104**, 14116–14121 (2007).
14. N. Benamer *et al.*, GluD1, linked to schizophrenia, controls the burst firing of dopamine neurons. *Mol. Psychiatry* **23**, 691–700 (2018).
15. S. C. Gantz, K. Moussawi, H. S. Hake, Delta glutamate receptor conductance drives excitation of mouse dorsal raphe neurons. *Elife* **9**, e56054 (2020).
16. J. Dai, C. Patzke, K. Liakath-Ali, E. Seigneur, T. C. Südhof, GluD1 is a signal transduction device disguised as an ionotropic receptor. *Nature* **595**, 261–265 (2021).
17. J. Elegheert *et al.*, Structural basis for integration of GluD receptors within synaptic organizer complexes. *Science* **353**, 295–299 (2016).
18. K. Matsuda *et al.*, Cbln1 is a ligand for an orphan glutamate receptor delta2, a bidirectional synapse organizer. *Science* **328**, 363–368 (2010).
19. E. Carrillo, C. U. Gonzalez, V. Berka, V. Jayaraman, Delta glutamate receptors are functional glycine- and D-serine-gated cation channels in situ. *Sci. Adv.* **7**, eabk2200 (2021).
20. A. P. Burada, R. Vinnakota, J. Kumar, The architecture of GluD2 ionotropic delta glutamate receptor elucidated by cryo-EM. *J. Struct. Biol.* **211**, 107546 (2020).
21. A. P. Burada, R. Vinnakota, J. Kumar, Cryo-EM structures of the ionotropic glutamate receptor GluD1 reveal a non-swapped architecture. *Nat. Struct. Mol. Biol.* **27**, 84–91 (2020).
22. M. N. Green *et al.*, Structure of the Arabidopsis thaliana glutamate receptor-like channel GLR3.4. *Mol. Cell* **81**, 3216–3226.e8 (2021).
23. D. Ramos-Vicente *et al.*, Metazoan evolution of glutamate receptors reveals unreported phylogenetic groups and divergent lineage-specific events. *Elife* **7**, e35774 (2018).
24. D. Stroebel, P. Paoletti, Architecture and function of NMDA receptors: An evolutionary perspective. *J. Physiol.* **599**, 2615–2638 (2021).

25. A. Hejnol, K. Pang, Xenacoelomorpha's significance for understanding bilaterian evolution. *Curr. Opin. Genet. Dev.* **39**, 48–54 (2016).
26. R. Yadav, R. Rimerman, M. A. Scofield, S. M. Dravid, Mutations in the transmembrane domain M3 generate spontaneously open orphan glutamate delta1 receptor. *Brain Res.* **1382**, 1–8 (2011).
27. L. Piot *et al.*, GluD1 binds GABA and controls inhibitory plasticity. *Science* **382**, 1389–1394 (2023), 10.1126/science.adf3406.
28. K. Williams, M. Dattilo, T. N. Sabado, K. Kashiwagi, K. Igarashi, Pharmacology of delta2 glutamate receptors: Effects of pentamidine and protons. *J. Pharmacol. Exp. Ther.* **305**, 740–748 (2003).
29. J. Boulter *et al.*, Molecular cloning and functional expression of glutamate receptor subunit genes. *Science* **249**, 1033–1037 (1990).
30. S. M. Schmid, S. Kott, C. Sager, T. Huelsken, M. Hollmann, The glutamate receptor subunit delta2 is capable of gating its intrinsic ion channel as revealed by ligand binding domain transplantation. *Proc. Natl. Acad. Sci. U.S.A.* **106**, 10320–10325 (2009).
31. M. Schonrock, G. Thiel, B. Laube, Coupling of a viral K(+)-channel with a glutamate-binding-domain highlights the modular design of ionotropic glutamate-receptors *Commun. Biol.* **2**, 75 (2019).
32. I. J. Reynolds, E. Aizenman, Pentamidine is an N-methyl-D-aspartate receptor antagonist and is neuroprotective in vitro. *J. Neurosci.* **12**, 970–975 (1992).
33. D. McNamara *et al.*, 5,7-Dichlorokynurenic acid, a potent and selective competitive antagonist of the glycine site on NMDA receptors. *Neurosci. Lett.* **120**, 17–20 (1990).
34. Y. P. Auberson *et al.*, N-Phosphonoalkyl-5-aminomethylquinoxaline-2,3-diones: In vivo active AMPA and NMDA(glycine) antagonists. *Bioorg. Med. Chem. Lett.* **9**, 249–254 (1999).
35. K. Menuz, R. M. Stroud, R. A. Nicoll, F. A. Hays, TARP auxiliary subunits switch AMPA receptor antagonists into partial agonists. *Science* **318**, 815–817 (2007).
36. A. S. Kristensen *et al.*, Pharmacology and structural analysis of ligand binding to the orthosteric site of glutamate-like GluD2 receptors. *Mol. Pharmacol.* **89**, 253–262 (2016).
37. K. B. Hansen *et al.*, Modulation of the dimer interface at ionotropic glutamate-like receptor delta2 by D-serine and extracellular calcium. *J. Neurosci.* **29**, 907–917 (2009).
38. E. C. Twomey, M. V. Yelshanskaya, R. A. Grassucci, J. Frank, A. I. Sobolevsky, Channel opening and gating mechanism in AMPA-subtype glutamate receptors. *Nature* **549**, 60–65 (2017).
39. S. Chen *et al.*, Activation and desensitization mechanism of AMPA receptor-TARP complex by cryo-EM. *Cell* **170**, 1234–1246.e14 (2017).
40. A. L. Carbone, A. J. Plested, Coupled control of desensitization and gating by the ligand binding domain of glutamate receptors. *Neuron* **74**, 845–857 (2012).
41. B. A. Daniels, E. D. Andrews, M. R. Aurousseau, M. V. Accardi, D. Bowie, Crosslinking the ligand–binding domain dimer interface locks kainate receptors out of the main open state. *J. Physiol.* **591**, 3873–3885 (2013).
42. Y. Stern-Bach, S. Russo, M. Neuman, C. Rosenmund, A point mutation in the glutamate binding site blocks desensitization of AMPA receptors. *Neuron* **21**, 907–918 (1998).
43. Y. Sun *et al.*, Mechanism of glutamate receptor desensitization. *Nature* **417**, 245–253 (2002).
44. J. Kehoe, Transformation by concanavalin A of the response of molluscan neurones to L-glutamate. *Nature* **274**, 866–869 (1978).
45. M. L. Mayer, L. Vyklicky Jr., Concanavalin A selectively reduces desensitization of mammalian neuronal quisqualate receptors. *Proc. Natl. Acad. Sci. U.S.A.* **86**, 1411–1415 (1989).
46. J. T. Cannon *et al.*, Xenacoelomorpha is the sister group to Nephrozoa. *Nature* **530**, 89–93 (2016).
47. D. Tapken *et al.*, The low binding affinity of D-serine at the ionotropic glutamate receptor GluD2 can be attributed to the hinge region. *Sci. Rep.* **7**, 46145 (2017).
48. A. C. Chin, R. A. Yovanno, T. J. Wied, A. Gershman, A. Y. Lau, D-serine potently drives ligand-binding domain closure in the ionotropic glutamate receptor GluD2. *Structure* **28**, 1168–1178.e2 (2020).
49. R. M. Klein, J. R. Howe, Effects of the lurcher mutation on GluR1 desensitization and activation kinetics. *J. Neurosci.* **24**, 4941–4951 (2004).
50. S. E. Murthy, T. Shogan, J. C. Page, E. M. Kasperek, G. K. Popescu, Probing the activation sequence of NMDA receptors with lurcher mutations. *J. Gen. Physiol.* **140**, 267–277 (2012).
51. M. Coutelier *et al.*, $GRID_2$ mutations span from congenital to mild adult-onset cerebellar ataxia. *Neurology* **84**, 1751–1759 (2015).
52. I. Nenadic *et al.*, Glutamate receptor delta 1 (GRID1) genetic variation and brain structure in schizophrenia. *J. Psychiatr. Res.* **46**, 1531–1539 (2012).
53. P. K. Panda, I. K. Sharawat, L. Dawman, GRID2 mutation-related spinocerebellar Ataxia type 18: A new report and literature review. *J. Pediatr. Genet.* **11**, 99–109 (2020).
54. R. W. Olsen, W. Sieghart, International Union of Pharmacology. LXX. Subtypes of gamma-aminobutyric acid(A) receptors: Classification on the basis of subunit composition, pharmacology, and function. Update. *Pharmacol. Rev.* **60**, 243–260 (2008).
55. S. Bossi *et al.*, GluN3A excitatory glycine receptors control adult cortical and amygdalar circuits. *Neuron* **110**, 2438–2454.e8 (2022).
56. R. Alberstein, R. Grey, A. Zimmet, D. K. Simmons, M. L. Mayer, Glycine activated ion channel subunits encoded by ctenophore glutamate receptor genes. *Proc. Natl. Acad. Sci. U.S.A.* **112**, E6048–6057 (2015).
57. A. A. Beg, E. M. Jorgensen, EXP-1 is an excitatory GABA-gated cation channel. *Nat. Neurosci.* **6**, 1145–1152 (2003).
58. D. F. Cully *et al.*, Cloning of an avermectin-sensitive glutamate-gated chloride channel from Caenorhabditis elegans. *Nature* **371**, 707–711 (1994).
59. C. Andrikou, D. Thiel, J. A. Ruiz-Santiesteban, A. Hejnol, Active mode of excretion across digestive tissues predates the origin of excretory organs. *PLoS Biol.* **17**, e3000408 (2019).
60. K. Katoh, K. Misawa, K. Kuma, T. Miyata, MAFFT: A novel method for rapid multiple sequence alignment based on fast Fourier transform. *Nucleic Acids Res.* **30**, 3059–3066 (2002).
61. B. Q. Minh *et al.*, IQ-TREE 2: New models and efficient methods for phylogenetic inference in the genomic era. *Mol. Biol. Evol.* **37**, 1530–1534 (2020).
62. B. Q. Minh, C. C. Dang, L. S. Vinh, R. Lanfear, QMaker: Fast and accurate method to estimate empirical models of protein evolution. *Syst. Biol.* **70**, 1046–1060 (2021).
63. S. Guindon *et al.*, New algorithms and methods to estimate maximum-likelihood phylogenies: Assessing the performance of PhyML 3.0. *Syst. Biol.* **59**, 307–321 (2010).
64. D. T. Hoang, O. Chernomor, A. von Haeseler, B. Q. Minh, L. S. Vinh, UFBoot2: Improving the ultrafast bootstrap approximation. *Mol. Biol. Evol.* **35**, 518–522 (2018).
65. M. Diez *et al.*, iCodon customizes gene expression based on the codon composition. *Sci. Rep.* **12**, 12126 (2022).
66. Y. Xia, W. Chu, Q. Qi, L. Xun, New insights into the QuikChange process guide the use of Phusion DNA polymerase for site-directed mutagenesis. *Nucleic Acids Res.* **43**, e12 (2015).
67. J. Schindelin *et al.*, Fiji: An open-source platform for biological-image analysis. *Nat. Methods* **9**, 676–682 (2012).
68. J. Jumper *et al.*, Highly accurate protein structure prediction with AlphaFold. *Nature* **596**, 583–589 (2021).
69. M. Mirdita *et al.*, ColabFold: Making protein folding accessible to all. *Nat. Methods* **19**, 679–682 (2022).
70. G. M. Morris *et al.*, AutoDock4 and AutoDockTools4: Automated docking with selective receptor flexibility. *J. Comput. Chem.* **30**, 2785–2791 (2009).
71. E. C. Meng *et al.*, UCSF ChimeraX: Tools for structure building and analysis. *Protein Sci.* **32**, e4792 (2023).
72. R. Gupta, S. Brunak, Prediction of glycosylation across the human proteome and the correlation to protein function. *Pac. Symp. Biocomput.*, 310–322 (2002).

SUPPORTING INFORMATION FOR:

Loss of activation by GABA in vertebrate delta ionotropic glutamate receptors

Giulio Rosano[a], Allan Barzasi[a], Timothy Lynagh[a,*]

[a] Michael Sars Centre, University of Bergen, 5008 Bergen, Norway

* Correspondence
tim.lynagh@uib.no
Michael Sars Centre, University of Bergen
Thomøhlensgate 55
5008 Bergen
Norway

This PDF file includes:

Figure S1. Animal iGluR phylogeny. (**A**) Maximum likelihood phylogeny with Q.pfam+G4 substitution model. *Branch support values*, SH-aLRT and ultrafast bootstrap (/100). Values near tips omitted for clarity. *Colors*, selected iGluR families. *Bold*, genes tested in our experiments. (**B**) Animal lineages and species used for iGluR search.

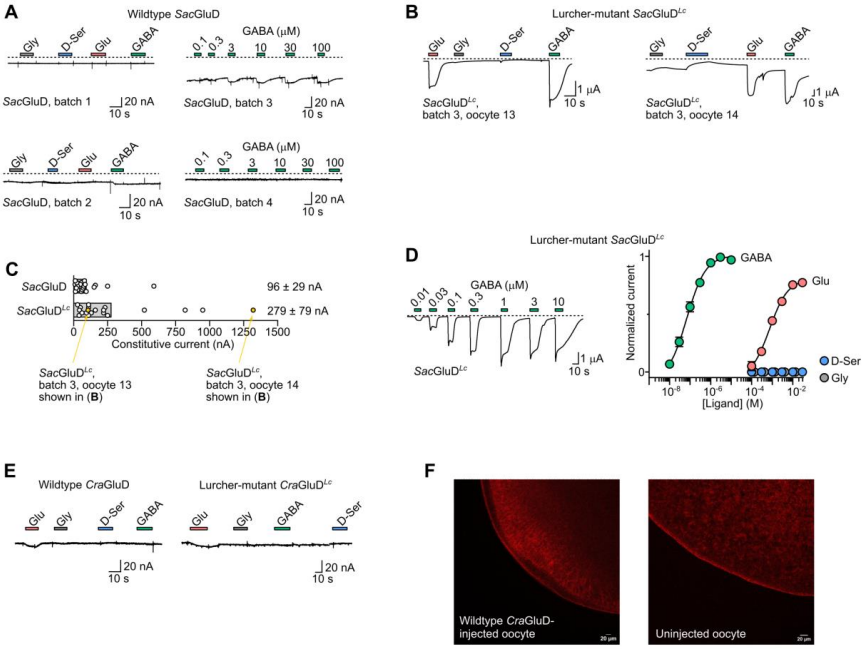

Figure S2. Characterization of *Saccoglossus kowalevskii* and *Crassostrea gigas* GluD iGluRs

(**A**) Two-electrode voltage clamp (TEVC) recordings in oocytes of four different batches, injected with wildtype *Saccoglossus kowalevskii* GluD (*Sac*GluD) mRNA, showing current responses to different potential ligands. *Dashed lines*, zero current.

(**B**) TEVC recordings of responses to different ligands in oocytes injected with lurcher-mutant *Sac*GluD^{Lc}. Oocyte batch number is separate from that in panel **A**. *Dashed lines*, zero current.

(**C**) Mean (bars) and individual data points (both n = 20 oocytes, over four different batches) of constitutive current in wildtype *Sac*GluD-expressing and lurcher-mutant *Sac*GluD^{Lc}-expressing oocytes. Two *Sac*GluD^{Lc} data points are highlighted: these are shown in panel **B**.

(**D**) *Left*, Representative recording, and *right*, mean ± SEM current responses (normalized to GABA-gated current amplitude) to increasing ligand concentrations in oocytes injected with lurcher-mutant *Sac*GluD^{Lc}. n = 4 (GABA), 3 (Glu), or 5 (D-Ser and Gly).

(**E**) Recordings in oocytes injected with wildtype or lurcher-mutant *Crassostrea gigas* GluD (*Cra*GluD or *Cra*GluD^{Lc}) mRNA.

(**F**) Anti-myc fluorescent immunolabelling of oocyte injected with *Cra*GluD-myc mRNA and uninjected oocyte suggests absence of *Cra*GluD surface expression.

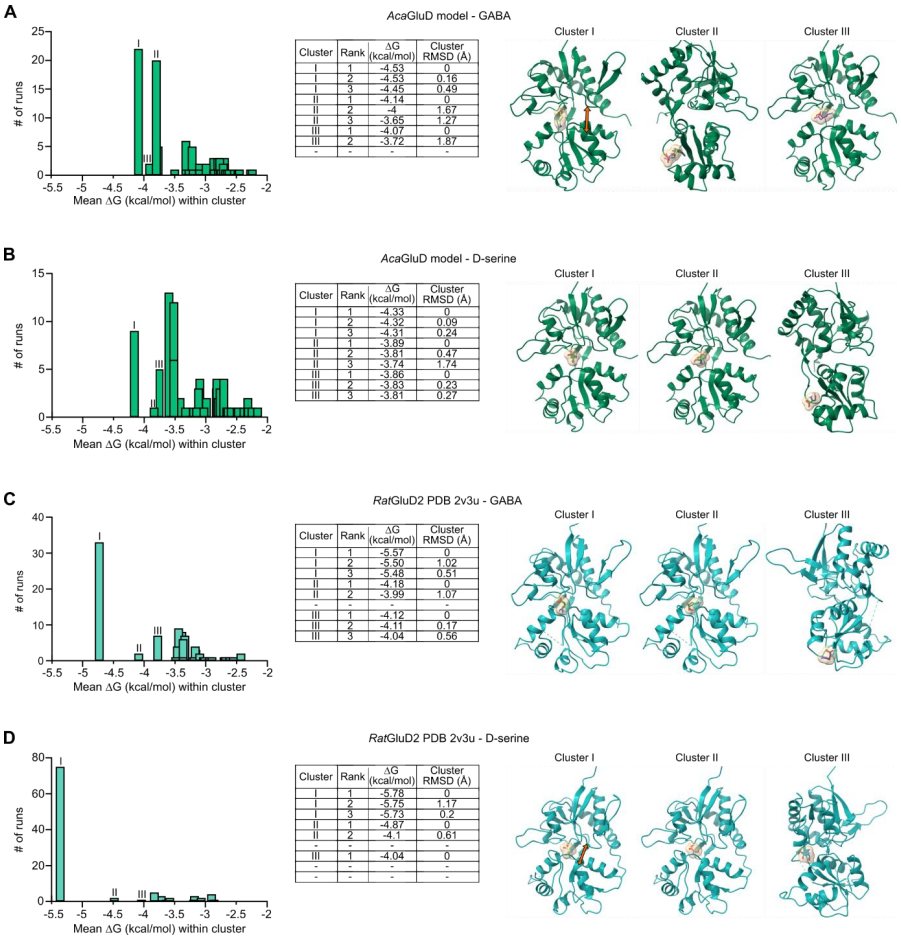

Figure S3. Computational ligand docking to *Aca*GluD and *Rat*GluD2.
(**A**-**D**) Analysis of dockings into clusters of ligand binding modes with <2 Å root mean squared deviation ("RMSD") from each other, for GABA and D-serine at our *Aca*GluD model (**A**,**B**) and the *Rat*GluD2/D-serine structure (PDB 2v3u) with D-serine removed (**C**,**D**). *Left*, number of runs yielding binding modes within clusters (clusters I-III indicated) of decreasing mean binding energy ("mean ΔG within cluster"). *Middle*, corresponding table showing the most favourable binding poses ("Rank 1-3") for the top three clusters. *Right*, graphical representation indicating ligand binding poses in top three clusters. Orange arrows in (**A**) and (**D**) represent *Aca*GluD E475-A747 (**A**) and *Rat*GluD2 E450-A727 (**B**) Cα-Cα distances of 12.4 Å and 12.0 Å.

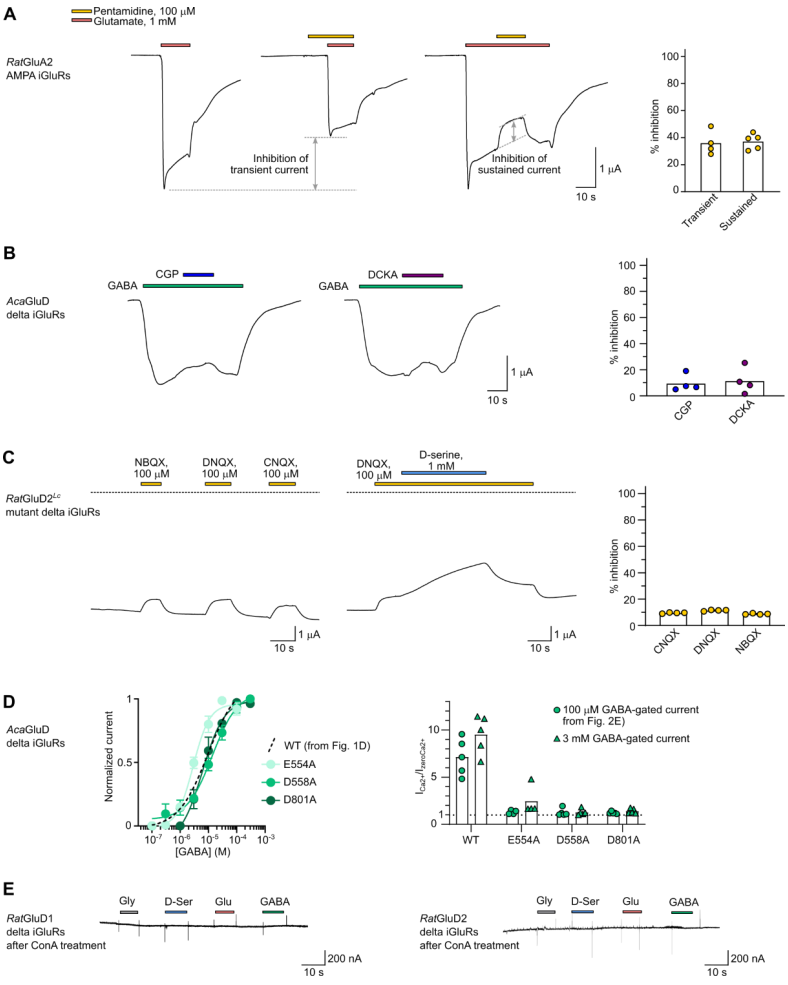

Figure S4. Pharmacological characterization of delta iGluRs and AMPA iGluRs

(**A**) *Left panels*, example recording of glutamate-gated current in an oocyte expressing *Rat*GluA2 and human TARPγ2 (CACNG2). *Right panel*, % inhibition of glutamate-gated current by pentamidine at different oocytes (dots) and resulting means (columns).

(**B**) *Left panels*, example recording of GABA-gated current in an oocyte expressing *Aca*GluD. *Right panel*, % inhibition of GABA-gated current at different oocytes (dots) and resulting means (columns).

(**C**) *Left panels*, example recordings of oocytes expressing A654T lurcher-mutant *Rat*GluD2 (*Rat*GluD2^{Lc}) in response to indicated AMPA iGluR antagonists and D-serine. *Dashed line*, zero current baseline. *Right panel*, % inhibition at different oocytes (dots) and resulting means (columns).

(**D**) *Left*, mean ± SEM (n = 3, D801A; n = 4, all others) normalized (to maximum GABA-gated current at each oocyte) current amplitude in response to increasing GABA concentrations. *Right*, Ca^{2+}-induced enhancement of GABA-gated currents ($I_{Ca2+}/I_{zeroCa2+}$) was similar for 100 µM GABA- and 3 mM GABA-gated currents.

(**E**) Example recordings of oocytes expressing wildtype *Rat*GluD1 or *Rat*GluD2 after oocytes were incubated in 10 µM concanavalin A for 5-10 min.

Figure S5. Alignment of active and inactive delta iGluRs

Major tertiary structural elements are indicated as boxes and labeled, as inferred from high-resolution structures of mouse GluD1 N-terminal domain(1) and rat GluD2 ligand-binding domain(2) and moderate-resolution structures of human GluD1 and GluD2 full-length receptors(3, 4). *Bold cyan and blue*, residues that differ between active *Aca*GluD, *Sac*GluD, and *Dio*GluD iGluRs and verified inactive vertebrate delta iGluRs receptors. Numbers refer to *Aca*GluD positions that were mutated. *Pink*, Lurcher mutant (Lc) position(5), mutated to threonine in several Lc mutants in this study. *Red*, potential Ca^{2+}-binding residues(6), mutated to alanine in several mutants in this study.

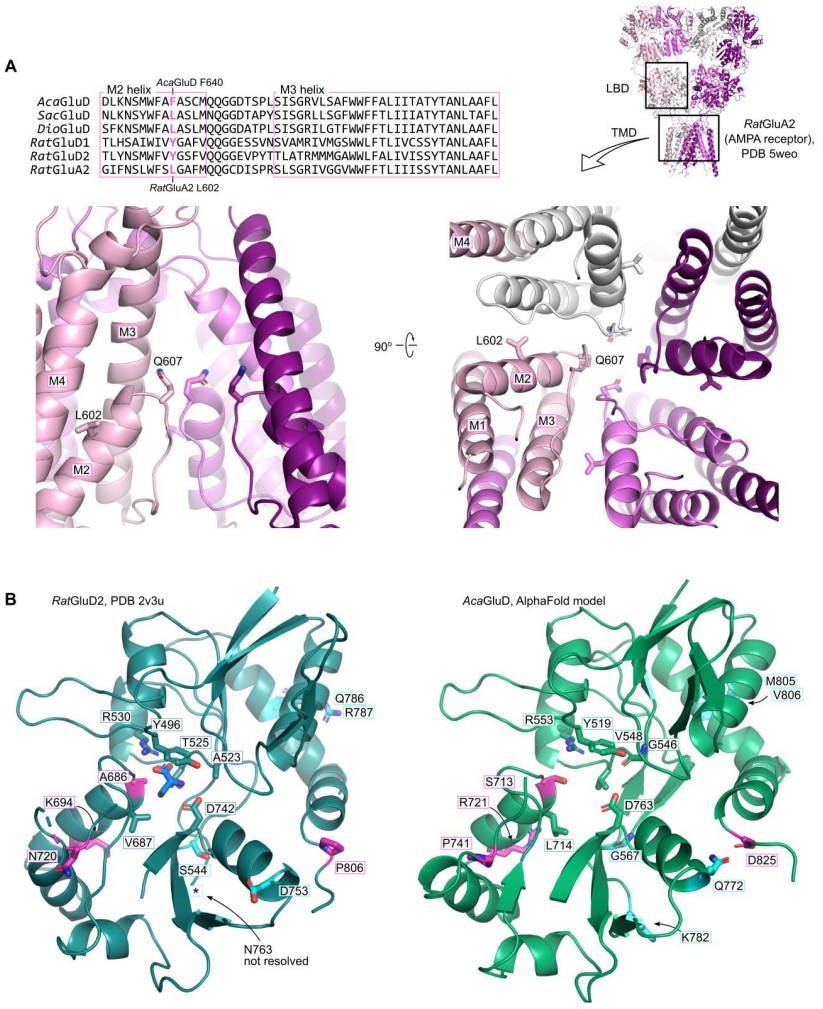

Figure S6. Position of selected amino acid residues in iGluR structures and AlphaFold *Aca*GluD model.
(**A**) Amino acid sequence alignment of membrane-embedded helical segments M2 and M3 from selected delta iGluRs and rat AMPA receptor (*Rat*GluA2, PDB 5weo), and magnified view of the channel pore from cryo-electron microscopy structure of *Rat*GluA2(7), showing the location of *Rat*GluA2 L602, equivalent to *Aca*GluD F640, in comparison to pore-lining residue *Rat*GluA2 Q607. Helices and selected residues for one subunit are labeled. One subunit removed from side view (left) for clarity.
(**B**) *Left*, X-ray structure of D-Serine (blue) -bound *Rat*GluD2 isolated ligand-binding domain (LBD) (2) and *right*, AlphaFold model of *Aca*GluD LBD, highlighting positions whose mutation in *Aca*GluD caused severe (magenta) and moderate (cyan) loss of function and positions that coordinate ligands in most iGluRs (teal in *Rat*GluD2, green in *Aca*GluD). Helix H (residues 723-736 in *Rat*GluD2 and 744-757 in *Aca*GluD) has been hidden from the foreground for clarity.

SUPPORTING TEXT

DNA constructs for expression in *Xenopus laevis* oocytes

All DNA constructs were based on a pSP64 vector (ProMega) modified for expression in *Xenopus* oocytes into which the following delta iGluR inserts were sub-cloned.

ATTTAGGTGACACTATAG, SP6 transcription promoter
AAGCTT, HindIII restriction site
GCTTG etc, beta globin 5' UTR
GTCGACTCTAGAGGATCC, SalI, XbaI, BamHI, restriction sites
ACC, loose Kozak consensus sequence
cMyc + TAA stop codon,
GGTTA etc, beta globin 3' UTR
AAAAA etc, poly(A) sequence
GAATTC, EcoRI restriction site

Modified pSP64 vector

ATTTAGGTGACACTATAGAATACAAGCTTGCTTGTTCTTTTTGCAGAAGCTCAGAATAAACGCTCAACTTTGGCGTCGACTCTAGAGGATCCGAGCAGAAGCTCATCAGTGAGGAAGATCTCTAA
GGTTACCACTAAACCAGCCTCAAGAACACCCGAATGGAGTCTCTAAGCTACATAATACCAACTTACACTTTACAAAATGTTGTCCCCCAAAATGTAGCCATTCGTATCTGCTCCTAATAAAAAGA
AAGTTTCTTCACATTCTAAAAAAAAAAAAAAAAAAAAAAAAAAAAAAAAAAAAAAGAATTCGTAATCATGTCATAGCTGTTTCCTGTGTGAAATTGTTATCCGCTCACAATTCCACACAACATACGAGCCGG
AAGCATAAAGTGTAAAGCCTGGGGTGCCTAATGAGTGAGCTAACTCACATTAATTGCGTTGCGCTCACTGCCCGCTTTCCAGTCGGGAAACCTGTCGTGCCAGCTGCATTAATGAATCGGCCAAC
GCGCGGGGAGAGGCGGTTTGCGTATTGGGCGCTCTTCCGCTTCCTCGCTCACTGACTCGCTGCGCTCGGTCGTTCGGCTGCGGCGAGCGGTATCAGCTCACTCAAAGGCGGTAATACGGTTATCC
ACAGAATCAGGGGATAACGCAGGAAAGAACATGTGAGCAAAAGGCCAGCAAAAGGCCAGGAACCGTAAAAAGGCCGCGTTGCTGGCGTTTTTCCATAGGCTCCGCCCCCCTGACGAGCATCACAA
AAATCGACGCTCAAGTCAGAGGTGGCGAAACCCGACAGGACTATAAAGATACCAGGCGTTTCCCCCTGGAAGCTCCCTCGTGCGCTCTCCTGTTCCGACCCTGCCGCTTACCGGATACCTGTCCG
CCTTTCTCCCTTCGGGAAGCGTGGCGCTTTCTCATAGCTCACGCTGTAGGTATCTCAGTTCGGTGTAGGTCGTTCGCTCCAAGCTGGGCTGTGTGCACGAACCCCCCGTTCAGCCCGACCGCTGC
GCCTTATCCGGTAACTATCGTCTTGAGTCCAACCCGGTAAGACACGACTTATCGCCACTGGCAGCAGCCACTGGTAACAGGATTAGCAGAGCGAGGTATGTAGGCGGTGCTACAGAGTTCTTGAA
GTGGTGGCCTAACTACGGCTACACTAGAAGAACAGTATTTGGTATCTGCGCTCTGCTGAAGCCAGTTACCTTCGGAAAAAGAGTTGGTAGCTCTTGATCCGGCAAACAAACCACCGCTGGTAGCG
GTGGTTTTTTTGTTTGCAAGCAGCAGATTACGCGCAGAAAAAAAGGATCTCAAGAAGATCCTTTGATCTTTTCTACGGGGTCTGACGCTCAGTGGAACGAAAACTCACGTTAAGGGATTTTGGTC
ATGAGATTATCAAAAAGGATCTTCACCTAGATCCTTTTAAATTAAAAATGAAGTTTTAAATCAATCTAAAGTATATATGAGTAAACTTGGTCTGACAGTTACCAATGCTTAATCAGTGAGGCACC
TATCTCAGCGATCTGTCTATTTCGTTCATCCATAGTTGCCTGACTCCCCGTCGTGTAGATAACTACGATACGGGAGGGCTTACCATCTGGCCCCAGTGCTGCAATGATACCGCGAGACCCACGCT
CACCGGCTCCAGATTTATCAGCAATAAACCAGCCAGCCGGAAGGGCCGAGCGCAGAAGTGGTCCTGCAACTTTATCCGCCTCCATCCAGTCTATTAATTGTTGCCGGGAAGCTAGAGTAAGTAGT
TCGCCAGTTAATAGTTTGCGCAACGTTGTTGCCATTGCTACAGGCATCGTGGTGTCACGCTCGTCGTTTGGTATGGCTTCATTCAGCTCCGGTTCCCAACGATCAAGGCGAGTTACATGATCCCC
CATGTTGTGCAAAAAAGCGGTTAGCTCCTTCGGTCCTCCGATCGTTGTCAGAAGTAAGTTGGCCGCAGTGTTATCACTCATGGTTATGGCAGCACTGCATAATTCTCTTACTGTCATGCCATCCG
TAAGATGCTTTTCTGTGACTGGTGAGTACTCAACCAAGTCATTCTGAGAATAGTGTATGCGGCGACCGAGTTGCTCTTGCCCGGCGTCAATACGGGATAATACCGCGCCACATAGCAGAACTTTA
AAAGTGCTCATCATTGGAAAACGTTCTTCGGGGCGAAAACTCTCAAGGATCTTACCGCTGTTGAGATCCAGTTCGATGTAACCCACTCGTGCACCCAACTGATCTTCAGCATCTTTTACTTTCAC
CAGCGTTTCTGGGTGAGCAAAAACAGGAAGGCAAAATGCCGCAAAAAAGGGAATAAGGGCGACACGGAAATGTTGAATACTCATACTCTTCCTTTTTCAATATTATTGAAGCATTTATCAGGGTT
ATTGTCTCATGAGCGGATACATATTTGAATGTATTTAGAAAAATAAACAAATAGGGGTTCCGCGCACATTTCCCCGAAAAGTGCCACCTGACGTCTAAGAAACCATTATTATCATGACATTAACC
TATAAAAAATAGGCGTATCACGAGGCCCTTTCGTCTCGCGCGTTTCGGTGATGACGGTGAAAACCTCTGACACATGCAGCTCCCGGAGACGGTCACAGCTTGTCTGTAAGCGGATGCCGGGAGCAG
ACAAGCCCGTCAGGGCGCGTCAGCGGGTGTTGGCGGGTGTCGGGGCTGGCTTAACTATGCGGCATCAGAGCAGATTGTACTGAGAGTGCACCATTCGACGCTCTCCCTTATGCGACTCCTGCATT
AGGAAGCAGCCCAGTAGTAGGTTGAGGCCGTTGAGCACCGCCGCCGCAAGGAATGGTGCATGCAAGGAGATGGCGCCCAACAGTCCCCCGGCCACGGGGCCTGCCACCATACCCACGCCGAAACA
AGCGCTCATGAGCCCGAAGTGGCGAGCCCGATCTTCCCCATCGGTGATGTCGGCGATATAGGCGCCAGCAACCGCACCTGTGGCGCCGGTGATGCCGGCCACGATGCGTCCGGCGTAGAGGATCT
GGCTAGCGATGACCCTGCTGATTGGTTCGCTGACCATTTCCGGGTGCGGGACGGCGTTACCAGAAACTCAGAAGGTTCGTCCAACCAAACCGACTCTGACGGCAGTTTACGAGAGAGATGATAGG
GTCTGCTTCAGTAAGCCAGATGCTACACAATTAGGCTTGTACATATTGTCGTTAGAACGCGGCTACAATTAATACATAACCTTATGTATCATACACATACG

*Aca*GluD (*Acanthaster planci* delta iGluR, after XM_022229986.1 from Genbank)

GTCGACACCATGGGAAATACCACAGTGGATAGCTTTAACCTGTCTCCTCCTCATGTATATTCTGGAAGGCGTTGTCACATCTGAGAGGCGTTTCCCGTCAGTCATAAAAGTTGGTCTAATATT
ACAACAGCCGTCGTCAGATGAGGACGAGATGATTCGACTCTCATTCCAACATATAAACCAAAACGGGAACATCTTACCGTCAACCCGATTGGATTATACCGTGGCAAGGATAGCCTCCACAGATC
CCTTTGCAGCGTTAAAGCAGCATCGTCAATGTTAAATACAACTGTCGCTGCACTTGTCTCTTCTACAAGCTGCGAGACGAGCCTAGCTTCCAGTCGCTGGCGAACTCTTTCGATGTCCCCAC
ATTATTGTGCCCGGCGAGGAATCCCTCTCGAAAGCATAACAGTTTACGGTTAACGTGCGACCAAGTCAAGTCTACCTGAGCCGAAGCCGTTCTGGACTTGGTATGGTGGCTGAAATGGAAGAG
TGTCTCTATGTTCTACGATTCAGAGAGGCCTATAAGAACGTGCAGCAGTTCCTGCATCTGGCGGCGACAATCGGAGGAGCGCAAGCCGCTGGAGGTGACGCTGTACCGGGTGGACGATAGGGACC
CGGCCAGCGGCGCGCTTGGGATGATTAACATCTTGCACAAAGCTAAGGATTCGGACGTCCAACACATGATCACCTTCTGCGACAGAGCCCAGAGCATGAGGCTGATTAGACAGGCTGCACGTTTT
GGGATGGCCGTGGGGAAATACCAATGGATTATTACAACACAGGACTGGGACATGATGGGAGATGGCGAGCCGGGGAGCTTCACGACGGCTGGCGGGGACATCTCTGAGGAAGAGGCATGAGATT
CCTCAATGGCTCCGAGGGCATCATCACCTTGATGAAGCAACAGGTCAAAGTTCAGACCCACCCTCTGCAGTTCTACAGCGCCTGGCAGATGCTCTACCCGGACATCGACAGGGAAGAGGACGCTA
ACTCCACTTACTTGTCGCCGGGGTATCTCAACACGATCCAGTTCAAAGCAGCCTATATGTACGACGCCGTACGAGTATTGGCAGTTGCCTTGAACGAACAGGTTGAGCGAGCAAGTACATTGAA
CCCGAGATACAGCATTGCTATGACAACAAACCCAAATCATGGAAAGGGGGCATTCGCCTCCGGAAGATGCTGCACAGGACGGAAACAACTGGGCTGATGGGACGGATGCGGTTTAATCACAGTAG
TCTGAATGATGAGATAGCGGTGGATGTCATTACCTTAGAAAGTGGCCGTAACCAGACCAAGGCATGGAAGATTGGCGGCTGGGACCCGGAAAATCGTCTAAATTTGGTCAAAACACCCTTTTCAA
GAGTTTTGCTGCTTTTATCAGTAACAACACCACATTTCGCATTGTAACCGTTGTGGAGGCGCCGTTCGTTAATCGGGACGAGACAGTGAATGGGTACAAGTACTCGGGGTTTTGCATCGACATG
TTAGAACTAATCGCCAAGGAGTTGAACCTGAAGTATGAGTTGTACCTTGTACCAGATGGAAACTACGGAGGAAAGAACGACGACGGGACGTGGAATGGCCTGATTGGGGAAGTTTATTATGGTAG
GGCGGACCTAGCGGTGGCCGGCATGGTCATCAACTCCGACCGCGAGGAAGTGGTGGACTTCACCAAGCCCTTCATGAACTACGGCGTTGGGATTCTCATGCAAAAGCCCAAGAAGAAGGCCAACA
TCTTCGCCTTCCTGGAGCCGCTCCACATCAAGGTCTGGGGCTGCGTGCTGGCCTCCCTCTTCGTGGTCGGGGTGCTGATCTACATCGTGGACCGGCTCAGCCCTTACAGCAGTTCCGGCGGGAG
AACAGTCCCAACCCGGAAGCCTTCGACTTGAAGAACAGCATGTGGTTTGCCTTCGCTTCCTGCATGCAACAGGGCGGCGACACCCTCCCGCTGTCCATTTCTGGTCGTGTCCTGAGCGCGTTCTG
GTGGTTCTTCGCCCTCATCATCACCGCTACGTACACCCGCAACCTGGCCGCCTTCCTGACCGTCACCCGCATGGAGAACCCCATCAACTCTCTAGAGGATTTGGCCACGCAGAAAACCGTGGTCT
ACGGCACCATCCTTAACAGCAGCCTGCATGACTTCTTCGAGAAGCGAAAGAATCAGGGTATCTACGAAAAGATGTGGAACTTCATGTCCACCTCCAAGATCGACCCCTGGGTGCCCAACGCCGAG
GCGGGGTACAAGCGCGTCCAGACAGAGGACTACGCCTCTTTTGGGACGCGCCGATCCTAGACTACATCAAGCAGGAGGAGTGTGACGTCATGACTGTGGGCAAGCCCTTCAACCTGAAGGGATA
CGGCATTGCTACGCCGCGGGGGGTTCCATGGAGAGACGAGATATCAATGGTAATCTTAAAAATGCAAGAGAGGGGCGAACTAGAAGAACTCCGTAAGAAGTGGTTCGACCGGGAATCCAGCTGCC
TGGATGAGACGGACAGCATGAATACGAAACATCGCGCCGCCCGGGCCGACATCAACCTGGACCAGATTGCCGGCGCCTTCTACGTCCTGATCATTGGGGCCGTGTTGTCCTTTGTGGTGGTCATT
GTGGAGCACGTTTGGCACAAGCCGTCCTTCTACAAGAAGCGGGAAAAGGAGACGGGAAGGACCACATTGGACTGGTCAGACAAACTCCCTCCACGGGAAACGAGAAACAATGGTCTTTCTAACAT
TGAAAATTGTTCTTCCAATAAGCATTTAGTTGTTCAAGAGAATGACTCTTTTGCGTTAACACCTTTGAGACCAAACCCATGGAGCACAACGACAATTCTTTCTGTCCCCCCTGAAGCGACAGAAA
ACTCTTGCGGATCC

*Cra*GluD (*Crassostrea gigantea* delta iGluR, after XM_011429946.3 from Genbank)

GTCGACACCATGATACAGTCTACTGGATTTATACTGTTTGTCCTAGCTATTCGATCTTCTGCTAACTGGACAGTGGGAGTCATCTACCAGAGTGACAAGTGGACTGATTTGGGTAAACCACTAAA
TAATGGAAAGGTCACTGCCGTTCAGGAATACCTGTTGCATCAAGTCGATAATTCGGACGCTTTTTCAATGTATCAGAAAGTTTCCAACTTTTCCGAGAGTGGTGTGATTGGAATCGTCGCTTTCA
CATCTTGCCCTACTGCTGCAGTTCTTCAGGAGCAGATCGCTTCTACGAACCTTCCACTGATCACCATAGATAATGAAGTCTGTCCACAAACCTATGACGGCCATCATCATCTGTCCGTGCTTCCA
AACTGCCATAGTCAAAATACACAGTTCATCGATATAGTGCTTCACATGAAGTGGGAACATGTCAACGTCATTTACGATTCAACATCTTCTTACTGCGTTCAGGAACTCATCGTGTTACTGACCAA
AAAGAATGTCTCCAGTAATGCCATATTTCTCCATGAAGGACAACATCTGACGCTGGAAATCTTCCCAGAACTATACTTGGAAGAAGTTATCTACGTGGCTACAGATAAGGAACGGACGCTGGGCA
TTGTCTCCGAGGCTATGACACTGGACATGTTCAACCGTTCCTTCTTCTGGGTTCTGAATTTAGACCCATACGCTCTGTGGAATAGCTCCTTGTATAAGCCTGTCCATGAAGGATGTGTTCTTCTG
ATATCCCTCTGGACTTCAACAGAACGAAACCACGGCAGCTGATTTGCTTTCGGAAGCCCTATCAATATTCCAGCGTGGAGATTAGATTCTATCGGAGATGGACGAAATATCACAGACTTAACATTTCT
TCGCTTTAACCTCAAGCAATACATGATGGGATCTTCCGACGAAACCGGATTAATAGGAAAGGAATCGCAGATCCGGGTTTTCAGTTCTACCAAAGATTACGAAACTCCGTTTGAAGAAGTTGCAG
GTTACTCACAGGATACTCGTAATTTTAATGTAGCTGACGATCGACTTTACAAGTGCATTTTCAAAGACTTTGGCAATAAGACGCTGAAGGTCGTTTCCGTCGAGGGAAAACCTTTCCAAATGCGA
GTGGATAAAGGCAATGGGTCCTTCTACTATTACGGATTTACATACGACCTGCTGAATGAGTTCGCCAAGCAGTTTAACTTCAGATACGAGTTCCTAGATTCAGTAGATGGCCTCTATGGAATAAC
TACAGATGATACCGAAAGTGCTTCAGGGATGATCGGAATGATCATGAGAGGGGAGGCTGATATTGCTGTCGGTGGATTTACAATAACAGCAGACAGAAGAAAAGTTGTAGACTTTCTCTATCCCT
TCCAAGAAGACGGTATCGGAATTATCATGCGAAAGGTTGATAACGAGGCTAACAAGATGTTTCGGGTCTTCAGTTCGCTGGGAACCGACTCTTGGCTTGCTACCGGCGCAGCTGCTTTTGTTGCT
GCCATAGTGTTGTCAATTATCGTCAAGCTGAGTCCGTTTAGTAAGGAGCTTCACAACAAGGTATCTGCTAGCTTTTGGTTGGTTTTCTCCGCTTTTCTCCAACAGGGTGAAGAAAATCCTCCAA
GTCTGCCCCTGCTCGTCTCGTGATAGGATTCTGGTGGATCTTCACAATTATCGTCATGTCCCTGTATACGGCTAACCTTGCTGCCTTTCTGACAGTATCCCTGGCAAAGGCACCAATAAAAACT

TGGAGGAACTTGCAGCTCAGTCCGTTTACAAGCCATTAATTAAGAATGGTTCCAATCTTCACACCCTATTCGAGAAAGCTGAAGGAGGTATCTATAAGAAGATTTGGGATATGATGAGAGATGTC
CCTAAAATCATCTCTCCCGATGAAGGATATGAGATGATCGTCAAAGGAAATTATGCTTACATGACTGATGAATCGGAAGCCCGTTTCAAAGCTATGAAAGACTGCAAGAATCTAGAAATGGCGGA
TGAAACCTTCCATAAAGCAGAGCTCTCTTTCGTTATACGTAAGAACGCAGAGTTTAAAGAGGCTTTCAATAAACACATGCTGAAAATGGTGCAAAATGGCATCGTGGATAAGTACAAGAAGATAT
GGTGGGATAAGCATTCTTGTCATTCGGCTAATACTGCTACTGAACTCGAATTTAAAAGTACAAGTGGAATATTCATTGTCTATTCCGGATTCATATTTATTTCGGTCATCTGCTGTCTTGTAGAG
CTGTACCTTCGAGGTCGTAAATACCCAAAGAACCGTGTCTCATCCAGTAAACAGAGTCTCGAAGATATTTCTGTCATCATGGTTGATTATGGATCC

*Dan*GluD2A (*Danio rerio* delta iGluR, after AAI62459.1from Genbank)

GTCGACACCATGAAAGTTTTTCCGGCAGTACTGTTTCTGATCACATTTTGGTCCCTGGAATGGGAACCTGTTCTTCCCGATTCAATCATTCACATCGGCGCCATTTTTGATGAGTCTGCCAAAAA
GGACGATGAGGTGTTCCGTATGGCAGTCGCGGATCTCAATCTCAACAATGAAATCCTGGAGACAGAGAAGATAACAGTGTCCGTGGAGTTTGTTGATGGAAACAACCCTTTCCAGGCTGTGCAGG
AAGCATGCGAGCTTATGAACAGAGGAATCCTCGCTCTGGTCAGTTCTATCGGCTGCATGTCCGCAGGCTCGCTGCAGTCTTTAGCTGATGCCATGCACATCCCTCACCTGTTCATCCAGAGGGCA
CCCGCGGGCACCCCTCGCTCCAGCTGCCCACCAACAACTCGTGCACAACCCGATGACTACACCCTGTTCGTCCGGCCTCCTGTCTATCTAAATGACGTCATCTTCCAAGTTGTGATGGAGTACAC
TTGGCAGAAGTTCATTATCTTCTACGATACAGACTATGATATCCGTGGAATAGAAAACTTCCTGGACCAGACGTCTCAGCAGGGGATGGATGTGTCTCTGCAGAAGGTTGAATCTAATATTAACA
TGATGATCACTGGAATGTTCCGCACCATGCGAGTGGAAGAACTGCATCGCTACCGAGACACACTGAGACGTGCTGTCCTGTTCATGTCACCCGCCACTGCCAAGGCCTTCATCACCGAAGTGGTG
GAGACCAACCTTGTGGCTTTCGACTGTCACTGGATCATCATAAATGAGGAGATTTCAGATATGGATGTGCAAGAACTGGTCATGAAGTCCATCGGTCGCTTGACCCTGGTGAGACAGACATTCCC
TTTGCCTCAAAACACGAGCCAGCGTTGCGTCCGTAACAATCACCGCATCAACACTTCTCTCTGCGATCCCAAAGACCCTAAGGCACAGATGCTGGAGATTACCAACCGCTACATCTACGACACAG
TACTGTTGCTGGCTAACACATTTCACCGTAAGCTGGAGGATCGTAAGTGGCATTCCATGGCGAGTCTTTCCTGCATCCGTAAGGGCTCCAAACCTTGGCAAGGAGGAAAGTCCATGCTGGAAACT
GTGAAAAAGGGAGGAGTATCTGGTCTGACCTCCCTGCTGGAGTTTAATGATAATGGGTCCAATCCCAACATCCATTTTGAAATCCTGGGTACCAACTACGGTGAGGATCGTGGTCGTGGAGTCTC
CCGTCTGGCTACCTGGGACCCAATCCACGGACTGAATGGAACACTGACCGATAGAAAGCTGGAAAATAACATGCGTGGTGTCGTCCTTCGTGTTGTCACTGTCCTGGAAGAACCGTTTGTTATGG
TGTCTGAAAATGTGCTGGGAAAACCTAAGAAGTACCAGGGATTCTCCATCGATGTGCTGGATGCTCTGGCCAACTATCTCGGATTCAAATATGAGATCTACGTGGCTCCTGATCACAAGTATGGC
AGCCAGCAGGCTGATGGAACGTGGAATGGTCTTATCGGAGAGCTGGTTTTCAAGAGAGCAGACGTAGGACTTTCCGCCCTGACCATCACCCCTGAACGGGAAAGCGTGGTCGATTTCACCACCCG
CTACATGGATTACTCTGTTGGAGTGCTGCTGAGGAAGGCGGAGAGGACCGTCGATATGTTTGCTTGCCTCGCGCCCTTCGACCTGTCCCTGTGGGCTTGTATAGCGGGTACCGTCCTGCTTGTGG
GAACTCTTGTCTATCTGCTCAACTGGCTTAATCCTCCTCGTCTTCCGATGGGCTCTGTCTCCTCAACCACACTCTACAACTCCATGTGGTTTGTCTACGGCTCTTTTGTCCAGCAGGGAGGCGAA
GTGCCCTACACAACTCTGGCTACCCGTATGATGATGGGTGTTTGGTGGCTGTTTGCTCTAATAGTCATCTCCTCCTACACGGCTAATCTGGCTGCTTTTCTTACCATCTCCCGCATTGAGAACTC
CATTCAATCACTGCAGGATTTGGCTAAGCAGACAGATCTCCCTTATGGCACGGTTCTGGACTCCGCCGTCTACGATCAGGTCCGTTCCAAAGGAATGAACCCTTTCGAACGAGACCCTATGTATT
CGCAGATGTGGCGTATGATCAACCGTACAGGAGGAGCCGAAAACAATGTGGAAGAATCAAAAGAAGGAATCCGGAAGGTGAAGTACGGACGTTTTGCATTCGTGTGGGATGCAGCTGTGCTGGAA
TATGTCGCCATTAATGACGAGGACTGTTCGCTGTACACCGTCTCTAACAATGTTGCTGATAGAGGATACGGCATGGCTATGCAGCATGGCAGTCCTTACAGAGACATTTTCTCTCAGCGTATCCT
GGAGCTTCAGCAGAATGGAGATATGGACATCCTGAAGCTTAAGTGGTGGCCAAGGGACAGTCCGTGCGACCTGTACTCTCCAGTCGGAACCCGTAAGAGTGGCAGCGCCCTGGACATCCACAGTT
TTGCTGGAGTCTTCTTTGTTCTAGCGGCAGGTGTGGTCCTGTCCTGTCTGATTGCCACCGTGGAAACGTGGTGGACACGACGTAAGGGCTCCCGTGTCCCATCGAAGGAAGACGATAAAGAAATC
GACCTGGAACACCTGCACCATCGTGTTAACAGCCTGTGCACTGAAGACGAGAGCCCCCACAAACAGTTCTCCACCTCCTCCATCGACCTGACGCCCCTTGATATGGATTCCCTCCCTGCTGCCCG
TCAGGCTCTCGAGCAGATAAGCGACTTCCGTAACACACACATCACCACCACCACCTTTATACCCGAGCAGATTCAGACTCTCTCACGTTCCCTGTCCGCCAAAGCCGCAGCTGGCTTCGCTTTCG
GGGCTGTACAGGATCACCGGACTGGGCGTCCCTTTCGTCAGCGTGCCCCTAATGGCGGCTTCTTTCGCAGCCCTGTCAAAACAATGTCTTCAATCCCTTATCAGCCCACCCCTGCTCCCAACTTT
AGCTATGGAAACGACCCGGATCGAGGAACTTCCATTGGATCC

*Dio*GluD (*Diopisthoporus longitubus* delta iGluR, after c29957 from transcriptome in Andrikou 2019)

GTCGACACCATGGTCAAGTTTACGCACATCGAACACGTGCTTTTCCTTCTGGCGACGTTATGCTCGTTTGTGCTGAAATCATCGGGTAGCAGTGGTGGAAGTGACTTCAGCTCGATACGGCTCGG
ATTCATCATAGAGCAGACGAGTGGAAGTGAGTTTCCACTTGATCAAGTCAATTCCCTGCTTCAGGATGAGGACGAGACAGCTCCTTCGCTCCTTAGCTATAGCATCGAAGTGATCGACTCTCAGA
ACCCGTACCTAGTAGTGCAGCGTGCGTGCGACATGCTAGCGACGTTCCCCGACCAGACGATCCTATTTGTCAGTCTGACAACGTGCATAACTCACCTGGTGCTACGATCGTTCACTGATCAGCAC
GCGCTGCCACACATTACGCTAGGTGGCATGGAAGGGTGTAATGCGCCGCCCAATAACACGTCCTCTCCATTAGGGGGCATCACGCTTACTTGGAATCTACAGGCCGACACAGAGAATACGGTGGA
TTCAGTGATTGCACACATTGTACACTTGGAAAAATGGACGAGTGTAATATTAATACGAGATGAAAGCATCAGCCAACAGCGGACGATCTCGCTACGGGAGCACATTGAAAGTCAGCGGGATAACG
TCAAATTCCATGAGATCAAACTCTTTCTTTACAATCACGATGAGCAGTTGAAGGACCGACTGCGTGACATCGTACCAGATGGAGAGTTTTTCAACTTCATCGTTCTAGCATCTGCTAGCTACACG
ATTGAAATTATACAGACGGCGATGCATCAAGAAATTAGAGGGACTGGAAACGTCAAGAAGTACAAATGGGTGATAGCTAATCAGGAGTTGAGTCTGGAGCAGATTTCGGTGATCGACCCCGAGAT
TCAGATAGTGTCGATTCTGCGATCATCACTCAAACCGTACAAGCTGAAGACAGACCGAAACTTGGAATACTTCAAGGATGCGATGAGTCTGATGGTTCTTGCACTGGAGAACCTTTCGGGAAGTC
TTTATGCTGATATTACTTGCGACAGAGATACAGTCTATCACCAAGGTGAGAACATCATCCAGGAGTTTAGGACTATGGATATCTACGATGGCCTTACTGGTTCGATCGAATCTCGCGAAGACAGA
TTTTACGACTACGTGGCATTGGACATTGTGCAAACAGCCAAGAATGCGACGTTTATCAATCGCTGGAACCTCATCGGTACGTGGAACAAGAGCGAAGGCCTAAACATGCCCGCGACGCGTGCGTT
TCTTCCCGAGTTCGATTCATTGGCGGGCATGACGCTACGAATTGTCACGCTAGTCGAACATCCATTCGTAATCAAAAAGTGGAATGCCGAAACGGGCCAAGCGGAGTACGAAGGCTGCGCTATCG
ACATTCTGAAGGCCATCCAGAAGGATTTGAAGGAAGAGAGTTTCACCTTCACAATGTACGAGGTGGCAGACAACAAATATGGAATTTTCGACGCTGAAACCAATCGCTGGACAGGCCTCGTCGGG
GATGTGAAAGAGCTGAGAGCGCAGATGGCGGTGGCGGGAATGATACGAAACTACAATCGAGAGATGGTAGTGGACTTCACCGCCTCTTACATGGACTACGGAGTGGGTATTCTCATCCCCAAACC
GTCCAAGACGACGAGCATCTTTGGATTTCTGGAGCCACTCAACGTGCAGGTCTGGATCTGTATCGCCGTGGCAACCTTCGGCGTTGGACTCGCGCTCTTCATCCTCTCCCGGTTCTCGCCCTTCA
GTCGGTTCAATCAACACGGAACCGACGAGTTCAGCTTCAAAAACTCAATGTGGTTTGCGCTCGCTAGCCTCATGCAGCAGGGAGGGGATGCGACGCCGCTCTCAATCTCGGGCAGAATCCTCGGC
ACCTTCTGGTGGTTCTTTACTCTTATTATCATAGCGACGTACACGGCGAATTTGGCGGCTTTCCTGACGGTGACGCGTATGGAGACGCCGATCGAGTCCCTTCAAGACCTGAGTAGCCAGACTCG
GATGCCGTATGGGACGGTGCGCGGCAGTTCGCTCGAACATTTCATACACCAGCAGGCGGAGGTAGACAAACTCTACGAGCGCATCTCAGCCTACTTCAGGACAACCGACCCTTCCCCGCTCGTAA
ACACATTCGAAGAAGGCAAAGATAAAGTCATCAGGGGCGATTACGCATTCCTGTGGGACGCTCCCGTGTTGGAGTACCACCGCAAATTACATTGCAGAGAGCTGGCGACGGTGGGAAAGCCATTT
AACCGCAAAAACTATGCCTTCGCCGTGCCAAAAAATGCGCCGTACCTCGAGACGATCACACTGAGCATCCTCCGTCTACAGGAGTCGGGCGAGCTCGACAAAATCAAGCAGAAGTGGTTCGAGGG
TGAGTCCCTGTGTTCGGAGGACGATTCGCTGACACCCGGTCAGGAGGCTGAGGGAATTGCCATCAAGAACGTCGCCGGTGTCTTTTACATACTGCTGATGGGCACCGGACTATCTTTCTTTACGG
CGATCATCGAGTTGATCTGGTATCGCTATTTCAGAGCGATGGAGGACCTGCGTCCTCCTCTACCCCAAAACAGACAGCGGGCCGAATTGTTGGCTCCTACGGGATCC

*Rat*GluD2 (*Rattus norvegicus* delta 2 iGluR, after NM_024379.2 from Genbank)

GTCGACACCATGGAAGTTTTCCCCTTGCTCTTCTTTCTATCCTTCTGGTGGTCTCGAACCTGGGACCTGGCGACCTCCGATTCCATCATCCACATCGGAGCAATTTTTGATGAATCTGCTAAAAA
AGATGATGAAGTATTCCGCACAGCAGTTGGTGACCTCAACCAGAATGAGGAAATCTTACAGACTGAGAAAATCACATTTTCAGTGACATTTGTGGATGGCAACAACCCTTTTCAAGCTGTTCAAG
AAGCATGTGAACTTATGAACCAGGGCATCTTGGCCTTGGTCAGCTCCATTGGTTGCACATCTGCTGGGTCCCTCCAGTCTTTGGCAGACGCCATGCATATCCCTCACCTCTTCATTCAGCGTTCA
ACAGCTGGGACCCCAAGAAGTGGCTGCGGCCTCACCAGGAGCAACAGAAACGATGACTATACCCTTTCAGTTCGTCCACCTGTCTACTTGAATGAAGTCATCCTAAGAGTAGTCACAGAGTATGC
ATGGCAGAAATTTATTATCTTCTATGATAGTGAATATGATATCCGTGGCATACAGGAATTTTTGGACAAAGTTTCCCAGCAGGGAATGGATGTTGCCCTTCAAAAGGTGGAAAACAACATCAATA
AAATGATCACCACGCTCTTTGACACCATGAGGATAGAGGAGTTGAATCGCTATCGAGACACTCTCAGAAGAGCCATCCTTGTTATGAACCCCGCCACAGCCAAATCCTTCATAAGTGAGGTGGTG
GAGACTAATCTGGTTGCTTTTGACTGTCACTGGATCATCATCAATGAGGAAATAAATGATGTGGATGTTCAGGAACTTGTCAGAAGGTCCATTGGAAGGTTAACAATTATTCGGCAGACATTTCC
AGTCCCCCAGAATATAAGTCAGCGCTGTTTCCGTGGCAACCATCGAATTTCTTCAACACTGTGTGATCCCAAGGACCCCTTCGCACAGAATATGGAGATTTCTAACCTTTACATCTATGACACGG
TGCTTCTGCTTGCAAACGCCTTTCATAAGAAGCTGCAGGACCGGAAGTGGCACAGCATGGCGAGCTTGTCCTGTATCAGGAAAAACTCCAAGCCCTGGCAGGGAGGGCGGTCCATGCTGGAGACC
ATCAAGAAGGGTGGAGTTAATGGATTGACTGGAGATCTAGAATTTGGAGAAAATGGAGGTAACCCCAATGTCCACTTCGAAATCCTTGGAACCAACTATGGAGAAGAACTTGGCAGGGGTGTCCG
TAAACTTGGGTGCTGGAATCCTGTCACAGGTCTGAATGGATCACTGACAGACAAGAAACTGGAGAATAACATGCGAGGTGTGGTTCTACGCGTGGTGACTGTATTGGAGGAGCCTTTTGTAATGG
TCTCTGAAAATGTCTTGGGAAAACCGAAGAAATACCAGGGCTTCTCCATTGATGTTTTAGATGCCCTATCTAACTATCTGGGTTTTAACTATGAAATTTATGTTGCACCGGACCACAAATATGGA
AGCCCACAAGAAGATGGGACATGGAATGGACTAGTAGGAGAACTTGTTTTTAAGAGAGCTGACATCGGGATTTCAGCTTTAACCATCACTCCAGACCGGGAGAATGTTGTGGATTTTACAACACG
CTACATGGACTACTCAGTAGGGGTCCTACTGCGAAGGGCAGAAAAAACAGTGGATATGTTTGCCTGCCTTGCACCATTTGATCTATCTCTGTGGGCCTGCATTGCCGGCACAGTCCTTCTTGTGG
GACTCCTGGTCTACCTCTTGAACTGGCTTAATCCCCCACGGTTGCAAATGGGATCAATGACATCTACTACACTCTATAACTCCATGTGGTTTGTGTACGGGTCCTTTGTACAGCAAGGTGGGGAA
GTACCATACACAACTTTGGCAACCCGAATGATGATGGGGGCTTGGTGGTTATTTGCTCTGATTGTCATCTCATCTTATACAGCAAATCTTGCCGCTTTCCTCACTATCACCCGCATTGAGAGCTC
CATCCAGTCTCTTCAGGATCTGTCCAAGCAAACGGATATCCCTTATGGCACAGTCTTGGATTCCGCAGTATATCAGCATGTTCGCATGAAGGGGCTGAATCCTTTTGAGAGGGACAGCATGTATT
CCCAGATGTGGAGGATGATCAACCGAAGCAATGGCTCAGAGAACAATGTTCTGGAGTCCCAAGCAGGCATTCAAAAGGTAAAATATGGAAACTATGCTTTTGTATGGGATGCAGCTGTGTTGGAA
TATGTGGCCATCAATGACCCCGACTGTTCCTTCTACACTGTTGGAAATACTGTTGCTGACCGGGGGTATGGCATCGCACTGCAGCATGGCAGTCCCTACCGTGATGTCTTTTCACAAAGGATTCT
GGAGCTGCAGCAGAGTGGCGACATGGACATCCTCAAGCACAAATGGTGGCCTAAGAATGGCCAGTGTGACCTGTACTCCTCAGTAGATGCAAAGCAGAAGGGAGGAGCCCTGGACATCAAGAGTC
TGGCAGGCGTGTTCTGCATCCTGGCCGCGGGGATTGTACTCTCCTGCCTCATAGCCGTCCTCGAGACATGGTGGAGTCGGCGGAAGGGCTCCCGAGTCCCATCGAAAGAGGATGACAAGGAAATT
GACCTGGAGCACCTCCATAGACGTGTAAATAGCTTGTGCACAGATGACGACAGCCCCCATAAACAGTTTTCCACCTCGTCAATTGACTTGACCCCTCTGGACATTGACACTTTGCCAACACGACA
AGCCCTGGAGCAGATCAGTGATTTCAGAAACACTCACATCACCACCACCACCTTCATCCCAGAGCAGATCCAGACTCTTAGCCGCACACTCTCAGCAAAAGCTGCCTTTGGCTTCACTTTCGGCA
GTGTGCCCGAGCACCGAACTGGCCCTTTTAGGCACAGGGCCCCTAATGGGGGCTTTTTCAGGAGTCCTATCAAAACAATGTCATCTATTCCTTATCAGCCTACTCCCACTCTGGGGCTCAATCTG
GGCAATGACCCCGACCGAGGCACGTCCATAGGATCC

*Rat*GluD1 (*Rattus norvegicus* delta 1 iGluR, after NM_024378.3 from Genbank)

GTCGACACCATGGAAGCGCTGACGCTGTGGCTTCTTCCCTGGATATGCCAGTGCGTTACGGTGCGGGCCGACTCCATCATCCACATCGGTGCCATCTTCGAGGAGAACGCAGCCAAGGACGACAG
AGTGTTCCAGTTGGCTGTATCAGACTTGAGCCTCAATGATGACATCCTGCAGAGTGAGAAGATCACCTACTCCATCAAGGTCATCGAGGCCAATAATCCGTTCCAGGCGGTGCAGGAAGCCTGTG
ACCTCATGACCCAGGGGATTTTGGCCTTGGTCACGTCCACGGGCTGTGCATCTGCCAACGCCCTGCAGTCCCTCACAGACGCCATGCACATCCCACACCTCTTTGTCCAGCGCAACCCCGGGGGT
TCACCACGTACTGCCTGCCACCTGAACCCTAGCCCCGACGGCGAGGCCTACACACTGGCTTCGAGACCGCCCGTCCGTCTCAATGATGTCATGCTCAGGCTGGTGACAGAACTGCGCTGGCAGAA
GTTCGTCATGTTCTATGACAGCGAGTATGATATCCGTGGGCTCCAAAGCTTTCTGGATCAGGCCTCACGGCTGGGTCTTGACGTCTCTTTACAAAAGGTGGACAAGAACATCAGTCACGTGTTCA
CCAGCCTCTTCACCACCATGAAGACGGAGGAGCTGAATCGCTACCGGGACACACTGCGCCGGGCCATCCTCCTGCTTAGCCCACAGGGGGCGCACTCGTTCATCAACGAGGCTGTGGAGACCAAC

TTGGCTTCCAAGGACAGCCACTGGGTCTTCGTGAATGAGGAAATCAGTGACCCCGAGATCCTGGATCTGGTCCACAGTGCCCTTGGCAGGATGACCGTGGTCCGGCAAATCTTCCCATCTGCAAA
GGACAACCAGAAATGCATGAGGAATAACCACCGCATCTCTTCCCTGCTCTGTGATCCACAGGAAGGCTACCTCCAAATGCTGCAGATCTCCAATCTCTATCTGTACGACAGTGTTCTGATGCTGG
CCAACGCCTTCCACAGGAAGCTGGAAGACCGGAAGTGGCATAGTATGGCAAGCCTTAACTGCATACGGAAATCTACCAAGCCATGGAATGGAGGGAGATCCATGCTAGACACCATTAAAAAGGGA
CACATCACCGGCCTCACAGGAGTTATGGAGTTTCGGGAAGACAGCTCAAATCCCTATGTCCAGTTGAAATCCTTGCACAACCTATAGTGAGACTTTTGGCAAAGCACTGGCGACAAGCTGGCGAC
CTGGGACTCAGAGAAGGGCCTGAATGGCAGTCTGCAGGAGAGACCCATGGGCAGCCGCCTCCAAGGACTGACTCTCAAAGTGGTGACTGTCTTGGAAGAGCCTTTTGTGATGGTAGCTGAGAATA
TCCTTGGACAGCCCAAGCGTTACAAAGGGTTCTCCATAGATGTGCTGATGCATTGGCTAAAGCTCTCGGATTCAAATACGAGATATACCAGGCCCCTGATGGCAGGTATGGCCACCAACTCCAT
AACACTTCCTGGAACGGGATGATCGGGGAGCTCATTAGCAAGAGAGCAGACTTGGCCATCTCTGCTATTACCATCACCCCGGAGAGAGAGAGCGTTGTGGACTTCAGCAAGCGATACATGGACTA
CTCAGTGGGGATTCTCATCAAGAAGCCGGAGGAGAAAATCAGCATCTTCTCCCTTTTCGCCCCCTTTGACTTTGCGGTGTGGGCCTGCATTGCTGCAGCCATTCCCGTGGTGGGTGTGCTCATAT
TCGTGTTGAATCGGATACAGGCTGTAAGGTCTCAGAGTGCCACCCAGCCTCGGCCCTCAGCTTCTGCGACTTTGCACAGTGCCATCTGGATCGTCTATGGAGCCTTTGTCCAGCAAGGTGGTGAG
TCTTCGGTGAACTCTGTGGCCATGCGCATCGTGATGGGCAGCTGGTGGCTCTTCACGCTCATTGTATGTTCCTCCTACACAGCCAACCTTGCTGCTTTCCTCACAGTGTCCAGGATGGACAGCCC
CGTAAGAACATTTCAGGACCTGTCCAAGCAACTGGAGATGTCTTATGGCACTGTCCGGGACTCTGCTGTCTATGAGTACTTCAGAGCCAAGGGGACCAATCCCCTGGAGCAGGATAGCACTTTTG
CTGAGCTCTGGCGGACCATAAGCAAGAATGGAGGGGCTGACAACTGTGTGTCCAATCCTTCAGAAGGTATCAGGAAGGCAAAGAAGGGGAACTACGCCTTTCTGTGGGATGTGGCCGTGGTTGAG
TATGCAGCCCTGACAGATGACGACTGCTCAGTGACTGTCATCGGCAACAGCATCAGCAGCAAGGGCTATGGGATTGCCCTGCAACATGGCAGCCCCTACAGGGACCTCTTCTCCCAGAGGATTCT
GGAGCTCGAAGACACAGGGGACCTGGATGTGCTCAAGCAGAAGTGGTGGCCACACACAGGCCGCTGCGACCTCACCAGCCATTCCAGTGCACAGACTGATGGTAAATCCCTTAAGCTGCACAGCT
TCGCTGGGGTCTTCTGCATTTTGGCCATTGGCCTCCTTCTCGCCTGCCTCGTGGCTGCTCTAGAGTTATGGTGGAACAGCAACCGGTGCCACCAGGAGACCCCCAAAGAGGACAAAGAAGTGAAT
CTGGAACAGGTGCACCGGCGCATCAACAGCCTCATGGATGAAGCATTGCTCACAAGCAAATTTCCCCAGCATCCATTGAGCTTGGCCTGGAGATGGGGGGCCTGGCTCCAAGCCAAGCTTT
GGAGCCCACGAGGGAGTACCAGAACACCCAGCTCTCAGTCAGCACCTTTCTGCCTGAGCAGAGCAGCCATGGCACCAGCCGGACACTGTCGTCAGGGCCCAGCAGCAACCTGCCACTGCCGCTGA
GCAGCTCAGCCACCATGCCCTCAATTCAGTGCAAACACAGGTCGCCCAATGGGGGACTGTTTCGACAGAGTCCGGTGAAGACCCCCATCCCTATGTCTTTCCAGCCCGTGCCTGGAGGCGTCCTT
CCAGAGGCCCTGGACACCTCTCATGGCACCTCCATCGGATCC

*Sac*GluD (*Saccoglossus kowalevskii* delta iGluR, after XM_002731960.1 from Genbank)

GTCGACACCATGGATCGACACGTGTCGTATATTCTGTTGTTGTTTTCGAGTATGTTGATAGGCTTGTTGTGTTTTCCGATTCAAGCAAGAGAAGGACTACCTCGCAACATCAGCATAGGTGTGTT
ATTCGAAGAAACTCAAGGAGATGAGAGAAAACTTTTAAAAGAAGCAATCAAAAAAGTTCAAAGGGATACTTCATTATTACCTCACACAGAATTAATTGTTCACTGGGAAAGGATTGGATTCACAG
ATCCGTACGACATGATTGAACAAGCATCGAGAATATATGGGAAGTCGCCTTCATTAATGATAACATTGACGTCCTGCCAGCCATCTACCTTACTGCAAAATGCTGCTAACGTGTTCAGGTTACCA
CATTTACAGATTGCTACGGAGACCTGCAGGATTAGTTCAGAATTTACGCTAAGTATGAATCCCGATGTCTATATGACTGACATGGCGCTGTTTTCGCTGATCAAGTTACAGGAATGGACTTCATT
TGTTGTTTACTATGACACCGATATGGCATACCACCGAGTGCAGAGCATTATTGAATCGGCCGATAATGGTAATCTAGTTTGGGAAGTCATTTTACTACGCTACATTGGCGATGAAGTGGGTACAC
GCTGGACATCACAACAACTCAAAAGAATGGACGGAATACATAATTATGTGATTGTATTTGAAACCAAAAATGTATTTAATCTTTTACGTACGGCAGGTAACATGGGTATGCGGTCACGTGAATAT
CACTGGATCGTTCTTTATCAGGGAATGACAGACACCCAGCTGGAAAATGTGCCTAAGGCATTGGGTATTGTCATATTTGTCAGACAACAACCTCTCATCATAGAAACGAACGAAGAGGAGGTGAG
AGGTCACAAAAAGAAGAAGAAAGATAGAATAAATAATGCAAGTATACCGTCCCTCTATCTCCATGATAGCGTCATTGTTGCTGCCATGGCACTAGATGCAGTTATCAAGAAACACAGGCATTTTA
TTTGGCCCGGCAGTAGACCCGTCGTTGTGTAGACCATTACAGTCTGATACTACTGTACATCATATCGGCAGGTCTGATACTATAGGGTCTCAGGAGGTAACGGATAGATATGCGCTAATGGATGCT
GTGCGAAAGATTGGCATATGGGACCCGGTCAACAGGCTGAACATGTCACACACCCCATTTCAGTCCACTTTTAAAGTTCTACAGAACAGGACTTTGAAGATTGTTACTATAGAGGAAGAGCCTTT
TGTTAGAAAAACCGAGATCCGCCCAGGAGTGTATGAATACACAGGTTTCTGCATAGACATATTAGACGAGATTTCACAATTCACGTATGTTGCTATATGATGTTCCTGATCTGAAAT
ACGGAGCTAAAGTGAATGGTACATGGAATGGGTAGTCGGAGAAGTGGCATATGGGAAAGCAGACATGGCAGTAGCTGGAATAACAATAATGGCTGAGCGAGAAGAAGTTGTTGATTTCACTAAA
CCGTATTATCAGTATGCCCTGGGAATTATTATCAGTAAGCCCGGACCGAGCGAGGCATCTTCGCCTTTATGGAACCATTAAGCGGTCCGGTGTGGGGATGTATAGCAGCAGCCTTGTTTGTAGT
GGGAATATTCCTGTTCGTCATAGCCAGGCTTAGTCCATATAGCTCGTTCAATTACTCTAAAAAAGAATATTGTGAATGTAAAGGCGATGACTTTAACTTGAAGAACAGCTACTGGTTTGCATTGG
CATCCCTTATGAACCAAGGTGGTGATACTGCTCCCTACCATCTCCGGGAGATTACTGAGCGGTTCTGGTGGTTTTTCACTTTAATAATCATAGCTACGTACACAGCTAATTTGACAGCATTT
CTGACAGTGAGCAGGATGGAAACGCCTATATCGTCTGTGGAGGAATTATCAACGCAATCTAAAATCAAATACGGTACAATCCGAGACAGTAGTGTAGTCTCATTTTTTAAAAGATCCACAATAAA
TCCTTATCAGCGAATGTGGCAGTTCATGAATACGACAGAGGTTGATCCATACGTAGACACTGTCACGGACGCATATCGTAGAGCGAAAGGGGAGGAGTATGCCTTCATGTGGGATTATCCCGTGT
TGGAGTTACAAAAAAGAATCGATTGCGATCTTATGACTGTGGGAAAGCCTTTCTATGAAAAGGGATACGGTTTTGTAACTCCACAAGGAGCGGATTGGAGAGATGATATATCCATGAGTATTCTG
GAGATGAGGGAGAATGGTCAACTAGAAAAATATCGCAAGAAGACCTGGGAAATCGAAAGCGAGTGTGAGGACGATGCGGCTATGATAAGAAGTTCCACAAATGAGATAGATATTCAAAGTGATTAC
TGGTGTGTTCTATATACTTATGATCGGTGCAGGTGTCTCCTTGATAACTGTCTCAGTAGAGATATTGTATTATCATTTTTGAGGAAGTGTTGCCGACAACTATAACAGTCCATCCCAACGTGG
ATGGTAAGGCTATTGAGGTCAGAGAAGAAAATGCTATAGAAGATGGTAAATCCTTGTCTAATTCCAGAGTTTGA

Chimera *Aca*GluD^{RatNTD} (*Acanthaster planci* delta iGluR with NTD replaced with *Rat*GluD2 NTD (purple). *Aca*GluD NTD-LBD linker underlined.)

GTCGACACCATGGAAATACCACAGTGGATAGCTTTAACCTGTCTCCTCCTCATGTATATTCTGGAAGGCGTTGTCACATCTGAGAGGCGTGTTTTCCCGTCCATCATCCACATCGGAGCAATTTT
TGATGAATCTGCTAAAAAAGATGATGAAGTATTCCGCACAGCAGTTGGTGACCTCAACCAGAATGAGGAAATCTTACAGACTGAGAAAATCACATTTTCAGTGACATTTGTGGATGGCAACAACC
CTTTTCAAGCTGTTCAAGAAGCATGTGAACTTATGAACCAGGGCATCTTGGCCTTGGTCAGCTCCATTGGTTGCACATCTGCTGGGTCCCTCCAGTCTTTGGCAGACGCCATGCATATCCCTCAC
CTCTTCATTCAGCGTTCAACAGCTGGGACCCCAAGAAGTGGCTGCGGCCTCACCAGGAGCAACAGAAACGATGACTATACCCTTTCAGTTCGTCCACCTGTCTACTTGAATGAAGTCATCCTAAG
AGTAGTCACAGAGTATGCATGGCAGAAATTTATTATCTTCTATGATAGTGAATATGATATCCGTGGCATACAGGAATTTTTGGACAAAGTTTCCCAGCAGGGAATGGATGTTGCCCTTCAAAAGG
TGGAAAACAACATCAATAAAATGATCACCACGCTCTTTGACACCATGAGGATAGAGGAGTTGAATCGCTATCGAGACACTCTCAGAAGAGCCATCCTTGTATTGAACCCCGCCACAGCCAAATCC
TTCATAAGTGAGGTGGTGGAGACTAATCTGGTTGCTTTTGACTGTCATCATCAATGAGGAAATAAATGATGTGGATGTTCAGGAACTTGTCAGAAGGTCCATTGGAAGGTTAACAAT
TATTCGGCAGACATTTCCAGTCCCCCAGAATATAAGTCAGCGCTGTTTCCGTGGCAACCATCGAATTTCTTCAACACTGTGTGATCCCAAGGACCCCTTCGCACAGAATATGGAGATTTCTAACC
TTTACATCTATGACACGGTGCTTCTGCTTGCAAACGCCTTTCATAAGAAGCTGCAGGACCGGAAGTGGCACAGCATGGCGAGCTTGTCCTGTATCAGGAAAAACTCCAAGCCCTGGCAGGGAGGG
CGGTCCATGCTGGAGACCATCAAGAAGGGTGGAGTTAATGGATTGACTGGAGATCTAGAATTTGGAGAAAATGGAGGTAACCCCAATGTCCACTTCGAAATCCTTGGAACCAACTATGGAGAAGA
ACTTGGCAGGGGTGTCCGTAAACTTGGGTGCTGGAATCCTGTCACAGGTCTGAATGGATCACTGCCCTTTTCAAGAGGTTTTGCTGCTTTATCAGTAACAACACCACATTTCGCATTGTAACCG
TTGTGGAGGGCGCGTTCGTTAATCGGGACGAGACAGTGAATGGGTACAAGTACTCGGGCGTTTGCATCGACATGTTAGAACTAATCGCCAAGGAGTTGAACCTGAAGTATGAGTTGTACCTTGTA
CCAGATGAAACTACGGAGGAAAGAACGACGACGGGACGTCGAATGGCCTGATTGGCGAAGTTATTATGGTAGGGCGGACCTACCGGTCGCCGGCATGGTCATCAACTCCGACCGCGAGCAAGT
GGTGGACTTCACCAAGCCCTTCATGAACTACGGCGTTGGGATTCTCATGCAAAAGCCCAAGAAGAAGGCCAACATCTTCGCCTTCCTGAGCCCGCTCCACATCAAGGTCTGGGGCTGGCTGTGG
CCTCCCTCTTCGTGGTCGGGGTGCTGATCTACATCGTGGACCGGCTCAGCCCTTACAGCAGTTTCCGGCGGGAGAACAGTCCCAACCCGGAAGCCTTCGACTTGAAGAACAGCATGTGGTTTGCC
TTCGCTTCCTGCATGCAACAGGGCGGCGACACCTCCCCGCTGTCCATTTCTGGTCGTGTCCTGAGCGCGTTCTGGTGGTTCTTCGCCCTCATCATCACCGCTACGTACACCCGCCAACCTGGCCGC
CTTCCTGACCGTCACCCGCATGGAGAACCCCATCAACTCTCTAGAGGATTTGGCCACGCAGAAAACCGTGGTCTACGGCACCATCCTTAACAGCAGCCTGCATGACTTCTTCGAGAAGCGAAAGA
ATCAGGGTATCTACGAAAAGATGTGGAACTTCATGTCCACCTCCAAGATCGACCCCTGGGTGCCCAACGCCGAGGCGGGGTACAAGCGCGTCCAGACAGAGGACTACGCCTTCTTTTGGGACGCG
CCGATCCTAGACTACATCAAGCAGGAGGAGTGTGACGTCATGACTGTCGGCAAGCCCTTCAACCTGAAGGGATACGGCATTGCTACGCCGCGGGGGGTCCATTGGAGAGCAGAGTATCAATGGT
AATCTTAAAAATGCAAGAGAGGGGCGAACTAGAAGAACTCCGTAAGAAGTGGTTCGACCGGGAATCCAGCTGCCTGGATGAGACGGACAGCATGAATACGAAACATCGCGCCGCCCGGGCCGACA
sTCAACCTGGACCAGATTGCCGGCGCCTTCTACGTCCTGATCATTGGGGCCGTGTTGTCCTTTGTGGTGGTCATTGTGGAGCACGTTTGGCACAAGCCGTCCTTCTACAAGAAGCGGGAAAAGGA
GACGGGAAGGACCACATTGGACTGGTCAGACAAACTCCCTCCACGGGAAACGAGAAACAATGGTCTTTCTAACATTGAAAATTGTTCTTCCAATAAGCATTTAGTTGTTCAAGAGAATGACTCTT
TTGCGTTAACACCTTTGAGACCAAACCCATGGAGCACAACGACAATTCTTTCTGTCCCCCCTGAAGCGACAGAAAACTCTTGCGGATCC

Chimera *Aca*GluD^{RatNTDlink} (*Acanthaster planci* delta iGluR with NTD and NTD-LBD linker replaced with *Rat*GluD2 NTD and NTD-LBD linker (purple). *Rat*GluD2 NTD-LBD linker underlined.)

GTCGACACCATGGAAATACCACAGTGGATAGCTTTAACCTGTCTCCTCCTCATGTATATTCTGGAAGGCGTTGTCACATCTGAGAGGCGTGTTTTCCCGTCCATCATCCACATCGGAGCAATTTT
TGATGAATCTGCTAAAAAAGATGATGAAGTATTCCGCACAGCAGTTGGTGACCTCAACCAGAATGAGGAAATCTTACAGACTGAGAAAATCACATTTTCAGTGACATTTGTGGATGGCAACAACC
CTTTTCAAGCTGTTCAAGAAGCATGTGAACTTATGAACCAGGGCATCTTGGCCTTGGTCAGCTCCATTGGTTGCACATCTGCTGGGTCCCTCCAGTCTTTGGCAGACGCCATGCATATCCCTCAC
CTCTTCATTCAGCGTTCAACAGCTGGGACCCCAAGAAGTGGCTGCGGCCTCACCAGGAGCAACAGAAACGATGACTATACCCTTTCAGTTCGTCCACCTGTCTACTTGAATGAAGTCATCCTAAG
AGTAGTCACAGAGTATGCATGGCAGAAATTTATTATCTTCTATGATAGTGAATATGATATCCGTGGCATACAGGAATTTTTGGACAAAGTTTCCCAGCAGGGAATGGATGTTGCCCTTCAAAAGG
TGGAAAACAACATCAATAAAATGATCACCACGCTCTTTGACACCATGAGGATAGAGGAGTTGAATCGCTATCGAGACACTCTCAGAAGAGCCATCCTTGTATTGAACCCCGCCACAGCCAAATCC
TTCATAAGTGAGGTGGTGGAGACTAATCTGGTTGCTTTTGACTGTCATCATCAATGAGGAAATAAATGATGTGGATGTTCAGGAACTTGTCAGAAGGTCCATTGGAAGGTTAACAAT
TATTCGGCAGACATTTCCAGTCCCCCAGAATATAAGTCAGCGCTGTTTCCGTGGCAACCATCGAATTTCTTCAACACTGTGTGATCCCAAGGACCCCTTCGCACAGAATATGGAGATTTCTAACC
TTTACATCTATGACACGGTGCTTCTGCTTGCAAACGCCTTTCATAAGAAGCTGCAGGACCGGAAGTGGCACAGCATGGCGAGCTTGTCCTGTATCAGGAAAAACTCCAAGCCCTGGCAGGGAGGG
CGGTCCATGCTGGAGACCATCAAGAAGGGTGGAGTTAATGGATTGACTGGAGATCTAGAATTTGGAGAAAATGGAGGTAACCCCAATGTCCACTTCGAAATCCTTGGAACCAACTATGGAGAAGA
ACTTGGCAGGGGTGTCCGTAAACTTGGGTGCTGGAATCCTGTCACAGGTCTGAATGGATCACTGACAGACAAGAAACTGGAGAATAACATGCGAATTTCTTCCGTCATCATCCACATCGGAGCAATTTT
CGTTCGTTAATCGGGACGAGACAGTGAATGGGTACAAGTACTCGGGCGTTTGCATCGACATGTTAGAACTAATCGCCAAGGAGTTGAACCTGAAGTATGAGTTGTACCTTGTACCAGATGAAACT
ACGGAGGAAAGAACGACGACGGGACGTCGAATGGCCTGATTGGCGAAGTTATTATGGTAGGGCGGACCTACCGGTCGCCGGCATGGTCATCAACTCCGACCGCGAGCAAGTGGTGGACTTCACC
AAGCCCTTCATGAACTACGGCGTTGGGATTCTCATGCAAAAGCCCAAGAAGAAGGCCAACATCTTCGCCTTCCTGGAGCCGCTCCACATCAAGGTCTGGGGCTGGCTGTGGCCTCCCTCTTCG
TGGTCGGGGTGCTGATCTACATCGTGGACCGGCTCAGCCCTTACAGCAGTTTCCGGCGGGAGAACAGTCCCAACCCGGAAGCCTTCGACTTGAAGAACAGCATGTGGTTTGCCTTCGCTTCCTGC
ATGCAACAGGGCGGCGACACCTCCCCGCTGTCCATTTCTGGTCGTGTCCTGAGCGCGTTCTGGTGGTTCTTCGCCCTCATCATCACCGCTACGTACACCCGCCAACCTGGCCGCCTTCCTGACCGT
CACCCGCATGGAGAACCCCATCAACTCTCTAGAGGATTTGGCCACGCAGAAAACCGTGGTCTACGGCACCATCCTTAACAGCAGCCTGCATGACTTCTTCGAGAAGCGAAAGAATCAGGGTATCT
ACGAAAAGATGTGGAACTTCATGTCCACCTCCAAGATCGACCCCTGGGTGCCCAACGCCGAGGCGGGGTACAAGCGCGTCCAGACAGAGGACTACGCCTTCTTTTGGGACGCGCCGATCCTAGAC
TACATCAAGCAGGAGGAGTGTGACGTCATGACTGTCGGCAAGCCCTTCAACCTGAAGGGATACGGCATTGCTACGCCGCGGGGGGTCCATTGGAGAGCAGAGTATCAATGGTAATCTTAAAAAT
GCAAGAGAGGGGCGAACTAGAAGAACTCCGTAAGAAGTGGTTCGACCGGGAATCCAGCTGCCTGGATGAGACGGACAGCATGAATACGAAACATCGCGCCGCCCGGGCCGACATCAACCTGGACC

AGATTGCCGGCGCCTTCTACGTCCTGATCATTGGGGCCGTGTTGTCCTTTGTGGTGGTCATTGTGGAGCACGTTTGGCACAAGCCGTCCTTCTACAAGAAGCGGGAAAAGGAGACGGGAAGGACC
ACATTGGACTGGTCAGACAAACTCCCTCCACGGGAAACGAGAAACAATGGTCTTTCTAACATTGAAAATTGTTCTTCCAATAAGCATTTAGTTGTTCAAGAGAATGACTCTTTTGCGTTAACACC
TTTGAGACCAAACCCATGGAGCACAACGACAATTCTTTCTGTCCCCCCTGAAGCGACAGAAAACTCTTGCGGATCC

SUPPORTING INFORMATION REFERENCES

1. J. Elegheert *et al.*, Structural basis for integration of GluD receptors within synaptic organizer complexes. *Science* **353**, 295-299 (2016).
2. P. Naur *et al.*, Ionotropic glutamate-like receptor delta2 binds D-serine and glycine. *Proc Natl Acad Sci U S A* **104**, 14116-14121 (2007).
3. A. P. Burada, R. Vinnakota, J. Kumar, The architecture of GluD2 ionotropic delta glutamate receptor elucidated by cryo-EM. *J Struct Biol* **211**, 107546 (2020).
4. A. P. Burada, R. Vinnakota, J. Kumar, Cryo-EM structures of the ionotropic glutamate receptor GluD1 reveal a non-swapped architecture. *Nat Struct Mol Biol* **27**, 84-91 (2020).
5. J. Zuo *et al.*, Neurodegeneration in Lurcher mice caused by mutation in delta2 glutamate receptor gene. *Nature* **388**, 769-773 (1997).
6. K. B. Hansen *et al.*, Modulation of the dimer interface at ionotropic glutamate-like receptor delta2 by D-serine and extracellular calcium. *J Neurosci* **29**, 907-917 (2009).
7. E. C. Twomey, M. V. Yelshanskaya, R. A. Grassucci, J. Frank, A. I. Sobolevsky, Channel opening and gating mechanism in AMPA-subtype glutamate receptors. *Nature* **549**, 60-65 (2017).

Graphic design: Communication Division, UiB / Print: Skipnes Kommunikasjon AS

uib.no

ISBN: 9788230862940 (print)
9788230842669 (PDF)